THE UNIVERSITY
of EDINBURGH

THE UNIVERSITY *of* EDINBURGH

A Synthetic Biology Approach towards Engineering of *Shewanella oneidensis* MR-1 for Microbial Fuel Cell Technologies

Beatrice Viviane Vetter-Ceriotti

Thesis presented for the Degree of Doctor of Philosophy

The University of Edinburgh

May 2019

DECLARATION

I declare that this thesis has been composed solely by myself and that it has not been submitted, in whole or in part, in any previous application for a degree. Except where states otherwise by reference or acknowledgment, the work presented is entirely my own.

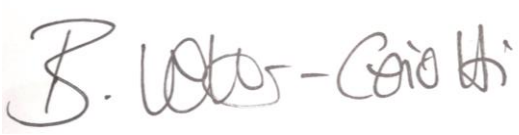

_____

Beatrice V. Vetter-Ceriotti

ACKNOWLEDGEMENTS

I would like to thank Prof Susan Rosser for her supervision and support over the past years and the many opportunities, as well as all members of the research group, especially Annegret, Mai-Britt and Maryia. I would also like to thank Dr. Louise Horsfall and Dr. Chris French for their support.

I would like to acknowledge and thank all my wonderful friends for their tremendous and inexhaustible support and encouragement over the last years, no matter how far we live apart.

I would like to dedicate this thesis to my husband Matteo and my family who sacrificed so much to enable me to complete this, especially my father Hans-Jürgen, Ingrid and Oma Helga and my mother-in-law Silvana and my late father-in-law Genesio. Without your unconditional love and support, I would not be the person that I am today.

TABLE OF CONTENTS

LAYMAN'S ABSTRACT

In the past decade the emerging field of microbial electrochemical technologies (METs) has gained increased attention due to their potential for bioenergy production and bioremediation. By utilizing pollutants or waste as carbon sources electroactive bacteria can convert chemical energy into electricity, thereby conceivably closing the waste disposal energy generation loop. One such organism is *Shewanella oneidensis* MR-1 (SOMR-1) already possesses a large respiration versatility. These traits make it a feasible synthetic biology chassis to increase predictability, stability and novel functionalities of MET applications. However, to precisely engineer this bacterium more genetic tools are needed to overcome the bottleneck for this new technology. In this study, a synthetic biology toolbox for SOMR-1 was expanded by establishing the Standardised European Vector Architecture (SEVA) plasmid platform and transcriptional regulation tools. In this work a novel cyclohexanone inducible promoter has been characterised and used to express a synthetic flavin gene operon to enhance SOMR-1' current output in novel small-scale MFCs with screen-printed electrode technology. Additional work is shown to test novel screening methods to identify optimised EAB capabilities in SOMR-1 using a colorimetric tungsten trioxide assay.

ABSTRACT

In the past decade the emerging field of microbial electrochemical technologies (METs) has gained increased attention due to its potential for bioenergy production and bioremediation. By utilizing pollutants or waste as carbon sources electroactive bacteria (EAB) can convert chemical energy into electricity, thereby conceivably closing the waste disposal energy generation loop. These EABs can generate current anaerobically by forming an electroactive biofilm on conductive electrode materials via extracellular electron transfer (EET). The genetically tractable EAB model organism *Shewanella oneidensis* MR-1 (SOMR-1) already possesses several EET routes and a large respiration versatility. These traits make it feasible as a synthetic biology chassis to increase predictability, stability and novel functionalities of MET applications. However, as synthetic gene circuits become more elaborate in size and complexity and only relatively few well-characterized biological parts have been described for this organism, precise genetic engineering increasingly presents a bottleneck for this new technology. Here, the synthetic biology toolbox for SOMR-1 was expanded by establishing the Standardised European Vector Architecture (SEVA) plasmid platform providing characterisation of plasmid maintenance with a large range of replication origins, quantification of plasmid copy numbers and their compatibility as multi-plasmid bearing systems in SOMR-1. Further, establishment of transcriptional regulation using oxygen independent inducible promoters was realised. In this work the novel cyclohexanone inducible promoter $P_{ChnB/ChnR}$ was introduced among others and characterised using oxygen independent reporter assays. A synthetic flavin gene operon under the control of $P_{ChnB/ChnR}$ was used to show enhancement of SOMR-1 EET in small-scale MFCs using screen-printed electrode technology. Additional screening methods are presented which were aimed to identify novel EET capabilities in SOMR-1 using a colorimetric tungsten trioxide (WO_3) assay.

ABBREVIATIONS

Antibiotics	
Am	Ampicillin
Cm	Chloramphenicol
Gm	Gentamicin
Km	Kanamycin
Na	Nalidixic acid
Sp	Spectinomycin
Tc	Tetracycline
A	Ampere
ara	Arabinose
ARB	Anode-respiring bacteria
AQDS	Anthraquinone-2,6-disulfonate
aTc	anhydrotetracycline
BBa	BioBrick (version alpha)
BES	Bio-electrochemical system
bp	Basepair
Btu	British thermal unit (1 Btu = 1055 J)
C	Celsius
CA	Chronoamperometry
c-di-GMP	Cyclic-dimeric-GMP
CE	Counter electrode
cfu	Colony forming unit
CH	Cyclohexanone
cm	Centimetre
CO_2	Carbon dioxide

CV	Cyclic Voltammetry
DAP	Di-aminopelic acid
DET	Direct Electron Transfer
DMSO	Dimethyl sulfoxide
DNA	Deoxyribonucleic acid
dNTPS	deoxyribonucleotide triphosphate
DSMZ	Leibniz-Institut DSMZ - Deutsche Sammlung von Mikroorganismen und Zellkulturen GmbH
EAB	Electroactive bacteria
EABf	Electroactive biofilm
ECM	Extracellular matrix
EDTA	Ethylenediaminetetraacetic acid
EET	Extracellular Electron Transfer
ES	Extracellular space
et al.	*et alteri* (lat.); Engl.: and other
EtOH	Ethanol
FAD	Flavin adenine dinucleotide
FMN	Flavin mononucleotide
g	Gram
gDNA	Genomic DNA
GFP	Green fluorescent protein
GMP	Guanosine monophosphate
h	Hour
HAc	Glacial acetic acid
HF	High fidelity
IET	Indirect electron transfer
IM	Inner membrane

IPTG	Isopropyl β-D-1-thiogalactopyranoside
IR	Inverted repeat
k	Kilo
KAc	Potassium acetate
kb	Kilobasepair
KOD	Recombinant *Thermococcus kodakaraensis* KOD1 DNA polymerase
L	Litre
LB	Lysogeny broth
LM	Lactate medium
m	Milli (10^{-3})
M	Molar concentration; 1M =1 molar = 1 mol· L^{-1}
MAE	Microbiallly assisted electrosynthesis
MCS	Multiple Cloning Site
MEC	Microbial Electrolysis Cell
MeOH	Methanol
MES	Microbial electrochemical systems
MES	Microbial electrosynthesis
MET	Mediated Electron Transfer
MFC	Microbial Fuel Cell
min	Minute
MU	Miller units
MQ	Menaquinone
MQH_2	Menaquinol
n	Nano (10^{-9})
NB	*Nota bene* (lat.); Engl.: note well
NCIMB	National Collection of Industrial Food and Marine Bacteria

NEB	New England Biolabs
nt	Nucleotide
OD_{600}	Optical density at 600 nm
OM	Outer membrane
OMC	Outer membrane cytochrome
ONPG	Ortho-Nitrophenyl-β-galactoside
oriT	Origin of transfer
oriV	Origin of replication
P	Promoter
PBS	Phosphate-buffered saline
PCN	Plasmid copy number
PCR	Polymerase chain reaction
PDB	Protein Database
PEC	Periplasmic electron carriers
PEG	Polyethylene glycol
PNK	Polynucleotide kinase
PP	Periplasmic
qPCR	Quantative PCR
RE	Reference electrode
RFU	Relative fluorescent unit
rpm	rounds per minute
s	Second
SD	Standard deviation
SDS	Sodium dodecyl sulfate
SEM	Scanning Electron Microscope
SEM	Standard error of the mean
SEVA	Standardised European Vector Architecture

SHE	Standard hydrogen electrode
SPE	Screen printed electrode
tDNA	Total DNA
V	Volt
v/v	volume/volume; volume part in total volume
WE	Working electrode
w/v	weight/volume; weight part in total volume
µ	Micro (10^{-6})
XRD	X-ray diffraction

LIST OF FIGURES

LIST OF TABLES

available pSEVA3X1 or pSEVA6X1. SOMR-1 transconjugants were grown overnight in LB with appropriate antibiotic selection (50 µg/mL Km and 20 µg/mL Cm, or 50 µg/mL Km and 10 µg/mL Gm) and plasmids confirmed by gel electrophoresis. 89

CHAPTER 1

1. INTRODUCTION

1.1 The Global Energy Challenge

With a growing global population living on the planet, currently estimated to be 9.4 billion in 2050, the greatest environmental challenge of our generation is to develop alternative ways to meet future energy needs (United Nations Department of Economic and Social Affairs Population Division 2017), and to address the pressing need to challenge the evermore omnipresent global impacts of climate change. While fossil fuels, such as oil, coal and natural gas, have been important in the industrialisation and economic growth worldwide, these resources are not only finite but are also releasing stored carbon dioxide (CO_2) into the atmosphere resulting in steadily rising global mean temperatures causing melting of glacier and rising sea levels (Wuebbles et al. 2017). Other energy sources such as nuclear energy are also limited. Uranium availability with its mining and lack of safe nuclear waste disposal options further poses risk of devastating, long-lasting environmental damage that can be caused by nuclear power plants accidents (Schneider and Froggat 2017). Renewable energy generation is therefore a solution that presents a cleaner and safer alternative to fossil fuels and nuclear power, such as harvesting solar and hydro-electric energy. However with the global energy consumption to be predicted to grow by 56 % between 2010 and 2040 (International Energy Agency, 2013), energy demands cannot be met with renewables alone and novel and innovative solutions should be invested in, both in terms of research and development, to meet these energy demands in a sustainable and environmentally friendly way.

1.2 Synthetic Biology Design Principles and Approaches to Address Global Challenges

1.2.1 *The Emerging Field of Synthetic Biology*

Synthetic biology has been an emerging field over the past two decades combining biological and engineering concepts to advance science for human health and the environment. In 2012, the UK Technology Strategy Board published the Synthetic Biology Roadmap (Clarke et al. 2012), and the UK has since invested approximately £300 million for Synthetic Biology Research which included funding for 6 new multidisciplinary research centres, DNA synthesis facilities, training centres and start-up companies.[1] As promising as Synthetic Biology is with its radical approaches to re-design life, it has to come with responsible research and innovation to solve our futures' great challenges whilst maintaining public acceptability and adhering to governance (Marris and Calvert 2019). While this nascent field is forming with deeply challenging ideas and pervasive assumptions on how these technological leaps could lead to ground-breaking innovation and economic progress, it also has to bridge between science, public acceptance and policy makers. Therefore, natural scientists are often required to include social scientists on their grants to demonstrate to the funding bodies that they are taking "ethical, legal and social implications" serious (Marris and Calvert 2019). With recent examples of public perception and the public condemnation of, e.g. *Golden Rice* where the functioning pro-vitamin A (β-carotene) biosynthetic pathway was cloned in rice defeat vitamin A deficiency, a serious public health problem Asia, Africa and Latin America (Beyer et al. 2002), it is important to

[1] https://www.gov.uk/government/groups/synthetic-biology-leadership-council (last accessed 12th May 2019)

assess Synthetic Biology's ambitious aims and its potential. These range from the production of drugs and their delivery, to biofuel, engineered tissue and genomically engineered organisms all of which are reporting stark progress over recent years, one of the best-known examples is the semi-synthetic production of the antimalarial drug, artemisinin, using engineered yeast (Keasling 2012). Hence, approaches for wastewater treatment and energy recovery should be carefully thought through, otherwise they could be endangered to not be accepted by not only the public, but also policy makers thereby halting its innovation.

1.2.2 *The Synthetic Biology Domain*

With the emergence of fast and cheaper sequencing options, genetic information and a more advanced biological understanding of organisms has never been more readily available. This plethora of biological information allows us now to apply design and engineering principals of characterisation, standardisation and modularisation to biology [see Figure 1.1] (Clarke and Kitney 2016). This vast knowledge and desire to re-design biological systems led to the development of more rapid and precise gene editing tools, such as CRISPR-Cas (Hofer 2014). Further, as a large deposit of standardised genetic components to enhance productivity emerge by several repositories such as the international genetically engineered machine (iGEM) competition and its registry[2] of standardised parts, these standardised genetic parts provide the basis for genetically engineering of microorganisms.

[2] http://igem.org/Registry

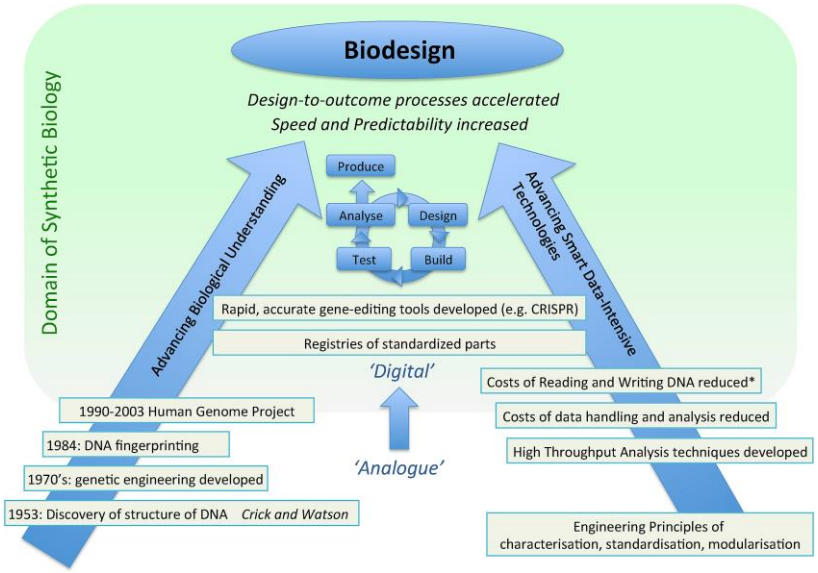

Figure 1.1 Schematic illustration of the synthetic biology domain. Image taken from (Clarke and Kitney 2016).

1.3 Microbial Electrochemical Technologies (METs)

A novel approach to harvest bioelectricity from bacterial biomass has gained increased attention during the past decades, even though its first observation of electrical current generated by bacteria was over a century ago (Potter 1911). Since then, the newly emerging discipline of electro-microbiology and its affiliated new technologies, such as microbial bio-electrochemical systems (BESs), is a highly inter-disciplinary field integrating, among others, microbiology, electrochemistry, material science and engineering (Wang and Ren 2013). BESs, such as microbial fuel cells (MFCs), have the potential to generate electricity by converting chemical energy from various dissolved organic materials, as found in industrial, agricultural and domestic wastewaters (Rozendal et al. 2008) through microbial metabolic oxidation in the anode chamber (see Figure 1.2).

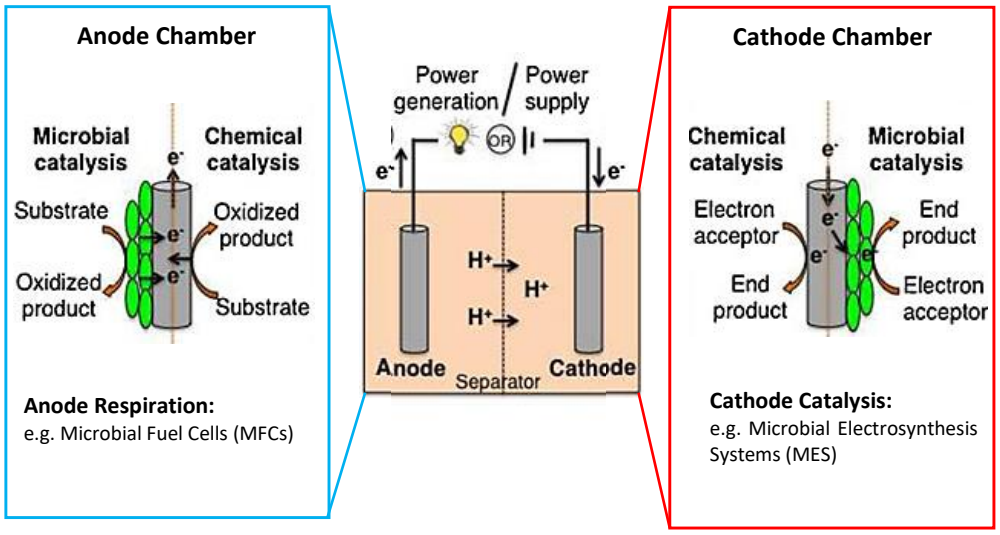

Figure 1.2. Overview of Bio-electrochemical systems (BES). Blue rectangle, Anode chamber with microbial respiration via substrate catalysis; Red rectangle, Cathode catalysis via microbial electrosynthesis. Image parts taken and amended from Patil et al. *(2012).*

Alternatively, electrons can also be accepted from the cathode to synthesise value-added organic compounds in microbial electrosynthesis cells [MESs] (Nevin et al. 2010). Due to the plasticity of BESs set-ups, a vast array of functions, beyond electricity production, is possible with ~47 different systems have been described so far ranging from bioremediation, water desalination, hydrogen production or other desired compounds such as ethanol, acetate and formate (Wang and Ren 2013).

1.4 Electromicrobiology: Exoelectrogens and Electroactive Biofilms

At the core of these technologies are a groups of electroactive bacteria (EAB's) called exoelectrogens which can form electrochemically active biofilms (EABfs) on electrode material. These EABfs are defined as microbial biofilms that exchange electrons with a conductive surface as illustrated in Figure 1.3 (Babauta et al. 2012).

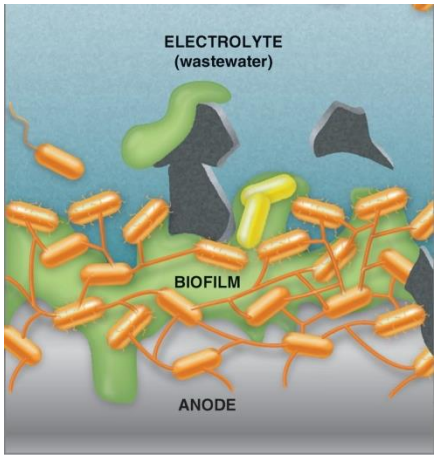

Figure 1.3 Schematic illustration of electrochemically active biofilm (EABf) attached to an anode. Image taken from (Logan and Rabaey 2012).

Many different bacterial species have been found to associate with electrodes. Mixed-species biofilms have been shown to produce high electrical conductivity (Malvankar et al. 2012a). However, only a few species have been isolated in pure culture with the ability to produce a high current density, which is not surprising considering that microbial attachment to mineral surfaces and their usage as final electron acceptors is omnipresent in natural environments and important for biogeochemical processes (Patil et al. 2012). Such as organisms include *Geobacter sulfurreducens* which can form a 40-50 μm thick biofilm (Bond et al. 2012) and has an electron transfer distance greater than 50 μm (Franks et al. 2010). In addition, a direct correlation between biofilm thickness and current production has been shown. Another prominent model

organism is facultative metal-reducing γ-proteobacterium *Shewanella oneidensis* MR-1 [SOMR-1] (Myers and Nealson 1988) which has been reported to form thinner biofilms (Franks et al. 2010).

1.4.1 *Microbial Extracellular Electron Transfer (EET)*

Model organisms, such as *G. sulfurreducens* and SOMR-1, have since been studied elucidate how these electroactive bacteria conduct electrons via electro-active biofilms in METs. Three modes of extracellular electron transfer (EET) to the electrode material are currently being proposed for anode respiring bacteria (ARB) as illustrated in Figure 1.4 (Kumar et al. 2012), i.e. directly through outer membrane cytochromes (OMC; Path 1), via pili or nanowires (Path 2) or via electron mediators (Path 3).

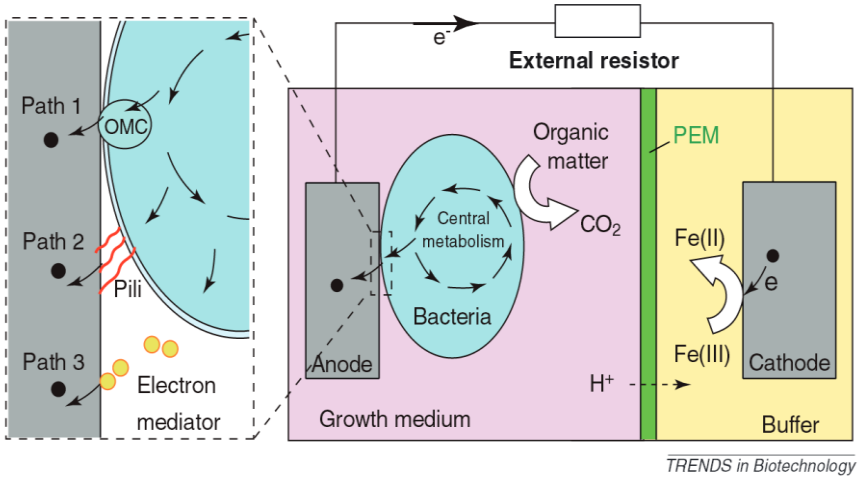

Figure 1.4. Working principles of a dual-chamber Microbial Fuel Cell (MFC) and direct and indirect electron transfer (DET; IET) mechanisms. Image taken from Qian & Morse (2011).

Figure 1.5 illustrated the three different pathways by which EAB have evolved to used different strategies to, either, donate electrons to external surfaces for the purpose of respiration (see Figure 1.5A), or alternatively, to accept electrons that can be channelled into the central metabolism (see Figure 1.5B). Three modes of electron

transfer to the electrode are currently proposed for anode respiring bacteria (ARB) in a BES set-up (Kumar et al. 2012; Patil et al. 2012):

- Direct electron transfer (DET; see section 1.4.1.1 and Figure 1.5, red box)
- Mediated electron transfer (MET; see section 1.4.1.2 and Figure 1.5, blue box)
- Indirect electron transfer (IET see section 1.4.1.3 and Figure 1.5, green box)

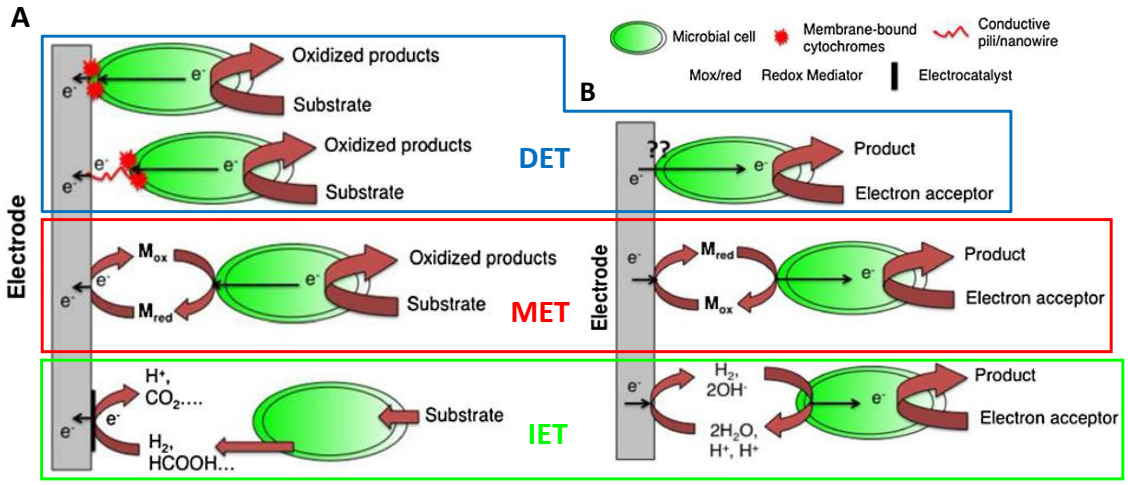

Figure 1.5. Electron Transfer Mechanisms. (A) EET from microorganism to electrode material; (B) EET from electrodes to microorganisms. DET, direct electron transfer; MET, mediated electron transfer; IET, indirect electron transfer. Images taken and amended from Patil et al. *(2012).*

1.4.1.1 *Direct Electron Transfer (DET)*

The molecular mechanisms of direct electron transfer (DET) have mainly been elucidated in metal-reducers and differ depending on environmental factors and between organisms. Currently, the understanding is that DET to electrodes is facilitated by outer-membrane bound proteins (OMPs) such as multihaeme c-type cytochromes which are both found in *Shewanella spp.* (Fredrickson et al. 2008) and *Geobacter spp.* (Methé et al. 2003; Busalmen et al. 2008). Additionally, conductive

extracellular filaments known as bacterial nanowires have also been shown to conduct electrons from (Gorby et al. 2006; Malvankar et al. 2012b; Boesen et al. 2013).

One of SOMR-1's major electron transfer pathway, the Mtr pathway (see section 4.1.1 for detailed pathway description), consists of an inner membrane tetraheme cytochrome, CymA, a periplasmic decahaeme cytochrome MtrA, an outer membrane β-barrel protein MtrB and the outer membrane decahaeme cytochromes OmcA and MtrC all of which enable direct EET to solid inorganic metals (Jensen et al. 2010).

There is still intensive debate around the physiological makeup and electron transfer mechanism of these nanowires. Whereas the nanowires in *G. sulfurreducens* are proposed to be type IV pili (Reguera et al. 2005) that conduct electrons through the aromatic amino acids of the PilA subunit (Vargas et al. 2013), the nanowires of SOMR-1 have just been identified to be outer membrane and periplasmic extensions that contain numerous multihaeme cytochrome complexes, rather than being based on pillin (Pirbadian et al. 2014). Furthermore, other metal containing proteins such as rusticyanin (Rus) of *Acidithiobacillus ferrooxidans* are being debated regarding their involvement in DET (Liu et al. 2011).

1.4.1.2 *Mediated Electron Transfer (MET)*

Mediated electron transfer MET via redox mediators, either exogenous or self-secreted, that shuttle electrons from cell to electrode and vice versa. This can be facilitated within the conductive extracellular biofilm matrix so-called nanowires, which are pilin nanofilaments with metallic-like conductivity properties, can transfer electrons to the electrode directly (Reguera et al. 2005; Franks et al. 2010; Malvankar

et al. 2011; Boesen et al. 2013). However, *G. sulfurreducens* and SOMR-1 nanowires are phylogenically (Reguera et al. 2005) and physically (Gorby et al. 2006) distinct.

In fact, flavins secreted by *Shewanella* (Marsili et al. 2008) account for 75% of EET to insoluble substrates (Kotloski and Gralnick 2013). Interestingly, *Geobacteraceae* do not secrete electron shuttling compounds or other small aromatic compounds (Nevin and Lovley 2000; Bond and Lovley 2003). Other mediators, like the redox-active antibiotic phenazine produced by *Pseudomonas spp.*, can also function as an electron carrier and have been shown to promote mineral reduction (Rabaey et al. 2005). In addition, chemicals such as neutral red (Park and Zeikus 2000), anthraquinone-2,6-disulfonate (AQDS), thionine, methyl viologen and methyl blue can also be utilised as added redox shuttles between cells and electrodes (Wang and Ren 2013).

1.4.1.3 *Indirect Electron Transfer (IET)*

Indirect electron transfer (IET) is facilitated by a range of microbial electron donors and acceptors, such as hydrogen, and secreted primary metabolites, such as formic acid. IET can be facilitated via soluble electron shuttles, also known as redox mediators. They can be transported or diffuse in and out of bacteria where they act as terminal electron acceptors, ultimately transporting electrons to the electrode. Examples include flavins, such as flavin mononucleotides (FMN) and other quinones produced by *Shewanella spp.* (Gorby et al. 2006; von Canstein et al. 2008; Okamoto et al. 2013). These account for 75% of EET in *SOMR-1* (Kotloski and Gralnick 2013).

In contrast to some mediators used in METs some of these electron shuttles can undergo an irreversible redox process when transferring electrons between EABs and

electrodes (Sydow et al. 2014). Furthermore, the redox-active antibiotic phenazine, produced by *Pseudomonas spp.* can function as electron carrier and have been shown to promote mineral reduction (Hernandez et al. 2004). In addition, chemicals such as neutral red, anthraquinone-2,6-disulfonate (AQDS), thionine, methyl viologen and methyl blue can also be utilised as redox mediators (Wang and Ren 2013).

1.4.1.4 *Reversible Electron Transfer*

Alternatively, electrons can be accepted by the microorganisms (see Figure 1.5B). However, the precise mechanisms have not been fully elucidated yet and knowledge is very limited. It is proposed that electrons can be accepted directly, as it has been shown that the Mtr pathway in *Shewanella* is reversible (Ross et al. 2011), but the precise mechanisms in other cathodic model organisms such as species of the Gram-positive genus of *Clostridium* are still unknown. As is the case with mediators, they can also function as an electron shuttle from electrode to microorganism. Further, H_2 can be produced at the cathode and oxidised by the microorganism and the electrons are fed into central metabolism (Patil et al. 2012).

1.5 Current Genetic Tools for Electroactive Model Organisms

Currently, the main model organisms of bio-electrochemical systems are SOMR-1 (Myers and Nealson 1988) and *G. sulfurreducens* (Caccavo et al. 1994). Both genomes have been sequenced (Heidelberg et al. 2002; Methé et al. 2003) which allowed for a detailed molecular and metabolic investigation and a systems-level analysis of *Shewanella* (Fredrickson et al. 2008). For these organisms, which are mainly used for the elucidation of EET and as a catalyst in the anode chamber of BES, there is only a limited number of genetic tools available (see Figure 1.6).

However, for other EABs that are used as cathodic catalysts in MES, such as *Clostridium spp.*, *Sporomusa spp.* and *A. ferrooxidans,* not only are genetic tools very limited (Sydow et al. 2014), but also the exact mechanisms of EET are yet unknown. First attempts to improve transformation efficiency in *C. ljungdahlii* have reported recently by Leang *et al.* (2013). For the acidophilic, obligate chemolithoautotrophic, Gram-negative *A. ferrooxidans* (Kelly and Wood 2000), however, which has a diverse metabolic network to oxidize several compounds such as sulphur and metals making it an important organism for bioleaching for the removal of heavy metal from sewage sludge (Murugesan et al. 2014), only a limited number of publications report successful genetic modification techniques (see Figure 1.6).

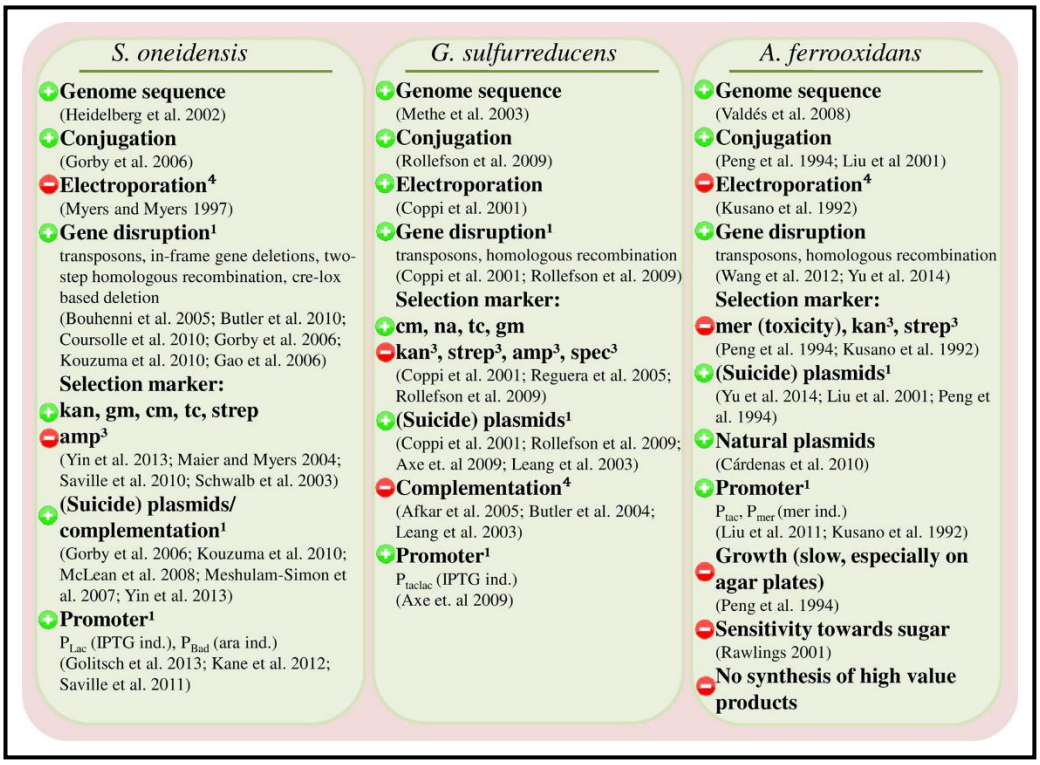

Figure 1.6 Overview of main genetic tools for SOMR-1, G. sulfurreducens, and A. ferrooxidans. kan kanamycin; strep, streptomycin; cm, chloramphenicol; na, nalidixic acid; tc, tetracyclin; spec, spectinomycin; amp, ampicillin; gm, gentamicin; neo, neomycin; clar, clarithromycin; tp, triamphenicol; mer, mercury; IPTG, isopropyl β-D-1-thiogalactopyranoside; ara, arabinose; ind., inducible; [1]examples, [2]unstable without selection pressure, [3]tolerance (antibiotic concentration >100 μg·ml-1), [4]inefficient. Image and legend taken from Sydow et al. (2014).

1.6 Synthetic Biology for Optimisation of Electroactive Microorganisms

The current bottleneck of METs is mainly the microbial efficiency of electron transfer. Recently, efforts have been made to overcome these existing limitations using synthetic biology approaches. Synthetic biology bio-engineering principles offer a starting point to accomplish this undertaking. Synthetic biology aims to use a rigorous engineering approach to design and build new standardised biological parts, devices and systems or to reconfigure existing ones to be more efficient or to carry out new functions (Kitney and Freemont 2012). However, to successfully apply these to enhance BES more genetic tools are needed for EAB model organisms

Jensen *et al.* (2010) successfully engineered a non-metal reducing *E. coli* strain by introducing a synthetic electron conduit, which bridges the cytosol to the extracellular space by using major components of the SOMR-1 *mtrCAB* electron transfer pathway allowing the reduction of inorganic. However, the resulting strain showed impaired cell growth and limited control of MtrCAB expression.

To overcome this, Ajo-Franklin's group then used an *E. coli* host with a more tuneable induction system (Goldbeck et al. 2013). Additionally, Goldbeck *et al.* demonstrated that minimal perturbations to cell morphology and MtrCAB expression are correlated with improved extracellular electron transfer and improved current production in *E. coli*. Albeit the modest efficiency of this engineered bacterial strain compared to naturally occurring dissimilatory metal-reducing bacteria, their work hallmarks the possibility to use a synthetic biology approach to introduce a molecularly defined extracellular electron transfer mechanism into another organism (Goldbeck et al. 2013).

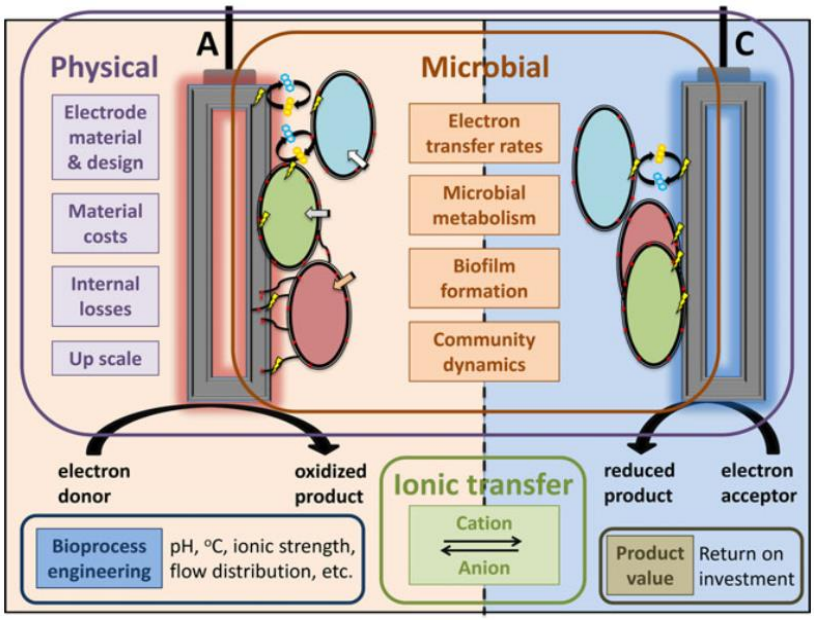

Figure 1.7 Central challenges for BES research and development in MES reactor. Left chamber (A) depicts bio-anode and bacterial biofilm transferring electrons to the anode by oxidative metabolism. Right chamber (C) shows bio-cathode and bacterial production of value-added products through reduction. Image taken from Rosenbaum & Franks (2013)

Even though tremendous breakthroughs in the past 2 decades have been made, there are central challenges (see Figure 1.7) that need to be overcome before BES technology can be effectively put to use (Rosenbaum and Franks 2014). Both fundamental research, to understand the molecular basis of electrogenic bacteria, and innovative novel approaches are needed to enhance these systems especially with regard to electron transfer rates, microbial metabolism, biofilm formations and physiology. Further, existing electron transfer systems do work, but the microorganisms used have not evolved to transfer electron effectively to anodes or from cathodes, therefore there is huge potential to genetically and metabolically engineer EABs to improve ET electrodes in BES (Sydow et al. 2014). One approach could be not only to elucidate remaining question of EET but also to design novel electrogenic bacteria using Synthetic Biology.

Synthetic biology aims to use a rigorous engineering approach to design and build new standardised biological parts, devices and systems or to reconfigure existing ones to be more efficient or to carry out new functions (Kitney and Freemont 2012). These bio-engineering principles offer methods of accomplishing engineering of electrogenic bacteria and could potentially allow increased predictability, stability and novel functionalities of BES applications for use in enclosed, controlled systems (Rosenbaum and Henrich 2014).

One approach is to use *E. coli* as a chassis for orthologous introduction of electron transfer pathways. Jensen *et al.* (2010) successfully engineered a non-metal reducing *E. coli* strain by introducing a synthetic electron conduit, that bridges the cytosol to the extracellular space by using major components of the SOMR-1 *mtrCAB* electron transfer pathway allowing the reduction of inorganic solids (see Figure 1.8). However, the resulting strain showed impaired cell growth and limited control of MtrCAB expression. To overcome this, Ajo-Franklin's group then used an *E. coli* host with a more tuneable induction system (Goldbeck et al. 2013). Additionally, Goldbeck *et al.* demonstrated that minimal perturbations to cell morphology and MtrCAB expression are correlated with improved extracellular electron transfer and improved current production in *E. coli*. Albeit the modest efficiency of this engineered bacterial strain compared to naturally occurring dissimilatory metal-reducing bacteria, their work hallmarks the possibility to use a synthetic biology approach to introduce a molecularly defined extracellular electron transfer mechanism into another organism (Goldbeck et al. 2013).

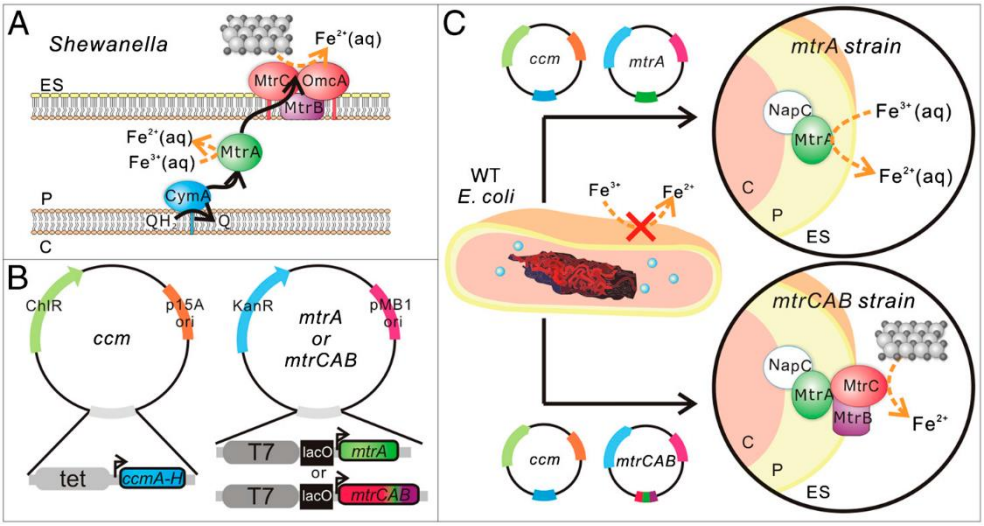

Figure 1.8 Engineering of a synthetic electron conduit in E. coli. (A) Schematic of proposed extracellular electron transfer pathway in Shewanella oneidensis MR-1. The silver and black spheres represent extracellular iron oxide. (B) Schematic of plasmids used to create the ccm, mtrA, and mtrCAB strains in E. coli. (C) Schematic of the engineered mtrA and mtrCAB strains for soluble and extracellular metal reduction. Image and legend taken from Jensen et al. (2010). ES, extracellular space; P, periplasm; C, cytoplasm

Another approach to improve BES is to tailor microbial interactions to electrode materials. Even though SOMR-1 can respire on more than 20 organic and inorganic compounds (Nealson and Scott 2006; Hau and Gralnick 2007), using gold anodes, which normally make an ideal material due to their high conductivity and resistance to oxidation, has failed with SOMR-1. To overcome this issue, Kane et al. (2013) successfully engineered a fusion protein to promote attachment of SOMR-1 to gold surfaces thereby providing a strategy to specifically immobilise bacteria to electrodes. However, the expression of the gold-binding peptide came at the cost of almost diminished levels of Mtr components and a decreased rate of riboflavin reduction, therefore highlighting the difficulties that still underline non-native pathway introduction in SOMR-1.

Other applications with electroactive bacteria also include using them for biosensors. Webster *et al.*(2014) developed a BES-based biosensor for the detection or arsenate by placing *mtrB* under the arsenic-inducible promoter (P_{ars}) in SOMR-1. This genetic circuit enabled the strain to have an increasing capacity to reduce Fe(III) to Fe(II) at increasing arsenate concentrations (40-100 μM) and ultimately produces increasing current in response to arsenate when inoculated in a BES.

In summary, there are distinct genetic tools available for EABs such as *Shewanella spp*. and *Geobacter spp*. but for other species, there are prominent restrictions when attempting to genetically modify these organisms. This emphasises the need for a standardised synthetic biology toolbox for a broad range of EABs to enable fine-tuning and enhancement of this technology.

1.7 Aims and Objectives

Even with the advances of the past years, the precise understanding electron transfer pathways and their molecular mechanisms in electroactive bacteria is still under debate. Furthermore, more genetic manipulation techniques are needed for the optimisation of EAB for industrial applications of BES technologies.

Expanding, synthetic biology toolbox for electroactive bacteria is essential to allow for increased predictability, stability and novel functionalities of BES applications. Given the lack of standardisation within Synthetic Biology and Electromicrobiology, I aimed to show that Standardised European Vector Architecture (SEVA) plasmids (Silvia-Rocha et al., 2013) can be used in the model organism *Shewanella oneidensis* MR-1.

Secondly, screening of electroactive bacteria still remains challenging with complex and large-sized reactors allowing for only a limited number of bacteria and settings to be tested. It was therefore aimed to establish screening methods for EABs that enable comparison of multiple engineered strains in parallel.

Combining these two outcomes will make it possible to not only genetically modify EABs quickly but also to test their EET capabilities effectively thereby advancing the field of electromicrobiology.

Therefore the key aims of this study were:

- The key aims in Chapter 3 were to establish a synthetic biology toolbox for SOMR-1 which included a plasmid platform, new inducible promoters and their verification suing novel reporter assays

- The key aims Chapter 4 were to establish and construct a new synthetic operon to increase SOMR-1 current output using novel miniaturised MFC technologies
- The key aim of Chapter 5 was establish a high-throughput screening assay of electroactive bacteria that can be used to identify enhanced EET phenotypes from transposon mutagenesis.

Chapter 2

2 MATERIALS AND METHODS

2.1 Materials

2.1.1 *Chemicals and Enzymes*

Unless otherwise stated, all chemicals and antibiotics were purchased from Sigma-Aldrich. All DNA restriction enzymes used, T4 DNA ligase (M0202), 50 bp and 100 bp DNA Ladder were purchased from New England Biolabs (NEB). 1 kb DNA ladder (G571A) was purchased from Promega. KOD Hot Start DNA Polymerase (71086) was purchased from Merck Millipore.

All kits, including QIAprep Spin Miniprep Kit (27104), QIAquick Gel Extraction Kit (28704), QIAquick PCR Purification Kit (28104), QIAamp DNA Mini Kit (51304), were bought from QIAGEN and used as per manufacturer's instructions; occasionally EZ-10 DNA Mini Spin Columns (SD5005, Bio Basic Inc.) were used instead of Qiagen columns. UltraPure™ Agarose and SYBR® Safe DNA Gel Stain (S33102) were purchased from Invitrogen. StrataClean resin (400714) was purchased from Agilent Technologies, Inc.

2.1.1.1 *Antibiotics*

A range of antibiotics was used in this study with different working concentrations for *E.coli* and SOMR-1, see Table 2.1.

Table 2.1 Antibiotics used and their working concentrations in E.coli and SOMR-1

Antibiotic	Solvent	Stock Concentration [mg·mL^{-1}]	Working Concentration	
			E.coli	SOMR-1
Ampicillin (Am)	dH_2O	50	50	–
Kanamycin (Km)	dH_2O	50	50	50/30
Chloramphenicol (Cm)	*EtOH*	40	40	20
Spectinomycin (Sp)	dH_2O	50	50	-
Tetracycline (Tc)	EtOH	5	5	5
Gentamicin (Gm)	dH_2O	10	10	10

dH_2O, deionized water; EtOH, ethanol.

2.1.2 *DNA Custom DNA Oligonucleotides and PCR Primers*

Single stranded DNA oligonucleotides and PCR Primers for cloning were designed using CLC Main Workbench software (QIAGEN Aarhus, version 7.7.1) and synthesised using either Integrated DNA Technologies or Eurofins Genomics.

2.1.3 *Bacterial Strains, Plasmids and Oligonucleotides*

The bacterial strains, plasmids and oligonucleotides used in this study are listed in Table 2.2, Table 2.3 and Table 2.4, respectively.

Table 2.2 List of Strains used in this study

Bacterial strains	**Relevant genotype**	**Source[a] or Reference**
Escherichia coli		
Invitrogen™ One Shot® TOP10 Chemically Competent	*F- mcrA Δ(mrr-hsdRMS-mcrBC) φ80lacZΔM15 ΔlacX74 recA1 araD139 Δ(ara-leu) 7697 galU galK rpsL (StrR) endA1 nupG λ-*	Life Technologies, C4040-10
E. cloni 10G Chemically Competent Cells >1x 10^9 cfu/µg	*F- mcrA Δ(mrr-hsdRMS-mcrBC) endA1 recA1 Φ80dlacZΔM15 ΔlacX74 araD139 Δ(ara,leu)7697galU galK rpsL nupG λ- tonA (StrR)*	Lucigen, 60107-2
DH5α-λ *pir*	*φ80dlacZΔ*M15 *Δ(lacZYA-argF)U196 recA1 hsdR17 deoR thi-1 supE44 gyrA96 relA1/λpir*	Miller and Mekalanos (1988)
WM3064	DAP[b] auxotroph donor strain for conjugation with SOMR-1; *thrB1004 pro thi rpsL hsdS lacZ M15 RP4-1360 (araBAD)567 dapA1341::[erm pir(wt)]*	(Saltikov and Newman 2003)
C118 *pir*	*phoA*$^-$; pSEVA host	(Silva-Rocha et al. 2013)
BL-21	*F2 ompT hsdSB(rB 2mB 2) gal dcm (DE3)*	Lab stock
Shewanella oneidensis		
MR-1	wild type; isolated from Lake Oneida, NY	NCIM14063[a]
MR-1 / JG274	*S. oneidensis* MR-1, wild type	(Myers and Nealson 1988)
JG665	*S. oneidensis MR-1*, ΔPEC (periplasmic electron carriers: Δ*mtrA*, Δ*mtrD*, Δ*cctA*, Δ*dmsE*, and Δ*SO4360*)	(Coursolle et al. 2010)
Δ*bfe*	*S. oneidensis MR-1*, Δ*bfe*	(Kotloski and Gralnick 2013)
JG686	*S. oneidensis MR-1*, Δ*fccA*	(Ross et al. 2011)
JG700	*S. oneidensis MR-1*, Δ*mtrB*	(Coursolle et al. 2010)
JG730	*S. oneidensis* MR-1, Δ*mtrA*	(Coursolle et al. 2010)
JG1064	*S. oneidensis* MR-1, Δ*cymA*	(Ross et al. 2011)

[a]NCIMB, National Collection of Industrial Food and Marine Bacteria, UK, available at:

https://www.ncimb.com/ (last accessed 7th May 2019. [b]DAP, di-aminopimelic acid

Table 2.3 List of plasmids used in this study

Plasmid	Description	Source, GenBank accession number or Reference
pSEVA		SEVA Collection, Madrid[3] (Silva-Rocha et al. 2013; Martinez-Garcia et al. 2014)
221	Km^R, $oriV_{RK2}$, MCS	JX560327
231	Km^R, $oriV_{pBBR1}$, MCS	JX560328
234	Km^R, $oriV_{pBBR1}$, $P_{trc/lacIq}$	KC847292
241	Km^R, $oriV_{ColEI}$, MCS	JX560329
251	Km^R, $oriV_{RSF1010}$, MCS	JX560330
261	Km^R, $oriV_{p15A}$, MCS	SEVA Collection, Madrid[4]
271	Km^R, $oriV_{pSC101}$, MCS	This study
281	Km^R, $oriV_{pUC}$, MCS	SEVA Collection, Madrid[5]
291	Km^R, $oriV_{pBBR322/ROB}$, MCS	This study
321	Cm^R, $oriV_{RK2}$, MCS	JX560332
331	Cm^R, $oriV_{pBBR1}$, MCS	JX560333
341	Cm^R, $oriV_{ColEI}$, MCS	JX560334
351	Cm^R, $oriV_{RSF1010}$, MCS	JX560335
621	Gm^R, $oriV_{RK2}$, MCS	JX560347
631	Gm^R, $oriV_{pBBR1}$, MCS	JX560348
641	Gm^R, $oriV_{ColEI}$, MCS	JX560349
651	Gm^R, $oriV_{RSF1010}$, MCS	JX560350
661	Gm^R, $oriV_{p15A}$, MCS	This study
pSEVA234::lacZ	Km^R, $oriV_{pBBR1}$, $P_{trc/lacIq}$ → *lacZ*	This study
pSEVA23::Ptet/TetR	Km^R, $oriV_{pBBR1}$, $P_{Tet/tetR}$	This study
pSEVA23::Ptet/TetR::lacZ	Km^R, $oriV_{pBBR1}$, $P_{Tet/tetR}$→ *lacZ*	This study
pSEVA2311	Km^R, $oriV_{pBBR1}$, $P_{ChnB/ChnR}$	(Benedetti et al. 2016b)
pSEVA2311::lacZ	Km^R, $oriV_{pBBR1}$, $P_{ChnB/ChnR}$→ *lacZ*	This study
pZJ56b	Km^R, $oriV_{ColEI}$, P_{J23119}→ *gfp*	Lab stock
pZJ56b::phiLOV_SO	Km^R, $oriV_{ColEI}$, P_{J23119}→ *phiLOV(SO)*	Lab stock
pZJ7::phiLOV_SO_opt	pBAD (Cm^R, $oriV_{p15A)}$, P_{ara}→ *phiLOV(SO)*	Lab stock
pBBR1	Km^R, $oriV_{pBBR1}$, MCS	(Kovach et al. 1995)
pBBR1::phiLOV	Km^R, $oriV_{pBBR1}$, P_{J23119}→ *phiLOV(SO)*	This study
pBAD33	Cm^R, $oriV_{p15A}$, P_{ara}	Lab stock
pBAD33::T7RNP	Cm^R, $oriV_{p15A}$, P_{ara}→ T7RNAP	This study
pSEVA23::PT7::phiLOV	Km^R, $oriV_{pBBR1}$, P_{T7}→ phiLOV	This study
pSEVA26::P_{bfe}::phiLOV	Km^R, $oriV_{p15A}$, P_{ara}→ phiLOV	This study

[3] http://seva.cnb.csic.es/?page_id=17 (last accessed 6th May 2019)
[4] http://wwwuser.cnb.csic.es/~seva/wp-content/uploads/docs/gbk/pSEVA261.gbk/ (last accessed 6th May 2019)
[5] http://wwwuser.cnb.csic.es/~seva/wp-content/uploads/docs/gbk/pSEVA281.gbk (last accessed 6th May 2019)

pSEVA23::Ptet/TetR::bfe::ushA	Km^R, $oriV_{pBBR1}$, $P_{tet/TetR}$ → *bfe/ushA*	This study
pSEVA2311::bfe::ushA	Km^R, $oriV_{pBBR1}$, $P_{ChnB/ChnR}$ → *bfe/ushA*	This study
pSEVA234:: bfe::ushA	Km^R, $oriV_{pBBR1}$, $P_{trc/lacIq}$→*bfe/ushA*	This study
pYYDT-C5	Km^R, $P_{trc/lacIq}$→*ribADEHC*	Hao Song, personal communications (Yang et al. 2015)
pSYedQ	Km^R, $oriV_{pBBR1}$, $P_{ChnB/ChnR}$→ *yedQ*	(Benedetti et al. 2016a)
pSYhjH	Km^R, $oriV_{pBBR1}$, $P_{ChnB/ChnR}$→ *yhjH*	(Benedetti et al. 2016a)

MCS, multiple cloning site; oriV, origin of replication.

Table 2.4 List of oligonucleotides used in this study

Name	**Sequence 5' to 3'[a,b]**	**Notes**
AvrII-RBS-lacZ FWD	GGTGGTCCTAGG*AAAGAGGAGAAA*TACTAGATGAC	Amplification primers
	CATGATTACGGATTCACTGG	
SalI-lacZ REV	ACCACCGTCGACTTATTTTTGACACCAGACCAACT	
	GG	
NheI – buffer FWD	GGTGGTGCTAGCTTTTTCCTCCTTATAAAGTTAAT	
	C	
AvrII-ptet-R24-xhol-	ACCACCCCTAGGGTGCTCAGTATCTCTATCACTGA	
Buffer REV	TAGGGATGTCAATCTCTATCACTGATAGGGATCCT	
	GTGTGAAATTGTTATCCGCTCTCGAGGTTTGACAG	
	CTTATCATCG	
NheI – FWD	GGTGGTGCTAGCATGTCCAGATTAGATAAAAG	
SalI-PacI-TetR REV	ACCACCGTCGACTTAATTAATTATTAAGCTACTAA	
	AGCG	
PT7_EcoRI-Xhol	GGTGGTGAATTCTAATACGACTCACTATAGGGAG	
FWD	ACTCGAG*CACCCATATCTTTACTCTAAGGCTAGGAAA*	
	*C*CATATGATCGAGAAAAGCTTCG	
phiLOV-XbaI REV	ACCACCTCTAGATTAAACATGATCGCTACC	
SacI -T7 RNAP-	GGTGGTGAGCTCATGAACACGATTAACATCGC	
FWD		
T7 RNAP-Xbal REV	ACCACCTCTAGATTACGCGAACGCGAAG	
P_{bfe} *- SacI FWD*	GGTGGTGAGCTCCTATGAACTCTCCTAATGATTTA	
	ATG	

P_{bfe} XbaI-NdeI REV	ACCACCTCTAGACATATGGGAGAAAATAGTGCCTTGTTTGCG	
PC_UF_bfe	GCCGAATTCTCTAGAGAAAGAGGAGAAATACTAGATGAAAGAC	Paperclip oligos
PC_UR_bfe	TTTCATCTAGTATTTCTCCTCTTTCTCTAGAGAATTC	
PC_DF_bfe	AACCGCCGACACCCTTTAGTACTAGTAGCGGCCGCTGCAG	
PC_DR_bfe	GGCCTGCAGCGGCCGCTACTAGTACTAAAGGGTGTCGGCG	
PC_UF_ushA	GCCGAATTCTCTAGAGAAAGAGGAGAAATACTAGATGACAAAT	
PC_UR_ushA	TGTCATCTAGTATTTCTCCTCTTTCTCTAGAGAATTC	
PC_DF_ushA	TAAGATTACAGCGAAGTAATACTAGTAGCGGCCGCTGCAG	
PC_DR_ushA	GGCCTGCAGCGGCCGCTACTAGTATTACTTCGCTGTAATC	
PC_UF_ushA_56bp	GCCGAATTCTCTAGAGAAAGAGGAGAAATACTAGATGACAAATATGCTTATTAAAGG	
PC_UF_cymA_60bp	GCCGAATTCTCTAGAGAAAGAGGAGAAATACTAGATGAACTGGCGTGCACTATTTAAACC	
PC_UF_cymA	GCCGAATTCTCTAGAGAAAGAGGAGAAATACTAGATGAACTGG	
PC_UR_cymA	GTTCATCTAGTATTTCTCCTCTTTCTCTAGAGAATTC	
PC_DF_cymA	CCCCTATCCAAAAGGATAATACTAGTAGCGGCCGCTGCAG	
PC_DR_cymA	GGCCTGCAGCGGCCGCTACTAGTATTATCCTTTTGGATAG	
PC_UF_ribF_56bp	GCCGAATTCTCTAGAGAAAGAGGAGAAATACTAGATGGAATTAATCCGCGGTATAC	
PC_UF_ribF	GCCGAATTCTCTAGAGAAAGAGGAGAAATACTAGATGGAATTA	
PC_UR_ribF	TTCCATCTAGTATTTCTCCTCTTTCTCTAGAGAATTC	

PC_UF_ribF_56bp	GCCGAATTCTCTAGAGAAAGAGGAGAAATACTAG ATGGAATTAATCCGCGGTATAC
PC_DF_ribF	TGGTAACGATGCAGGCTGATACTAGTAGCGGCCG CTGCAG
PC_DR_ribF	GGCCTGCAGCGGCCGCTACTAGTATCAGCCTGCA TCGTTA
PC_UF_ribE_59bp	GCCGAATTCTCTAGAGAAAGAGGAGAAATACTAG ATGAACGTAGTTCAAGGTAATATCG
PC_UF_ribE	GCCGAATTCTCTAGAGAAAGAGGAGAAATACTAG ATGAACGTA
PC_UR_ribE	GTTCATCTAGTATTTCTCCTCTTTCTCTAGAGAATT C
PC_DF_ribE	GCTTGAACAACAGTTGTAATACTAGTAGCGGCCG CTGCAG
PC_DR_ribE	GGCCTGCAGCGGCCGCTACTAGTATTACAACTGTT GTTCA
PC_UF_cctA_59bp	GCCGAATTCTCTAGAGAAAGAGGAGAAATACTAG GTGAGCAAAAAACTATTAAGTGTGC
PC_UF_cctA	GCCGAATTCTCTAGAGAAAGAGGAGAAATACTAG GTGAGCAAA
PC_UR_cctA	GCTCACCTAGTATTTCTCCTCTTTCTCTAGAGAAT TC
PC_DF_cctA	GTCTGTTCTGAAGAAGTAATACTAGTAGCGGCCG CTGCAG
PC_DR_cctA	GGCCTGCAGCGGCCGCTACTAGTATTACTTCTTCA GAACA
PC_UF_fccA_60bp	GCCGAATTCTCTAGAGAAAGAGGAGAAATACTAG ATGTTCACAAGAAAGATTCAAAAAAC
PC_UF_fccA	GCCGAATTCTCTAGAGAAAGAGGAGAAATACTAG ATGTTCACA
PC_UR_fccA	GAACATCTAGTATTTCTCCTCTTTCTCTAGAGAAT TC
PC_DF_fccA	ATTCGCTAAAGATAATTAATACTAGTAGCGGCCG CTGCAG
PC_DR_fccA	GGCCTGCAGCGGCCGCTACTAGTATTAATTATCTT TAGCG
PC_UF_TetR-Ptet	GCCTTATTAAGCTACTAAAGCGTAGTTTTCGTCGT TTGCAGCG

PC_UR_TetR-Ptet	TGCAAACGACGAAAACTACGCTTTAGTAGCTTAA TAA	
PC_DF_TetR-Ptet	TGACATCCCTATCAGTGATAGAGATACTGAGCAC CCTAGG	
PC_DR_TetR-Ptet	GGCCCTAGGGTGCTCAGTATCTCTATCACTGATAG GGATG	
PC_UF_PChnB/R	GCCTCAAAAAACAATAGAGGAGACTGAATTTTCA GACACGAGA	
PC_UR_PChnB/R	CGTGTCTGAAAATTCAGTCTCCTCTATTGTTTTTTG A	
PC_DF_PChnB/R	AGTGCAGATTTTGAATAAATTCACATGTCGTAATC CTAGG	
PC_DR_PChnB/R	GGCCCTAGGATTACGACATGTGAATTTATTCAAA ATCTGC	
PC_UF_PChnB	GCCGCAACTAAAAGAGATTGTTTGGATCAGTTAC CCAAAATCG	Paperclip linker
PC_UR_PChnB	TTTTGGGTAACTGATCCAAACAATCTCTTTTAGTT GC	
pMH_rev_p23119_speI	ACCACCACTAGTGAATTGACGCGTCGAATTAATT CCGCGAACCCCAG	pminiHimar primers
pMH_fwd_p23119	TTGACAGCTAGCTCAGTCCTAGGTATAATGCTAGC GAGCTCGGGTATCGCTCTTGAAGG	

FWD, forward; REV, reverse. [a]RBS in italics. [b]restriction site or scar for paperclips is highlighted in grey

2.1.4 *Designing of Ribosomal Binding Sites (RBS) for SOMR-1*

To design SOMR-1 specific ribosomal binding sites (RBS) the RBS Calculator 2.0 was used.[6]

2.1.5 *DNA Sequencing*

Sanger DNA sequencing (Sanger et al. 1977) was performed by DNA Sequencing and Services, University of Dundee, Dundee, UK.

[6] https://www.denovodna.com:4433/ (last accessed 7th May 2019)

2.1.6 *Molecular weight markers and DNA ladders*

DNA ladders used in this work were the 1 kb DNA Ladder (Promega, #G571A), the 50 bp DNA Ladder (New England Biolabs, #N3236L) and the 100 bp DNA Ladder (New England Biolabs, #N3231L), the different band size fragments as run on agarose gel are shown in Figure 2.1.

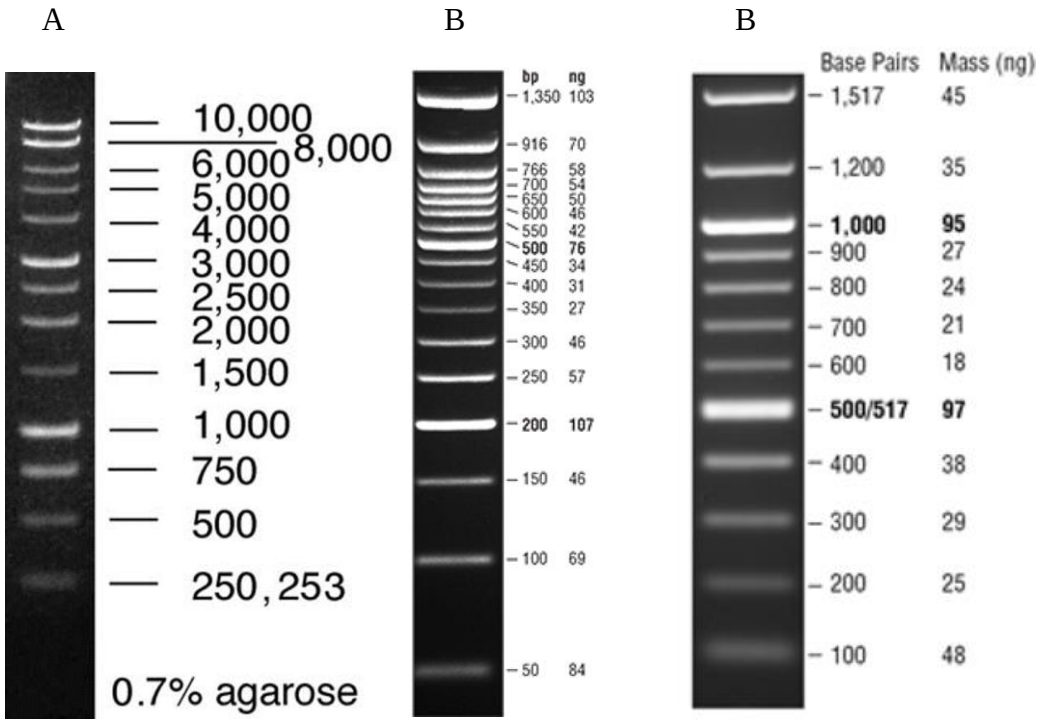

Figure 2.1 DNA ladders used in this work. (A) 1kb DNA Ladder (Promega, #G571A). (B) 50 bp DNA Ladder (New England Biolabs, #N3236L). (C) 100 bp DNA Ladder (New England Biolabs, #N3231L).

2.1.7 *Media*

All media was prepared with dH_2O and the pH was adjusted to 7.0 - 7.2 for all recipes with either 5M NaOH and 37% (v/v) HCl prior to autoclaving (121°C for 20 min) unless otherwise stated. If required, media were supplemented with appropriate antibiotics (Table 2.1). When required, media were solidified with 1.5% (w/v) agar.

2.1.7.1 *Lysogeny Broth Medium*

Lysogeny Broth (LB) medium was prepared as follows using the Miller variation:

10g Bacto-tryptone

5g yeast extract

10g NaCl

per litre dH20

pH adjusted to 7.5

(15 g agar for solid medium)

2.1.7.2 *Shewanella Basal Medium (SBM)*

Shewanella basal medium (SBM) was prepared per litre as stated below. Prior ro sterilisation, the medium was sparged with N2 gas that and adjusted to pH 7.2, and then autoclaved. After autoclaving, filter sterilised vitamin and mineralmix, as well as casamino acids were added, in addition to electron acceptor and donors, i.e. sodium fumarate and lactate.

0.46 g NH_4Cl

0.225 g K_2HPO_4

0.225 g KH_2PO_4

0.117g $MgSO_4 \cdot 7H_2O$

0.225 g $(NH_4)_2SO_4$

5 ml mineral mix

5 ml vitamin mix

100 mM HEPES

After sterilisation:

5 ml mineral mix (see 2.1.8.1)

5 ml vitamin mix (see 2.1.8.2)

0.05% (w/v) casamino

15 mM sodium lactate

40 mM sodium fumarate

2.1.7.3 *Lactate Medium (LM) for Biofilm Assays*

Lactate medium (LM) was prepared per litre as follows and components sterilised as for SBM: 10 mM HEPES, 100 mM NaCl, 0.02% yeast extract, 0.01% peptone, and 0.5 mM, 5 mM, or 15 mM lactate, respectively, as per desired experiment. The pH was adjusted to 7.3 (Gödeke et al. 2011a).

2.1.8 *Buffers*

The following buffers were used to supplement media or in assays:

2.1.8.1 *SBM Mineral Mix*

SBM mineral mix was prepared containing following per liter

1.5 g Nitrilotriacetic acid (NTA)

0.1 g $MnCl_2$ $4H_2O$

0.3 g $FeSO_4 \cdot 7H_2O$

0.17 g $CoCl_2 \cdot 6H_2O$

0.1 g $ZnCl_2$

0.04 g $CuSO_4 \cdot 5H_2O$

0.005 g $AlK(SO_4)2 \cdot 12H_2O$

0.005 g H_3BO_3

0.09g Na_2MoO_4

0.12 g $NiCl_2$

0.02 g NaWO4·2H2 O

0.10 g Na_2SeO_4

2.1.8.2 *SBM Vitamin Mix*

SBM vitamin mix was prepared containing the following per liter:

0.002 g biotin

0.002 g folic acid

0.02 g pyridoxine HCl

0.005 g thiamine

0.005 g nicotinic acid

0.005 g pantothenic acid

0.0001 g of B-12

0.005 g of p-aminobenzoic acid

0.005 g of thioctic acid

2.1.8.3 *CPH Z-Buffer*

Cold Spring harbour laboratory (CPH) Z-Buffer was prepared containing as listed below per liter H_2O. The pH was adjusted to 7.0 with 1M Na_2HPO_4/ NaH_2PO_4 stock solution and stored at 4°C.

8.518 g Na_2HPO_4 (0.06M)

4.775 g NaH_2PO_4 (0.0398M)

0.75 g KCl (0.01M)

0.246 g $MgSO_4 \cdot 7H_2O$

2.7 mL β-mercaptoethanol (*NB only added immediately prior to experiment)*

2.1.8.4 *10 % SDS Stock Solution*

Sodium Sodecyl Sulfate (SDS) Stock Solution at 10% (w/v) was prepared by dissolving 10 g of electrophoresis-grade SDS in 90 mL of H_2O and then heated to 68°C while being stirred with a magnetic stirrer to assist dissolution. If necessary, pH was adjusted t to 7.2 by adding a few drops of concentrated HCl. Finally, the total volume was made up to 100 mL.

2.1.8.5 *1M $Na_2 \cdot CO_3$ Stock Solution*

To make 1M Na2·CO3 stock solution 10.6 g of anhydrous Na_2Co3 was dissolved in 100 mL of dH_2O.

2.1.8.6 *1X ONPG Solution*

To make2.1.8.6 1X Ortho-Nitrophenyl-β-galactoside (ONPG) solution, ONPG was dissolved at a concentration of 4 mg/mL in 0.1 M phosphate buffer (pH 7.5).

2.2 Methods

2.2.1 *Bacterial Propagation*

Strains purchased from culture collections (i.e. NCIMB) were revived from freeze-dried condition following provided instructions and media recipes (see 2.1.7).

E. coli strains used in this study (Table 2.2) were cultivated in LB medium at 37°C. For strain WM3064, 2,6-diaminopimelic acid (DAP) was added to the medium to a final concentration of 300 µM (Gödeke et al. 2011b). For propagation, SOMR-1 was grown aerobically in LB medium at 30°C, depending on protocol at 225 rpm. For electrochemical analysis, SOMR-1 was grown anaerobically in SBM supplemented with additional carbon source, e.g. sodium lactate.

Stock cultures were stored at -80°C using 7 % dimethyl sulfoxide (DMSO) as cryo-protectant for *E.coli* and SOMR-1.

2.2.2 *Bacterial Strain Construction*

In this study bacterial strains were transformed chemically, by electroporation or using conjugation as describes in section 2.2.2.1 for *E. coli* strains and section 2.2.2.2 for SOMR-1.

2.2.2.1 *Strain Construction E. coli*

Replicative plasmids were introduced into *E. coli* by transformation using chemically competent cells.

2.2.2.1.1 *Transformation of E. coli*

Competent *E. coli* cells are prepared and transformed according to Chris French's[7] protocol and an adaptation of (Green et al. 2012). In brief, bacterial cells were made competent and stored in 1 x transformation and storage (TSS) solution (17 mL LB broth, 5 mL 40% (w/v) PEG 3350, 1 mL 1 M $MgCl_2$, 1 mL DMSO). To transform, cells were briefly thawed on ice, 10 ng plasmid DNA added and incubated on ice for 30-60 min. Cells were then heat-shocked at 42°C for 90 s and further incubated on ice for 90 s. Immediately after, preheated LB recovery medium was added and cells were incubated at 37°C for 1 h at 200 rpm. Finally, cells were plated onto LB agar plates containing the appropriate antibiotic to select plasmid-bearing transformants.

2.2.2.1.2 *Transformation of Commercial Chemically Competent E. coli*

Invitrogen™ One Shot® TOP10[8] or E. cloni® 10G[9] (Lucigen) Chemically Competent *E.coli* cells were transformed according to manufacturer's protocol.

2.2.2.2 *Strain Construction of SOMR-1*

Replicative plasmids were introduced into *SOMR-1* by transformation, electroporation or conjugations as described in the following sections.

2.2.2.2.1 *Electroporation of SOMR-1*

Protocol was performed and adapted according to (Myers and Myers 1997a). A 2 mL overnight culture of SOMR-1 from a single colony was used to inoculate 50 mL LB in a 500 mL flask and aerobically grown to mid-log phase (OD_{600} 0.4) at

[7] http://openwetware.org/wiki/Cfrench:compcellprep1; last accessed 19.08.2014
[8] https://assets.thermofisher.com/TFS-Assets/LSG/manuals/oneshottop10_man.pdf; last accessed 07.05.2019
[9] https://www.lucigen.com/docs/manuals/MA010-Ecloni-10G-Chem-Comp.pdf; last accessed 07.05.2019

30°C/225 rpm. Aliquots of 1 mL SOMR-1 culture were centrifuged for 1 min at 12000 g in 1.5 ml microfuge tubes, washed once in 330 µL and resuspended in 40 µL 1M D-sorbitol (pH 7.59). Cells were placed on ice and used within 15 min of preparation. Approximately 0.1-0.5 µg of plasmid DNA was added to iced SOMR-1 cells and then transferred in a pre-cooled 0.1 cm electro cuvette (Bio-Rad Laboratories Ltd, UK). Cells were electroporated at 200 Ω resistance; 25 µFD capacitance; 0.55 kV voltage (BioRad Gene PulserTM with Pulse Controler). After electroporation, 500 µL LB broth was immediately added to the cuvette and cells were transferred into 1.5 mL tube and incubated for 1 h at 30°C / 225 rpm. Finally, cultures were centrifuged for 1 min at 12000 g and resuspended in residual 200 µL of media. Transformants were selected by plating cells on LB agar plates with appropriate antibiotic selection and incubated overnight at 30°C static incubation.

2.2.2.2.2 *Conjugation of SOMR-1*

E. coli WM3064 was used as the conjugal donor strain for mating with SOMR-1. Conjugation was performed as described in (Paulick et al. 2015). In brief, the plasmid of interest was transformed into *E. coli* WM3064 as described above by chemical transformation and 1 mL of each donor and recipient overnight culture were centrifuged for 1 min at high speed and washed three times with LB media to remove residual antibiotics from inoculation media. Cell pellets were resuspended together in 250 µL of fresh LB media. The entire suspension was plated onto an LB plate containing 300 µM DAP and without antibiotics, and incubated at 30°C for 6-12 h. A loopful of cells were collected and were resuspended and washed three times in 2 mL LB media to remove any residual DAP to prevent further propagation of the donor strain. To select for SOMR-1 transconjugants, 50 µL of the washed 2 mL suspension

was plated on LB agar plates containing appropriate antibiotic without DAP to counter-select against donor cells and incubated at 30°C for 12-16 h statically.

2.2.2.2.2.1 Conjugation Frequency Determination

To determine the conjugation frequency between *E. coli* strain WM3064 harbouring various plasmids and SOMR-1 the protocol as described in section 2.2.2.2.2 was altered as follows: 500 µL overnight culture of recipient and donor strains were prepared as described above and plated onto a sterile 0.45 µm Millipore S-Pak Filters (HAWG047S6) which was positioned on an LB agar plate containing 300 µM DAP, without antibiotics, and incubated at 30°C for 6 h. After incubation, the filter paper was transferred into 50 mL falcon tube with 1.5 mL LB and cells were resuspended via vortexing until fully immersed. The cell suspension was washed 3x times in LB media to remove residual DAP. Serial dilutions of donor, recipient and transconjugants were prepared and plated in triplicate to determine the colony forming unit (cfu) per mL (cfu/mL).

2.2.3 *Plasmid Maintenance Determination*

Stability of plasmid maintenance during bacterial growth was determined by culturing SOMR-1 harbouring pSEVA plasmids containing the kanamycin resistance cassette and varying oriV cassettes (pSEVA2X1; where X represents a different oriV) (Silva-Rocha et al. 2013; Martinez-Garcia et al. 2014).

SOMR-1 strains were streaked out on LB agar containing 50 µg/mL Km from -80°C stock and grown overnight at 30°C in a static incubator. Single colonies were used to inoculate biological triplicates in 10 mL LB also containing Km as above. Overnight cultures were washed twice with SBM to remove residual antibiotics. Fresh LB media

containing no antibiotics was inoculated with washed cells to a final OD_{600} of 0.05 using glass tubes with butyl stoppers. After 24 h of shaking incubation at 200 rpm in 30°C and serial dilutions of culture were plated onto new LB agar plates containing 50 µg/mL Km and LB agar only plates and incubated overnight. The plasmid-containing fraction was calculated by dividing the number of SOMR-1 cfu on antibiotic selection and cfu without antibiotic selection.

2.2.4 *Nucleic Acid Manipulation and Detection Methods*

2.2.4.1 *DNA Purification*

Plasmid DNA was purified using QIAGEN QIAprep spin miniprep kit. Genonic DNA was purified using the QIAGEN DNeasy blood & tissue kit. Total DNA was extracted from bacterial cells using the QIAGEN QIAamp DNA Mini kit. Linearised DNA from PCR amplification was purified with the QIAGEN QIAquick PCR. Linearised DNA cut from agarose gels was purified with the QIAquick gel extraction kit. All purifications were performed according to manufacturer specifications and DNA was eluted in either AE buffer or dH_2O.

2.2.4.2 *Agarose Gel Electrophoresis*

Agarose gels were made from UltraPure™ Agarose (Thermo Fisher) and TAE buffer ranging from 0.8% to 4% (w/v) depending on DNA size and stained with SYBR Safe DNA Gel Stain (Thermo Fisher). Agarose gel electrophoresis was performed using BioLab RunOne for nucleic acids system at either 25 V, 50 V or 100 V depending on desired speed and fragment sizes.

2.2.4.3 *Restriction Enzyme Digest*

Restrictions reactions for screening and cloning of vectors were set up using the recipes in Table 2.5. Restriction Enzyme Digest for Screening of Cloning VectorsTable 2.5 and Table 2.6, respectively.

Table 2.5. Restriction Enzyme Digest for Screening of Cloning Vectors

Plasmid DNA	5 µl
NEB Buffer 10X	2 µl
NEB Enzymes	1 µl (each)
Nuclease-free water	11 µl
Total Volume	**20 µl**

Table 2.6. Restriction Enzyme Digest for Ligation Cloning

Plasmid DNA (2 µg)	Y µl
NEB Buffer 10X	10 µl
NEB Enzymes	2 µl (each)
Nuclease-free water	X µl
Total Volume	**100 µl**

Y, volume required to add 2 µg od plasmid DNA; X, volume of water required to make up the total volume of 100 µl.

2.2.4.4 *Ligation*

Ligations reactions were set up with overnight digested and purified vector and insert DNA using NEB T4 ligase and the reaction mix stated in Table 2.7. Unless otherwise

stated 50 ng of vector DNA was used and the mass of insert required at insert-vector ratio of 1:3 was calculated using the NEB ligation calculator[10] using Equation 1.

Equation 1. Determination of DNA Insert Mass

$$required\ mass\ insert\ (g) = \frac{desired\ insert}{vector\ molar\ ratio\ \cdot\ mass\ of\ vector\ (g) \cdot\ ratio\ of\ insert\ to\ vector\ lengths}$$

Table 2.7. T4 DNA Ligase Reaction

Component	Quantity
10X T4 DNA Ligase Buffer*	2 µl
Vector DNA	50 ng
Insert DNA	Y ng
Nuclease-free water	to 20 µl
T4 DNA Ligase	1 µl
Total Volume	**20 µl**

Y, insert vector mass as calculated using Equation 1

In brief, the reaction was mixed by pipetting up and down and microfuged for 30s. The reaction was incubated at 16ºC overnight and 5µL transformed into competent *E. coli* the next day.

[10] http://nebiocalculator.neb.com/#!/ligation

2.2.4.5 *Polymerase Chain Reaction*

To amplify linear double stranded DNA fragments the following standard reaction setup (see Table 2.8) and cycling conditions (see Table 2.9) for KOD Hot Start Polymerase were used unless otherwise stated.

Table 2.8 PCR Reaction Setup

Component	Volume	Final Concentration
10x KOD Buffer	5 µl	1x
25 mM $MgSO_4$	3 µl (3.5)	1.5 mM or 1.75 mM
dNTPs (2 mM each)	5 µl	0.2 mM (each)
Nuclease-free Water	X µl	
Forward Primer (10 µM)	1.5 µl	0.3 µM
Reverse Primer (10 µM)	1.5 µl	0.3 µM
Template DNA (100 ng genomic DNA, 10 ng plasmid DNA)	Y µl	
KOD Hot Start DNA Polymerase (1 U/µl)	1 µl	0.02U/µl
Total reaction volume	**50 µl**	

Table 2.9 PCR Cycling Conditions

	Temperature	Time
1. Polymerase activation	95°C	3 min
2. Denature	95°C for 20 s	20 s
3. Annealing	Lowest Primer Tm°C	10 s
4. Extension	70°C	10-25 s/kb
Step 2-4	30x cycles	
5. Final Extension	70°C	5 min

Tm, melting temperature; kb, kilobase pair.

2.2.4.6 *Colony PCR Screening*

To screen bacterial strains containing cloned vectors colony PCR was performed. A small amount of a single bacterial colony was transferred into 10 µl dH_2O, in parallel to re-streaking onto a fresh agar plate and then heated to 100ºC for 10 min to lyse cells, centrifuged briefly to remove cell debris and 1 µl of DNA-containing supernatant was added as template to the PCR reaction mixture as described in Table 2.8.

To visualise amplified DNA, 0.8% (products >3kb), 1% (products >1kb) or 2% (products <500bp) were used. Ultrapure agarose was melted in 1X TAE (made from Thermo Scientific 50X TAE Buffer (Tris-acetate-EDTA)) buffer and stained with SYBR safe gel stain at a concentration of 1:10000. Gels were run at 50V and visualised using Gel Doc™ XR+ Gel Documentation System (Bio-Rad)

2.2.5 Sanger Sequencing to Confirm Constructs

Plasmid DNA and PCR products to be Sanger dideoxy sequenced were submitted to Dundee Sequencing Services (University of Dundee)[11] in the Applied Biosystems 3730 DNA analyzers. 20 ng/µl of plasmid DNA and depending on size 2-200 ng, i.e. 0.0667-6.667 ng/µl, of PCR product were sent. Oligonucleotides were synthesised, stored and added to reactions by Dundee Sequencing Services at a concentration of 3.2 pM. Augmented protocol was routinely used for pSEVA sequencing to alleviate sequencing reaction inhibition by secondary plasmid structures.

[11] https://www.dnaseq.co.uk/

2.2.5.1 *Real-time Quantitative PCR (qPCR)*

For quantitative detection of target nucleic acid sequences, fluorescent-based, real-time PCR analysis was performed using Applied Biosystems StepOnePlus™ (Thermo Fisher).

2.2.5.1.1 *Preparation of Template DNA for Real-Time qPCR*

Bacterial culture were grown in LB with 50 µg/mL Km overnight from single colonies and sub-cultured and grown to mid-exponential phase (OD_{600} 0.7). One mL of culture was used to extract the total DNA using the QIAamp DNA Mini kit (Qiagen) following the protocol for Gram-negative bacteria. DNA eluted in 200 µL AE and normalised to 2 ng/mL with deionised H_20.

2.2.5.1.2 *Real-time qPCR Reaction Protocol*

Real-time qPCR reactions were set up using Power SYBR® Green PCR Master Mix (Applied Biosystems™, 4368706) (see Table 2.10). MicroAmp® EnduraPlate™ Optical 96-Well Fast Clear Reaction Plate (Applied Biosystems™**,** 4483485) covered with MicroAmp® Optical Adhesive Film **(**Applied Biosystems™, 4360954) were using. The qPCR thermal cycling protocol is described in Table 2.11.

Table 2.10 Real-time qPCR reaction mixture per well

Component	Volume	Final Concentration
Nuclease-free Water	6 µl	
Forward Primer (10 µM)	1.0 µl	0.5 µM
Reverse Primer (10 µM)	1.0 µl	0.5 µM
2x SYBR Green® PCR Master Mix	10 µl	1x
DNA template (2 ng/µl)	2.0 µl	0.2ng/ µl
Total Reaction	**20 µl**	

Table 2.11 Real-time qPCR thermal cycling protocol

Stage	**Holding**	**Cycling**		**Melt curve**		
Cycles		35x				
Step	1	1	2	1	2	3
Ramp rate	100%	100%	100%	100%	100%	100%
Temperature	95 ºC	95 ºC	61ºC	95 ºC	61ºC	95 ºC
Time	10 min	15s	1 min	15s	1min	15 s
Temperature increment						0.3

2.2.5.1.3 *Real-time qPCR data analysis*

Data for primer standard curves and efficiencies, melting curves and threshold cycle (C_T) was analysed using StepOne software v 2.3[12].

2.2.5.1.4 *Calculations Plasmid Copy Numbers*

Change in cycle threshold ΔC_T was calculated using Equation 2 and the relative expression fold change was calculated using Equation 3 resulting in the relative plasmid copy numbers.

Equation 2 Change in cycle threshold

ΔC_T: CT of the target (*neo*) − CT of the reference (*dxs*)

Equation 3 Expression Fold Change

$2^{-\Delta CT}$: (-ΔCT) *(-ΔCT)

[12] https://www.thermofisher.com/uk/en/home/technical-resources/software-downloads/StepOne-and-StepOnePlus-Real-Time-PCR-System.html; last accessed 08.05.19

2.2.6 *PaperClip Multipart Gene Assembly*

To assemble multi-part gene constructs the PCR-based Paperclip assembly method was used as described in (Trubitsyna et al. 2014) to design clip oligonucleotides, and prepare half-clips, which were obtained from IDT and rehydrated in nuclease-free water to a final concentration of 100 µM, and full clips. Clips were prepared by ligation of the 5'-GCC and 3'-CGG half-clip overhangs (see Table 2.12)

Table 2.12 Clip Ligation and Phosphorylation

COMPONENT	**10 µl REACTION**
DOWN	3.5 µL
UP	3.5 µL
NEB T4-ligase buffer	1 µL
T4 Ligase	1 µL
T4 PNK	1 µL
	17.5 µM final Concentration

In detail, the ligation reaction was incubated at 37 ºC for 30min, further incubated at 16ºC for 1h and finally heat inactivated for 20 min at 65ºC. Yielding in 17.5 µM final Clip concentration a Ligations was verified by running 1 µL on a 4% ultrapure TAE agarose gel. Further, for higher accuracy in the assembly reaction, clips were diluted 1:10 to 1.75 µM final clip concentration. Paperclip DNA assembly parts were made by amplifiying from plasmid or genomic DNA using the appropriate UF and DR oligonucleotides of the corresponding part as primers for the PCR reaction, which was

prepared in 50 µl volume using KOD Hot Start DNA polymerase (Novagen) as described in section 2.2.4.5. Adjustment of KOD extension time was generally to 20 kb/s per desired size of the part with appropriate Tm for each primer set. PCR products were verified using gel electrophoresis. Remaining PCR product was digested with DpnI for 1 h at 37°C to prevent carryover of template DNA. DNA bands of parts were excised from agarose gel, purified and eluted in 10-15 µL dH_2O. Part concentration was measured using NanoDrop spectrophotometer.

2.2.6.1 *Paperclip Assembly Procedure using PCR*

The paperclip assembly procedure was slightly altered from Trubitsyna *et al.* (2014) and thessembly mixture was prepared as described in Table 2.13 and a two-step PCR was performed as described in Table 2.14.

Table 2.13 Paperclip assembly reaction mixture

Component	**Volume / Final concentration**
Parts	200 ng/ 3.3 nM final concentration
Clips (1.75mM))	66 nM concentration each
KOD buffer 10x	5 µL
dNTPSs (2mM each)	5 µL
$MgSO_4$ (25 mM)*	3.5 µL
Glycerol (50% v/v)	5 µL
KOD hot start polymerase	1 µL
ddH2O	Make up to V_{final} = 50 µL

**$MGSO_4$ was increased to 3.5µl due to larger product size*

Table 2.14 PaperClip assembly reaction conditions

Stage	Step	Temperature	Time
A	Initial denaturation	95°C	2 min
B (20 cycles)	1. Denaturation	95°C	20 s
	2. Annealing and Extension	70°C	30 s/kb

2.2.7 *Shewanella β-Galactosidase Assay*

For β -galactosidase assays to determine specific promoter activities a modified Miller method was used (Müller et al. 2013). In brief, SOMR-1 strains were grown overnight in biological triplicates from single colonies at 30°C and 250 mL flasks containing 25 mL of either LB medium or SBM were inoculated at OD_{600} 0.05 and further grown at 220 rpm until mid-log phase (OD_{600} 0.5-0.7) and induced. Culture samples were taken before induction and immediately refrigerated. Harvested cells were washed in CPH Z-buffer (see section 2.1.8.3) and resuspended to an OD_{600} of 0.5-0.7. 100 µL of cell suspension was added to pre-aliquoted tubes of 900 µL Z-buffer containing 0.27% (v/v) β - mercaptoethanol, as well as 50 µL chloroform and 100 µL 0.1 % SDS and vortexed for 10 seconds. SOMR-1/Z-buffer mixtures were equilibrated at 30°C for 10 minutes, to allow for the chloroform to sink to the bottom of the well. The reaction was started by adding 200 µL freshly prepared 1X ONPG (4 mg/mL) and was incubated at room temperature until yellow colour developed. The reaction was stopped with 500 µL 1M $Na_2 \cdot CO_3$ immediately and reaction time recorded for each sample. Samples were centrifuged for 5 minutes at 13,000 rpm. 100 µL of supernatant was transferred to a 96-well plate and OD_{420} was measured.

Specific enzyme activities were expressed as Miller Units and calculated as follows:

Equation 4. Miller Unit Calculation

$$\text{Miller Unit} = 1000 * \frac{(OD420)}{(t * V * OD600)}$$

$$where\ t = time; V = volume;\ OD = optical\ density$$

2.2.8 *SOMR-1 Bulk Flavin Assays*

Bulk flavin assays were performed as previously described in (Covington et al. 2010). In brief, strains were propagated as previous described in appropriate media and antibiotic selection. OD_{600} was measured for each sample which was then centrifuged and 300 µL of cell-free supernatant were transferred to 96-well Greiner fluorescence plate and fluorescence was measured at 440/520 mn as described below.

2.2.8.1 *Propagation of SOMR-1 Strains*

As described in Covington *et al.* (2010), SOMR-1 strains overnight cultures were grown at 30°C at 200 rpm (see section 2.2.1). Then 2 mL of culture were harvested and washed twice in SBM containing 20 mM sodium lactate and OD_{600} measured to inoculated 11 ml of sterile SBM medium at a ratio of 1:100 and grown overnight at 30°C at 200 rpm. OD_{600} of overnight cultures was measured and fresh SBM was then inoculated at OD_{600} 0.01-0.05 in glass tubes with a diameter 1.5 cm sealed by a butyl stopper.

2.2.8.2 *Induction of SOMR-1*

Cultures were grown until exponential phase and induced with either IPTG with a final concentration of 1 mM IPTG from a 100 mM stock or cyclohexanone (Sigma; 9.6495 M stock) with a final concentration 1 mM, unless otherwise stated.

2.2.8.3 *Flavin Excitation and Measurement*

OD_{600} and OD_{450} emissions were measured using the FLUOstar Omega platereader (BMG LABTECH GmbH). 160 µl of culture were added in technical triplicate to a Greiner 96-well flat bottom clear plate for optical density at 600 nm to measure growth. 1-2 ml of culture were centrifuged at high speed for 2 min and 300 µl of supernatant added to black Greiner 96-well flat bottom plate for excitation/emission at 450/520 nm. Gain adjusted to highest expected fluorescence

2.2.8.4 *Data Analysis*

To calculate relative fluorescence units (RFU), fluorescence readings were blank-corrected by the OD_{600} average of corresponding biological sample from which RFU average and standard deviation (SD) were calculated.

2.2.9 *SOMR-1 Biofilm Assay*

The biofilm assay used here was adapted from (Paulick et al. 2009). Overnight cultures were grown in LB and 10 µl of the culture for each sample were added to 165 µl LM with 0.5 mM, 5 mM or 15 mM sodium lactate in 96-well polystyrene plates (Greiner) which were then incubated at 30°C for 24 h. Prior to processing, OD_{600} was measured and planktonic cells were removed. Wells were washed once with water. Then, 0.1% crystal violet solution (Sigma) was added to each well. After circa 15-20 minutes, wells were washed 4 times with 200 µl water or until washes were clear of purple appearance. The remaining crystal violet was then resuspended in 200 µl of 98 % ethanol. Absorbance at 570 nm was measured using a Fluostar Omega spectrophotometer (BMG Labtech).

2.2.10 *pMiniHimar Transposon Mutagenesis*

pMiniHimar transposon mutagenesis was carried out as previously described in (Bouhenni et al. 2005) using *E.coli* WM3064 as the donor strain.

2.2.11 *Electrochromic Detection of Electrochemically Active Bacteria (EAB) using a Tungsten Trioxide (WO_3) Assay*

EABs can be identified and screened for their electron transfer capabilities using crystalline tungsten trioxide (WO_3) nanoclusters (Yuan et al. 2013; Yuan et al. 2014). In brief, once the WO_3 was synthesised, the bacteria under investigation are incubated anaerobically in a 96-well plate using appropriate media suspension in addition to 5 $g \cdot L^{-1}$ WO_3 media suspension. Following incubation, depending on the ET capabilities of each strain a colour change from white to blue should be visible. The 96-well plate was then imaged and the colour intensity of each well is measured *in silico*. The protocol was performed as described in (Yuan et al. 2013; Yuan et al. 2014) with some alterations as described in the following sections.

2.2.11.1 *Hydrothermal Synthesis of Tungsten Trioxide (WO_3)*

Crystalline WO_3 nanoclusters were synthesized using a hydrothermal process with sodium tungstate dehydrate ($Na_2WO_4 \cdot 2H_2O$) as a precursor as described in (Yuan et al. 2013; Yuan et al. 2014) using an Acid Digestion Bomb with Teflon liner (Model 4744, Parr Instruments, USA).

For a Teflon liner with 20 mL capacity 0.4125 g of $Na_2WO_4 \cdot 2H_2O$ (Sigma-Aldrich) and 0.145 g of NaCl (Fisher Scientific) are dissolved in 10 mL of deionized water; amounts were doubled when using an acid digestion bomb with 40 mL capacity. The pH was lowered to 2.0 by slowly adding 3 M HCl under stirring. The solution was

then transferred into the Teflon liner and heated in the hydrothermal reactor bomb at 180°C for 16 h in an oven (Heratherm™, Germany). After cooling down to ambient temperature, a white powder of WO3 nanocluster was obtained and washed thoroughly with deionized water, and then filtered through a 0.45 µm membrane (Millipore, UK) to collect the solid using a bottle top vacuum filter unit. The powder was dried in an oven at 60°C for 8 h and then stored at room temperature in an air-sealed container.

2.2.11.2 *Verification of WO_3 Nanorods*

The phase of the obtained WO_3 powder was determined using X-Ray diffraction using a Bruker D2 Phaser. A small sample of pestled powder was placed in the centre of a sample disk and mixed with a drop of absolute EtOH to flatten the sample on the disk. The morphology of the synthesised WO_3 was confirmed using a Scanning Electronic Microscope (Hitachi 4700 II, Cold Field Emission). The sample was coated with 20 nm Au Palladium (E306A Coating System) prior to imaging.

2.2.11.3 *WO_3 96-Well Plate Assay*

As population density is directly proportional to the chromaticity of the WO_3 nanorods, the initial cell density of each strain was determined by OD_{600} measurement. Various strains of SOMR-1 were incubated overnight from frozen -80°C stock in 40 mL LB medium at 30°C/125 rpm. to achieve logarithmic growth phase for the assay. For each strain, the reaction was set up in triplicate. Using a flat bottom, clear polystyrene 96-well plate (GreinerBio), a mixture of 100 µL ($1\text{-}2\cdot10^9$ CFU/mL) bacteria resuspended in SL-MSM and 80 µL of 5 $g\cdot L^{-1}$ sterile WO_3/SL-MSM suspension were transferred in each well and immediately 80 µL of mineral oil (Acros Organics, Belgium) were added to ensure anaerobic conditions. To ensure credibility of the electro-chromic

results, the following controls were added to each plate in triplicate: an abiotic control WO_3 and SL-MSM only, SOMR-1 only in SL-MSM in addition to *E. coli* DH5α and DET deficient control strains. The plate was further incubated at 30°C and colour development was checked after ~30 min.

2.2.11.3.1 *Image Acquisition, Processing and Data Analysis*

Brightfield images of the 96-well plates were acquired using a scanner (EPSON Scanner V370). As the density mean gives a positive correlation to EET activity of each strain, the colour density mean of the wells was determined using ImageJ (1.48v) software. The WO_3 blank density mean was subtracted from all measurements and these were normalised with the mean of S. oneidensis MR-1 wild type. Standard error means were calculated from three different well measurements and statistical significance tested using Mintab v16.

2.2.11.4 *WO_3 Sandwich Plate Screen*

To screen potential electrochemical properties of SOMR-1 enhancer transposon mutants, colonies were tested using a WO_3 sandwich plate screen. SOMR-1 colonies were grown on SBM medium containing 20 mM sodium lactate. Colonies were overlaid with a tungsten top agar (containing 5 $g \cdot L^{-1}$ WO_3) prior to anaerobic incubation at 30°C in a 2.5 L-anaerobic jar (Merck Millipore; Cat. Number 116387) over the course of 3 days. Anaerobic conditions were maintained using Anaerocult® (Merck Millipore; Cat. Number 113829) sachets to remove oxygen (O_2) from the jar while releasing CO_2. WO_3 sandwich plates were scanned at regular intervals and returned back in the anaerobic vessel replacing the anaerobic sachet each time.

2.2.12 *Electrochemical Analyses*

Experimental set-up of miniaturisation of three-electrode MFC was adapted from (Gimkiewicz and Harnisch 2013) and all experiments performed at 30°C under anaerobic environment using Whitley A95TG Workstation (Don Whitley Scientific, UK) with a N_2 / H_2 / CO_2 atmosphere.

2.2.12.1 *MFC Set-Up and Maintenance*

SOMR-1 cultures grown overnight in LB from single colonies and grown aerobically in SBM medium (20 mM sodium lactate) containing appropriate antibiotic selection as described in section 2.2.1. 3 mL of fresh anaerobic SBM medium (20 mM sodium lactate, 40 mM sodium fumarate) was inoculated with 1mL of overnight culture in a 5 mL Eppendorf tube. Screen printed electrodes (#DRP-C110, Metrohm DropSens, Spain) containing a pseudoreference electrode, working electrode (Carbon 110, 4 mm diameter) and counter electrodes made of carbon were used.

Chronoamperometry as described in section 2.2.12.2 was performed to grow electroactive biofilm. Cyclic voltammetry was performed after steady state biofilm growth as measured by chronoamperometry as described in the section below. Upon substrate depletion, 100 µl of 1 M sodium fumarate and sodium lactate were added to the culture and chronoamperometry commenced.

2.2.12.2 *Chronoamperometry and Chronoamperometric Biofilm Growth*

Chronoamperometry was performed using Potentiostat / Galvanostat µStat 8000 (DRP-STAT8000) [Metrohm DropSens, Spain]. The working electrode was set to a constant potential of E=0.24 V measuring current (µA) every 600 s.

2.2.12.3 *Cyclic Voltammetry*

Cyclic voltammetry was adapted from Gimkiewicz and Harnisch (2013) and performed using Potentiostat/Galvanostat µStat 8000 (DRP-STAT8000) [Metrohm DropSens, Spain]. Cycling potential was set to E_i=-0.7V, E_1 = 0.5V and E_2 = -0.7V.

2.2.12.4 *Current Density Calculation*

Current density *j* ($\mu A \cdot cm^{-2}$) was calculated using the following equations:

Equation 5. Electrode Surface Area

$$\text{Electrode Surface Area } (cm^2) \quad = \pi \cdot r^2$$

The SPE DRP-C110 has a circular working electrode with a diameter of 4 mm, therefore the calculated electrode surface area is 0.12567 cm^2 which was rounded to 0.13 cm^2.

Equation 6 Current Density

$$Current\ density\ j = \frac{Current\ (\mu A)}{Electrode\ surace\ area\ A\ (cm^2)}$$

Chapter 3

3 A SYNTHETIC BIOLOGY TOOLBOX FOR SOMR-1

3.1 Introduction

The driving force behind synthetic biology is the desire to simplify and rationally design biological systems for biotechnology applications (Freemont et al. 2012). Microbial synthetic biology efforts have resulted in several repositories such as the international genetically engineered machine (iGEM) competition and its registry[13] of standardised parts, which provide standardised genetic parts for genetically engineering of microorganisms. Furthermore, non-profit repositories like addgene[14] allow easy and fast plasmid exchange between researchers of different labs. However, previous research efforts to improve reliability and to fine-tune gene expression systems have been mostly characterised in well-established model organisms such as *E. coli* (Nielsen et al. 2013; Segall-Shapiro et al. 2018). To translate synthetic biology into a wider applied biotechnology, more diverse molecular genetic tools are needed. Establishing procedures to engineer niche model organisms, such as SOMR-1, would greatly advance the field of electromicrobiology.

Recently, more and more of the genes and components that build the microbial extracellular electron transfer (EET) pathway have been elucidated for the most prominent electrogenic bacteria, i.e. *Geobacter* and SOMR-1, which can both respire on insoluble extracellular entities such as solid-state electrodes (Coursolle et al. 2010; Strycharz et al. 2011). With the advances in both of these fields, there is the potential

[13] http://igem.org/Registry
[14] https://www.addgene.org/

to precisely engineer electromicrobial systems where SOMR-1's extracellular electron transfer is dynamically controlled by utilising synthetic gene regulatory networks. However, this requires more tools that function in SOMR-1. SOMR-1 itself has only been a nascent model organism, and genetic tools and plasmids are limited so far.

3.1.1 *Establishing the pSEVA Plasmid Platform in SOMR-1*

Plasmids have been used in molecular biology for decades since they are easy to manipulate with standard and inexpensive molecular techniques and can be transferred into a wide range of host cells where they autonomously replicate from the host's chromosome (Kües and Stahl 1989; Meyer and Dehio 1997) making them an essential tool for biotechnology. However, the plethora of cloning vectors used world-wide in research labs are rarely well-characterised. Besides they seldom adhere to any strict nomenclature for their parts including antibiotic resistance cassettes, origins of transfer and replication, all of which makes prediction and standardisation of parts difficult. As the field of systems and synthetic biology expands and moves towards handling complex genetic circuits (Anderson et al. 2007) implementing novel functionality into the workhorses of biotechnology, there is an imminent need for vector organisation and designation. Not least because many of these advances in synthetic biology have been made in and for *E.coli*. However, although it is an excellent host for the physical assembly of DNA constructs, *E.coli* is not suitable for many biotechnical applications where synthetic biology could aid solve environmental problems, and non-model organisms which possess an inert wealth of other characteristics making them uniquely suitable for such applications. One of these is SOMR-1, albeit being a nascent model-organism in the field of electromicrobiology, synthetic biology tools and methods for this bacterium are limited. Even though, advances have been made recently to

genetically engineer SOMR-1 (Baron et al. 2009; Kane 2011; Choi et al. 2013; Webster et al. 2014), it is vital to have a vector platform that can be reliably used to introduce exogenous DNA into SOMR-1 with high efficiency and that can be easily adapted to further these efforts.

Recently, the Standard European Vector Architecture (SEVA) platform was developed and has a growing repository of standardised vector parts making the adaptation of each vector to a specific host more rapidly achievable by exchanging either oriV, AB or cargo cassette using restriction enzyme cloning (Silva-Rocha et al. 2013; Martinez-Garcia et al. 2014). To date, there are six different antibiotic resistance cassettes, nine different origins of vegetative replication (oriV) and a range of cargo cassettes including the default multiple cloning site (MCS), green fluorescent protein (GFP), lacZ or the luxCDABE operon (see Figure 3.1). [(Jahn et al. 2016)].

The most common origins of replication (oriV) are for Gram negative bacteria, namely E. coli, only. Currently used oriVs include ColEI, p15A, pMB1, with its derivatives, R6K, pUC and pSC101. Depending on their regulation, host cells produce anything from one plasmid copy per cell to many copied (Jahn et al. 2016). This control is usually referred to as being relaxed or stringent (see Table 3.1) and is dependent on whether these oriV are positively regulated by, for example by an RNA protein. Small mutations can increase plasmid copy numbers from 20 to as high as 700, such as in the case of pMB1 and pUC, which only differs from pMB1 in two mutations. Figure 3.2 shows the organisation of pSEVA replication origins. A frequently used suicide origin, R6K, which is dependent on the Π replication protein, can only be maintained if the *pir* is expressed in the host cell in *trans.* The RK2 origin of replications requires next

to oriV the replication protein trfA, which is a similar architecture to pBBR1. The pSEVA pRO1600/ColE1 hybrid origin is combines pRO1600 origin and the ColE1 replication sequence allowing further replication in not only *E.coli* but also *Pseudomonas aeruginosa* isolate. As for RSF1010 has been altered to limited the number of mob genes and the new synthetic sequence has the oriV and the repBAC genes (see Figure 3.2) (Silva-Rocha et al. 2013).

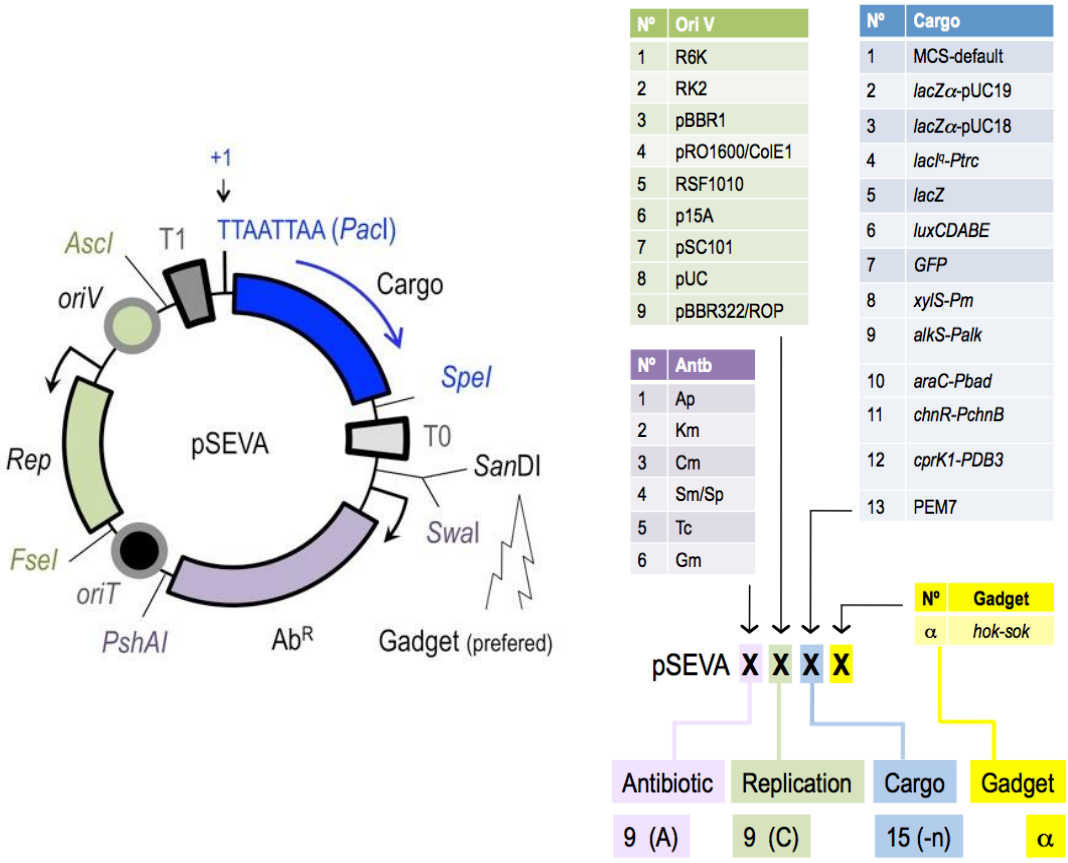

Figure 3.1 pSEVA vector organisation (left) and available vector combinations and their nomenclature (right). Image taken from http://wwwuser.cnb.csic.es/~seva/ (last accessed 8th June 2018).

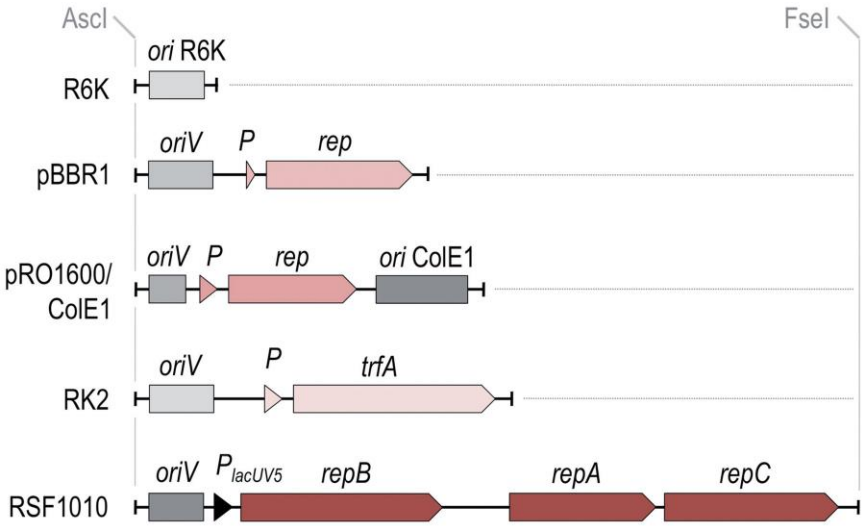

Figure 3.2 Organisation of the pSEVA replication origins. Image taken from (Silva-Rocha et al. 2013).

An imminent bottleneck of combining synthetic biology approaches with electromicrobiology in SOMR-1 is the lack of a vector toolbox for this organism. From the 9 different oriV available from the SEVA collection, only some have been used in SOMR-1 research (see Table 3.1) with the prominent example being the pBBR1-MCS-3 plasmid (Kovach et al. 1995) that has been used in a number of complementation studies (Marsili et al. 2008; Covington et al. 2010; Brutinel and Gralnick 2012a; Kotloski and Gralnick 2013). Furthermore, the pBAD33 plasmid with the p15A oriV (Myers and Myers 1997a) has already been used successfully in SOMR-1 (Rachkevych et al. 2014). The R6K oriV can also be used as a suicide origin of replication in SOMR-1 since no *lamba pir* gene is present to allow for replication. This has been shown to work for transposon mutagenesis with a pminiHimar transposon using R6K oriV (Bouhenni et al. 2005).

However the other six oriV available in the SEVA collection have either not been described in the literature for SOMR-1 or been shown to work less efficiently. Functionality of RSF1010 has not been reported in the literature so far. Another *Shewanella* strain, *S. baltica*, has been shown to replicate ColE1-like oriV plasmids (Milewska et al. 2015). Successful transformation with pSC101in *Shewanella* has not been described in the literature so far, and some efforts to show the replication of the pBR322 plasmid have been unsuccessful (Myers and Myers 1997a). However, the removal of *claI* restriction sites has been shown to improve transformation efficiency in a number of plasmids including pBR322 (Rachkevych et al. 2014). Coincidentally, *claI* restriction sites are absent from most pSEVA plasmids with the exception of pSEVA221 (Kan^R; RK2 oriV; MCS).

Table 3.1 Usage of most common SEVA oriV (1-9) in SOMR-1.

SEVA number	**oriV**	**Copy Number**	**Compatibility group**[a,b]	**Notes**	**Reference** in SOMR-1
1	R6K	~15-20[a]	C (stringent)[a]	Suicide origin, no *lamda pir* in SOMR-1, used in pMiniHimar transposon	(Bouhenni et al. 2005)
2	RK2		ND	"RK2 origin of transfer (oriT) cassette effectively ports a modular plasmid system"	(Gralnick and Hajimorad 2016)
3	pBBR1	~15-20[a]	A (relaxed)	Numerous papers for complementation studies pBBR1-MCS-3	(Covington et al. 2010; Brutinel and Gralnick 2012b)
4	ColEI	~15-20[a]	A (relaxed)[a]	*S. baltica* shown to replicate ColE1-like vector, otherwise no papers showing plasmid with cole1 replicates in SOMR-1	(Milewska et al. 2015)
5	RSF1010	Low copy, broad host range[c]	ND	"able to replicate in nearly all gram-negative bacteria", not published for SOMR-1	(Kües and Stahl 1989)
6	p16A	~10[a]	B (relaxed)[a]	Numerous papers with pBAD33 Myers p15A 1997	(Myers and Myers 1997a; Rachkevych et al. 2014)
7	pSC101	~5[a]	C (stringent)[a]	not determined	
8	pUC (pMB1 derivative)	~500-700 [a]	A (relaxed)[a]	electroporation efficiency is very low despite high copy number but yield higher protein for study of c cytochromes	(Ozawa et al. 2001; Rachkevych et al. 2014)
9	pBR322 (pMB1)	~15-20[a]	A (relaxed)[a]	Not determined, irrespective of *claI* restriction site, Tc^R	(Myers and Myers 1997a; Rachkevych et al. 2014)

[a]https://blog.addgene.org/plasmid-101-origin-of-replication (accessed 24 June 2018); [b]compatibility groups are an arbitrary designation, and plasmids from the same incompatibility group should not be co-transformed; [c]*(Frédéricq et al. 1971).*

3.1.2 *Transcriptional Regulation in SOMR-1*

Transcriptional regulation is a crucial bioengineering approach to optimising the performance of bacteria in biotechnological applications. Over the past decades genetic regulatory tools for gene expression have been developed predominantly for *E.coli* research and for biotechnology applications, including a variety of constitutive and inducible promoters. Hence, engineered gene expression in SOMR-1 has been only seen a few non-native promoters being applied to this organism so far (see Table 3.2). This includes arabinose and arsenic-inducible *E. coli* promoters, P_{ara} and $P_{ars,}$ respectively, which have been applied for SOMR-1 biosensor applications (Golitsch et al. 2013; Webster et al. 2014). Further, the *lac* promoter, P_{lac}, (Bouhenni et al. 2005), as well as $P_{tac,}$ a hybrid of P_{lac} and P_{trp} promoter, both inducible by IPTG, have also been shown to work in SOMR-1 in gene complementation studies in knockout strains (Liu et al. 2015; Yang et al. 2015; Wan et al. 2017).

The main limitations of these inducible expression systems are basal expression rates in the absence of the inducer, especially seen in P_{BAD} (Kane et al. 2013). Basal expression is a major drawback of inducible promoters, especially considering the metabolic burden they pose on the bacterial cell. Therefore, tight and timely induction of desired genes is needed.

Consequently novel, more tightly regulated and potentially titratable gene expression systems are needed to engineer and ultimately optimise extracellular electron transfer in SOMR-1 bioreactors.

Table 3.2 Inducible promoters previously used in SOMR-1

Promoter	Inducer	Notes	Reference
P_{lac}	Isopropyl β-D-1-thiogalactopyranoside (IPTG)	• Used in pMiniHimar for transposes without repressor • Complementation promoter for *mtrC*	(Bouhenni et al. 2005) (Beliaev et al. 2001)
P_{tac}	IPTG	Hybrid of P*lac* and P*trp*	(Liu et al. 2015; Yang et al. 2015)
$P_{ara/BAD}$	Arabinose (ara)	Arabinose-inducable promoter	(Kane et al. 2013)
$P_{ars/ArsR}$	As(II)	• arsenic-inducible promoter (P_{ars}) is negatively regulated by ArsR • arsenite-responsive transcriptional circuit in in plasmid pArsR/ MtrB. • arsR is a negative auto-regulator	(Webster et al. 2014)
Promoters not used in SOMR-1 before:			
$P_{ChnB/ChnR}$	Cyclohexanone	• Used for *P. putida* catalytic biofilms	(Benedetti et al. 2016b; Benedetti et al. 2016a)
$P_{tet/TetR}$	anhydrotetracycline (aTc)	• Not used in SOMR-1 before	(Bertram and Hillen 2008)
P_{T7}		• Not used in SOMR-1 before	(Tabor 2001)

3.1.3 *Aims of Work Presented in this Chapter*

The aim of this chapter was to create a synthetic biology toolbox for SOMR-1 by establishing a standardised vector platform and novel transcriptional regulation systems for this organism to allow for more fine-tuned genetic engineering of this organism in order to enhance its EET capabilities.

These aims included:

- Establishment of efficient transformation and maintenance protocols of the pSEVA plasmids containing previously established and novel oriV and resistance cassettes in SOMR-1;
- Identification of plasmid copy numbers, efficiency and maintenance of pSEVA plasmids in SOMR-1 compared to *E. coli;*
- Demonstration of SOMR-1's ability to harbour a combination of pSEVA plasmids with different replication systems;
- Development and establishment of transcriptional regulation using oxygen independent inducible & constitutive promoters: $P_{ChnB/ChnR}$, $P_{tet/TetR}$, P_{T7};
- Development of promoter activity using oxygen independent reporter *phiLOV* and *lacZ* assay

Promoter	**Inducer**	**Notes**	**Reference**
$P_{ChnB/ChnR}$	Cyclohexanone	Not used in SOMR-1 before Used for *P. putida* catalytic biofilms	(Benedetti et al. 2016b; Benedetti et al. 2016a)
$P_{tet/TetR}$	aTc	Not used in SOMR-1 before	(Bertram and Hillen 2008)
P_{T7}	NA	Not used in SOMR-1 before	(Chamberlin et al. 1970; Studier and Moffatt 1986)

3.2 Results

3.2.1 *Minimum Inhibitory Concentration for Common Antibiotics in SOMR-1*

The literature presents various concentrations of standard antibiotics used in molecular biology for the selection of recombinant SOMR-1. Following some unsuccessful cultivations with the pSEVA collection, especially those containing gentamicin and chloramphenicol resistance cassettes, the minimum inhibitory concentrations (MIC) (Andrews 2001) for ampicillin (Am), kanamycin (Km), chloramphenicol (Cm), spectinomycin (Sp/Sm), tetracyclin (Tc) and gentamicin (Gm) were determined.

For this, ~5 single colonies of wild type (WT) SOMR-1 were subcultured together and used to inoculate MIC test cultures containing antibiotics ranging from 0.125 to 128 µg/mL. After an overnight incubation, growth of wild type SOMR-1 and cultures with ranging concentrations of antibiotics were measured using $OD_{600.}$ As previously described, SOMR-1 is endogenously resistant to ampicillin (Yin et al. 2013), which was confirmed here, by an average growth reduction of 25.9 ± 7.9% compared to the negative control culture with LB medium only, ranging from a reduction of 14.1% at 0.125 µg/mL to 32.4% at 128 µg/mL Am. The second least effective antibiotic appears to be spectinomycin (standard working concentration 50 µg/mL), which reduced SOMR-1 growth to up to 28.2% up to a concentration of 32 µg/mL and only 50.7% at 62 µg/mL and finally 90.8% at 128 µg/mL, the latter being the minimum bactericidal concentration for this antibiotic.

The most commonly used antibiotic, kanamycin, inhibited growth by ≤26.1% compared to WT for concentrations of up to 8 µg/mL, while 16 µg/mL Km reduced growth by 83.1% and ≥32 µg/mL by ≥ 94.4%. At 50 µg/mL, the standard

concentration, growth was inhibited by 96.5% and even at 25 µg/mL by 93.7%, which is also the lowest MBC where new colonies were observed.

Both gentamicin and chloramphenicol inhibited growth even at the lowest concentration of 0.125 µg/mL by 27.5% and 28.9%, respectively. Gentamicin steadily reduced growth by ≤ 40.1 up until 2 µg/mL. A concentration of 8 µg/mL Gm inhibited growth by 90.8%, however only ≥10 µg/mL prevented growth by ≥ 95.8% and growth of colonies on subsequent cultivation. Similarly, chloramphenicol inhibited 77.5% of growth with a concentration of 1 µg/mL, compared to any concentration ≥2 µg/mL preventing growth by up to 98.6 % in liquid media. Table 2.1 summarises the MIC of antibiotics in SOMR-1 used in the following experiments in this work.

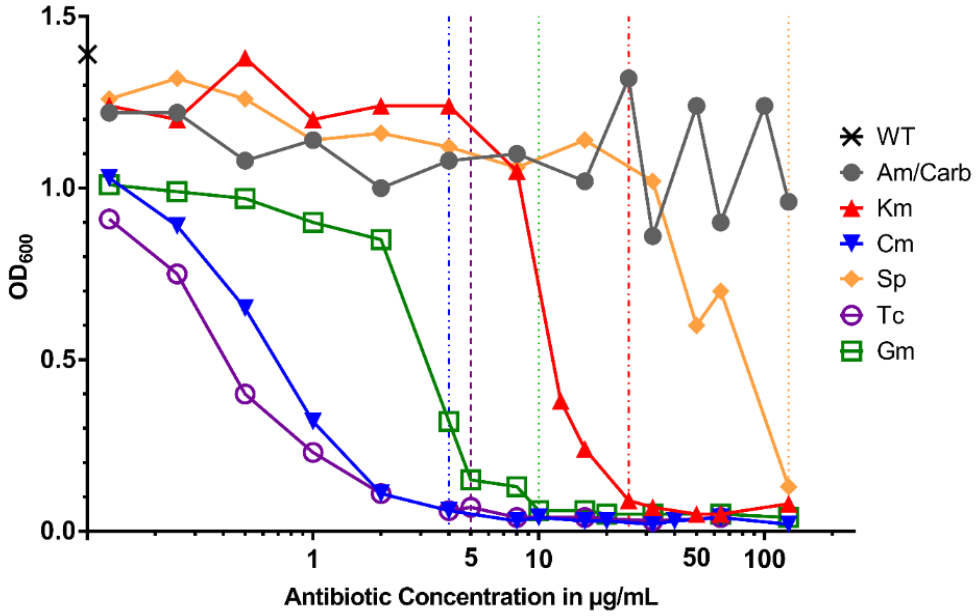

Figure 3.3 Minimum Inhibitory Concentrations (MIC) of commonly used antibiotics in SOMR-1. MIC were regarded as any OD_{600}≤0.08 after 16 h incubation in LB medium, i.e. no visible growth can be seen. Minimum bactericidal concentrations (MBC) are indicated as dashed lines, i.e. when no growth was observed after sub-plating on fresh LB plates without antibiotic.

3.2.2 *pSEVA Multi-plasmid Platform in SOMR-1*

3.2.2.1 *pSEVA in SOMR-1 Strain NCIMB14063*

Initially, SOMR-1 strain NCIMB14063 was obtained from the National Collections of Industrial, Food and Marine Bacteria (NCIMB) and was successfully transformed via electroporation with pSEVA with three different oriV (RK2, pBBR1, p15A using 3 different antibiotic markers (Km, Cm, Gm) (see Figure 3.4A) and the commonly used plasmids pBBR1-MCS-2 (Km^R) and pBBR1-MCS-5 (Gm^R) (Kovach et al. 1995) [see Figure 3.4B and Figure 3.4E].

Since $oriV_{p15A}$ has been shown to work in SOMR-1 in the commonly used plasmids pBBR1-MCS (see Figure 3.4E), and only pSEVA261 was available at the time in the SEVA collection, the kanamycin resistance cassette from pSEVA261 (Km^R, $oriV_{p15A}$, MCS) was replaced with the gentamicin resistance cassette from pSEVA631 (Gm^R, $oriV_{pBBR1}$, MCS) via *Fse*I and *Asc*I digestion and ligation resulting in the pSEVA661 (Gm^R, $oriV_{p15A}$, MCS, size: 2,211 bp) [see Figure 3.4D]. This plasmid is now available at the SEVA collection.

Unexpectedly, restriction digestion analysis of plasmids isolated from the modified NCIMB14063 strain showed many more additional bands than anticipated and DNA smear compared to plasmid DNA isolated from *E. coli* DH5α. A restriction digestion of plasmid miniprep DNA from a wild type culture of NCIMB14063 showed a large band for uncut plasmid DNA, 2 bands after *Pvu*II digestion of 5.5 kb and approximately ≥ 12 kb, while *Dra*I and *BstE*II digestion resulted in a band at circa 6 kb and a large number bands ≤2.5 kb. The bands from the *Pvu*II digestion from the wild type plasmid DNA are identical in size to those seen in the pSEVA231 digest with

*Pvu*II in Figure 3.4A, while two of the four bands seen correspond exactly with the bands expected from the digested pSEVA231 at 2.3 kb and 0.8 kb as seen in the miniprep DNA isolated from *E. coli* in Figure 3.4C. It indicated that this particular SOMR-1 strain must have already possed a large cryptic plasmid of ≥ 20kb (see Figure 3.4C and Figure 3.4E).

Natural plasmids have been previously reported for a number of *Shewanella* isolates, and have been seen to carry putative toxin and antitoxin systems for plasmid stabilization and hypothetical genes involved in conjugation (Milewska et al. 2015). However, not knowing what metabolic function and burden this plasmid poses for SOMR-1 application in MFCs, a new wild type strain from the Gralnick lab was sourced, SOMR-1 (JG274), for further experiments (Coursolle and Gralnick 2010). A plasmid miniprep of SOMIR-1 JG274 showed no presence of plasmid DNA (agarose gel not shown). Nevertheless, the available pSEVA plasmids with three different oriV (RK2, pBBR1 and p15A) were successfully replicated and maintained SOMR-1 (NCIMB14063) despite the cryptic plasmid, warranting further exploration of this platform in *Shewanella*.

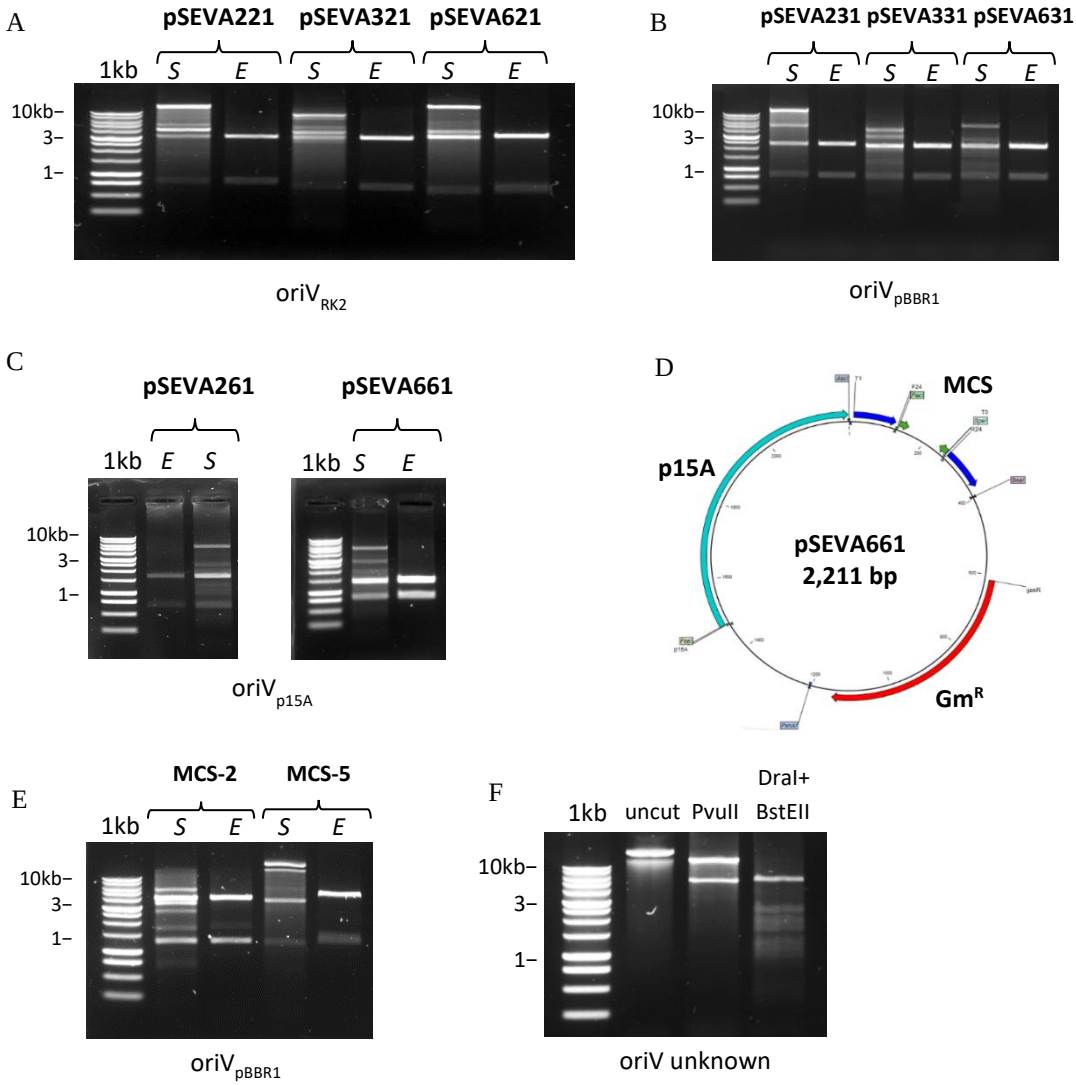

Figure 3.4. 1% agarose gel showing restriction digests of plasmid DNA isolated from SOMR-1 (NCIMB14063) and E. coli harbouring pSEVA with (A) oriV$_{RK2}$ i.e. pSEVA221 [digested with NdeI and BstEII-HF (expected band size 3022bp and 808 bp)], pSEVA321 [digested with NdeI and NcoI (expected band size 2976bp and 698 bp)], pSEVA621 [digested with NdeI and EcoRV-HF (expected band size 3064 and 639 bp)];(B) oriV$_{pBBR1}$ i.e. pSEVA231 [digested with PvuII-HF], pSEVA331 [digested with NcoI and HindIII-HF], and pSEVA631 [digested with with DraI and PshAI]; (C) oriV$_{p15a}$ i.e. pSEVA261 [digested with DraI and BstEII-HF (expected band sizes 1698 and 687) and pSEVA661 [digested with DraI and PshAI (expected band size 1397 and 814 bp)]. (D) vector map of pSEVA661 (Gm^R, orivV$_{p15A}$, MCS). (E) SOMR-1 (NCIMB14063) and E.coli harbouring pBBR1-MCS-2 [digested with PstI], and pBBR1-MCS-5 [digested with with EcoRV-HF]. (F) SOMR-1 (NCIMB14063) wild type miniprep showing unknown endogenous plasmid [uncut plasmid DNA and plasmid DNA digested with PvuII-HF and DraI + BstEII]. DNA ladder, Promega 1kb; MCS, multiple cloning site; S, NCIMB1406; E, E. coli.

3.2.2.2 *Effect of pSEVA oriV on transformation efficiency in SOMR-1 JG274*

Electroporation, as used in the previous section, can yield stark differences in transformation efficiency where only a few colonies were obtained after overnight cultivation (data not shown). Additionally, electrocompetent SOMR-1 are not storable at -80°C and their competency decreases rapidly once prepared. Therefore conjugation using the conjugal donor strain *E.coli* WM3064 for mating with SOMR-1 provided a more reliable and feasible solution to transforming large numbers of constructs and to acquiring a larger number of SOMR-1 transconjugants for screening and further experiments.

Table 3.3 Efficiency of conjugation of pSEVA plasmids with varying oriV between E. coli WM3064 and SOMR-1 JG274.

Conjugative plasmid/oriV	**Number of *E.coli* WM3064 donors (cfu·mL^{-1})**	**Number of SOMR-1 recipients (cfu·mL^{-1})**	**Donor: recipient ratio**	**Total number of SOMR-1 trans-conjugants (cfu·mL^{-1})**	**Total number of SOMR-1 trans-conjugants (mean±SD of $\log_{10}$ cfu·mL^{-1})**	**% Efficiency of conjugation trans-conjugants per donor**
pSEVA221/ $oriV_{RK2}$	1.34×10^9	1.76×10^{10}	1:13	6.04×10^7	7.78±0.01	85.3%
pSEVA231/ $oriV_{pBBR1}$	1.36×10^9	1.76×10^{10}	1:13	1.38×10^8	8.14±0.08	89.1%
pSEVA241/ $oriV_{ColEI}$	3.87×10^7	1.76×10^{10}	1:447	3.41×10^9	9.53±0.05	125.6%
pSEVA251/ $oriV_{RSF1010}$	2.22×10^9	1.76×10^{10}	1:8	1.11×10^7	6.75±0.81	72.3%
pSEVA261/ $oriV_{p15A}$	2.07×10^9	1.76×10^{10}	1:9	2.58×10^9	9.89±0.01	106.2%

Here, an initial selection of pSEVA plasmids was chosen, all Km^R, which is denoted in the first number of each vector name (i.e. pSEVA2XY). These plasmids only vary in their origin of replications (oriV), which is denoted in the second position of the SEVA nomenclature (i.e. pSEVA2X1, where X stands for $oriV_{RK2}$ [221]), $oriV_{pBBR1}$ [231], $oriV_{ColEI}$ [241], $oriV_{RSF1010}$ [251] or $oriV_{p15A}$ [261]) [see Figure 3.1]. Conjugation of SOMR-1 with this set of pSEVA plasmids was successfully achieved using *E. coli* WM3064 donor strain harbouring the selected plasmids. The efficiency of conjugation ranges from 72.3% for $oriV_{RSF1010}$, ≥85% for $oriV_{RK2}$ and $oriV_{pBBR1}$, ≥100 % for $oriV_{p15A}$ and $oriV_{ColEI}$ (see Figure 3.5). While notable differences can been seen in the efficiency, especially for the low copy number $oriV_{RSF1010}$, all conjugations yielded in viable transconjugants in orders of magnitude 1-3 times higher than previously reported in the literature for plasmids with $oriV_{p15A}$ and $oriV_{pBBR1}$ (see Table 3.3) (Rachkevych et al. 2014). However, as conjugation efficiencies were ≥100 % for $oriV_{p15A}$ and $oriV_{ColEI}$, these data indicate that there were multiple conjugative transfers, which indicates that incubation of donor and recipient cells was too long resulting in these multiple transfers and the incubation time should be shortened for high-copy number plasmids.

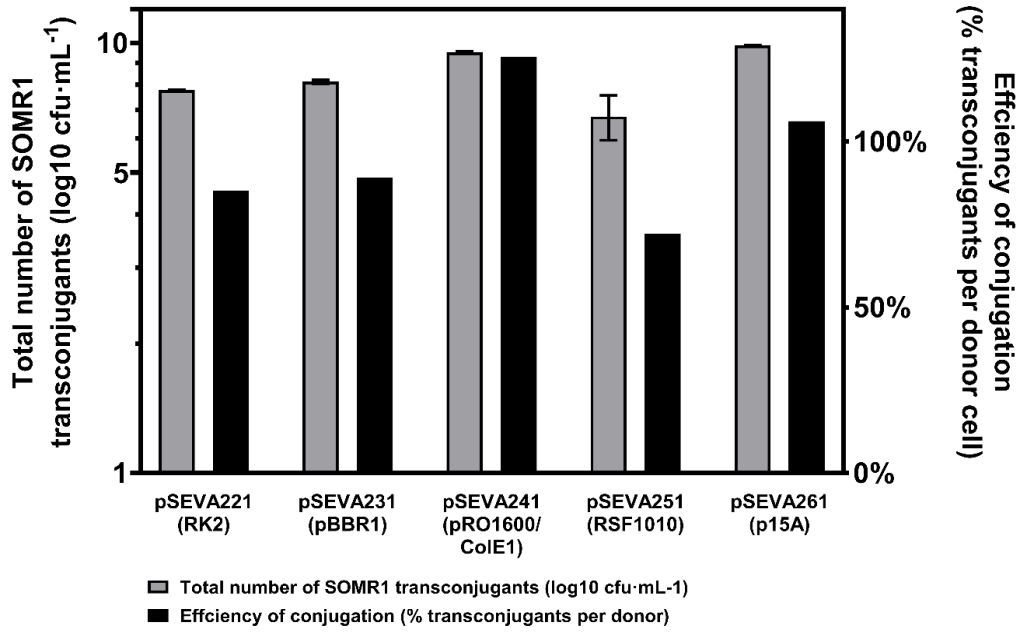

Figure 3.5 Conjugation efficiency of SOMR-1 with pSEVA plasmids in relation to total number of transconjugants per donor cell. For each strain SOMR-1 was conjugated with E. coli WM3064 harbouring the relevant pSEVA plasmid. Strains were mated on filter paper on DAP-containing LB agar plate for 6 h at 30°C. All cells were harvested and washed twice with LB liquid medium. Resuspended culture mixture was plated onto selective LB media containing 50 µg/mL Km and incubated at 30°C for 16 h to isolate transconjugants of SOMR-1. Colonies were counted from serial dilutions plated for SOMR-1 transconjugants, donor strain and SOMR-1 wild type. Conjugation efficiency was calculated by dividing the number of SOMR-1 transconjugants counted on LB agar plate with antibiotic selection by the number of donor cells. Bars represent data of three replicates with error bars showing standard deviation.

3.2.2.3 *Plasmid maintenance of pSEVA oriV range in SOMR-1*

Bioreactors such as MFCs can run over several days. By nature, the electroactive biofilms hinder antibiotic diffusion, thereby depleting antibiotic pressure on the cells, a known problem in clinical settings (Hall and Mah 2017). Even in the absence of antibiotic pressure, plasmid maintenance and stability is of great importance to make sure that all cells in the bioreactor are able to express the desired gene circuit system. Therefore, after every cell division both daughter cells need to carry at least one copy of the plasmid. Although plasmids are not essential and present a needless metabolic

burden for their host cells under non-selective conditions, they can still be maintained in a bacterial population cultivated in non-selective media (Milewska et al. 2015). Hence, to test whether SOMR-1 can reliably maintain plasmids and effectively conserve stable plasmid segregation in dividing cells without antibiotic pressure, seven pSEVA plasmids were tested in SOMR-1 for plasmid retention after 24h without antibiotic selection. For this experiment two additional new pSEVA plasmids were cloned to increase the selection available oriV with the same vector backbone and antibiotic selection cassettes. This allows to meaningfully discern between the effects of oriV mechanisms under identical metabolic burdens posed by the remaining genes of the plasmid backbone other than the oriV itself. There were pSEVA271 (KmR, $oriV_{pSC101}$, MCS; AscI and FseI ligation of $oriV_{pSC101}$ from pSEVA471 into the pSEVA2X1 backbone, data not shown) and pSEVA291 (KmR, $oriV_{pBBR322/ROP}$, MCS; AscI and FseI ligation of $oriV_{pBBR322/ROP}$ from pSEVA191 into the pSEVA2X1 backbone, data not shown).

These pSEVA vectors were conjugated using the *E.coli* WM3064 donor strain harbouring the pSEVA vectors [2.2.2.2.2]. SOMR-1 and *E. coli* WM3064 were washed in LB medium three times to remove residual antibiotics and mated on LB plates containing DAP in 30°C static incubation for 6h. Bacterial cells were harvested from the plate and washed three times in sterile LB medium to remove residual DAP from the culture and resuspended in 1-2 mL LB depending on the amount of biomass. 50 µL of cell suspension was then plated onto LB argar containing 50 µg/mL Km and incubated overnight at 30°C, only allowing survival of SOMR-1 cells who had acquired the new plasmid. Since DAP is absent from the media, the ΔDAP *E. coli* helper strain should not propagate. Single colonies were picked for each SOMR-1 mutant and grown in liquid media overnight at 30°C, shaking at 200 rpm. Cells were

washed twice in LB, and liquid LB media without antibiotic selection was inoculated and grown for 24 under the aforementioned conditions. Serial dilutions were then plated on LB only and on LB containing 50 µg/mL Km, and the plasmid retaining fraction was calculated. In addition, using the same culture, a plasmid DNA was extracted and gel electrophoreses of restriction digested plasmids were performed to verify that plasmids were maintained in each strain.

Five of the seven plasmids tested were maintained after 24h cultivation in SOMR-1 without antibiotic selection pressure and showed to have a ≥94% plasmid-containing fraction in their population (see Figure 3.6). In contrast, a fourth of the SOMR-1 population lost pSEVA221, and more than half of the SOMR-1 population harbouring pSEVA251 lost their plasmid. Figure 3.7 shows plasmid DNA isolated from SOMR-1 mutants after digestion with AscI. Notably, there is no visible band at 5.3kb for pSEVA251. Additionally, the aerobic growth of SOMR-1 harbouring pSEVA221, 231 and 251 was slightly slower compared to the other plasmids and to WT (see Figure 3.8). To further investigate this, plasmid copy numbers in SOMR-1 for these oriV was quantified next.

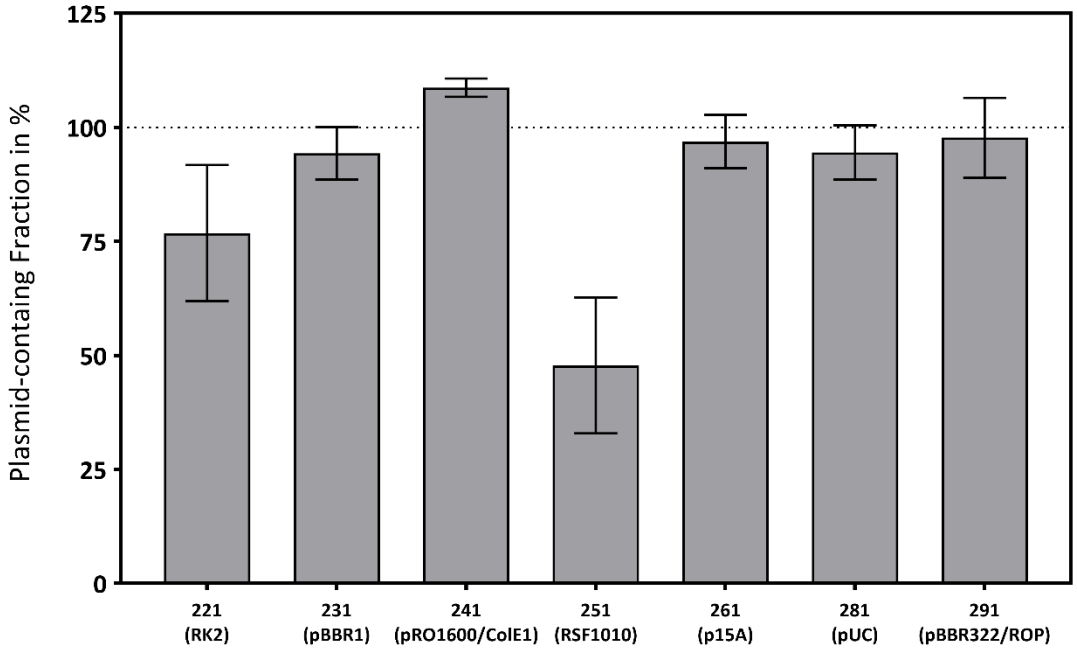

Figure 3.6 Stability of plasmid maintenance during bacterial growth of SOMR-1 harbouring plasmids: pSEVA221, 231, 241, 251, 261, 281, 271, 291 were cultivated in LB liquid medium without antibiotic selection for 24h. Percentage of plasmid retention in the culture was calculated by dividing the number of CFU with antibiotic selection of 50 µg/mL Km by the number of total CFU per dilution. The data are from at least 3 biological replicates with SEM.

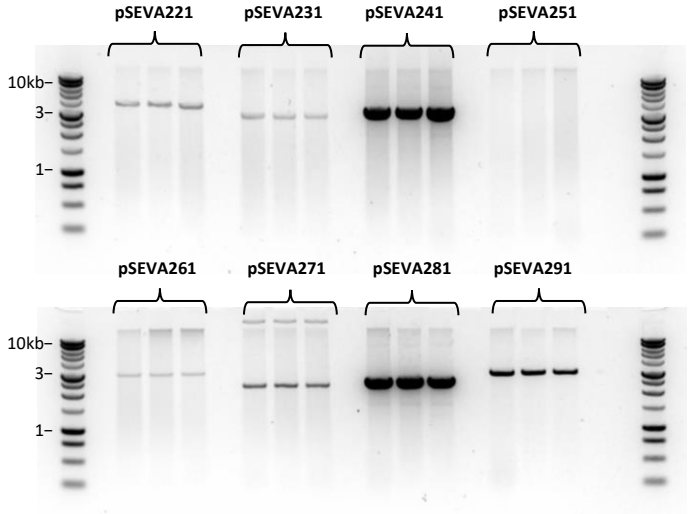

Figure 3.7 1% agarose gel showing linearised plasmid DNA of pSEVA 221-291 isolated from SOMR-1 cut with AscI. Expected band sizes are pSEVA221 (3823 bp), pSEVA231 (3123 bp), pSEVA241 (357 0bp), pSEVA251 (5275 bp), pSEVA261 (2334 bp), pSEVA271 (3061 bp), pSEVA821 (2530 bp), pSEVA291 (2986 bp).

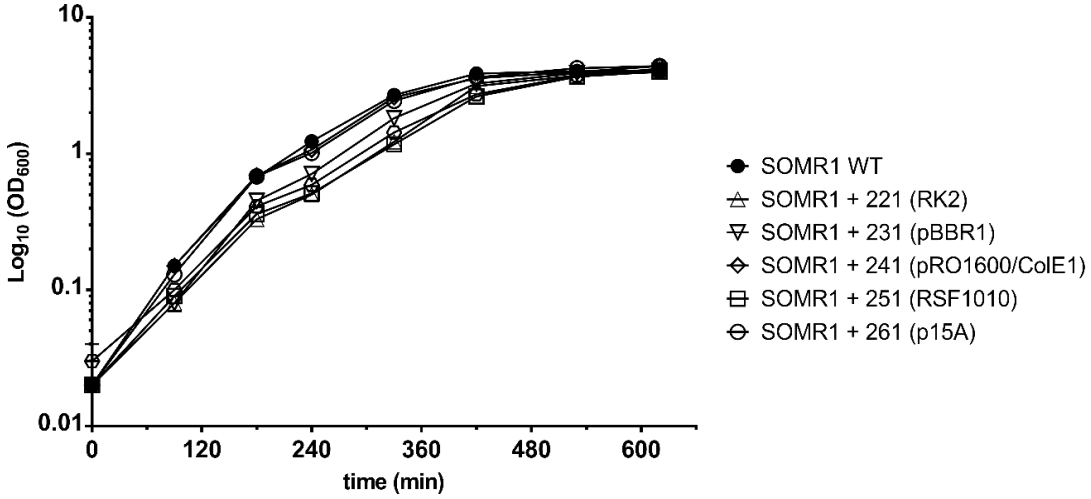

Figure 3.8 Aerobic growth curves of SOMR-1 harbouring pSEVA (Kan^R) with varying oriV. Cultures were inoculated from overnight cultures with a starting OD_{600} of 0.02 for 10 h. Data points show mean OD_{600} (n=3) with SD.

3.2.2.4 *Determination of Plasmid Copy Numbers of pEVA Expression Vectors in SOMR-1*

Since gene dosage can be crucial in biotechnological applications, knowing the plasmid copy number (PCN) in a given host, either to ensure that plasmids are passed to daughter cells reliably in case of low mean PCN or to avoid potential metabolic burden to host cells for high copy-number plasmids, can be essential for efficient protein production and fine-tuning of gene expression (Jones et al. 2000).

Here, to determine pSEVA plasmid copy numbers in recombinant SOMR-1 cultures, real-time quantitative PCR (qPCR) technology was used. This offers fast and sensitive quantification of any target sequence in a sample. Real-time qPCR was performed as described in Lee *et al*. (2006) with alterations [2.2.5.1] (Lee et al. 2006).

To determine the PCN of pSEVA vectors with different oriV in SOMR-1, two separate, single-copy genes were chosen as detection targets (see Table 3.4). The SOMR-1chromosomal gene target was chosen to be 1-deoxy-D-xylulose-5-phosphate synthase (*dxs*; SO1525). The plasmid gene target was the pSEVA kanamycin

resistance gene, i.e. neomycin phosphotransferase (*neo*). Subsequently, since both *neo* and *dxs* are single-copy genes of pSEVA2X1 and SOMR-1 chromosomal DNA, respectively, the plasmid copy number can be determined as the copy ratio of *neo* to *dxs*.

Table 3.4 Primer Sequences for real-time qPCR.

Target	**Accession number**	**Primers (5'→3')**	**Length (nt)**	**Primer position**	**Product size (bp)**
dxs	Q8EGR9	F: GCCGTCCCTAAATTTGACCC	20	1602020-1602039	233
		R: CCTAAGGTCACCGCATGTTG	20	1601807-1601826	
neo	AFV59772.1	F: GATCGTGTGTTTCGTCTGGC	20	810-829	90
		R: CCAGCCGTTACGTTCATCAT	20	880-899	

Bp = base pair; F = forward; nt = nucleotide; R = reverse.

3.2.2.4.1 *Amplification Specificity of Real-time qPCR Primer sets*

Amplification specificity of primer sets (see Table 3.4) were confirmed by Real-time qPCR melting curve analysis and gel electrophoresis (see Figure 3.9; 1B and 2B) with the *dxs*-set (1) and *neo*-set (2). Both sets showed a sharp single melting peak at 81.24°C and 81.84°C for *dxs* and *neo* set, respectively, using total DNA (tDNA) from SOMR-1 WT and from those harbouring pSEVA221-261 as template. Correspondingly, every PCR generated prominent single bands at the expected sizes of 233 bp and 90 bp for the *dxs* and *neo*-set respectively. These results confirm that the selected primer sets do not produce non-specific PCR products that can be detected in the analysed temperature range.

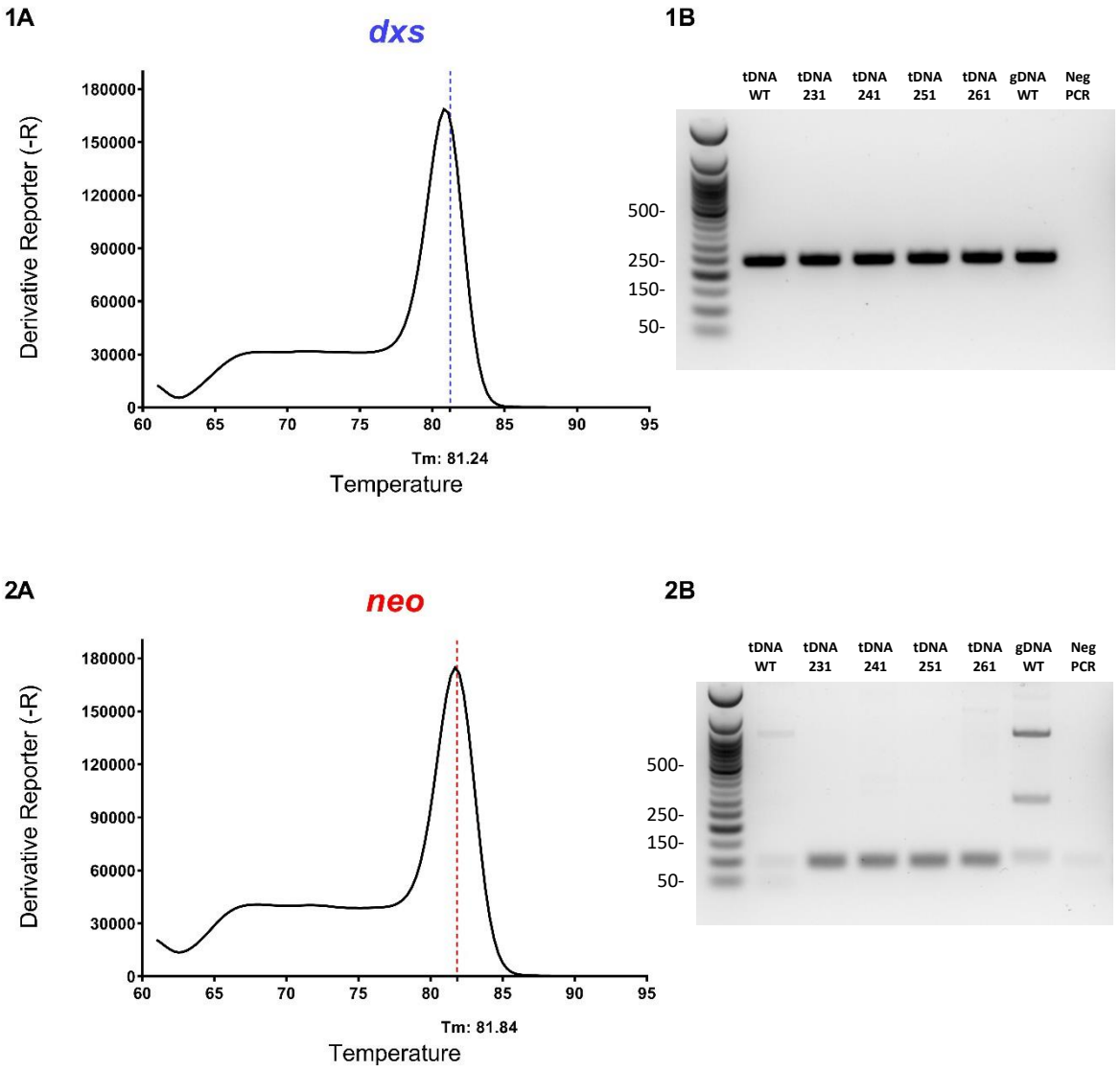

Figure 3.9 Confirmation of qPCR primer amplification specificities of dxs and neo primers using tDNA from SOMR-1 WT and pSEVA2X1 samples (n=18). Left panel: Melting curves of dxs primers (1A) and neo primers (2A). Right panel: 2% agarose gels showing PCR products for dxs primers (1B, expected band size 233 bp) and neo primers (2B, expected band size 90 bp). NEB 50 bp ladder. Tm = melting temperature; tDNA = total DNA; gDNA= genomic DNA.

3.2.2.4.2 *Real-time qPCR primer set standard curves and amplification efficiencies*

Further, standard curves and amplification efficiencies were calculated for both *dxs* and *neo* primer sets to ensure that their amplification efficiencies matched (Figure 3.10). Both curves were generated using 10-fold serial dilutions of tDNA from SOMR-1 harbouring pSEVA261 in the quantities of 20ng, 2ng, 0.2ng. Regression curves for *dxs* and *neo* were both linear with an $R^2 \geq 0.98$. The slopes of the standard curves for *dxs* and *neo* were nearly identical with -3.309 and -3.299 respectively, with amplification efficiencies of 100.56% and 100.99% validating the suitability of these primer sets to calculate the relative ratio of chromosome amplicon to plasmid (Lee et al. 2006).

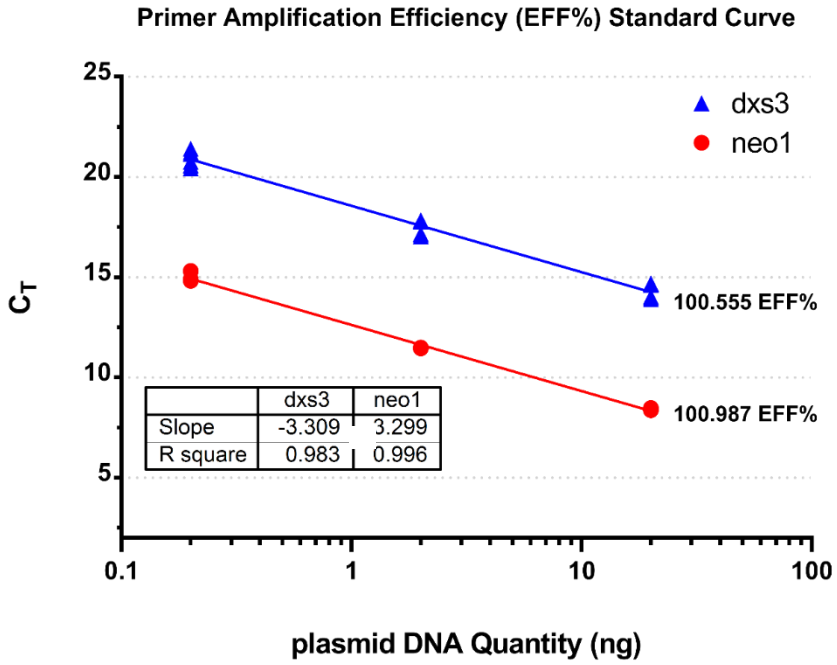

Figure 3.10 Primer amplification efficiencies standard curve of qPCR primer sets neo and dxs. Each curve was generated with 10-fold serial dilutions of tDNA (SOMR-1 WT and SOMR-1 harbouring pSEVA261) at 20 ng, 2 ng, and 0.2 ng. Each dilution was amplified by real-time qPCR using the neo and dxs primers in triplicate. Primer set dxs3 (n=18) has efficiency of 100.555% with a linear regression slope of -3.309. Primer set neo1 (n=9) has efficiency of 100.987% with a linear regression slope of -3.299.

3.2.2.4.3 *Determination of pSEVA plasmid copy number*

To determine the mean relative copy numbers of pSEVA plasmids in SOMR-1, *Shewanella* transconjugants harbouring pSEVA vectors with varying oriV (i.e. pSEVA221-291) and SOMR-1 WT were grown in biological triplicate in LB with 50µg/mL Km overnight from single colonies. These were sub-cultured and grown to mid-exponential phase (OD_{600} 0.7). Upon reaching the desired OD_{600} 4h post-inoculation, 1 mL of culture was harvested for total DNA extraction using the QIAamp DNA Mini kit (Qiagen) [2.2.4.1]. The protocol was amended for Gram-negative bacteria, and tDNA eluted in 200 µL AE and normalised to 2 ng/mL with deionised H20. Real-time QPCR amplification reaction mixtures were prepared as described in section [2.2.5.1] and the qPCR thermal cycling protocol. All tested samples of tDNA from SOMR-1 transconjugants showed expected melting curves at the predicted temperatures (data not shown). Additionally one of each technical triplicate sample for both primer sets was run on a 4 % agarose gel (see Figure 3.11) to further verify correct amplification of qPCR products and controls.

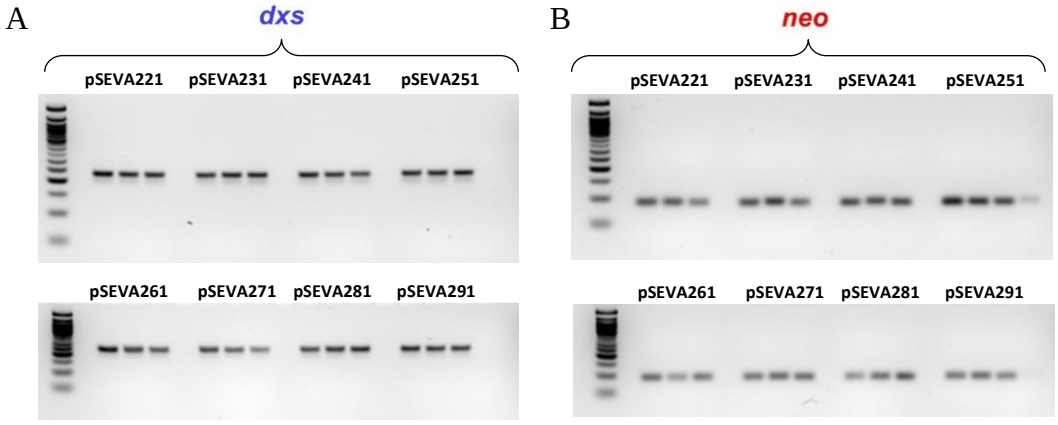

Figure 3.11 4% agarose gel showing qPCR products for SOMR-1 harbouring pSEVA plasmids 221-291 for each biological culture. A: dxs primer-set QPCR product (expected size 233 bp). B: neo primer-set qPCR product (expected size 90 bp). NEB 50 bp ladder.

All samples with *dxs* primer-set showed a band at the expected size of 233 bp, as well as the *neo* primer-set showing a band at the expected size of 90 bp (see Figure 3.11).

The threshold cycle (C_T) data for each reaction was analysed and exported using StepOne software v2.3 [see section 2.2.5.1.3]. To determine the mean relative copy numbers of pSEVA plasmids in SOMR-1, first, for each reaction the corresponding ΔC_T values were calculated by subtracting the C_T of the reference gene (*dxs*) from of amplicon C_T value of the target gene (*neo*). Then the expression fold change, i.e. the ratio of plasmid amplicon versus genomic amplicon, which gives the relative plasmid copy number (PCN) using the $2^{-\Delta CT}$ calculation of pSEVAs in SOMR-1, was calculated. The results of the relative quantification and the corresponding mean PCN for each vector are shown in Table 3.5 and Figure 3.12. The obtained plasmid copy numbers of these pSEVA vectors in SOMR-1 ranged from 1 to 21, however low copy numbers were dominant (see Table 3.5). Grouping these into low (PCN of 1-10), medium (PCN of 10-20) and high, (PCN of 20-100), $oriV_{pBBR1}$, $oriV_{RSF1010}$ and $oriV_{pSC101}$ were low copy in SOMR-1 with ≥2 copies, while $oriV_{RK2}$, $oriV_{p15A}$ and $oriV_{pBR322}$ ranged from circa 3 to 7 copies. Only the pUC and ColE1 oriV had the highest copy number with ~12 and ~21 plasmids per genome, respectively.

Table 3.5 Relative plasmid copy number.

Sample	ΔC_T[a,b]	PCN in SOMR-1 $2^{-\Delta C_T}$	Copy number group[c]	PCN in *E.coli*[d]
pSEVA221/oriV_{RK2}	-1.51±0.49	2.95±0.97	low copy	3 (low copy)
pSEVA231/oriV_{pBBR1}	-0.76±0.56	1.79±0.75	low copy	4.3 (low copy)
pSEVA241/oriV_{ColEI}	-4.36±0.29	20.83±3.9	high copy	30.8 (high copy)
pSEVA251/ori$V_{RSF1010}$	-0.28±0.36	1.24±0.32	low copy	3.9 (low copy)
pSEVA261/oriV_{p15A}	-2.49±0.70	7.40±2.30	low copy	6.5 (low copy)
pSEVA271/oriV_{pSC101}	-0.49±0.54	1.65±0.73	low copy	3.2 (low copy)
pSEVA281/oriV_{pUC}	-3.87±0.49	12.23±2.12	medium copy	7.8 (low copy)
pSEVA291/oriV_{pBR322}	-2.42±0.42	5.88±2.17	low copy	ND

[a]mean±SD (n=9); [b]ΔCT: CT of the target (neo)−CT of the reference (dxs);clow copy number = PCN 1-10; medium copy number = PCN 10-20; high copy number = PCN 20-100; [d]PCN of pSEVA vectors reported in E.coli DH5α (Jahn et al. 2016); ND = not determined.

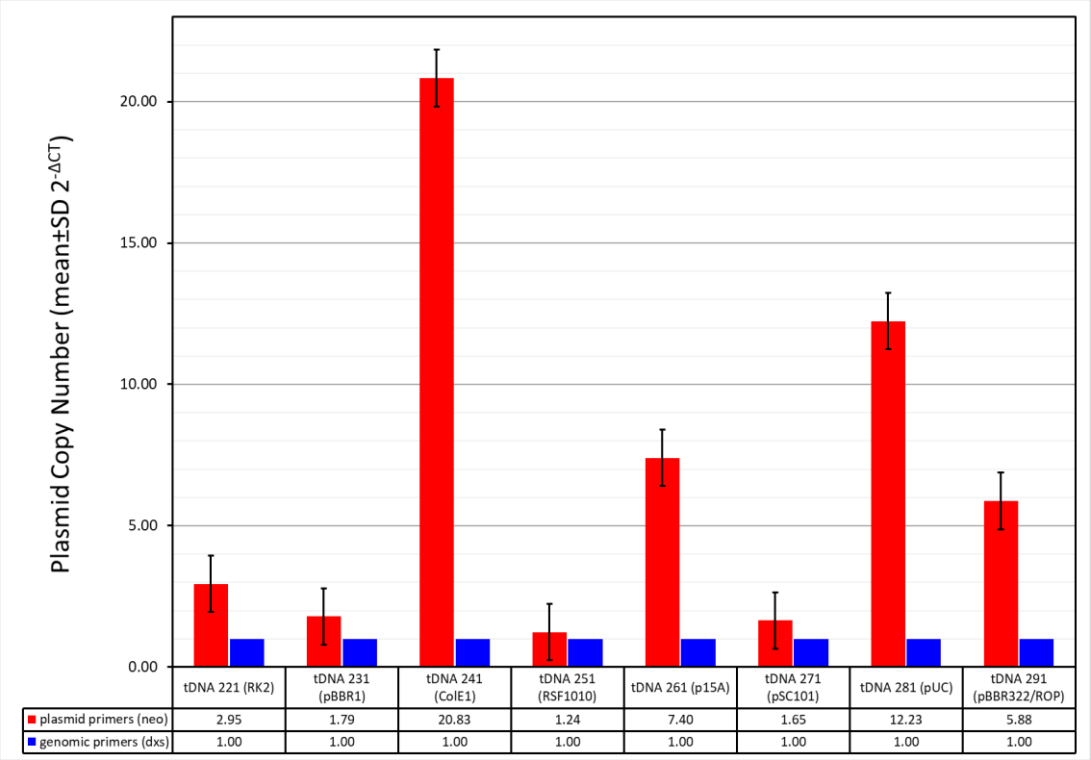

Figure 3.12 Average plasmid copy number (PCN) of pSEVA2X1 vectors in SOMR-1. tDNA of representative samples for each vector were extracted from batch culture at OD600 0.7. Bars show mean ± SD (n=9).

3.2.2.5 *pSEVA Plasmid oriV Compatibility for Multi-Plasmid Bearing Systems*

As synthetic gene circuits become more elaborate in size and complexity, it has become increasingly necessary to express these on multiple plasmids with different transcriptional regulators in a single host cell. To ensure stable plasmid maintenance and minimal metabolic burden and stress during bacterial propagation, these systems require to be fine-tuned in terms of origin of replication, antibiotic markers and transcriptional expression systems to optimise the desired biotechnological output. Current limitations in the field of synthetic biology are proving to be a true bottleneck, especially for novel model organism such as SOMR-1, for which quantative and qualitative data is lacking (Lee et al. 2011; Schmidt et al. 2012). Taking the pSEVA platform which has been shown to offer a range of vectors for SOMR-1, this section

aims to determine whether SOMR-1 can support maintenance of multiple pSEVA plasmids.

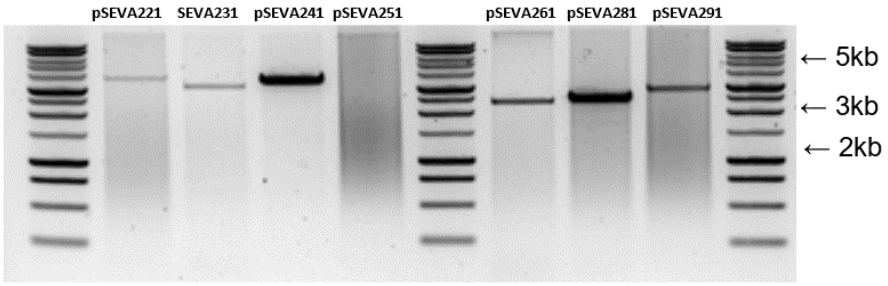

Figure 3.13 1% agarose gel showing AscI digestion of plasmid DNA isolated from SOMR-1 pSEVA2X1 mutants. Expected band sizes are pSEVA221 (3823bp), pSEVA231 (3123bp), pSEVA241 (3570 bp), pSEVA251 (5275 bp), pSEVA261 (2334 bp), pSEVA281 (2530 bp), pSEVA291 (2986 bp). DNA ladder: 1kb Promega.

Using the pSEVA vector set with Km resistance (2X1) as baseline which were at the time, conjugations between SOMR-1 and *E.coli* W3064 as the donor strain were performed as described in section 2.2.2.2.2. As previously shown in Figure 3.7, recipient SOMR-1 strains harbour the pSEVA2X1 plasmids and were verified by plasmid DNA digestion with *AscI,* which cuts pSEVAs only once, and gel electrophoresis (see Figure 3.13). Only pSEVA251 plasmid DNA could not be verified and did not show a band despite growth of the culture being normal. SOMR-1 harbouring pSEVA271 repeatedly failed to grow in overnight cultures for this experiment.

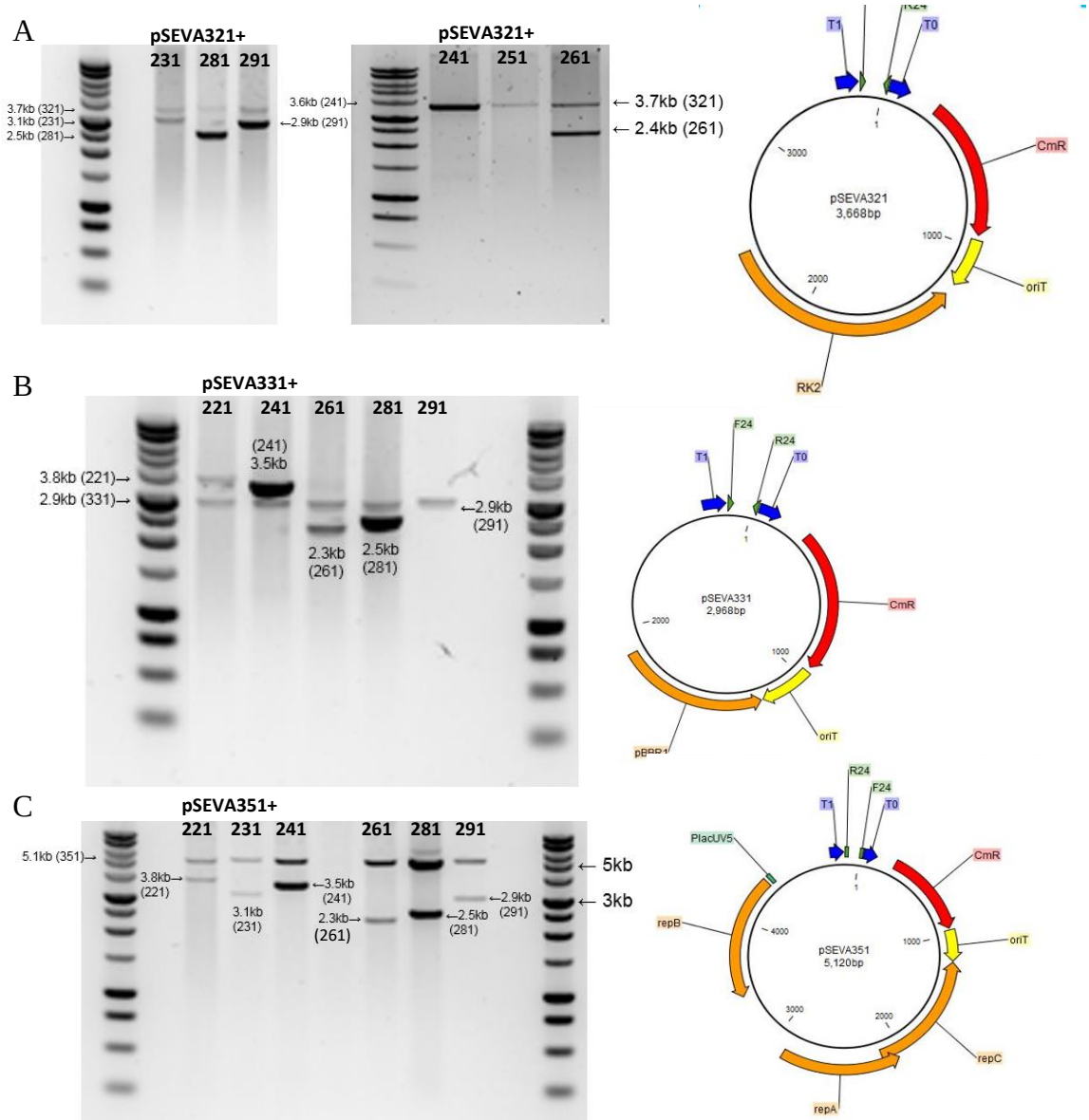

Figure 3.14 1%. Agarose gel showing AscI digestion of plasmid DNA isolated from SOMR-1 mutants harbouring: (A) pSEVA2X1 and pSEVA321 plasmids, (B) pSEVA2X1 and pSEVA331 plasmids, (C) pSEVA2X1 and pSEVA351 plasmids with accompanying plasmid vector maps. Expected band sizes are pSEVA221 (3823bp), pSEVA231 (3123bp), pSEVA241 (3570bp), pSEVA251 (5275bp), pSEVA261 (2334bp), pSEVA281 (2530bp), pSEVA291 (2986bp), pSEVA321 (3668bp), pSEVA331 (2968bp), pSSEVA351 (5120bp). DNA ladder: 1kb Promega.

Most dual-plasmid combinations yielded viable colonies. SOMR-1 transconjugants were then grown overnight in LB with appropriate antibiotic selection (50 µg/mL Km and 20 µg/mL Cm, or 50 µg/mL Km and 10 µg/mL Gm) and plasmid DNA extracted. To detect whether the tested plasmids were present in SOMR-1 transconjugants the extracted plasmid DNA was again digested with *AscI* restriction enzyme. Figure 3.14A shows successful dual-plasmid systems.

The pSEVA321 (Cm^R, $oriV_{RK2}$, MCS) was maintained with pSEVA231 (Km^R, $oriV_{pBBR1}$, MCS), pSEVA241 (Km^R, $oriV_{ColEI}$, MCS), pSEVA261 (Km^R, $oriV_{p15A}$, MCS), pSEVA281 ($oriV_{pUC}$) and pSEVA291 (Km^R, $oriV_{ppBBR322/ROB}$, MCS). Similarly, pSEVA331 (Cm^R, $oriV_{pBBR1}$, MCS; see Figure 3.14B) was compatible with the same range of pSEVA2X1, with the exception of pSEVA231 ($oriV_{pBBR1}$) and pSEVA251. However, pSEVA221 (Km^R, $oriV_{RK2}$, MCS), was also compatible. Lastly, pSEVA351 (Cm^R, $oriV_{RSF1010}$, MCS; Figure 3.14C), an oriV which has proven difficult to maintain with Km resistance in SOMR-1, appeared to not only replicate well with this resistance cassette, but also was compatible with all seven oriV tested in this experiment, with the exception of pSEVA251 which did not yield in viable transconjugants.

Dual plasmid systems for pSEVA6X1 (Gm^R) were equally successful. Figure 3.15A shows the successful dual-plasmid systems.

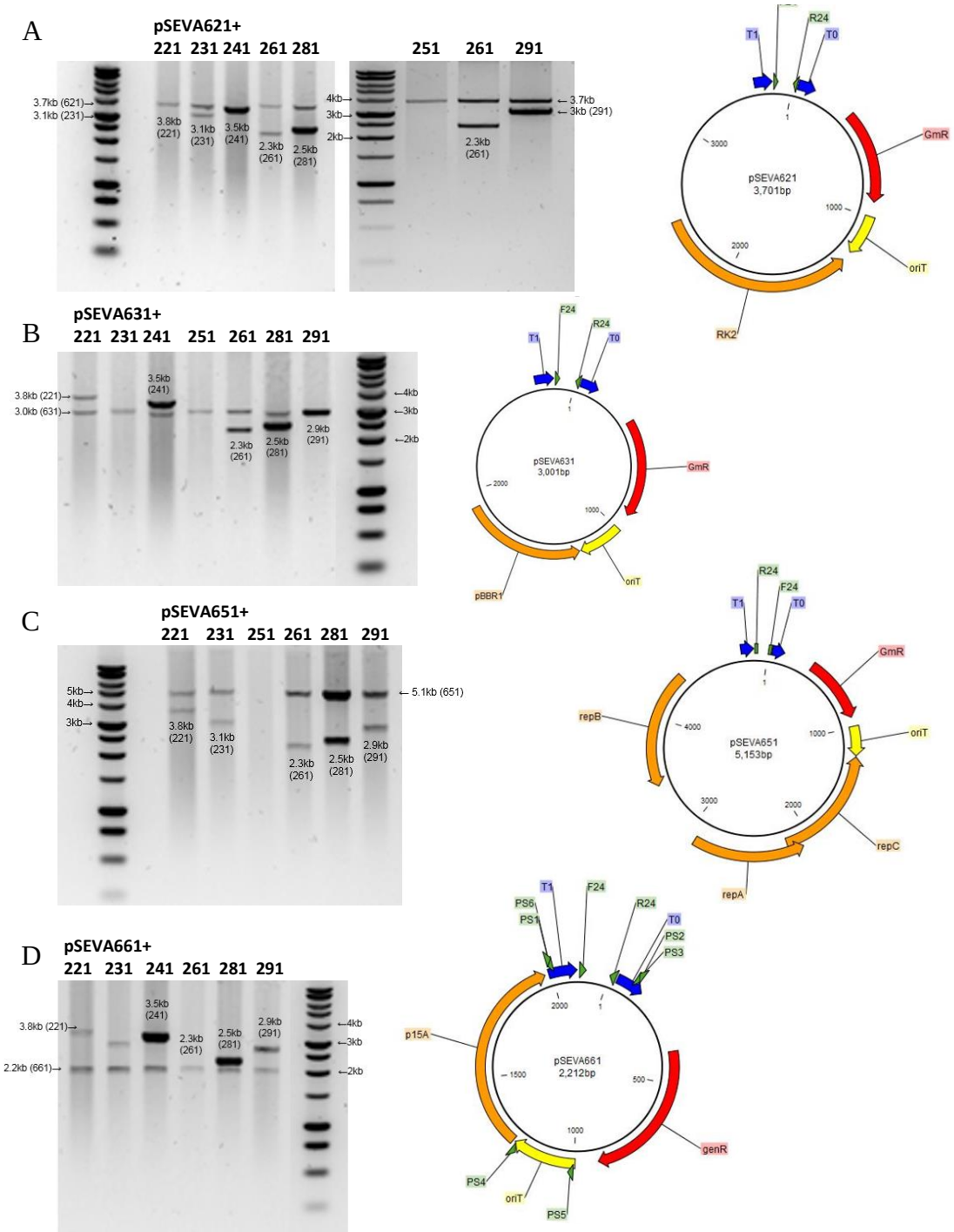

Figure 3.15 1% Agarose gel showing AscI digestion of plasmid DNA isolated from SOMR-1 mutants harbouring: (A) pSEVA2X1 and pSEVA621 plasmids, (B) pSEVA2X1 and pSEVA631 plasmids, (C) pSEVA2X1 and pSEVA651 plasmids with accompanying plasmid vector maps. Expected band sizes are pSEVA221 (3823bp), pSEVA231 (3123bp), pSEVA241 (3570bp), pSEVA251 (5275bp), pSEVA261 (2334bp), pSEVA281 (2530bp), pSEVA291 (2986bp), pSEVA621 (3701bp), pSEVA631 (3005bp), pSEVA651 (5153bp), pSEVA661 (2212bp). oriV pSEVA2X1 = RK2 (221), 3: pBBR1 (231), 4: ColEI (241), 5: RSF1010 (251), 6:p15A (261), 8: pUC (281), 9:pBBR322 (291); DNA ladder: 1kb Promega.

Table 3.6 pSEVA multi-plasmid compatibility in SOMR-1. SOMR-1 harbouring pSEVA2X1 were conjugated with E.coli WM3064 as donor strain harbouring available pSEVA3X1 or pSEVA6X1. SOMR-1 transconjugants were grown overnight in LB with appropriate antibiotic selection (50 µg/mL Km and 20 µg/mL Cm, or 50 µg/mL Km and 10 µg/mL Gm) and plasmids confirmed by gel electrophoresis.

pSEVA/ oriV	Antibiotic	RK2	pBBR1	ColE1	RSF1010	p15A	pSC101	pUC	pBBR322/ ROB
	Km/Cm	321	331	341	351	361	371	381	391
RK2	221	x	✓	o	✓	NA	NA	NA	NA
pBBR1	231	✓	x	o	✓	NA	NA	NA	NA
ColE1	241	✓	✓	o	✓	NA	NA	NA	NA
RSF1010	251	✓*	x	o	x	NA	NA	NA	NA
p15A	261	✓	✓	o	✓	NA	NA	NA	NA
pSC101	271	o	o	o	o	NA	NA	NA	NA
pUC	281	✓	✓	o	✓	NA	NA	NA	NA
pBBR322/ROB	291	✓	✓	o	✓	NA	NA	NA	NA
	Km/Gm	621	631	641	651	661	671	681	691
RK2	221	✓	✓	o	✓	✓	NA	NA	NA
pBBR1	231	✓	**x**	o	✓	✓	NA	NA	NA
ColE1	241	✓	✓	o	**x**	✓	NA	NA	NA
RSF1010	251	✓*	✓*	o	**x**	**x**	NA	NA	NA
p15A	261	✓	✓	o	✓	✓	NA	NA	NA
pSC101	271	o	o	o	o	o	NA	NA	NA
pUC	281	✓	✓	o	✓	✓	NA	NA	NA
pBBR322/ROB	291	✓	✓	o	✓	✓	NA	NA	NA

*251 not visible on gel; x=plasmid not maintained; o = no growth in liquid culture; ✓ = both plasmids maintained; NA = plasmid not available.

3.2.3 *Effect of Plasmid Maintenance on Flavin Production*

Recently, the bacterial flavin exporter (Bfe) was identified in SOMR-1 and is encoded by the *bfe* gene (SO_0702) (Kotloski and Gralnick 2013). To establish whether plasmid maintenance of pSEVA vectors affects flavin production, one of the main EET mechanism for this organism, bulk flavin assays were performed. the on SOMR-1 harbouring pSEVA2X1 and further SOMR-1 *Δbfe* harbouring pSEVA2X1. All plasmids were conjugated into SOMR-1. LB Overnight cultures were used to freshly inoculate SBM medium with 30 µg/mL Km. After 12 h of growth at 30°C shaking t 200 rpm, samples were taken and OD_{600} measure and 1 mL of culture centrifuged to obtain cell-free portion which was transferred to a fluorescence 96-well plate (Greiner,

see section 2.2.8). Figure 3.16 shows no negative effect of plasmid maintenance with respect to flavin production compared to WT, additionally there are no stark difference in flavin output from *Δbfe* between the different vectors.

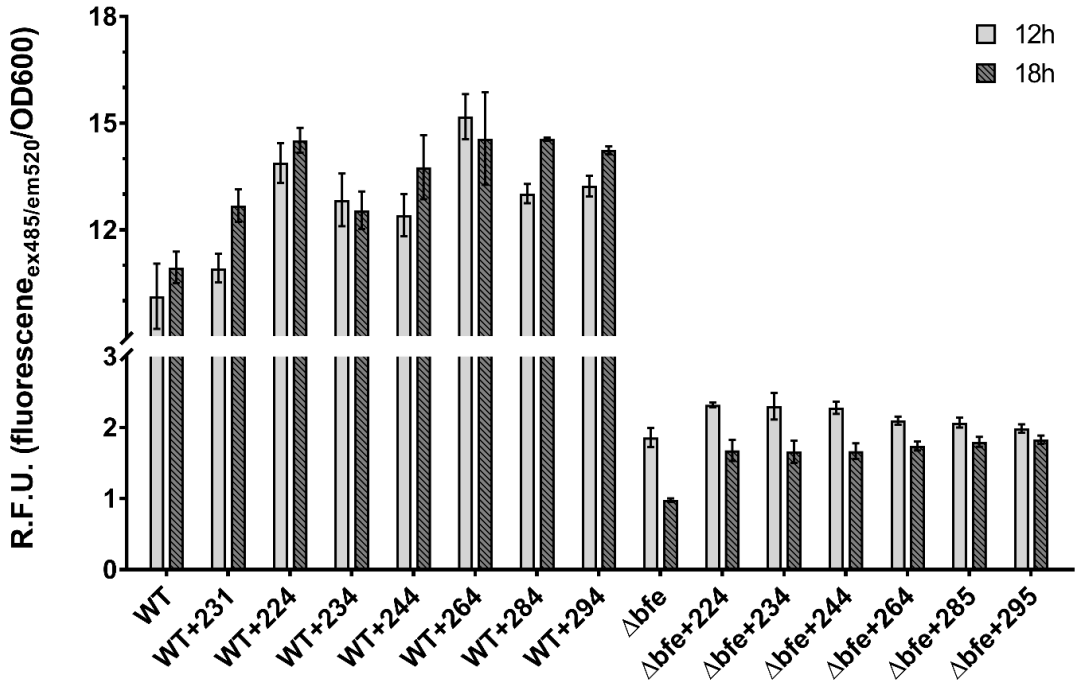

Figure 3.16 Bulk flavin production by SOMR-1 harbouring pSEVA2X1 and Δbfe harbouring pSEVA2X1. LB Overnight cultures were used to freshly inoculate SBM medium with 30 µg/mL Km. After 12 h and 18 h of growth at 30°C shaking at 200 rpm, samples were taken and OD_{600} measure and 1 mL of culture centrifuged to obtain cell-free portion which was transferred to a fluorescence 96-well plate (Greiner). Bar represent triplicates mean with SD. RFU, relative fluorescence unit; WT, wild type.

3.2.4 *Establishing phiLOV as a New Fluorescence Reporter Tool in SOMR-1*

The discovery of green-fluorescent protein (GFP) and their numerous derivatives has been a powerful tool for molecular biology in the past 2 decades having had a tremendous impact to elucidate molecular mechanisms in a diverse range of organisms (Tsien 1998). One drawback of these reporter molecules, however, is their oxygen-dependent fluorescence (Remington 2006). As a consequence, GFP-based proteins fluorescent only minimally or are non-fluorescent in hypoxic and anoxic environments, making investigation of bioprocesses such as microbial fermentation, bioremediation, and biofilm formation challenging (Mukherjee et al. 2013). Therefore, GFP-based fluorescent proteins are only marginally suitable to characterise SOMR-1 under anaerobic conditions and to further investigate the mechanisms of their electroactive biofilms in MFC settings. Recently, a novel class of oxygen-independent fluorescent reporter proteins was developed based on bacterial and plant photosensory flavoproteins (Drepper et al. 2007; Chapman et al. 2008). One of these, the fluorescent flavoprotein phiLOV is derived from the light, oxygen, or voltage (LOV) domain of the plant blue light receptor phototrophin (Gawthorne et al. 2012; Christie et al. 2012) (see Figure 3.17A). The main advantage over green fluorescent protein (GFP) is its small size, its photostability and its efficacy under anaerobic conditions. The latter is especially important when characterising anaerobic electro-active biofilms in MFCs. These attributes make this reporter a promising candidate to add to the SOMR-1 toolbox for screening gene expression outputs but also potentially for further investigating the structure and composition of SOMR-1 electro-active biofilms.

To allow for optimal expression of this reporter in the bacterium SOMR-1, the gene sequence of phiLOV was codon-optimised for expression in SOMR-1 (see Figure 3.17B). To preliminary test whether the obtained synthesised gene works in SOMR-1,

it was cloned into pZJ56b (Km^R, $oriV_{ColEI}$, $P_{J23119} \rightarrow$ *gfp*) and placed under the constitutive Anderson promoter J23119[15] (Mai-Britt Jensen, personal communications) (see Figure 3.18A). Further, phiLOV was also cloned into pZJ7::phiLOV_SO_opt [pBAD33 (Cm^R, $oriV_{p15A}$), $P_{ara} \rightarrow$ *phiLOV_SO*] and placed under the induciable P_{ara} promoter (Mai-Britt Jensen, personal communications) (see Figure 3.18A).

A

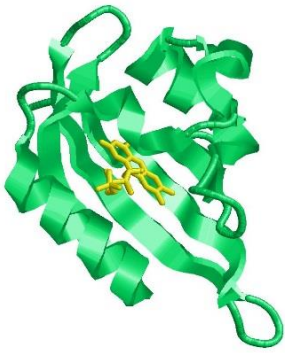

B

phiLOV	ATG	ATC	GAG	AAA	AGC	TTC	GTT	ATT	ACC	GAT	CCA	CGT	TTA	CCG	GAT	TAT	CCA	ATT	ATC	TTT	GCA	AGT	GAT								
Translation ORF/CDS	M	I	E	K	S	F	V	I	T	D	P	R	L	P	D	Y	P	I	I	F	A	S	D								
phiLOV	GGT	TTT	CTG	GAA	TTA	ACC	GAA	TAT	AGC	CGT	GAA	GAA	ATT	ATG	GGT	CGC	AAT	GCA	CGT	TTT	CTG	CAG	GGT								
Translation ORF/CDS	G	F	L	E	L	T	E	Y	S	R	E	E	I	M	G	R	N	A	R	F	L	Q	G								
phiLOV	CCA	GAA	ACC	GAT	CAG	GCA	ACC	GTT	CAG	AAA	ATT	CGT	GAT	GCC	ATT	CGC	GAT	CAG	CGT	GAA	ACC	ACC	GTT								
Translation ORF/CDS	P	E	T	D	Q	A	T	V	Q	K	I	R	D	A	I	R	D	Q	R	E	T	T	V								
phiLOV	CAG	TTA	ATT	AAC	TAT	ACC	AAA	AGC	GGC	AAA	AAA	TTC	TGG	AAT	CTG	TTA	CAT	CTG	CAG	CCA	GTT	CGC	GAT								
Translation ORF/CDS	Q	L	I	N	Y	T	K	S	G	K	K	F	W	N	L	L	H	L	Q	P	V	R	D								
phiLOV	CGT	AAA	GGT	GGT	CTG	CAG	TAT	TTT	ATC	GGT	GTT	CAG	TTA	GTT	GGT	AGC	GAT	CAT	GTT	TAA											
Translation ORF/CDS	R	K	G	G	L	Q	Y	F	I	G	V	Q	L	V	G	S	D	H	V	*											

Figure 3.17 (A) phiLOV2.1 tertiary crystal protein structure (green) with cofactor FMN (yellow) (PDB: 4EEU[16,17,18]). (B) phiLOV gene and amino acid sequence codon optimised for SOMR-1 (Mai-Britt Jensen, personal communication).

[15] http://parts.igem.org/Part:BBa_J23119
[16] http://www.ebi.ac.uk/pdbe/entry/pdb/4EEU
[17] http://www.uniprot.org/uniprot/P93025
[18] http://www.rcsb.org/pdb/explore/remediatedSequence.do?structureId=4EEU

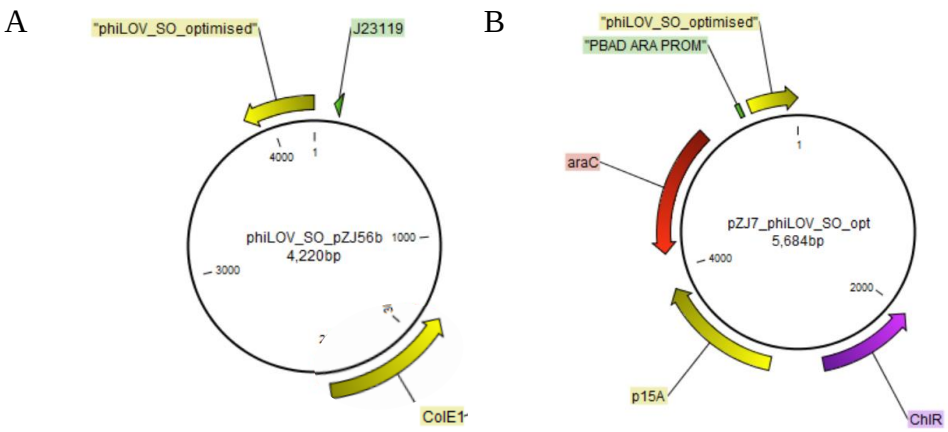

Figure 3.18 Vector maps of (A) pZJ56b::phiLOV_SO [Km^R, $oriV_{ColEI}$, P_{J23119}→ phiLOV_SO*] and (B) pZJ7::phiLOV_SO_opt [pBAD (Cm^R, $oriV_{p15A)}$, P_{ara}→* phiLOV_SO].

SOMR-1 was transformed with these plasmids using electroporation as described in section 2.2.2.2.1. Transformants were screened using plasmid restriction digestion (data not shown). SOMR-1 WT and SOMR-1 harbouring pZJ56b::phiLOV_SO were grown overnight in LB media containing 50 µg/mL Km shaking at 30°C at 200 rpm. Cells were washed twice in PBS (see section 2.2.8) to remove excreted endogenous flavins. Pelleted cell mass showed fluorescence under blue light (470 nm) (see Figure 3.19).

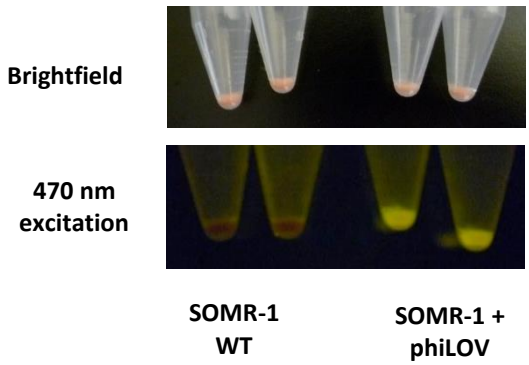

Figure 3.19 Fluorescence of phiLOV under blue light (470 nm) in SOMR-1 harbouring pZJ56b::phiLOV_SO. SOMR-1 WT and SOMR-1 harbouring pZJ56b::phiLOV_SO were grown overnight in LB media containing 50 µg/mL Km shaking at 30°C at 200 rpm. Cells were washed twice in PBS.

3.2.4.1 *Fluorescent Intensity of phiLOV under Constitutive Promoter P_{23119} in SOMR-1*

The codon optimised phiLOV gene was also cloned in two vectors with $oriV_{ColEI}$ and $oriV_{pBBR1}$ under the constitutive promoter P_{23119} (kindly provided by Mai-Britt Jensen). Aerobic flavin assays were performed as described in section 2.2.8. Relative fluorescence seen from SOMR-1 mutants expressing phiLOV under $P_{23119,}$ $oriV_{ColEI}$ increased 2-fold compared to SOMR-1 WT. Relative fluorescence seen from SOMR-1 mutants expressing phiLOV under $P_{23119,}$ $oriV_{pBBR1}$ only increased 1.2-fold compared to SOMR-1 WT (see Figure 3.20A). This makes a meaningful distinction of fluorescence between SOMR-1 endogenous flavins and phiLOV challenging. Furthermore, comparing this to the fluorescence intensity of GFP (see Figure 3.20B), an almost 9-fold increase can observed between phiLOV and GFP in SOMR-1.

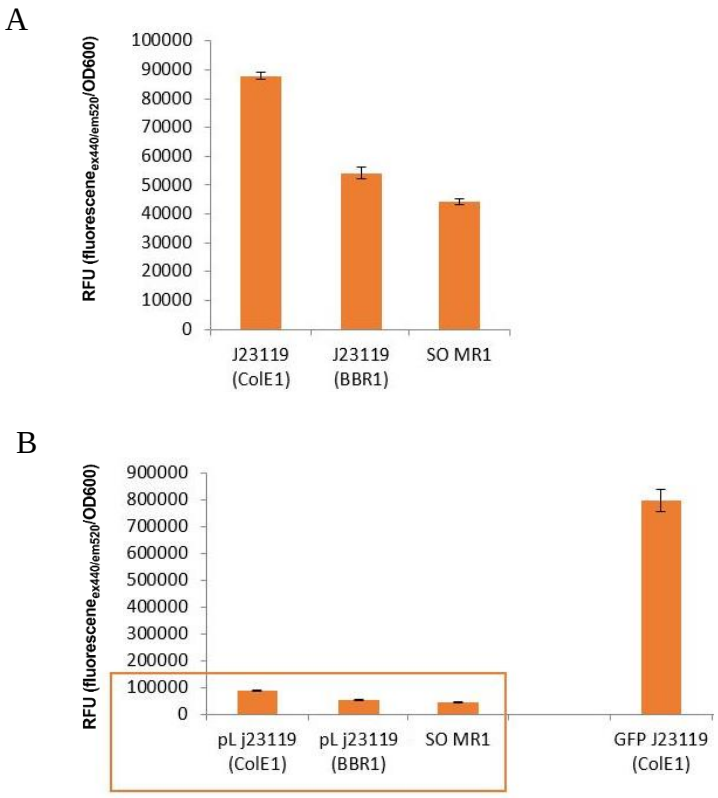

Figure 3.20 Relative fluorescence units ($Ex_{420nm}/Em_{520nm}/OD_{600}$) of SOMR-1 expressing phiLOV under (A) strong constitutive promoter P_{J23119} in a vector backbone with high-copy number $oriV_{ColEI}$ and $oriV_{pBBR1}$ versus WT and (B) SOMR-1 expressing P_{J23119}→GFP ($oriV_{ColEI}$) (data kindly provided by Mai-Britt Jensen, personal communications).

3.2.4.2 *A two-plasmid orthogonal expression system using P_{T7}, T7 RNA polymerase and phiLOV in SOMR-1*

T7 RNAP has long been the workhorse for molecular engineering and synthetic biology applications. This single polypeptide polymerase allows the transcription of target genes in high abundance using the highly specific, however short 17 bp promoter sequence (Chamberlin et al. 1970; Studier and Moffatt 1986). Establishing this expression system in SOMR-1 for the first time would be therefore highly desirable, allowing gene expression that is independent to SOMR-1's host machinery and promoters.

To further investigate whether phiLOV is a suitable reporter, a two-plasmid orthogonal expression system, using P_{T7} and T7 RNA polymerase (RNAP), was designed (see Figure 3.21A). T7 RNA polymerase was PCR amplified using *E. coli* BL-21 gDNA as template; primers were designed to add *Sac*I to the 5'end and *Xba*I to the 3'end. PCR product was verified using aragose gel electrophoresis and bands of the correct size were cleaned up, and restriction digestion for 2 h with *Sac*I and *Xba*I of the purified DNA and pBAD33 was performed and further cleaned up before ligation with T4 ligase (see section 2.2.4.4). Ligations were transformed into *E. coli* TOP10 and transformants were screened for correct plasmids using restriction digestion, then further verified using sanger sequencing resulting in plasmid (Figure 3.21B). Similarly, an oligonucleotide was designed to add the P_{T7} promoter, a specifically designed SOMR-1 RBS using the RBS calculator version 2.0[19] (Figure 3.21D) with a 5' EcoRI restriction site. The reverse primer to amplify phiLOV was designed to add *Xba*I restriction site to the 3' end of the phiLOV gene. Touchdown PCR was performed with previously mentioned primers and pZJ56b::phiLOV_SO as template DNA; the PCR product was verified using agarose gel electrophoresis and bands of the correct size were cleaned up, then restriction digestion for 2h with *Eco*RI and *Xba*I of the purified DNA and pSEVA231 was performed and further cleaned up before ligation with T4 ligase. Ligations were transformed into *E. coli* TOP10 and transformants were screened for correct plasmids using restriction digestion and further verified using sanger sequencing resulting in plasmid (Figure 3.21C).

[19] https://www.denovodna.com/software/

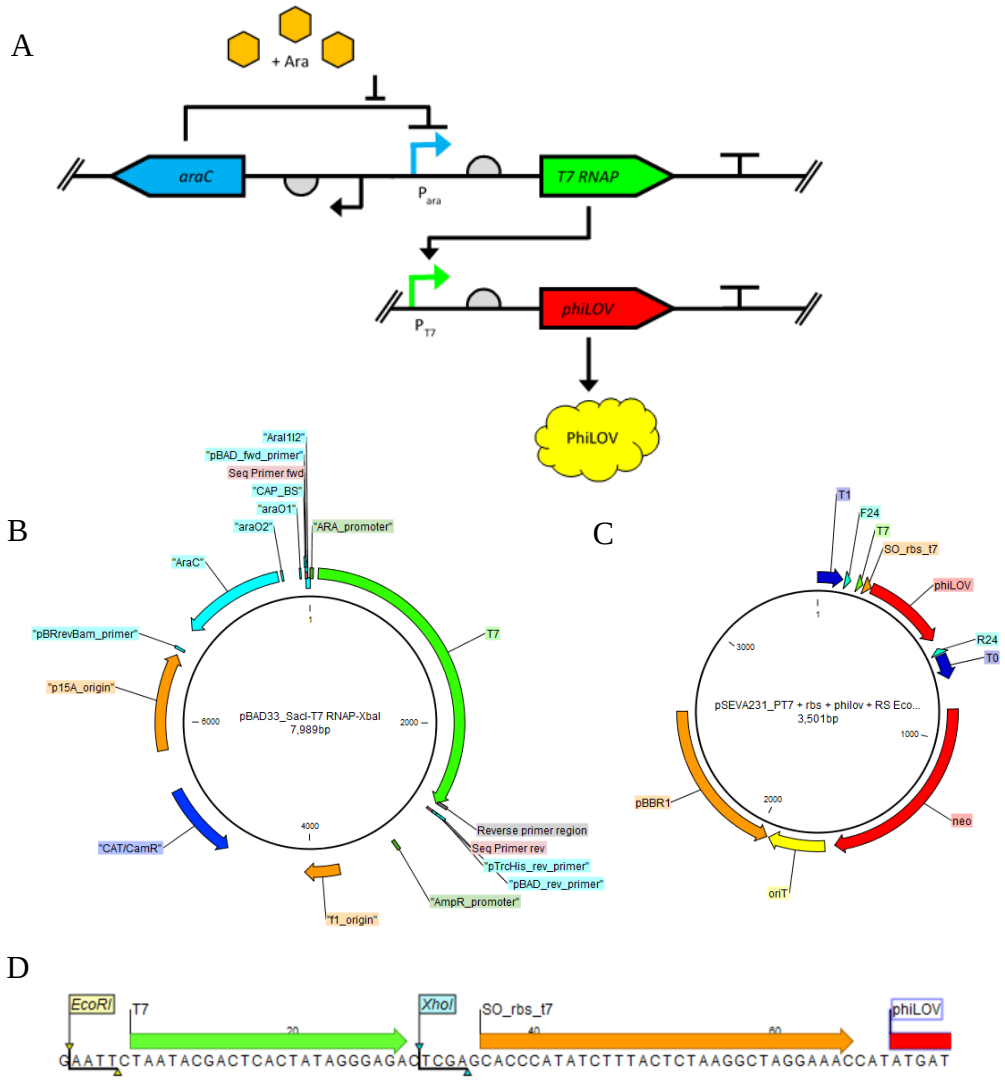

Figure 3.21 Schematic two-plasmid T7 RNAP - PT7 expression system with phiLOV reporter. (A) Transcriptional regulation of T7 RNAP is negative regulated with araC and P_{ara} is induced with arabinose allowing transcription of T7 RNAP which will bind the P_{T7} allowing phiLOV expression. (B) Vector map of pBAD33::T7RNP (Cm^R, $oriV_{p15A}$, P_{ara}→T7RNAP). (C) Vector map of pSEVA23::P_{T7}::phiLOV (Km^R, $oriV_{pBBR1}$, P_{T7}→ phiLOV. (D).

SOMR-1 strains were sequentially transformed via electroporation (*NB* these experiments were carried out prior to acquisition of conjugation donor strain *E. coli* WM3064) with pSEVA23::P_{T7}::phiLOV and pBAD33::T7RNP. Transformants were selected on Km, Cm and Km plus Cm containing agar plates at 30°C static incubation. Triplicate cultures were inoculated and grown overnight in liquid LB media containing the appropriate antibiotic at 30°C shaking incubation at 200 rpm. Fresh cultures of LB media were inoculated at OD_{600} 0.02 and grown

aerobically to mid-exponential phase before being induced with 0.01%, 0.05% 0.1% and 2.0% (v/v) arabinose. Samples were taken 7 h post induction, washed in sterile PBS to remove SOMR-1 endogenous flavins, and fluorescence was measured using FLUOstar Omega microplate reader at 450 nm. Figure 3.22A shows SOMR-1 WT, SOMR-1 each harbouring pSEVA23::P_{T7}::phiLOV, pBAD33::T7RNP and both plasmids together, relative fluorescence measured and normalised to the mean wild type fluorescence emission level which was set to 1 RFU. All controls show the same baseline auto-fluorescence ≤ 2 RFU. Given that pBAD33::T7RNP does not express any fluorescent gene, having pSEVA23::P_{T7}::phiLOV RUF level at the same indicates that firstly the pSEVA backbone offers adequate insulation of the cargo gene and that the P_{T7} promoter sequence is not recognised by SOMR-1 endogenous polymerases, making this expression system independent and orthogonal. Increasing the concentration of arabinose induction from 0.01% to 2% only increases RFU 1.2-fold. Compared to the single vector controls, all induced two-plasmid systems show increased fluorescence 2-fold. Hence, further experiments were induced with 0.05% arabinose. Anaerobic cultures were grown in SBM media containing the appropriate antibiotic selection and were induced with 0.05% arabinose. However, no fluorescence increase was seen in the two-plasmid system, be it 3 h, 7 h, or 21 h post induction (see Figure 3.22B). In fact the auto-fluorescence from SOMR-1 harbouring pBAD33::T7RNP was highest.

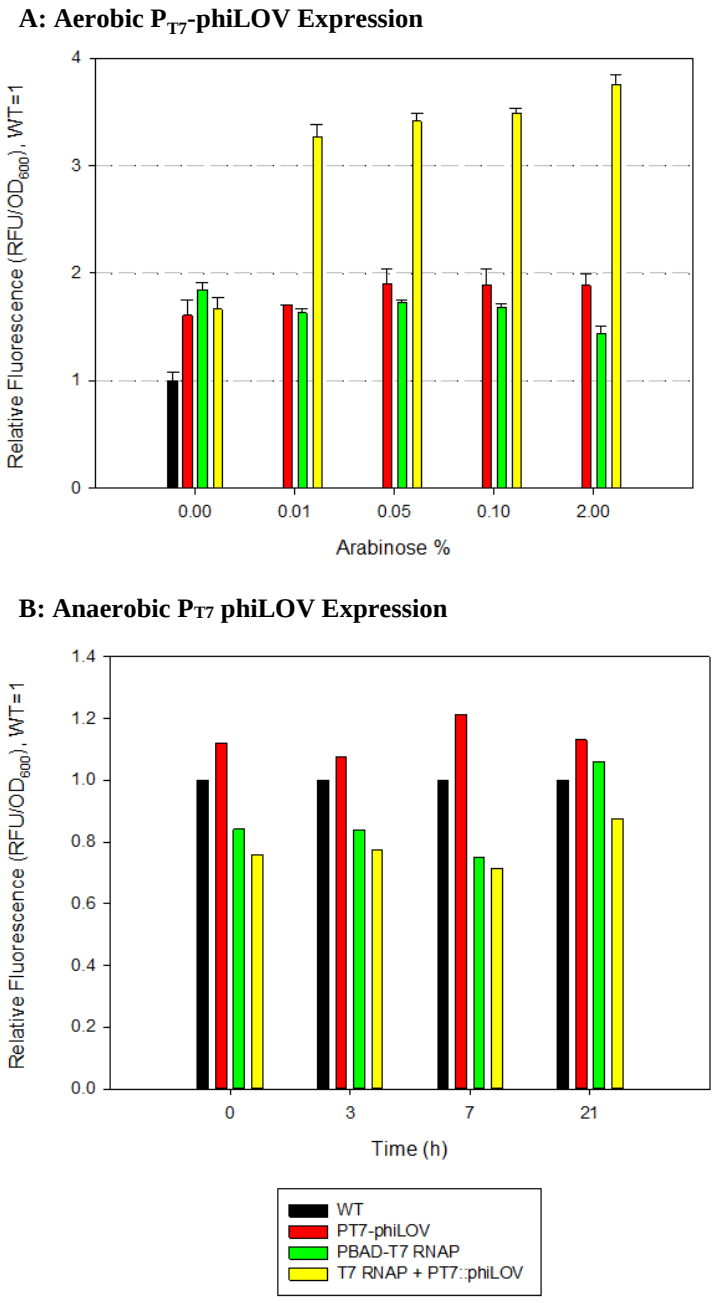

Figure 3.22 Fluorescence output of phiLOV expression driven by P_{T7} and T7 RNA Polymerase under P_{ara} promoter in SOMIR-1. (A) phiLOV expression under aerobic conditions with increasing arabinose concentrations 7 h post induction of SOMR-1 WT and transformants harbouring either pSEVA23::P_{T7}::phiLOV and pBAD33::T7RNP or both. (B) phiLOV expression under anaerobic conditions over time induced with 0.05% arabinose. Fluorescence was measured using FLUOstar Omega microplate reader. Bar graphs show relative fluorescence normalised to wild type fluorescence of triplicate samples with SEM error bars.

3.2.4.3 *Characterisation of SOMR-1 Endogenous Promoter of its Bacterial Flavin Exporter (Bfe) using phiLOV*

To test whether phiLOV could be used to characterise endogenous SOMR-1 promoters that are important to EET, the promoter of the bacterial flavin exporter (Bfe) (Kotloski and Gralnick 2013) was cloned. The 227 bp region upstream of the *bfe* gene (SO_0702) up to the preceding gene *groES* (SO_0703) (see Figure 3.23A) was amplified using touchdown PCR with primers which were designed to add *Sac*I to the 5' end and *Nde*I restriction sites to the 3' end using SOMR-1 gDNA as PCR template. The PCR product was verified by gel electrophoresis. Then the appropriate band was excised, gel purified and digested with *Sac*I and *Nde*I. The vector pSEVA23::phiLOV was digested with *Sac*I and *Nde*I for 2 h. The promoter and vector backbone were then ligated to yield vector pSEVA26::P_{bfe}::phiLOV (see Figure 3.23B). The resulting plasmid was verified by restriction digestion and sanger sequencing and transformed via electroporation into SOMR-1. Transconjugants were grown overnight in LB containing 50 µg/mL from single colonies. SOMR-1 WT and SOMR-1 harbouring pZJ56b::phiLOV_SO with the constitutive P_{23119} were used as controls. Samples were taken and washed twice in PBS to remove excreted flavins from the media. Relative fluorescence of phiLOV under P_{bfe} were similar to the fluorescent intensity of phiLOV under and P_{23119} and ~3-fold higher than the WT control (see Figure 3.23C).

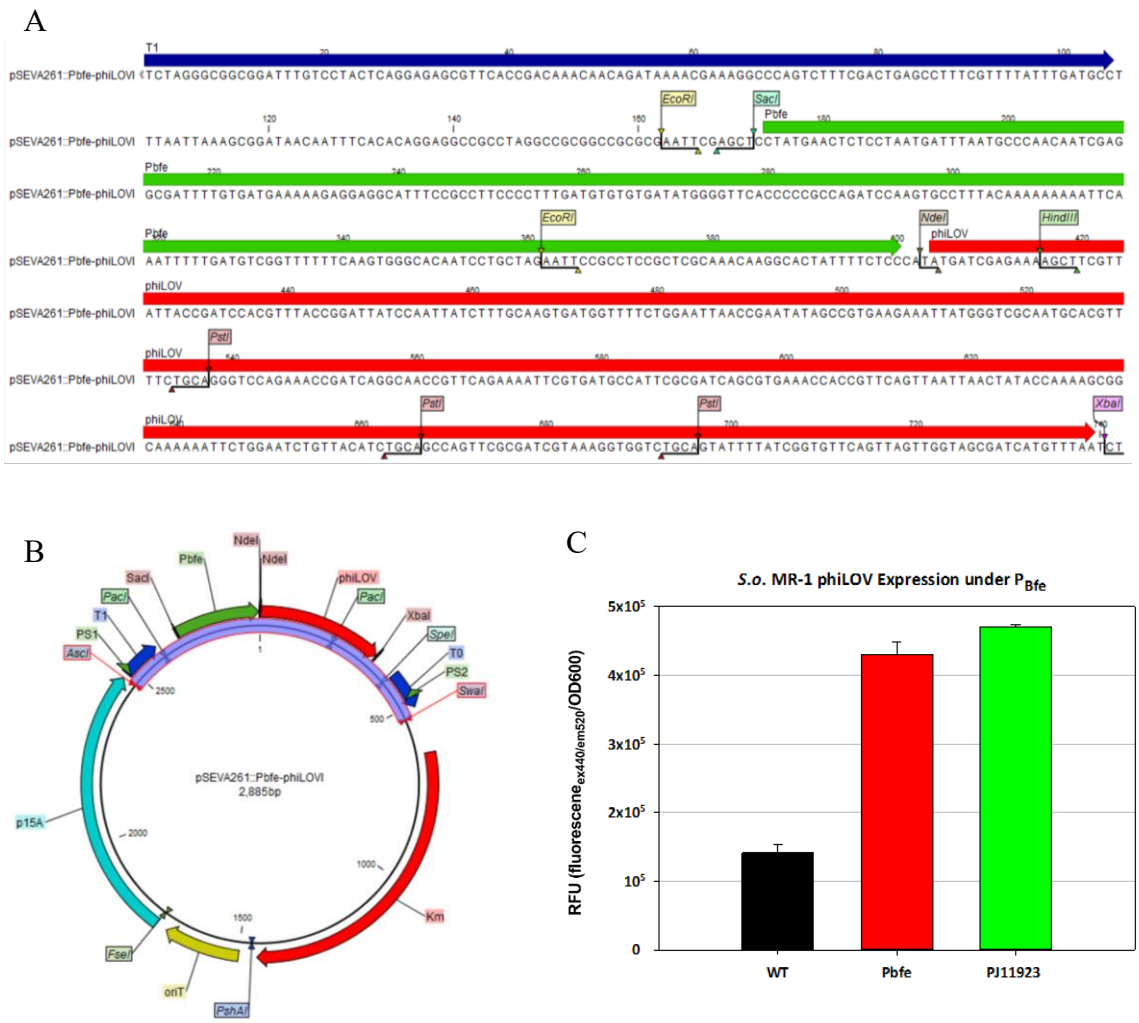

Figure 3.23 SOMR-1 endogenous promoter of bacterial flavin exporter (bfe) using phiLOV. Promoter region of bfe (A) that was cloned into pSEVA261::phiLOV (B). (C) Relative fluorescence of phiLOV under P_{bfe} and P_{23119}; samples were taken, washed twice in PBS and fluorescence measured at 440/520 nm. Bars represent triplicated with SEM error bars.

3.2.5 *Development and Validation of an SOMR-1-specific lacZ Reporter System using the pSEVA Vector Platform*

As seen from the results described preciously, using phiLOV as a reporter has a number of drawbacks when it comes to effectively discerning and characterising transcriptional and translational regulation in SOMR-1. It is not a sensitive enough reporter giving the interference with SOMR-1's endogenous flavin production and the lack of reporter output strength (see section 3.2.3).

To further characterise promoters in this work and expand the synthetic biology toolbox with transcriptional and translational regulators for SOMR-1, a *lacZ* gene reporter system was developed using the pSEVA vector platform. The β-Galactosidase assay was chosen, since it is a widely used and more established reporter enzyme in the field of molecular biology (Casadaban et al. 1980; Fried et al. 2012). The 120 kDa tetramer is encoded by the *lacZ* gene of the lac operon in *E. coli* which cleaves lactose into glucose and galactose to be utilised as carbon sources. For this assay, o-nitrophenyl-β-D-galactoside (ONPG), which is also recognized as a substrate, is used as a substrate yielding galactose and the yellow o-nitrophenol which can be measured at OD_{420} and quantified using the Miller method to determine the relative enzyme concentration expressed (Miller 1972). However currently available vectors, such as *E. coli* reporter vector pCM62 (Marx and Lidstrom 2001), typically only express the *lacZα* gene which encodes the lacZα peptide that complements the host cells lacZβγ peptide forming the functional b-galactosidase tetramer for this assay. As SOMR-1 lacks the *lacZ* homologue, available vectors for this assay are again not suitable for this niche model organism (Gao et al. 2010b).

3.2.5.1 *Promoter Characterisation of $P_{ChnB/ChnR}$ and $P_{tet/TetR}$ in SOMR-1 using a β-Galactosidase Reporter System*

The generated reporter system will allow easy replacement of promoters, thereby retaining the fluidity of this platform to rapidly change parameters from promoters, oriV and antibiotic resistance cassettes to enable fine-tuned gene expression in SOMR-1. For this, the full length *lacZ* gene (3075 bp; GeneID: 8181469; protein ID: WP_000177906) was amplified by PCR from genomic DNA (gDNA) purified from *E. coli* BL-21. The forward primer was designed to add *Avr*II restrictions site at the 5' end followed by a strong RBS (BBa_0034) and the biobrick scar (TACATAG) before the start codon of *lacZ*. The reverse primer was designed to add the *Sal*I restriction site to the 3'end (see Figure 3.24 and Table 2.4). This ensures that the *Avr*II restriction site, which is flanking the terminator T1 in pSEVAs without cargo, i.e. the first restriction site of the MCS, and the promoter sequence in e.g. pSEVA2311. This allows to preserve the promoter sequence for future replacement while removing any unnecessary distance from promoter sequence to RBS, spacer and start codon. The PCR amplification was performed as described in section 2.2.4.5 and the PCR product was digested with *Dpn*I for 1h prior to being run on an agarose to excise DNA at the correct size and purified as described previously. The purified PCR product and appropriate pSEVA vector backbone were digested with *Avr*II and *Sal*I for 2 h, cleaned up and ligated, then transformed in *E. coli* Invitrogen™ One Shot® TOP10 Chemically Competent cells. Clones were verified by plasmid restriction digestion with *Nhe*I and *Sac*I and sanger sequencing. A promoter-less copy of *lacZ* in the appropriate pSEVA vector backbone was also cloned and served as a negative control.

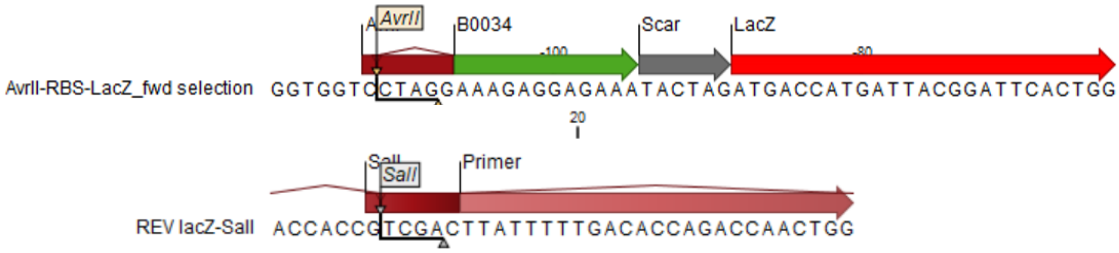

Figure 3.24 Forward and reverse oligonucleotide in 5'-3' orientation for the fusions of restriction sites, RBS and biobrick scar to lacZ gene amplicon.

3.2.5.1.1 *Cloning of pSEVA2311 ($P_{ChnB/ChnR}$) → lacZ*

Recently, a novel expression systems for Gram-negative bacteria was developed by (Benedetti et al. 2016a; Benedetti et al. 2016b) using a cyclohexanone-responsive ChnR regulator and the P_{ChnB} promoter from the Gram-negative bacterium *Acinetobacter johnsonii*. It was standardised in line with the pSEVA platform (Silva-Rocha et al. 2013; Martinez-Garcia et al. 2014) resulting in the vector pSEVA2311 (Km^R, $oriV_{pBBR1}$, $P_{ChnB/ChnR}$). This promoter has been successfully used in *Pseudomonas putida* biofilms (Benedetti et al. 2016a) which makes this promoter uniquely applicable to be tested in SOMR-1 with further applications in enhancing EET in MFCs. The expression vector pSEVA2311 has only been parameterised in *E. coli* and has shown to have extremely low basal expression levels in the absence of inducer, a large transcriptional capacity, as well as being usable in both rich and minimal media, which is further applicable to test whether the same holds true when used in SOMR-1 which is routinely grown in minimal media (Benedetti et al. 2016b).

To test whether the $P_{ChnB/ChnR}$ expression system works in SOMR-1, the *lacZ* gene was cloned into the pSEVA2311 backbone (see Figure 3.25A) as described in the previous section 3.2.5.1, resulting in the plasmid pSEVA2311::*lacZ* (see Figure 3.25B).

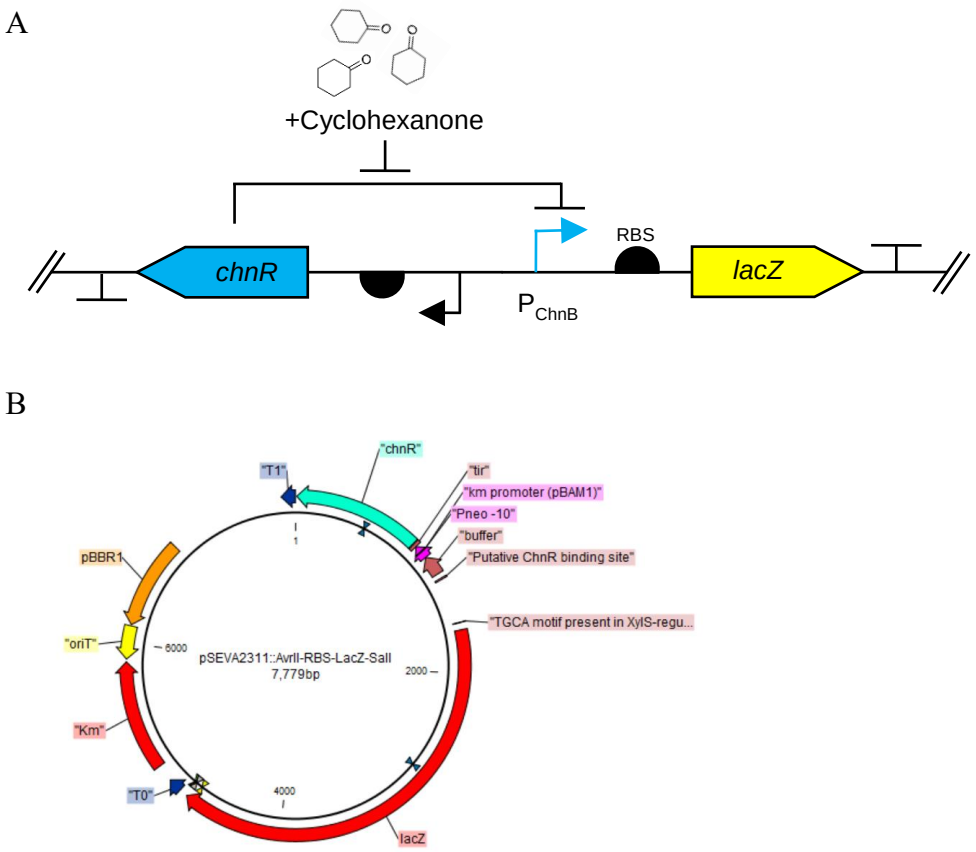

Figure 3.25 Schematic scheme of lacZ gene under $P_{ChnB/\ ChnR}$ (A) gene regulation in 5'-3' orientation and (B) vector map of pSEVA2311::lacZ.

3.2.5.2 *Promoter characterisation of $P_{ChnB/ChnR}$*

To characterise the output of the pSEVA $P_{ChnB/ChnR}$ expression system in SOMR-1, first the inducer strength needed was tested. Previously described for *E. coli* expression cyclohexanone was directly added to the cultures at a final concentration of 1mM (Benedetti et al. 2016b). To test what quantity of cyclohexanone in SOMR-1 was needed for induction, and to establish if gene induction could be achieved at all in SOMR-1, SOMR-1 was conjugated with pSEVA2311::*lacZ* and pSEVA231::*lacZ*, the latter lacking a promoter cassette as negative control. Cultures were grown overnight, inoculated from single colonies, and fresh medium was inoculated at a starting OD_{600} 0.02 and grown at 30°C shaking at 200 rpm. At mid-exponential phase at OD_{600} 0.7, liquid cyclohexanone (CAS Number 108-94-1) was added at concentrations ranging

from 0.1 mM to 2 mM. After 3 h further incubation at 30°C shaking at 200 rpm, samples were taken and the β-galactosidase assay was performed with modifications specific for SOMR-1 as described in section 2.2.7. The reaction was stopped after 4 min, OD_{420} was measured and Miller units calculated. The promoter-less pSEVA231::*lacZ* did not give any positive readings confirming the insulating strength of T1 and T0 of the backbone architecture (data not shown as reading were ≤ 0). The uninduced pSEVA2311::*lacZ* had a mean ± SEM basal expression of 2518 ± 55 Miller units (MU). In the range of concentrations tested there was a stark difference in expression output, 0.1 mM CH added to the culture resulted in an output of 11038 ± 616 MU, 0.2 mM CH yielded 12348 ± 666 MU, 0.5 mM CH yielded 12793 ± 334 MU. The recommended inducer concentration of 1mM did indeed give the highest enzyme expression output with 13047 ± 653 MU, ≥ 5-times higher than in the uninduced control. Interestingly, increasing the concentration to 2 mM did not yield in a higher expression rate and MU decreased to 12373 ± 100 MU (see Figure 3.26). The following experiments using this promoter were therefore induced with an inducer concentration of 1 mM cyclohexanone.

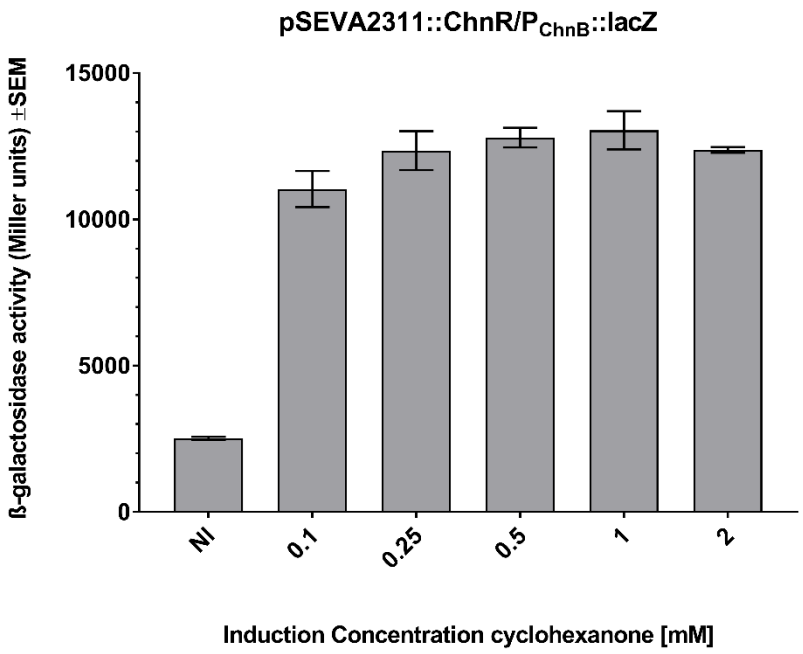

Figure 3.26 Determination of induction concentration of cyclohexanone for the ChnR/ChnB promoter in SOMR-1. SOMR-1 carrying pSEVA2311::lacZ was grown until mid-exponential phase (OD_{600} 0.7) and induced with cyclohexanone at varying concentrations from 0.1 to 2 nM. Samples were taken 3 h after induction and assayed for β-galactosidase activity, expressed as Miller Units (MU). β-galactosidase assay was performed in triplicate for each sample from biological triplicates. Error bars represent standard error of the mean (SEM).

3.2.5.3 *Cloning of pSEVA2311 ($P_{tet/TetR}$) → lacZ*

Another broadly applied tool in molecular genetics is the inducible gene expression using the Tet repressor (tet regulation) which is encoded by the tetR gene. Naturally, tetracycline (tc) resistance is controlled TetR negatively in bacteria, where in the presence of tc TetR detaches from its cognate DNA sequence ”tetO”, inducing the expression of the tc antiporter protein and thereby conferring resistance (Bertram and Hillen 2008). Owing to its versatile nature, a large number of novel tet-controllable artificial or hybrid promoters have been developed for target gene expression in bacteria providing a rarely found combination of low basal expression with efficient induction (Bertram and Hillen 2008).

To test whether a $P_{tet/TetR}$ works in SOMR-1 using the pSEVA vector architecture, this expression system was cloned using pSEVA2311 as a template. For this the *tetR* gene was amplified using the iGEM biobrick part BBa_C0040[20] as template. Primers were designed to add *Nhe*I restriction site to the 5' end of tetR and *Pac*I to the 3' prime end to replace *chnR.* To change the promoter sequence, the pSEVA2311 buffer sequence and promoter for ChnR were amplified using primers adding the P_{tet} promoter and the *Avr*II restriction site to the 3'end to place the promoter directly adjacent to the MCS. The pSEVA2311 vector backbone was digested with *Avr*II and *Pac*I removing the $P_{ChnB/ChnR}$ cassette, and PCR products were also digested and cleaned up before a 3-part ligation was performed and transformed in *E. coli* Invitrogen™ One Shot® TOP10 Chemically Competent cells. Clones were verified by plasmid restriction digestion with *Nde*I and *Xho*I and sanger sequencing. The resulting plasmid pSEVA23::$P_{tet/TetR}$ (4072 bp) is shown in Figure 3.27B. Furthermore, the *lacZ* gene was also cloned into this vector resulting in the plasmid pSEVA23::$P_{tet/TetR}$::*lacZ* (as described in section 3.2.5.1; see Figure 3.27C for corresponding vector map and gene regulation in Figure 3.27A).

[20] http://parts.igem.org/Part:BBa_C0040 (last accessed 25.06.2018)

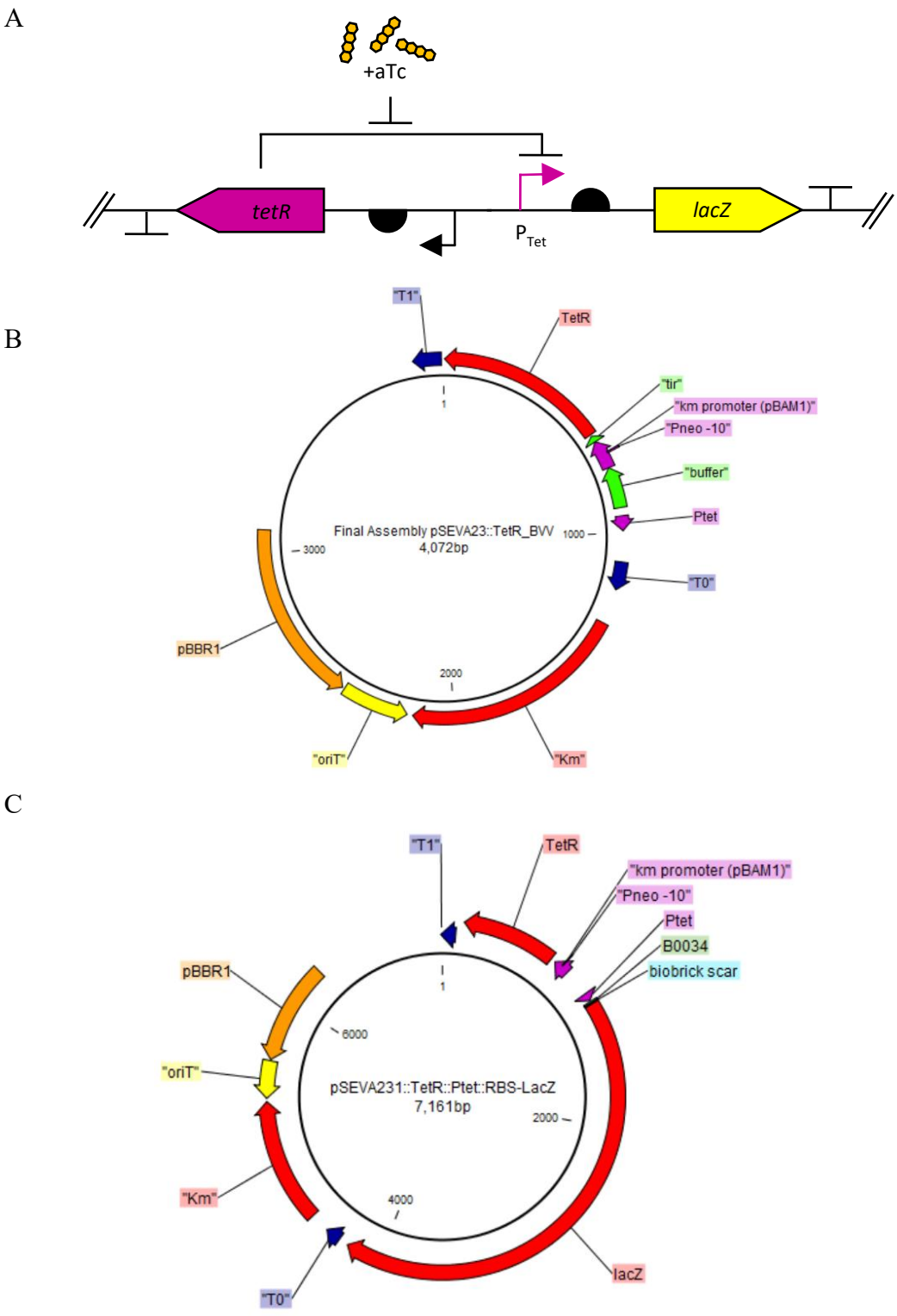

Figure 3.27 Schematic cloning scheme of $P_{tet/TetR}$. (A) Organisation of P_{tet} promoter and repressor tetR in 5'-3' orientation with fusions of lacZ gene. (B) Vector backbone of pSEVA23::$P_{tet/TetR}$::1 ($oriV_{pBBR1}$, Km^R) and (C) pSEVA23::$P_{tet/TetR}$::lacZ.

3.2.5.4 *Promoter characterisation of $P_{tet/TetR}$*

To characterise the output of the pSEVA $P_{tet/TetR}$ expression system in SOMR-1, SOMR-1 was conjugated with pSEVA23::$P_{tet/TetR}$::*lacZ* and pSEVA231::*lacZ*, the latter lacking a promoter cassette as negative control. Cultures were grown overnight inoculated from single colonies and new medium was inoculated at a starting OD_{600} 0.02 and grown at 30°C shaking at 200 rpm. At mid-exponential phase at OD_{600} 0.7, anhydrotetracycline (aTc) (CAS Number 13803-65-1) was added at concentrations ranging from 0.05 to 1 µM which is equivalent to 23 to 263 ng/mL. After 3 h further incubation at 30°C shaking at 200 rpm, samples were taken and the β-galactosidase assay was performed with modifications specific for SOMR-1 as described in section. The reaction was stopped after 4 min and OD_{420} was measured and Miller units calculated as described in section. The promoter-less pSEVA231::*lacZ* did not give any meaningful reading confirming the insulating strength of T1 and T0 of the backbone architecture (data not shown as readings were ≤ 0). The uninduced pSEVA23::$P_{tet/TetR}$::*lacZ* had a mean ± SEM basal expression of 1973 ± 41 Miller units (MU). In the range of concentrations tested there was only a minimal difference in expression output, 0.05 µM aTc added to the culture resulted in an output of 2078±50 MU, 0.1 µM aTc yielded 2727 ± 159 MU, 0.25 µM aTc yielded 3632 ± 39 MU. The recommended inducer concentration of 1mM did indeed give the highest enzyme expression output with 4198 ± 355 MU, $\geq$ 2-times higher than in the uninduced control. Interestingly, doubling the concentration to 1 µM aTc did not yield in a higher expression rate and the mean MU decreased to 3895 ± 84 MU (see Figure 3.28), which is giving the same level of expression as 0.25 µM. The following experiments using this promoter were therefore induced with an inducer concentration of 0.5 µM aTc.

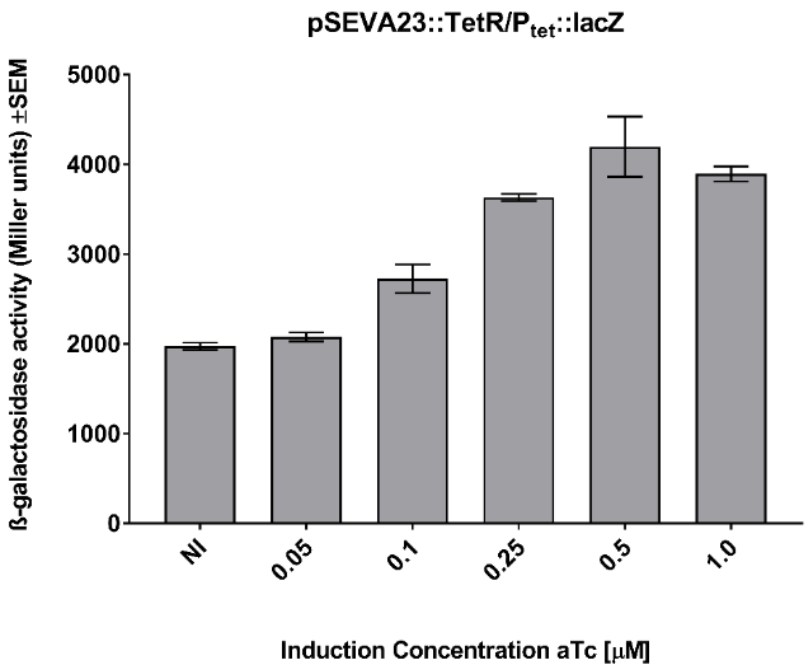

Figure 3.28 Determination of induction concentration of anhydrotetracycline (aTc) for $P_{TetR/tet}$ in SOMR-1. SOMR-1 carrying pSEVA231::$P_{tet/TetR}$::lacZ was grown until mid-exponential phase (OD_{600} 0.7) and induced with cyclohexanone at varying concentrations from 0.05 to 1 μM aTc. Samples were taken 3 h after induction and assayed for β-galactosidase activity, expressed as Miller Units (MU). β-galactosidase assay was performed in triplicate for each sample from biological triplicates. Error bars represent standard error of the mean (SEM)

3.2.5.5 *Comparing $P_{ChnB/ChnR}$ and $P_{tet/TetR}$ in SOMR-1 under Aerobic and Anaerobic Conditions*

To evaluate whether either $P_{ChnB/ChnR}$ or $P_{tet/TetR}$ expression kinetics are stable not only in minimal media which is routinely used for SOMR-1, especially in MFC settings, but also under anaerobic conditions, β-galactosidase assays were performed.

For this SOMR-1 harbouring pSEVA231::$P_{tet/TetR}$::*lacZ*, pSEVA231::$P_{tet/TetR}$, pSEVA2311::*lacZ* and empty vector pSEVA2311 were grown from single colonies from -80°C DMSO stocks in LB media at 30°C shaking at 200 rpm overnight. Aerobic SBM media (containing 20 mM sodium lactate as carbon source) and anaerobic SBM media (containing 20 mM sodium lactate and 40 mM sodium lactate) were inoculated and fresh cultures of minimal SOMR-1 basal medium were inoculated at OD_{600} of 0.06 and grown at 30°C shaking at 200 rpm (see section 2.1.7.2). Cultures were induced with appropriate inducer in mid-exponential phase and samples were taken for β-galactosidase assays (see section 2.2.7). Figure 3.29A illustrates the difference between $P_{ChnB/ChnR}$ and $P_{tet/TetR}$ in SOMR-1, where a 5-time increase in expression levels was seen for $P_{ChnB/ChnR}$ compared to a 2-times increase for $P_{tet/TetR}$ as opposed to uninduced basal expression. Further growth of SOMR-1 bearing pSEVA231::$P_{tet/TetR}$::lacZ is slightly reduced (Figure 3.29B). Figure 3.30A shows the expression level differences between the two promoter constructs under aerobic and anaerobic conditions in minimal media. A 20 h growth curve showed prolonged-exponential phase for SOMR-1 harbouring the promoter vectors grown anaerobically (Figure 3.30B). A prominent difference in expression level was observed between aerobic and anaerobic conditions. For $P_{ChnB/ChnR}$ mean ± SEM for aerobic basal uninduced expression was 4626 ± 348 MU and remained constant with a 2.5-fold increase post-induction with a mean 11292 ±283 MU and 11959 ± 726 MU at 2 h and

13 h time-points, respectively. Anaerobically, $P_{ChnB/ChnR}$ mean ± SEM for basal uninduced expression levels is 2-fold lower than under aerobic conditions with a mean ± SEM of 2405 ± 185 MU. Post induction, expression levels increased also 2-fold with a mean 4742 ± 65 MU and 4332 ± 90MU at 2 h and 13 h time-points, respectively. Although, there was a 2-fold expression level increase after induction under both aerobic and anaerobic conditions compared to baseline, an absolute reduction of 30 % in expression output was observed (see Figure 3.30A).

For $P_{tet/TetR}$ mean ± SEM for aerobic basal uninduced expression was 2072 ± 168 MU and remained constant with a ≥ 1.8-fold increase post-induction with a mean 3718 ± 46 MU and 4453 ± 115 MU at 2 h and 13 h time-points, respectively (see Figure 3.29A). Anaerobically, $P_{tet/TetR}$ mean ± SEM for basal uninduced expression levels was constant to that under aerobic conditions with a mean ± SEM of 1946 ± 49MU (see Figure 3.30A). Post induction, expression levels increased only 1.3-fold with a mean 2529 ± 33MU and 2343 ± 209 MU at 2 h and 13 h time-points, respectively. Although, the expression level increase after induction under both aerobic and anaerobic conditions compared to baseline, an absolute reduction of 1.5-fold and 1.9-fold in expression output was observed after 2 h and 13 h, respectively (see Figure 3.30A).

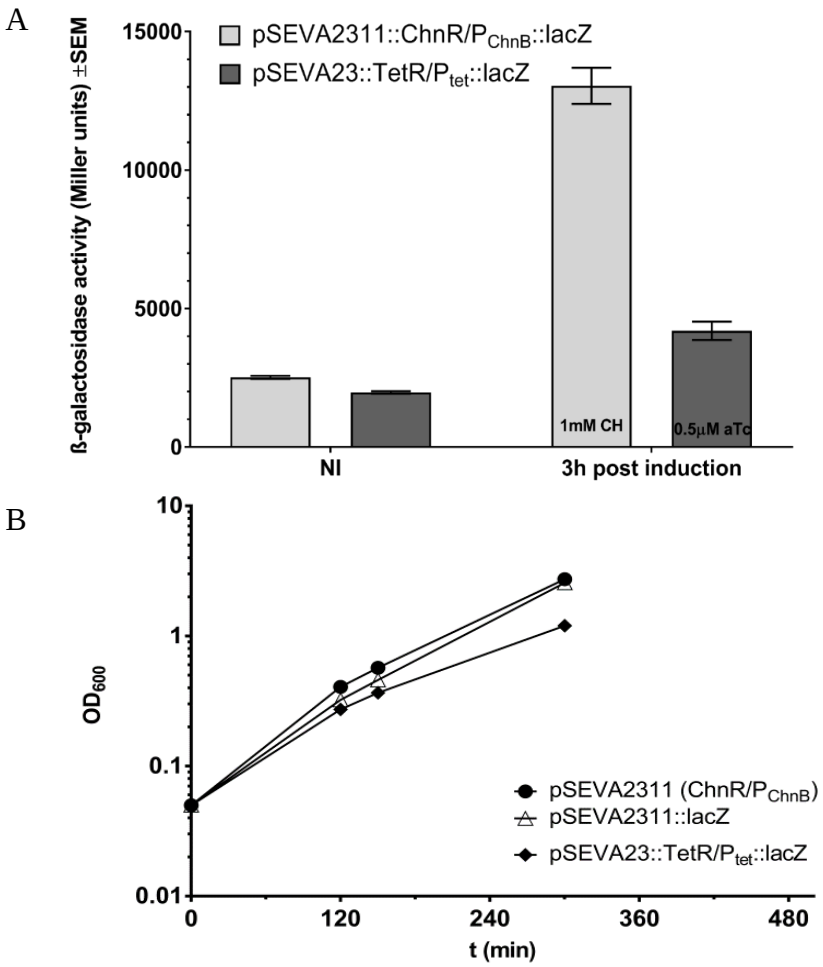

*Figure 3.29 Comparison of $P_{ChnB/ChnR}$ and $P_{tet/TetR}$ expression levels in SOMR-1 under aerobic as expressed by Miller units (A) and corresponding growth curves (B). SOMR-1 cultures harbouring pSEVA231::$P_{tet/TetR}$::lacZ, pSEVA231::$P_{tet/TetR}$, pSEVA2311::lacZ ($P_{ChnB/ChnR}$) and empty vector pSEVA2311 were grown in LB media (50 µg/mL Km) and were induced with appropriate inducer in mid-exponential phase and samples were taken for β-galactosidase assays at indicated time points. β-galactosidase assay and OD_{600} measurements were performed in triplicate for each sample from biological triplicates. Error bars represent standard error of the mean (SEM); ** $p<0.05$ uninduced vs induced. NI, not induced control; PI, post induction.*

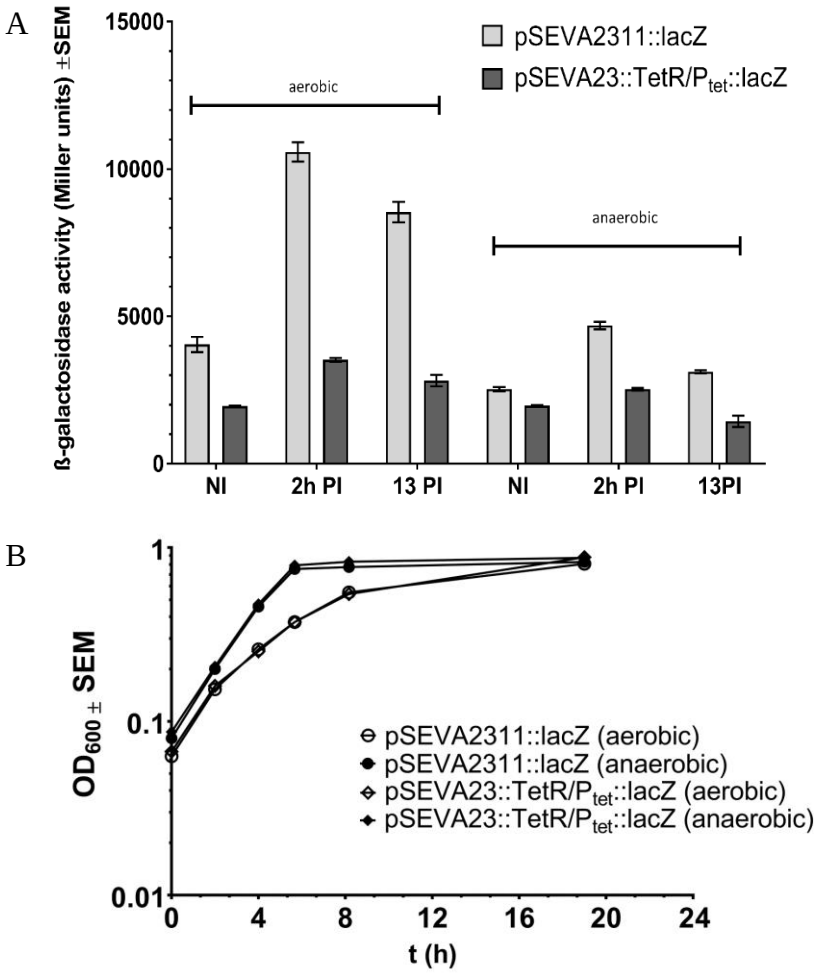

*Figure 3.30 Comparison of $P_{ChnB/ChnR}$ and $P_{tet/TetR}$ expression levels in SOMR-1 under aerobic and anaerobic conditions as expressed by Miller units (A) and corresponding growth curves (B). SOMR-1 cultures harbouring pSEVA231::$P_{tet/TetR}$::lacZ, pSEVA231::$P_{tet/TetR}$, pSEVA2311::lacZ ($P_{ChnB/ChnR}$) and empty vector pSEVA2311 were grown aerobically in SBM media (20 mM sodium lactate) and anaerobically SBM media containing 20 mM sodium lactate, 40 mM sodium lactate and 30 µg/mL Km. Cultures were induced with appropriate inducer in mid-exponential phase and samples were taken for β-galactosidase assays at indicated time points. β-galactosidase assay and OD_{600} measurements were performed in triplicate for each sample from biological triplicates. Error bars represent standard error of the mean (SEM); ** $p<0.05$ uninduced vs induced. NI, not induced control; PI, post induction.*

Further, to characterise how SOMR-1 growth conditions could affect the pSEVA2311 expression system, SOMR-1 harbouring pSEVA2311::*lacZ* was grown under varying conditions, i.e. in rich medium (LB) and in minimal media (SBM) under aerobic and anaerobic conditions (see Figure 3.31). It can be observed that the expression of *lacZ* is reduced depending on growth conditions, however, between induced and uninduced culture there are significant differences. Increasing the inducer concentration in SBM can provide a slight advantage under anaerobic conditions to counteract the slowed metabolism and expression levels.

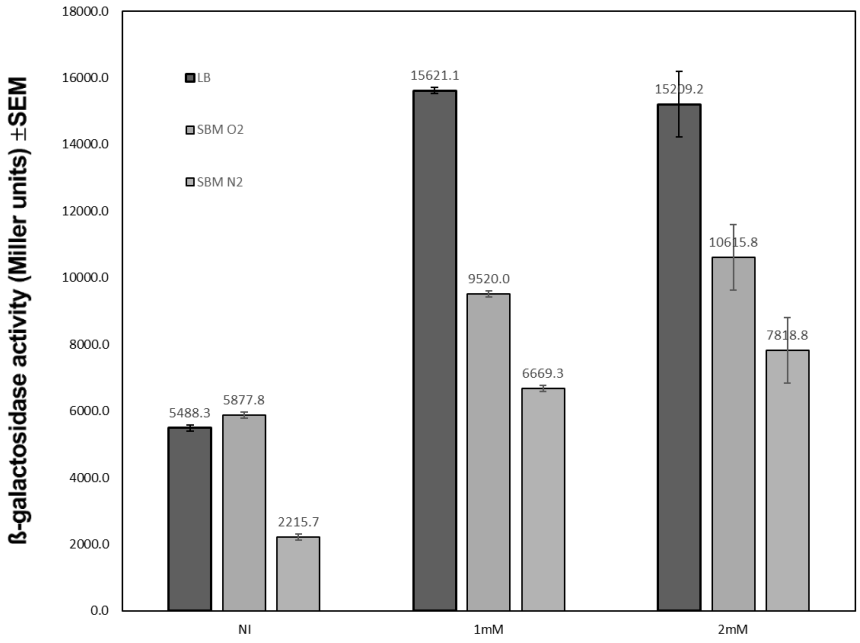

Figure 3.31 Comparison of pSEVA2311::lacZ expression system output in different media. B-galactosidase assay was performed 15 h post induction. Bars show data for triplicate samples as mean plus SD.

3.3 Discussion

3.3.1 *pSEVA Platform in SOMR-1*

The pSEVA vector platform has been shown here to offer a wide spectrum of plasmids and replication systems that can be used in SOMR-1. The assumption that most vectors that work in *E. coli* also function seamlessly in SOMR-1 has however also been disproven. While a large proportion of the pSEVA vectors work effortlessly and are proven to be maintained by SOMR-1, pSEVA271 and pSEVA251 are unreliable in this host. Interestingly, despite conferring kanamycin resistance, pSEVA251 cannot be extracted using a standard plasmid miniprep. This further indicates that this origin of replication, RSF1010, is not truthfully maintained in SOMR-1. This could be due to either its known low-copy number oriV making unequal distribution into daughter cells not only a stochastic process, but it could also be that the RSF1010 replication system interferes with SOMR-1 host factors as previously seen in *E. coli* DH5α (Jahn et al. 2016). If this was the case for *Shewanella*, it would explain the drastic loss in the plasmid-containing population, making pSEVA215 an unsuitable vector backbone for use in SOMR-1. However, pSEVA351 and pSEVA651 are maintained with almost all other pSEVAs tested, except for the aforementioned, and are clearly visible on the gels. The obtained results for plasmid copy numbers are, however, comparable with recently published PCN data for *E. coli* DH5α harbouring pSEVA vectors (Jahn et al. 2016). Compared to *E. coli,* SOMR-1 exhibits the same copy number groups for these replication machineries. However, PCNs for $oriV_{pBBR1}$, $oriV_{pSC101}$ and $oriV_{pRSF1010}$ are more than half of those seen in *E. coli*. PCNs. $OriV_{pUC,}$ however, has a 1.5-times higher PCN in SOMR-1 than in *E. coli.* While $oriV_{ColEI}$ is a high copy plasmid in both organisms, the average PCN is reduced by a third in SOMR-1.

The pSEVA621 (Gm^R, $oriV_{RK2}$, MCS) was maintained with pSEVA231 ($oriV_{pBBR1}$), pSEVA241 ($oriV_{ColEI}$), pSEVA261 ($oriV_{p15A}$), pSEVA281 ($oriV_{pUC}$) and pSEVA291 ($oriV_{ppBBR322/ROB}$). Notably, SOMR-1 was able to maintain both $oriV_{RK2}$ vectors here, i.e. pSEVA221 and pSEVA621. Similarly, pSEVA631 (Gm^R, $oriV_{pBBR1}$, MCS; see Figure 3.15B) was compatible with the same range of pSEVA2X1. Again SOMR-1 grew maintaining both $oriV_{pBBR1}$ containing vectors pSEVA231 and pSEVA631. Transconjugants harbouring pSEVA251 and pSEVA651 did grow in liquid culture, however no band is visible for pSEVA251. Additionally, pSEVA651 (Gm^R, $oriV_{RSF1010}$, MCS; Figure 3.15C) was also compatible with all vectors, with the exception of pSEVA241 ($oriV_{ColEI}$) and pSEVA251 ($oriV_{RSF1010}$). Lastly, pSEVA661 (Gm^R, $oriV_{p15A}$, MCS; Figure 3.15D), was also compatible with all vectors with the exception of pSEVA251 ($oriV_{RSF1010}$). However, neither pSEVA341 nor pSEVA641, both using $oriV_{ColEI}$ with Cm and Gm resistance cassette, respectively, yielded in any viable transconjugants with any of the kanamycin resistant pSEVAs in SOMR-1. This is interesting considering that $oriV_{ColEI}$ is maintained with other vectors, i.e. pSEVA321, 331, 631, 621 and 661, when conferring kanamycin resistance instead (pSEVA241). One could therefore speculate that it is not the replication system per se that confers incompatibility of these plasmids, but potentially the metabolic burden of expressing these resistance genes from a high copy number plasmid not allowing the cells to propagate efficiently.

Due to time constrains the missing pSEVA vectors from Table 3.1 were not cloned and tested for compatibility. However, taken together with the results from the PCN analysis it can be deducted that these vectors can be combined in a number of

combinations with varying replication systems ranging from low to high copy numbers and at least 3 different antibiotic markers.

Further, the results for multi-plasmid bearing systems are in accordance with a recently published study on a multi-origin based conjugal transfer suit for SOMR-1 where different replication origins were maintained in *Shewanella* (Gralnick and Hajimorad 2016). Their results however, only tested oriV_{RK2} and oriV_{pBBR1} using Km and Cm as antibiotic markers, therefore the results presented here offer a wider scope of tools available for this organism now. It would be interesting to analyse whether SOMR-1 harbouring these plasmids show a relation between plasmid maintenance and antibiotics on doubling time and current production, which has been recently reported for *Geobacter* (Kan, RK2, pBBR1) (Chan et al. 2015).

3.3.2 *Anaerobic Reporters*

Despite phiLOV's great advantages for anaerobic research such as which has been shown in *Clostridium* recently (Buckley et al. 2016), it has not proven to be a reliable and intense enough reporter tool in SOMR-1 in this work. However, low intensity was also reported for the aforementioned study, the endogenous flavin production of SOMR-1 masks any significant signal from phiLOV making it an unsuitable reporter for electrochemical studies where SOMR-1 main EET mechanism is flavin export (Kotloski and Gralnick 2013). However, these experiments showed that while pBAD33::T7RNP does not express any fluorescent gene, having pSEVA23::P_{T7}::*phiLOV* RUF levels at the same indicates that firstly the pSEVA backbone offer adequate insulation of the cargo genes and that P_{T7} promoter sequence is not recognised by SOMR-1 endogenous polymerases, making this expression

system truly orthogonal. If possible this system should be further investigated using another report assay such as *lacZ.*

3.3.3 *Transcriptional Regulation in SOMR-1*

The newly established $P_{ChnB/ChnR}$ and $P_{tet/TetR}$ expression systems produced in this work are adding to the only slowly expanding transcriptional regulation tools available for SOMR-1. Only recently West *et al.* developed a native inducible expression system utilising the Tor pathway for TMAO respiration (West et al. 2017). So only a small number of studies have realised synthetic biology applications (Gao et al. 2010b; Kane 2011; Fried et al. 2012) making these new promoter systems a valuable addition, especially considering their efficacy under minimal media and anaerobic conditions which is vital for SOMR-1 studies in MFCs.

3.4 Conclusion

The expansion of a SOMR-1 specific synthetic biology toolbox has been shown in this chapter systematically approaching known bottlenecks in SOMR-1's genetic manipulation tools. By realising the pSEVA platform, showing for the first time plasmid copy numbers for this organism, characterising new expression systems and reporter tools in SOMR-1 future research with this organism can realised and enable fine-tune gene expression.

CHAPTER 4

4 ENGINEERING OF SOMR-1 ELECTRON TRANSFER OUTPUT USING A SYNTHETIC OPERON

4.1 Introduction

SOMR-1 has been intensively studied to understand the mechanisms of its extracellular electron transfer (EET) and related metabolism which govern the performance of this organism in bioelectrochemical systems (BES) (see Chapter 1). Being a facultative anaerobic bacterium makes this organism an ideal workhorse as a tractable model organism for molecular engineering, however, biofilm formation of SOMR-1 on anode material under anaerobic conditions in MFCs has been described to be usually less dense and thick in comparison to its sibling model organism *Geobacter* (Liu and Bond 2012; Malvankar and Lovley 2012). Therefore, a number of advances have been made to engineer SOMR-1 to overcome these shortcomings compared to *Geobacter* and enhance its EET and electroactive biofilm formation capabilities using molecular engineering approaches and ultimately increase biocurrent output.

4.1.1 *Key Mechanisms in SOMR-1 Extracellular Electron Transfer (EET)*

To complete its respiration chain, electrons have to be shuttle across both inner and outer membrane in SOMR-1 to reach extracellular electron acceptors (see Figure 4.2) (Fredrickson et al. 2008; Coursolle and Gralnick 2010). Firstly, electrons are carried across the inner membrane via the menaquinol pool and reduce the tetraheme c-type cytochrome (c-Cyt) CymA (Marritt et al. 2012). Electrons are then further shuttled to

the Mtr complex which consists of the periplasmic decaheme c-Cyts MtA (Schuetz et al. 2009), the trans-outermembrane β-barrel MtrB (Myers and Myers 2002) and two decahaeme c-cyts MtrC and OmcA that are able to directly reduce extracellular electron acceptors (Wang et al. 2014).

Another route for EET in SOMR-1 that has been recently elucidated is via the flavin secretion pathway. In fact, SOMR-1 main respiratory capacity is directed towards its flavin secretion. Flavin electron shuttling has been reported to account for ~75% of extracellular electron transfer to insoluble substrates in SOMR-1 (Kotloski and Gralnick 2013). Flavin adenine dinucleotide (FAD) is transferred through the inner membrane via the bacterial flavin exporter (Bfe) (Kotloski and Gralnick 2013) into the intermembrane space. There FAD is hydrolysed to flavin mononucelotide (FMN) and adenosine monophosphate (AMP) via the recently elucidated UshA (Covington et al. 2010). AMP is then dephosphorylated by UshA and re-assimilated by the cell (see Figure 4.1 and Figure 4.2B). FMN then diffuses through a yet unknown outer membrane porin where it accelerates extracellular electron transfer to suitable electron acceptors, e.g. FMN can carry up to two electrons per molecule to reduce extracellular iron oxide (von Canstein et al. 2008; Covington et al. 2010).

Hence, it is becoming increasingly more evident that flavins play a major role in cellular physiology of SOMR-1. The precursor of FMN and FAD is riboflavin, also known as vitamin B2, which is an essential co-factor for many redox reactions and further mediate a variety of processes including the aforementioned extracellular respiration and iron acquisition (Brutinel et al. 2013). Considering its crucial role in SOMR-1's anaerobic respiration of insoluble substrates, SOMR-1 possess a multitude

of genes, duplicated and fused variations, involved in the riboflavin biosynthesis including two copies of ribE and a fusion gene of ribBA (Brutinel et al. 2013).

Another postulated way for SOMR-1 to complete is EET chain is via "nanowires" (El-Naggar et al. 2010; Pirbadian et al. 2014) (see Figure 4.2D). These however differ greatly from those described for *Geobacter* species where *Gebacter* nanowires are thought to be Type IV pili; it is proposed that their conductance stems from a metallic-like band transport due to the stacking of aromatic amino acids along the subunit PilA (Malvankar et al. 2011; Malvankar and Lovley 2012; Vargas et al. 2013). However, Piradian *et al.* recently proposed that nanowires in SOMR-1 are in fact outer membrane and periplasmic extensions that are clustered with extracellular electron transport components, such as the Mtr complex (see Figure 4.2C) (Pirbadian et al. 2014).

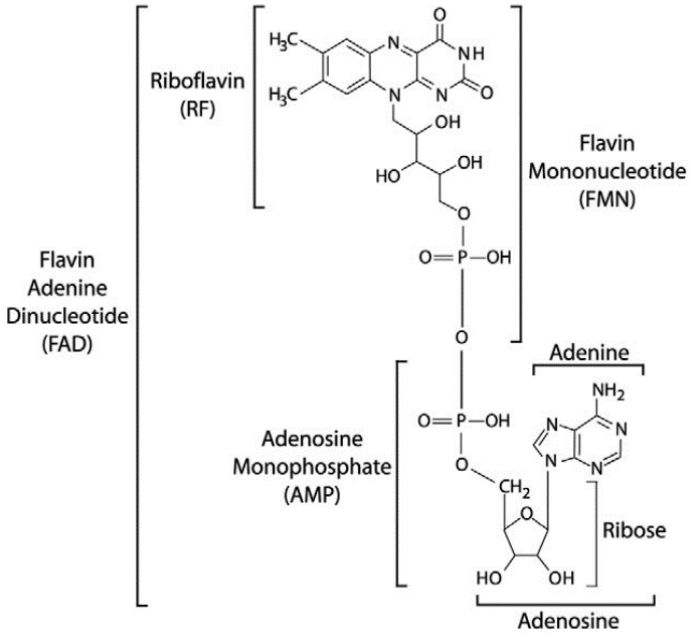

Figure 4.1 Structure of flavin adenine dinucleotide (FAD) and its moieties. Image taken from (Covington et al. 2010).

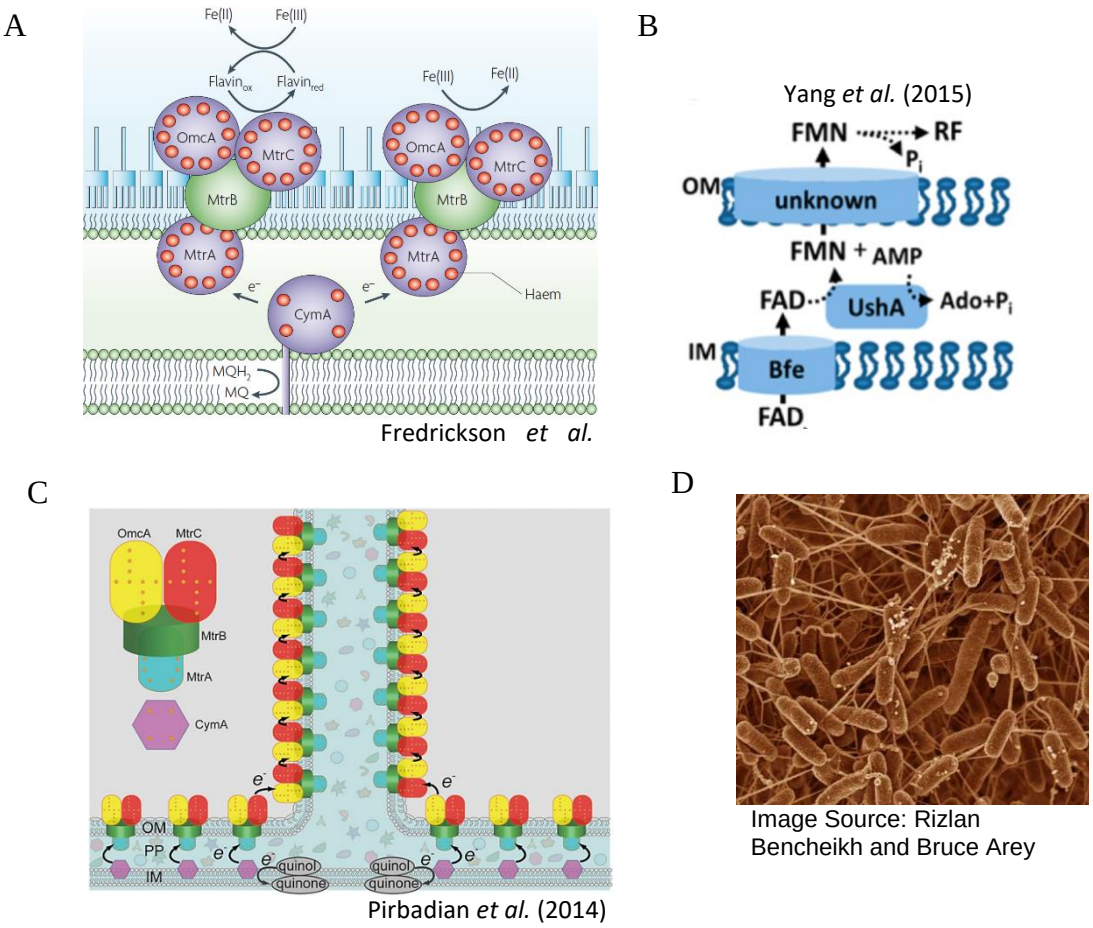

Figure 4.2 Shewanella EET meachnisms (A) Electron transfer across inner and outer membrane via the Mtr pathway [image taken from (Fredrickson et al. 2008)]. (B) FAD is shuttled via Bfe across the inner membrane, converted to FMN via UshA and exported across the outer membrane [image taken from (Yang et al. 2015)*]. (C) Proposed SOMR-1 nanowire structure [image taken from* (Pirbadian et al. 2014)*]. (D) SEM of SOMR-1 nanowires UshA [image taken from the New Scientist[21]].*

4.1.2 *Electroactive Biofilms in SOMR-1*

Bacterial biofilms formation is regulated by cyclic dimeric guanosine monophosphate (c-di-GMP), a second messenger which promotes the formation of biofilm by signalling the expression of adhesive matrix components at high levels, low levels of c-di-GMP lead to planktonic lifestyle of the bacterium (Thormann et al. 2005;

[21] https://www.newscientist.com/article/dn9526-bacteria-made-to-sprout-conducting-nanowires/ (last accessed 30th June 2018)

Benedetti et al. 2016a). Figure 4.3 illustrates how the diguanylate cyclase YedQ increases c-di-GMP, thereby enhancing biofilm formation, in contrast to the phosphodiesterase YhjH which lowers levels of c-di-GMP thereby increasing tendency of planktonic bacterial growth (Benedetti et al. 2016a).

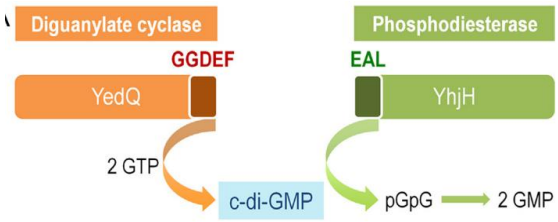

Figure 4.3 Regulation of c-di-GMP via expression of yedQ and YhjH. Image taken from (Benedetti et al. 2016a).

4.1.3 *Screening Tools Available for Electroactive Bacteria*

Microbial electrochemical technologies offer a variety of potential applications. Traditionally, current output and electroactive biofilm formation is generated and monitored using microbial fuel cells (MFC) using electrochemical approaches, such as chronoamperometric assays, namely cyclic voltammetry (CV) and chronoamperometry (Harnisch and Freguia 2012).

Figure 4.4 shows cyclic voltammograms of *Shewanella* spp. directly after inoculation and after 24he reduction process occurs from the initial potential (E_i) up to the switching potential where the potential is scanned negatively to cause a reduction; this resulting current is known as cathodic current (I_{pc}) and the corresponding is called the cathodic peak potential (E_{pc}) which is reached as all substrate present at surface of the electrode has been reduced. Anodic current (I_{pa}), i.e. where oxidation occurs, happens after the switching potential has been reached and the potential is positively scanned. As with the E_{pc}, the anodic peak potential (E_{pa}) is reached as all of the substrate present at the surface of the electrode has been oxidized.[22] As microbially produced flavins accumulate and are adsorbed at the electrode, anodic current increases (Marsili et al. 2008).

[22] https://chem.libretexts.org/Bookshelves/Analytical_Chemistry/Supplemental_Modules_(Analytical_Chemistry)/Instrumental_Analysis/Cyclic_Voltammetry (last accessed 12th May 2019)

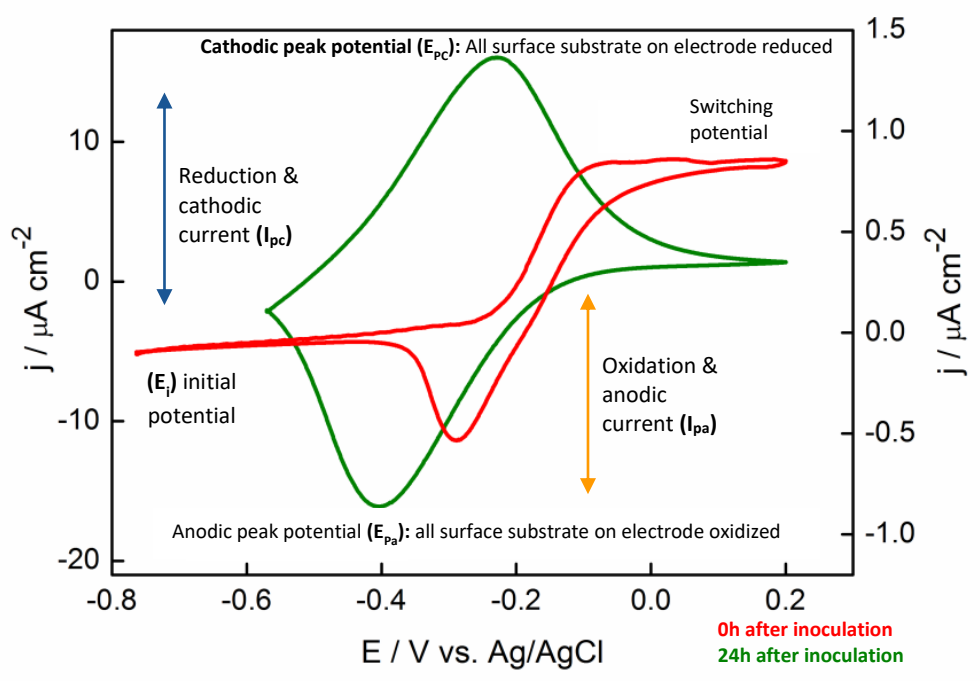

Figure 4.4 Cyclic voltammogram of a Shewanella spp. cell suspension (a) immediately after inoculation (red trace) and 24 h after inoculation (green trace). Scan rate: 1 mV·s^{-1}. Image taken and amended from (Jain and Connolly 2013).

A standard set-up for a MFC, as shown in Figure 4.5A, is using a three-electrode set up where the working, reference and counter electrode are immersed in one chamber instead of the classic 2-chamber MFC (Gimkiewicz and Harnisch 2013). This eliminates common disadvantages of this set up, such as the aeration of the solution cathode to deliver O_2 to the cathode (Liu and Logan 2004). However, much focus has been made on reactor design to investigate electroactive bacteria with typical reactor volumes of ~250 mL in the research lab setting, as well as scale up these reactors to industrial sizes. Miniaturisation of MFCs for research and screening purposes, is therefore desirable. Recently, disposable screen-printed electrodes (SPE) have been developed offering a range of different electrode materials. SPEs are comprised of a variable number of electrodes to complete an electric circuit with electrode and

material similar to that used in conventional MFCs can be chosen. These properties make them an ideal candidate to down-scale MFCs to allow for fast-screening of electroactive microorganisms and their physiology and/or metabolism (Metrohm Dropsense, see Figure 4.5B). Estevez-Canales *et al.* (2015) have recently established a 75 µL drop-assays to screen electrochemical behaviour of *Geobacter* species, thereby circumventing time-consuming and complex experimental set-ups which has the potential to enable more a rapid screening approach of EABs than traditional MFC setups.

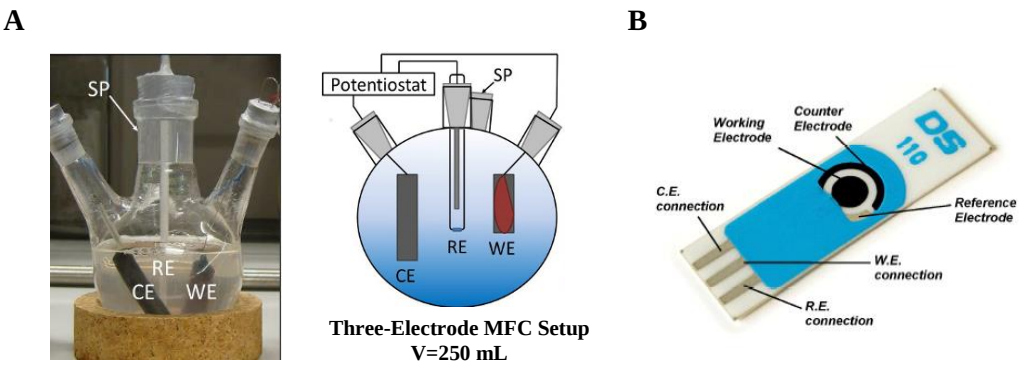

Figure 4.5 Experimental set-up of a three-electrode MFC. (A) Conventional three-electrode MFC set-up in a 250 mL vessel with reference electrode (RE), working electrode (WE) and counter electrode (CE) [image taken from (Gimkiewicz and Harnisch 2013)*]. (B) Screen-printed electrode (SPE) with a pseudo-reference electrode, working electrode (e.g. carbon or graphene) and counter electrode [image taken from Dropsense[23]].*

[23] http://www.dropsens.com/en/screen_printed_electrodes_pag.html (last accessed 30th June 2018)

4.1.4 *Aims of Work Presented in this Chapter*

This chapter uses a synthetic biology approach to increase SOMR-1's bio-electrochemical performance by applying the tools established in Chapter 3.

These aims included:

- To construct of a synthetic gene operon that combines known key genes involved in SOMR-1 flavin production, including *bfe* and *ushA*, to supplement the SOMR-1 EET chain
    - Operon to be used with modular pSEVA platform
    - Operon to be cloned using Paperclip gene assembly with novel inducible promoter $P_{Chnb/ChnR}$ and $P_{tet/TetR}$
- To assess biofilm formation by overexpressing *yedQ* and *yhjH* under $P_{Chnb/ChnR}$
- To establish miniaturisation of SOMR-1 three-electrode MFCs using screen-printed electrode (SPE) technology
- To combine SPE technology with the constructed synthetic operon to enhance microbial electrochemical activity

4.2 Construction of a Synthetic EET Enhancer Pathway in SOMR-1

Utilising the components of the synthetic tool box for SOMR-1 from Chapter 3, a synthetic operon using the modular pSEVA platform and the with newly established inducible Promoter $P_{Chnb/ChnR}$ was designed to combine and overexpress key proteins involved in SOMR-1's EET chain.

4.2.1 *Design of SOMR-1 EET Multi-gene Operon using the Paperclip Assembly Method*

To accomplish this, the Paperclip gene assembly method, which allows a flexible approach of multi-part assembly, was used owing to its rapid and ease of use to create this operon (Trubitsyna et al. 2014). This assembly method works in a restriction site-independent manner which is achieved by defining order of DNA parts and so-called oligonucleotide clips that are then fused using a two-step PCR reaction (see section 2.2.6). However, a 3 bp scar (5'-GCC-3') between the assembled parts, therefore oligonucleotide were synthesised which already possess an RBS s part of the DNA gene to be assembled. Figure 4.6A shows designed gene architecture including the Biobrick RFC10 prefix adding in EcoRI and Xbal as spacer before the strong RBS BBa_0034, follwoed by the biobrick scar (5'TACTAG'3), the open reading frame (ORF) which is proceeded by Biobrick RFC10 suffix and lastly the 3'end Paperclip scar (5'-GCC-3'). This way the Paperclip scar does not affect transcription of the correlating gene by being near the RBS and start codon (see Figure 4.6B for gene sequence). Figure 4.6C shows an overview of the designed components of this operon; see Table 2.4 for all paperclip oligonucleotides used. Vector assembly was carried out as described in the section 2.2.6 and assembly reactions were transformed into

E.coli TOP10. Colonies obtained were screened using colony PCR as described in section 2.2.4.5 using primers KAN_UR and oriV_DF which amplified the pSEVA vector insert of the desired genes. Colonies positive from colony PCR were grown overnight on LB agar with selective antibiotic and plasmid DNA extracted and further verified using restriction digesting and sanger sequencing. Despite numerous attempts and troubleshooting of the assembly methods, including PCR extension times, magnesium concentration, DMSO addition to reaction or glycerol only assembly of pSEVA23::$P_{tet/TetR}$::*bfe*::*ushA* (7208 bp) was successful. It was desired to also have SOMR-1's flavin synthesis genes *ribC*, *ribE/H* and *ribF* as well as the periplasmic election carriers STC and the fumarate reductase *fccA* to complement the over expression of *bfe* and *ushA* to increase power output; however due to time-constraints, it was not possible to complete the assembly of the full operon as described in Figure 4.6C and carry out these experiments. Therefore, to still test whether the overproduction of *rib* genes in this experimental set up would result in increased EET output (see section 4.3.3; Figure 4.6), the plasmid pYYDT-C5 was sourced from Hao Song's research group which has been shown to enhance bidirectional electron transfer in SOMR-1 by overexpressing the *rib* genes from *Bacillus subtilis* under $P_{trc/lacIq}$ control (Yang et al. 2015). However, this vector uses the $P_{trc/lacIq}$ promoter, to therefore be able to compare the expression of the *rib* genes from pYYDT-C5 with the pSEVA platform used in this study, the paperclip assembled plasmid pSEVA23::$P_{tet/TetR}$::*bfe*::*ushA* cargo was cloned into pSEVA234 (Km^R, $oriV_{pBBR1}$, $P_{trc/lacIq}$) using restriction-ligation cloning as described in section 2.2.4.4. All plasmids were conjugated into SOMR-1 as previously described (see section 2.2.2.2.2).

A

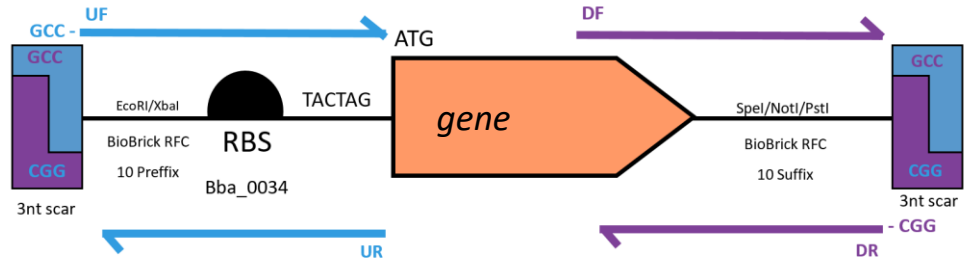

B

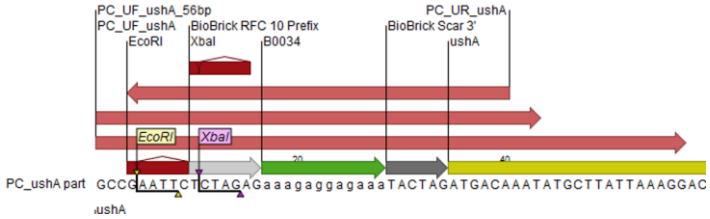

C

Backbone	Promoter	bfe	ushA	SO_ribC	SO_ribE/H	SO_ribF	STC/ cctA	fccA
pSEVA	ChnB	FAD export, FMN production		RF->FAD/FMN synthesis			Periplasmic e-shuttle pair	
2.9k	1kb	1.4+1.7=3.1kb		0.9, 0.5, 0.6=2kb			1.8kb+0.35	

D

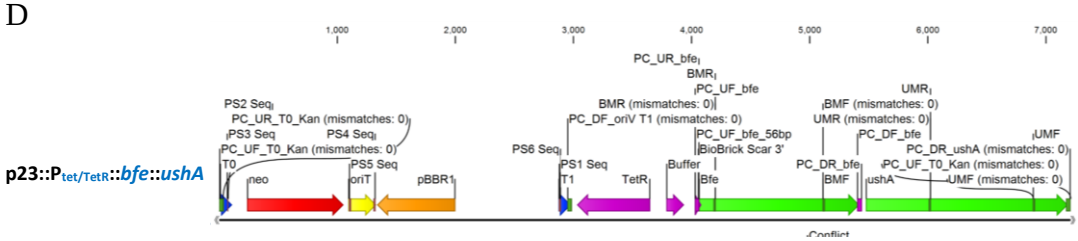

E

pYYDT-C5

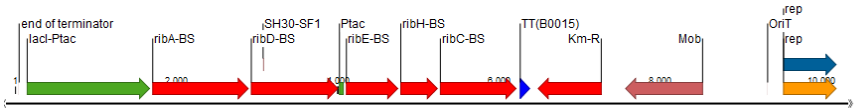

Figure 4.6 Schematic gene architecture of (A) EET operon gene component with paperclip parts and added RBS and pre-and suffix; (B) DNA sequence of paperclip oligo PC_UF_ushA as representative to illustrate added retriction sites, BBa_0034 and Biobrick scar; (C) proposed vector organisation with pSEVA backbone, promoter and EET genes. (D) Vector map of pSEVA23::$P_{tet/TetR}$::bfe::ushA. (E) Vector map of pYYDT-C5 expressing B. subtilis rib genes under P_{trc}. RBS, ribosome binding side; UF, up forwards; UR, up reverse; DF, down forward; DR, down reverse; nt, nucleotide.

4.2.2 *Overexpression of bfe and ushA Gene Fusion under $P_{tet/TetR}$ to enhance SOMR-1 Bulk Flavin Output*

SOMR1- harbouring p23::$P_{tet/TetR}$::*bfe*::*ushA* and pDDYT-C5 as well as SOMR-1 *Δbfe* WT as negative controls were cultivated as previously described and bulk flavin assay was performed as described in section 2.2.8. The overexpression of the *bfe*::*ushA* fusion under the control of $P_{tet/TetR}$ showed a significantly increase bulk flavin production compared to WT (3.5-fold increase) and *Δbfe* (11-fold increase) [see Figure Figure 4.7A]. Furthermore, as expected, the expression of the *B. subtilis rib* gene cluster in SOMR-1 resulted in a 33-fold increase in mean RFU compared to WT, and 111-fold increase compared to SOMR-1 *Δbfe.* This is comparable to the data reported in (Yang et al. 2015). *The growth curves of the c*ultures are shown in Figure 4.7B; notably, SOMR1- harbouring p23::$P_{tet/TetR}$::*bfe*::*ushA*, both uninduced and induced culture, showed slowed growth compared to its controls. Taken these results, however, there seems to be only a marginal difference between induced and uninduced culture of SOMR1- harbouring p23::$P_{tet/TetR}$::*bfe*::*ushA*, therefore it was decided to change the promoter to P_{ChnB} and P_{trc} (see section 4.2.3) to test whether a different promoter can further increase flavin production and reduce metabolic burden.

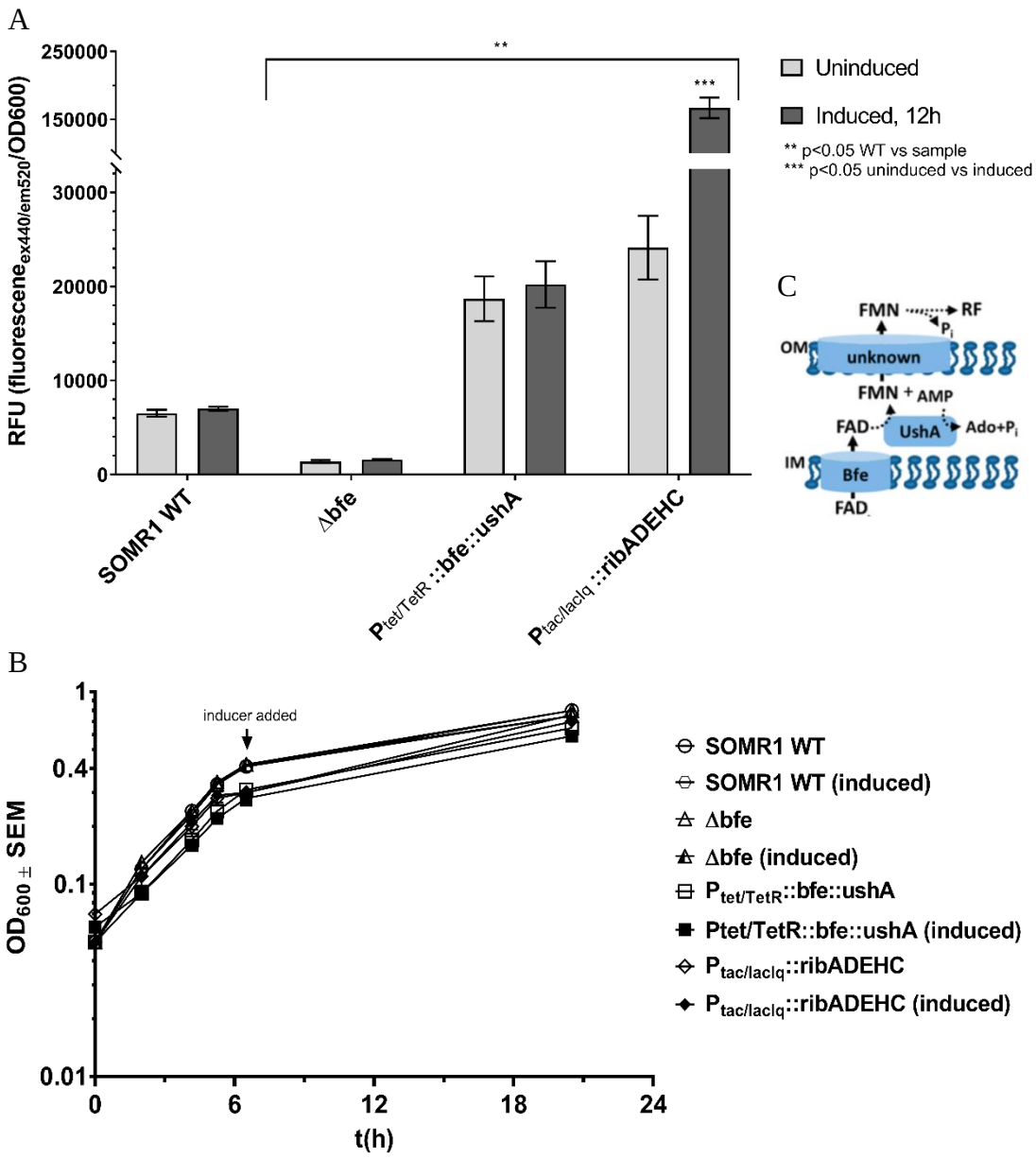

Figure 4.7 Bulk flavin production by SOMR-1 overexpressing bfe::ushA under $P_{tet/TetR}$ compared to SOMR-1 expressing the synthetic rib gene cluster under P_{trc} (pYYDT-C5) with SOMR-1 WT and Δbfe knock out as controls in relative fluorescent units (A). (B) Growth curve in SBM containing 20 mM sodium lactate as electron donor, 40 mM sodium fumarate and 30 µg/mL Km. Cultures were induced late-log phase with 0.5 µM aTc. Data shows triplicates with SD. (C) Schematic flavin pathway trough SOMR-1 outer membranes; image taken from (Yang et al. 2015).

4.2.3 *Overexpression of bfe::ushA Fusion under $P_{Chnb/ChnR}$ and P_{trc} to enhance SOMR-1 Bulk Flavin Output*

As the previous experiment showed only a marginal increase in flavin excretion between induced and uninduced SOMR-1 cultures, the *bfe::ushA* fusion was sub-cloned into pSEVA2311 ($P_{Chnb/ChnR}$) and pSEVA234 ($P_{trc/lacIq}$) using restriction digestion and ligation as previously described (see sections 2.2.4.3, 2.2.4.4 and 3.2.5.1.1) resulting in the plasmids pSEVA2311::*bfe::ushA* and *pSEVA234::bfe::ushA* (see Table 2.3) which were conjugated into SOMR-1 as previously described in section 2.2.2.2.2.

A bulk flavin assay was performed as described in the previous experiment and flavin production monitored over the course of 48 h (see Figure 4.8, Figure 4.9, Figure 4.10 and Figure 4.11). As expected, growth of SOMR-1 harbouring the plasmids pSEVA2311::*bfe::ushA and pSEVA234::bfe::ushA* was slightly slower than the WT and *⊿bfe* control strains (see Figure 4.8A and Figure 4.9A).

Overall bulk flavin production increased for *bfe::ushA* overexpressing strains under both $P_{Chnb/ChnR}$ (Figure 4.8B, Figure 4.10) and $P_{trc/lacIq}$ (and Figure 4.9B, Figure 4.11) over time. There was a 3.1-fold increase in flavin production between SOMR-1 harbouring pSEVA2311::*bfe::ushA* and WT and a 12-fold increase compared to *⊿bfe* knockout strain (see Figure 4.8B). Further, there was a 1.4-fold difference between induced and uninduced *bfe::ushA* expression of under $P_{Chnb/ChnR}$ (Figure 4.10), which is similar to findings of the previously characterised promoter $P_{Chnb/ChnR}$ in section 3.2.5.2 and Figure 3.26, verifying that this expression system can reliably overexpress physiologically important genes for SOMR-1's EET output (see Figure 4.8B and

Figure 4.10). Similarly, SOMR-1 harbouring pSEVA234::*bfe*::*ushA* ($P_{trc/lacIq}$) showed a 4.7-fold increase in flavin production compared to SOMR-1 WT and a 15-fold increase compared to the *Δbfe* strain (see Figure 4.9B and Figure 4.11). Equally, there was also a 1.4-fold difference between induced and uninduced samples, as previously characterised showing that this expression system can reliably overexpress physiologically important genes for EET (see Figure 4.9B and Figure 4.11).

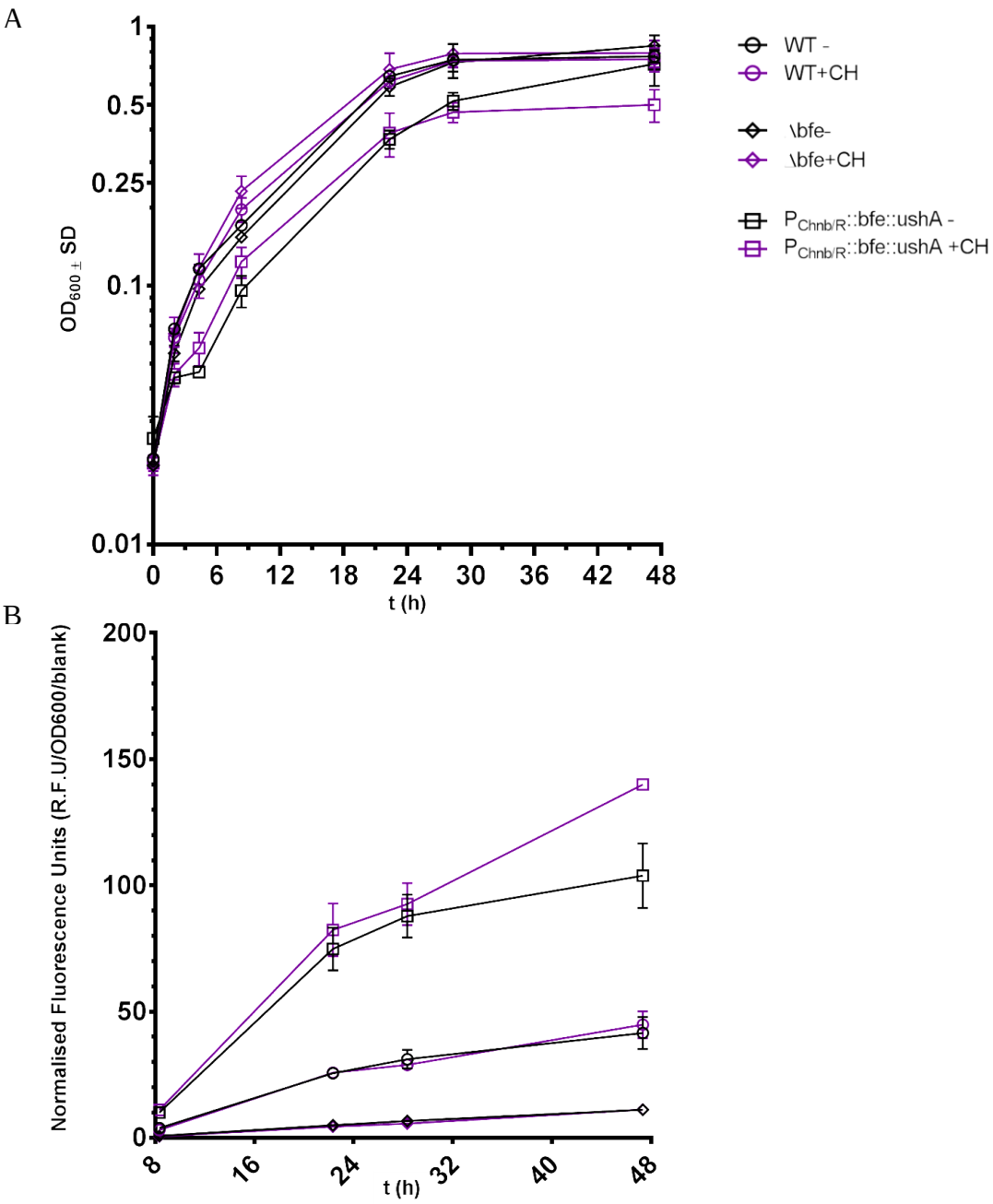

Figure 4.8. Bulk flavin production of SOMR-1 overexpressing bfe::ushA under $P_{Chnb/ChnR}$ over 48h [violet, induced; black uninduced]: (A) ~4h, (B) ~8h, (C) ~22h, (D) ~47h. Cultures harbouring pSEVA2311::bfe::ushA were grown in SBM with 20 mM sodium lactate and 40 mM sodium fumarate and 30 µg/mL Km. Cultures were induced mid-log phase with 1 mM cyclohexanone. Data shows triplicates with SD. Different time-point data was normalised by dividing RFU by OD_{600} and blank-adjusted.

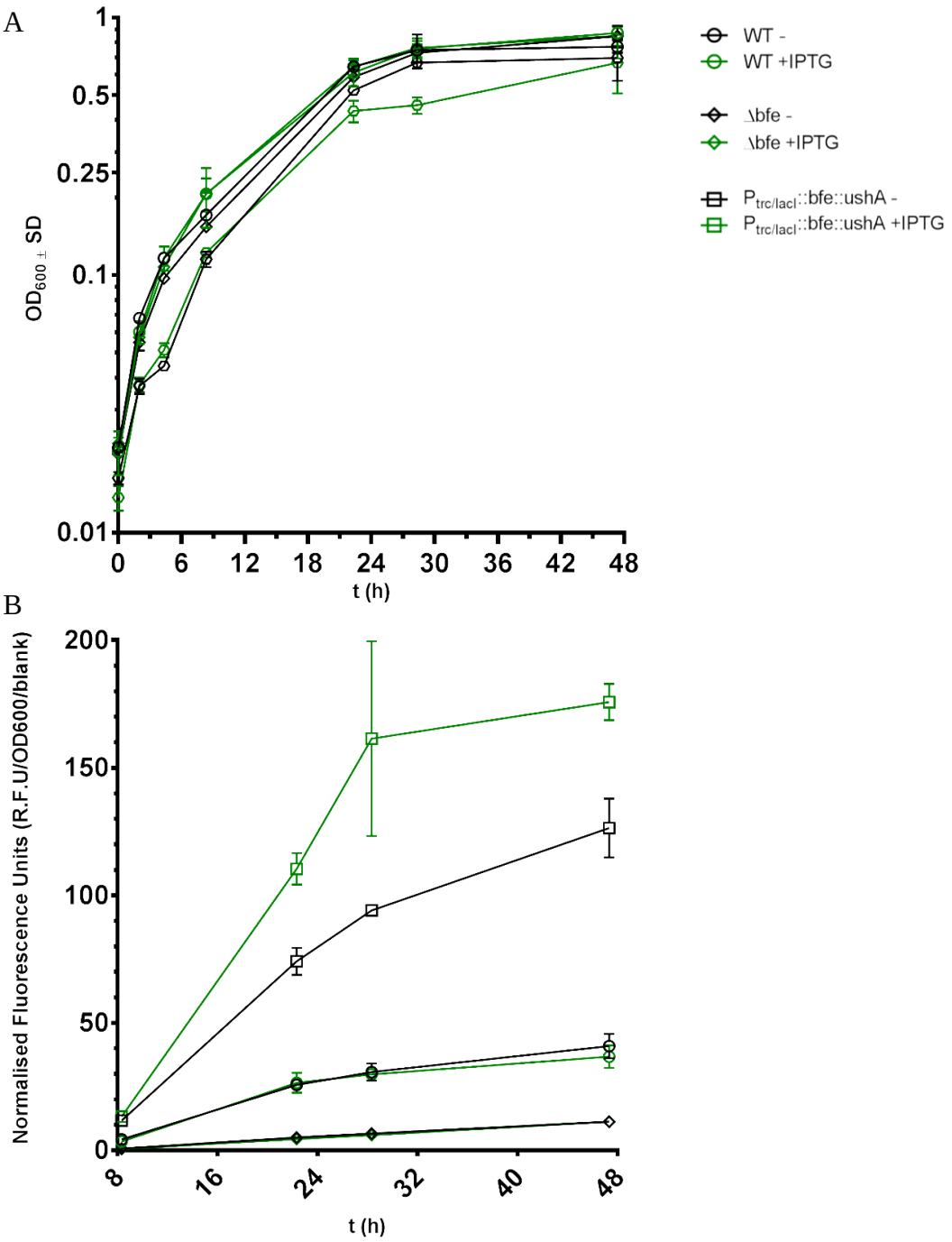

Figure 4.9. Bulk flavin production of SOMR-1 overexpressing bfe::ushA under $P_{trc/lacIq}$ [green, induced; black uninduced]: over 48 h: (A) ~4 h, (B) ~8 h, (C) ~22 h, (D) ~47 h. Cultures harbouring pSEVA234::bfe::ushA were grown in SBM with 20 mM sodium lactate and 40 mM sodium fumarate and 30 µg/mL Km. Cultures were induced mid-log phase with 1 mM IPTG. Data shows triplicates with SD. Different time-point data was normalised by dividing RFU by OD_{600} and blank-adjusted.

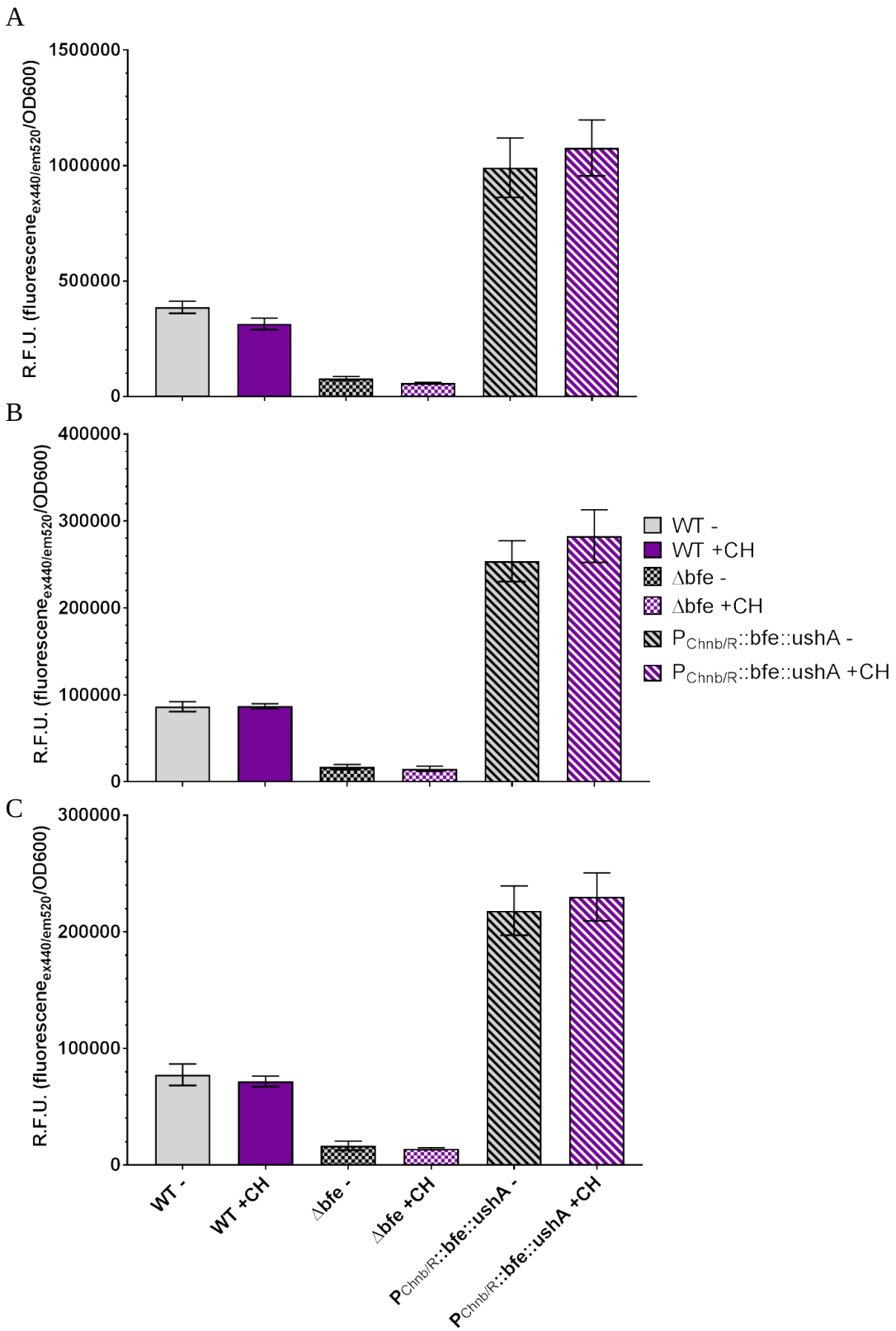
A
B
C
R.F.U. (fluorescene$_{ex440/em520}$/OD600)
1500000
1000000
500000
0
400000
300000
200000
100000
WT -
WT +CH
Δbfe -
Δbfe +CH
P$_{Chnb/R}$::bfe::ushA -
P$_{Chnb/R}$::bfe::ushA +CH

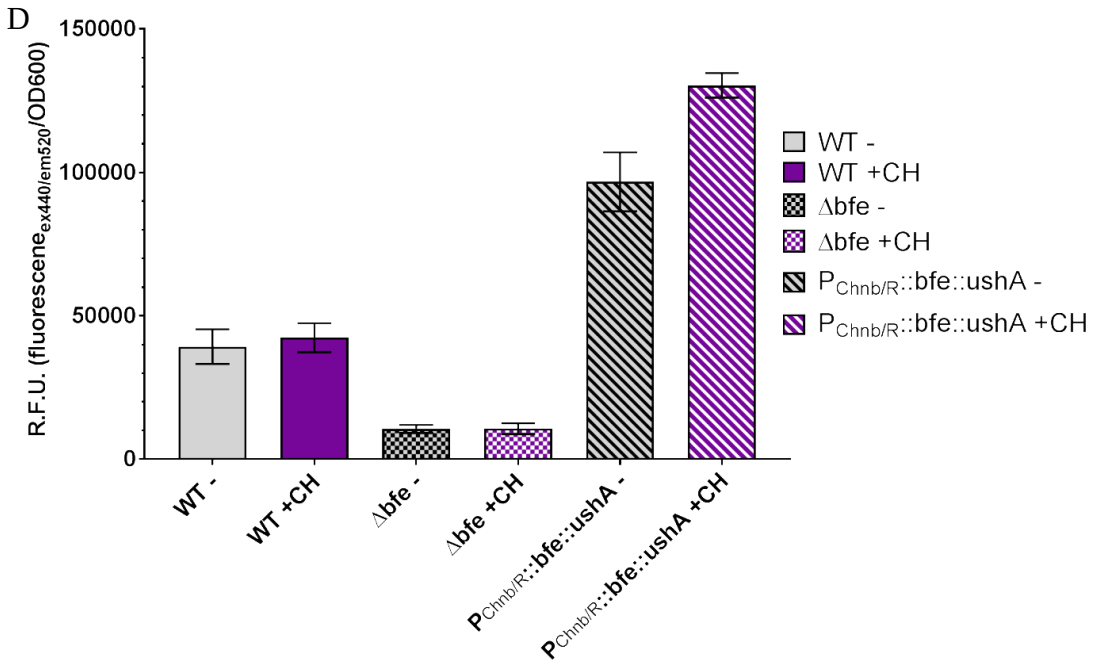

Figure 4.10. Bulk flavin production of SOMR-1 harbouring pSEVA2311::bfe::ushA [violet, induced; grey uninduced] over 48h post induction: (A) ~4h, (B) ~8h, (C) ~22h, (D) ~47h. Cultures were grown in SBM with 20 mM sodium lactate and 40 mM sodium fumarate and 30 µg/mL Km. Cultures were induced mid-log phase with 1 mM cyclohexanone. Data shows biological triplicates with SD.

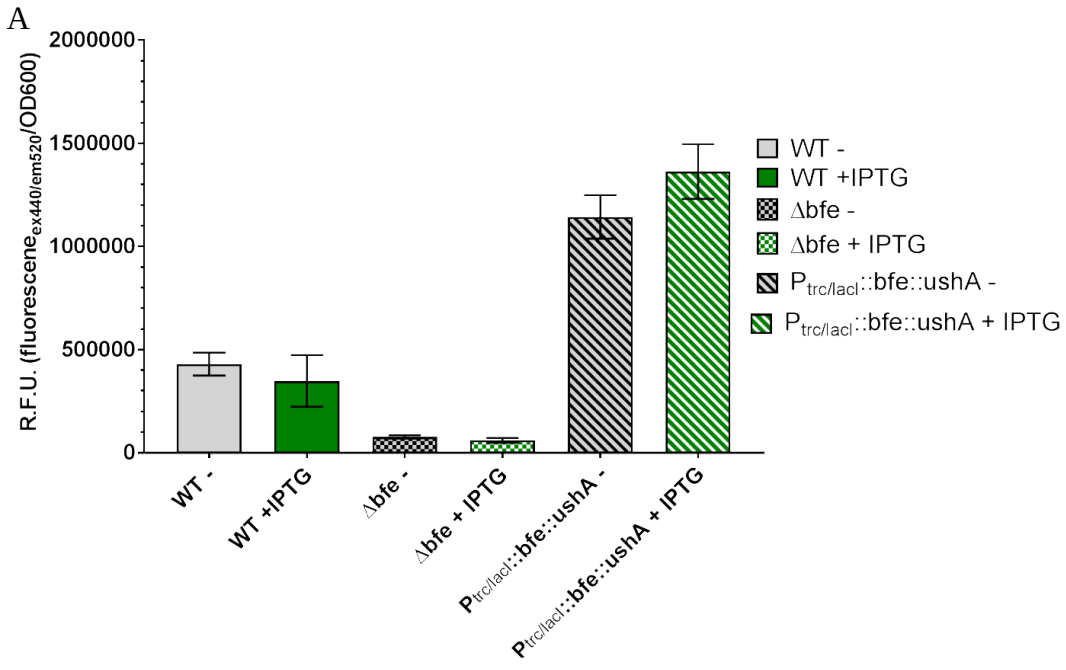

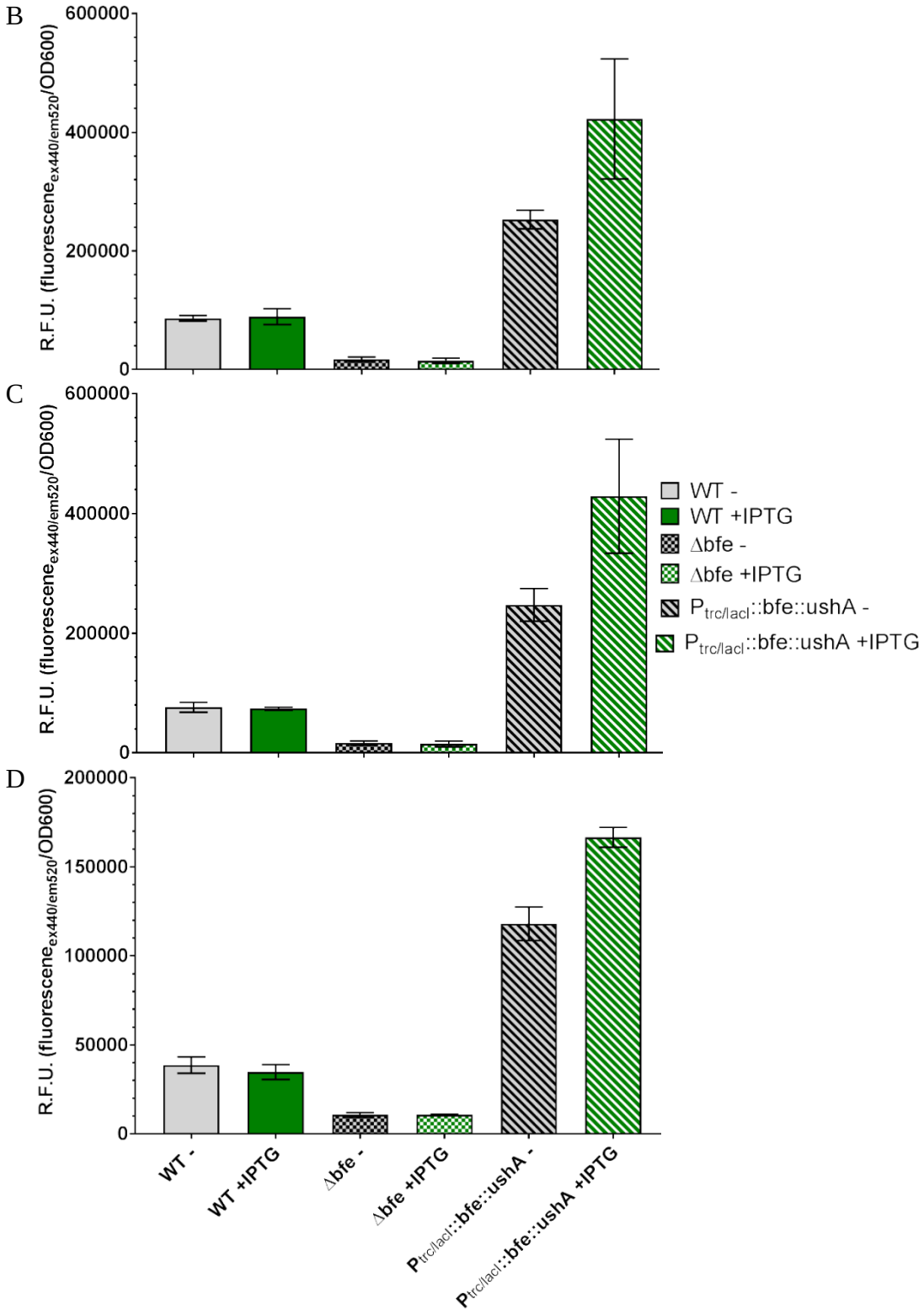

Figure 4.11. Bulk flavin production of SOMR-1 harbouring pSEVA234::bfe::ushA [green, induced; grey uninduced] over 48h post induction: (A) ~4h, (B) ~8h, (C) ~22h, (D) ~47h. Cultures were grown in SBM with 20 mM sodium lactate and 40 mM sodium fumarate and 30 µg/mL Km. Cultures were induced mid-log phase with 1 mM IPTG. Data shows biological triplicates with SD.

4.2.4 *Enhancing SOMR-1 Biofilm Growth using c-di-GMP Biosynthesis Gene yedQ under $P_{ChnB/ChnR}$*

Recently *Liu et al.* realised enhanced biofilm formation and power output in SOMR-1 by overexpressing of *ydeH*, a c-di-GMP biosynthesis gene that promotes biofilm formation in *E. coli*, under the control of IPTG-inducible promoter $P_{lacIq1\text{-}lacIq1}$-P_{tac} (Liu et al. 2015). Additionally, it has been recently shown that transcription of either *yedQ*, a diguanylate cyclase, or *yhjH*, a c-di-GMP phosphodiesterase, from *E. coli* in *P. putida* KT2440 can enable control of transition between bacterial planktonic and biofilm lifestyles. Benedetti *et al.* (2016) placed both genes were under the control of $P_{ChnB/ChnR}$ using pSEVA2311 (Benedetti et al. 2016b). These vectors, pSYedQ (Km^R, $oriV_{pBBR1}$, $P_{ChnB/ChnR}\rightarrow$ *yedQ*) and pSYhjH (Km^R, $oriV_{pBBR1}$, $P_{ChnB/ChnR}\rightarrow$ *yhjH*), were kindly provided by Pablo Nikel (Benedetti et al. 2016a) [see Table 2.3]. Having established the cyclohexanone-responsive expression system $P_{ChnB/ChnR}$ in SOMR-1 in this study, it was tested whether SOMR-1 biofilm formation is controllable using cyclohexanone-inducable expression system and whether it effects biofilm formation. The obtained plasmids pSYedQ and pSYhjH were verified by restriction digestion and gel electrophoresis, as well as sanger sequencing, and conjugated into SOMR-1 using the donor strain *E.coli* WM3064 as previously described. Overnight cultures from single colonies of SOMR-1 harbouring pSYedQ, pSYhjH and pSEVA2311 (negative control) were incubated in LB at 30°C shaking at 200 rpm. The biofilm assay was performed to measure biofilm mass as described in section 2.2.9 (Paulick et al. 2009; Gödeke et al. 2011a). Overnight SOMR-1 cultures harbouring pSEVA311, pSYedQ or pSYhjH grown in LB were added to LM media containing either 0.5 mM, 5 mM or 15 mM sodium lactate. Inoculated 96-well plates were incubated at 30°C for 24 h.

Prior to processing OD_{600} was measured, planktonic cells were aspirated and wells were washed once with water. The remaining bacterial mass was stained with 0.1% crystal violet solution and was resuspended in absolute ethanol (>96 %), before absorbance at 570 nm was measured.

The results in Figure 4.12 indicate that SOMR-1 harbouring pSYedQ (Figure 4.12C) formed more biofilm than SOMR-1 harbouring the empty vector pSEVA2311 (Figure 4.12A). SOMR-1 harbouring pSYhjH showed reduced biofilm formation compared to SOMR-1 harbouring the empty vector pSEVA2311 (Figure 4.12B). An increase in biofilm production was observed which was anti-proportional to the decreasing concentration of sodium lactate available in the media for all three strains. The highest biofilm production was generally seen at 0.5% sodium lactate in LM media, with a mean ± SD biofilm mass (OD_{570}) of 0.59 ± 0.09 for induced cultures of SOMR-1 harbouring pSEVA2311, 1.32 ± 1.22 for pSYedQ and 0.27 ± 0.06 for pSYhjH, compared to the slowest in rich LB media for all strains, with a mean ± SD biofilm mass (OD_{570}) of 0.28 ± 0.15 for induced cultures of SOMR-1 harbouring pSEVA2311, 1.05 ±1.17 for pSYedQ and 0.13±0.02 for pSYhjH (Figure 4.13). Furthermore, the use of cyclohexanone does not negatively affect biofilm mass under the conditions tested in the negative control (Figure 4.12A). A stark overall reduction of biofilm mass was seen in SOMR-1 harbouring pSYhjH by 2.2-fold reduction compared to pSEVA2311 and 5-fold decrease when compared to SOMR-1 harbouring pSYedQ (Figure 4.13). However, induction of pSYhjH does not have a more profound effect on biofilm reduction than the induced control in either LB or LM (Figure 4.12B). Induced overexpression of *yedQ* showed an increase in biomass with a mean ± SD biofilm mass (OD_{570}) of 1.25 ± 0.14 at 5 % (a 1.24-fold increase compared to uninduced control)

and 1.32 ± 0.12 at 0.5 % sodium lactate containing LM media (a 1.44-fold increase compared to uninduced control) [Figure 4.12C]. However, increase in induced versus uninduced cultures was only 1.1-fold in LB media with a mean ± SD biofilm mass (OD_{570}) of 1.05 ± 0.17 in the induced culture and a 1.05-fold increase of 1.039 ± 0.242 at 15 % sodium lactate concentration (Figure 4.12B and Figure 4.12D). Overall, *yedQ* expression significantly increased biofilm formation 5-fold, while overexpression of *yhjH* reduced biofilm formation 2.2-fold, compared to empty vector control (Figure 4.13).

These results indicate that this expression system can be used not only to manipulate biofilm formation and dispersal in SOMR-1 but it also confirms that cyclohexanone as an inducer does not negatively affect SOMR-1 biofilm production and therefore making it an ideal candidate for MFC applications.

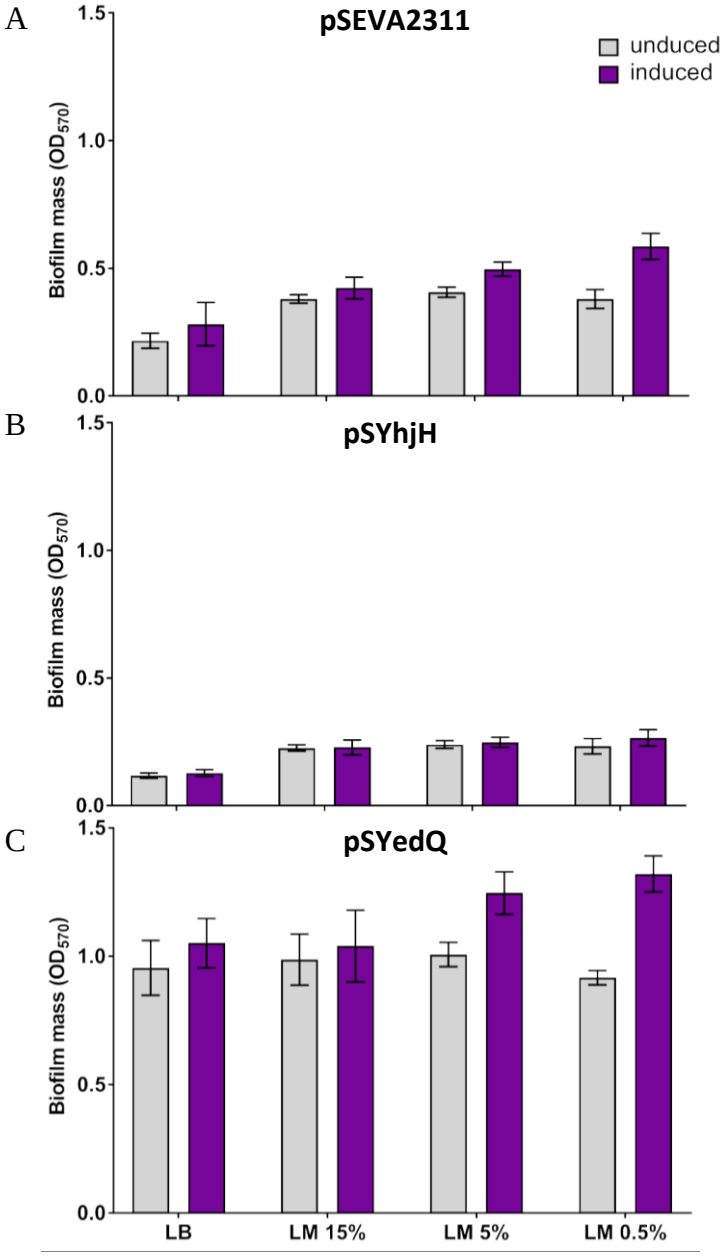

Figure 4.12 SOMR-1 biofilm formation after overexpression of yedQ and *yhjH under* $P_{ChnB/ChnR}$. *Overnight SOMR-1 cultures harbouring empty pSEVA2311 (A), pSYedQ (B) or pSYhjH (C) were grown in LB and 10 µl of the culture was added to 165 µl (175 µl total) of Lactate medium (LM) with 0.5 mM, 5 mM or 15 mM sodium lactate in 96-well polystyrene plates (Greiner). The plates were incubated at 30°C for 24 h and cultures were induced with 1 mM cyclohexanone at the onset of the cultivation. After incubation,* OD_{600} *was measured immediately prior to processing. Planktonic cells were aspirated and wells washed once with water. 180 µl of 0.1% crystal violet solution (Sigma) was added to each well and left for 15-20 minutes, before washing 4 times with 200 µl water (until washes are clear of purple). Remaining crystal violet was resuspended in 200 µl 96% ethanol, before absorbance at 570 nm was measured using a Fluostar Omega spectrophotometer (BMG Labtech). Bars show data in triplicate as mean with SD error bars.*

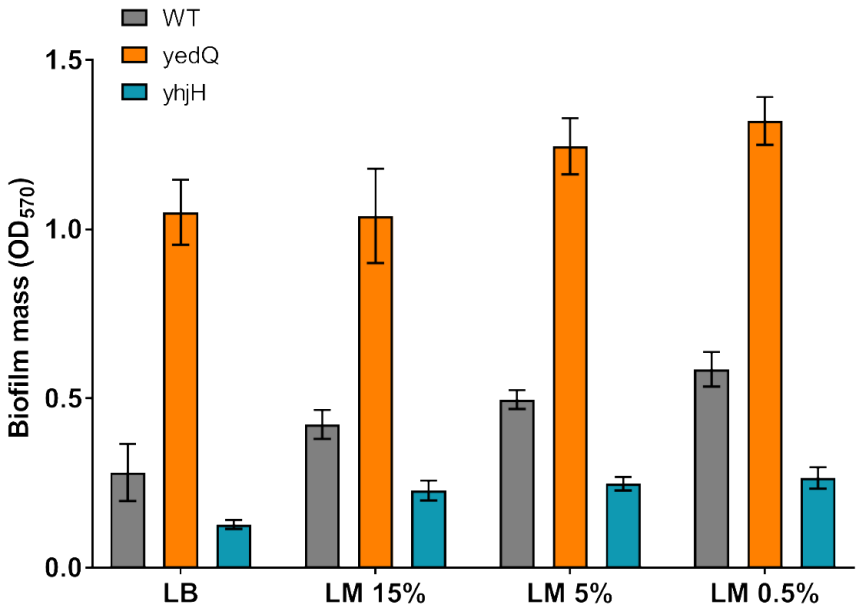

Figure 4.13 Comparison of SOMR-1 biofilm formation after overexpression of yedQ and *yhjH under* $P_{ChnB/ChnR}$*. Overnight SOMR-1 cultures harbouring empty pSEVA2311 (grey), pSYedQ (orange) or pSYhjH (blue).*

4.3 Miniaturisation of SOMR-1 MFCs using Screen-Printed Electrodes

To characterise and test the effect that novel promoters and gene constructs have on SOMR-1's EET performance, a miniaturised SOMR-1 three-electrode MFC reactors set-up was developed using screen-printed electrodes (SPE) for the bio-electrochemical analyses of SOMR-1.

4.3.1 *Design of Experimental Set-up of Screen-Printed Electrode MFCs*

To miniaturise a classic MFC reactor, the volume was reduced from 250 mL to 5 mL using a 5 mL Eppendorf tube a MFC chamber and the Dropsense multichannel potentiostat SPE system. Figure 4.14A illustrates the 5 mL MFC setup. The SPEs used in this system have with a pseudo-reference electrode (RE), working electrode (WE; carbon or graphene) and counter electrode (CE) [see Figure 4.14B]. SPE's were immersed into 5 mL Eppendorf tube containing anaerobically grown SOMR-1 culture in SBM medium containing 20 mM sodium lactate as electron donor and 20 mM sodium fumarate as electron acceptor to facilitate survival of bacteria during conditioning, as well as 30 µg/mL Km and inducer as appropriate. Figure 4.14C illustrates the MFC set-up in the anaerobic chamber where the SPE is connected to an 8-channel potentiostat (Dropsense multichannel potentiostat, see section 2.2.12). Each Eppendorf lid had been modified to allow the SPE to slit thought and immersed chip and lid were additionally sealed with parafilm to prevent contamination in the anaerobic chamber. SOMR-1 cultures were prepared as described in section 2.2.12.

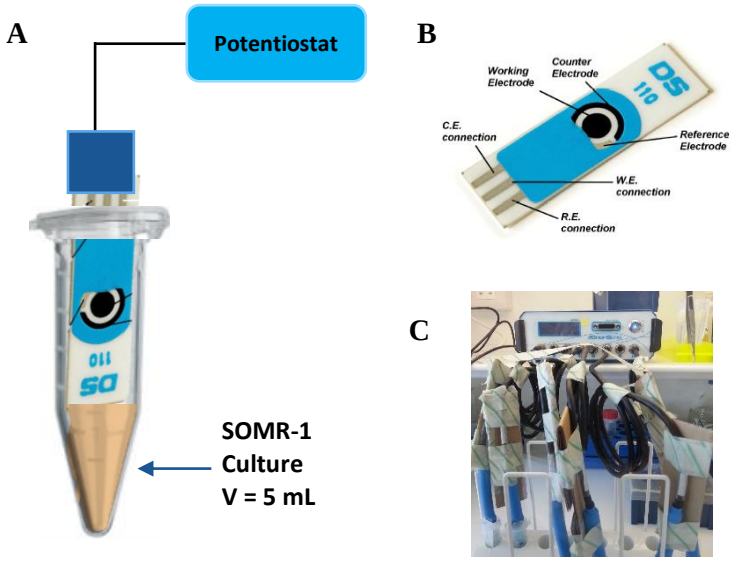

Figure 4.14 Experimental set-up of miniaturisation of three-electrode MFC. (A) Schematic setup of 5 mL SOMR-1 MFC using SPE system using Dropsense multichannel potentiostat and (B) screen printed electrodes with a pseudo-reference electrode, working electrode (Carbon 110) and counter electrode. SPE's are immersed into 5 mL Eppendorf tube containing anaerobic SOMR-1 culture in SBM medium contain 20 mM sodium lactate as electron donor and 20 mM sodium fumarate as electron acceptor to facilitate survival of bacteria during conditioning.

4.3.2 *Proof of Concept Performing Electrochemical Analysis of SOMR-1 Current Production in SPE MFC Set-Up*

To demonstrate whether the miniaturised SPE MFC can be used to facilitate current production of SOMR-1 and to test whether it is sensitive enough to provide meaningful data. SOMR-1 WT and known EET knockout mutants were therefore used with this set-up (as described in section 4.3.1) to understand whether this technique is sensitive enough to discern current analyses using chronoamperometry (CA) and cyclic voltammetry (CV) under the ascribed conditions.

Chronoamperometric (CA) detection and chronoamperometric biofilm growth of SOMR-1 WT and targeted kock-out mutants of the Mtr pathway (*ΔPEC*, *ΔcymA*; *ΔmtrB*; *ΔfccA*) which are impaired in their EET capabilities and should have this reflected in their CA as well as their CV output.

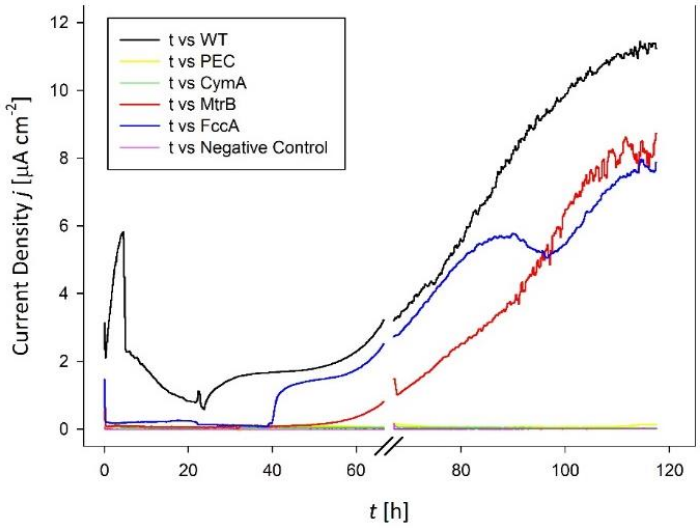

Figure 4.15 Chronoamperometric detection and chronoamperometric biofilm growth of SOMR-1 and EET targeted knock-out mutants (ΔPEC, ΔcymA; ΔmtrB; ΔfccA). E = +0.2 V constant potential applied to WE, measuring every 600 s.

Chronoamperometry was performed using Potentiostat / Galvanostat µStat 8000 (DRP-STAT8000) [Metrohm DropSens, Spain] set to constant potential applied to WE of E = +0.2 V, measuring current (µA) every 600 s using the MFC set up as described in section 4.3.1. Figure 4.16 shows the chronoamperometric current density over the course of 5 days of SOMR-1 and kock-out strains. Peak current density was reached by SOMR-1 WT with ~12 µA·cm^{-2}, whereas *ΔmtrB and ΔfccA* reached ~8 µA·cm^{-2} and ~7.5 µA·cm^{-2}, respectively. There was no detectable current from *ΔPEC*, *ΔcymA* and the medium only control (see Figure 4.16). To further characterise the sensitivity of the SPE electrode for substrate reduction across a range of imposed potentials cyclic voltammetry method was adapted from Gimkiewicz and Harnisch (2013) and performed with the cycling potential set to E_i=-0.7V, E_1 = 0.5V and E_2 = -0.7V.

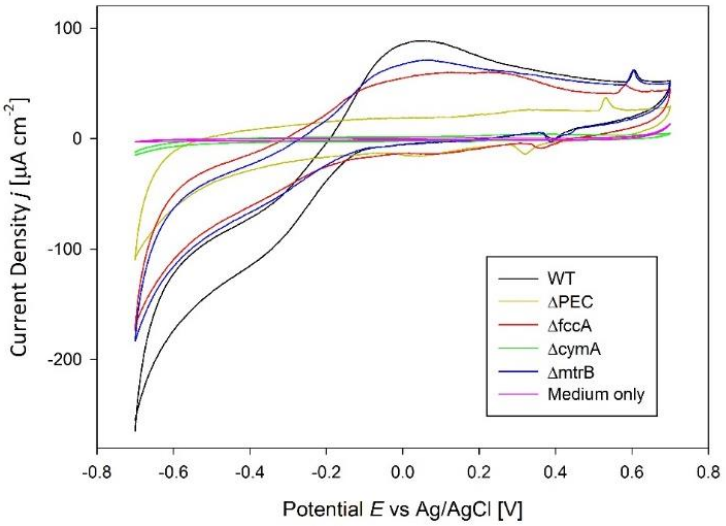

Figure 4.16 Cyclic voltammetry of SOMR-1 WT and mutants with the cycling potential set to E_i=-0.7V, E_1 = 0.5V and E_2 = -0.7V at a scan rate: 1 mV/s.

Figure 4.16 shows the electrochemical current profile, i.e. CV, during oxidation and reduction processed at the surface of the working electrode after ~65 h of chronoamperometric biofilm growth. Voltammograms of SOMR-1 of *ΔcymA* showed

no notable potential changes, similar to the negative medium control. However, SOMR-1 WT showed a distinctive change in its anodic peak potential (E_{pa}) at -0.7V and to a lesser extend *ΔmtrB, ΔfccA* and *ΔPEC* kock-out strains. The redox peak of WT, *ΔmtrB* and *ΔfccA* is centred at 0.1 V. However, there was no notable current peaks from *ΔPEC*, *ΔcymA* and the medium only control (see Figure 4.16). This in line with the assumption that these know-out strains are impaired in their EET capability, meaning as microbially produced flavins and/or outer-membrane bound cytochromes cannot be deposited at the electrode, anodic current decreases compared to WT (Marsili et al. 2008).

4.3.3 *Electrochemical Analysis of EET Enhancer Pathway using SPE MFCs*

As demonstrated in the previous section, the miniaturised SPE MFC can be used to test current production of SOMR-1 strains. As described in section 4.2, the proposed enhancer pathway of the *bfe*::*ushA* gene fusion results in increased bulk flavin production. To see whether this can be translated directly into increased current production by SOMR-1 harbouring the same construct, chronoamperometric (CA) detection and chronoamperometric biofilm growth as described in the previous section 4.3.2. Cultures of SOMR-1 strains were prepared as described in section 2.2.12 and set up in anaerobic SBM containing 20 mM sodium, lactate 40 mM sodium fumarate and 30 µg/mL Km. Cultures were induced with 1 mM cyclohexanone and 1 mM IPTG as appropriate once transferred to the MFC vessel.

Figure 4.17 shows the chronoamperometric detection over the course of over ~40 h. Current increased steadily for all strains over time with the exception of SOMR-1 harbouring pYDTT-C5. Maximum current was reached at the end of the experiment and SOMR-1 controls, i.e. WT plus empty pSEVA2311 and Δbfe plus pSEVA2311, reached current densities of 7.7 $\mu A \cdot cm^{-2}$ (Figure 4.17A) and 9.6 $\mu A \cdot cm^{-2}$ (Figure 4.17B), respectively (Figure 4.17A). SOMR-1 overexpressing *bfe*::*ushA* under the control of $P_{Chnb/ChnR}$ (Figure 4.17C) and $P_{trc/lacIq}$ (Figure 4.17D) yielded in current densities of 6.2 $\mu A \cdot cm^{-2}$ and 6.9 $\mu A \cdot cm^{-2}$, respectively. SOMR-1 expression *B. subtilis rib* genes (pYDTT-C5; Figure 4.17E) gave a maximum current density of 8.8 $\mu A \cdot cm^{-2}$, a 1.14-fold increase compared to WT. This was even further increased when *bfe*::*ushA* under the control of $P_{Chnb/ChnR}$ was added, resulting in a total current density of 11.5 $\mu A \cdot cm^{-2}$, 1.5-fold increase compared to WT, and 1.9-fold increase to *bfe*::*ushA* and 1.3-fold increase when compared to the *rib* gene overexpression alone.

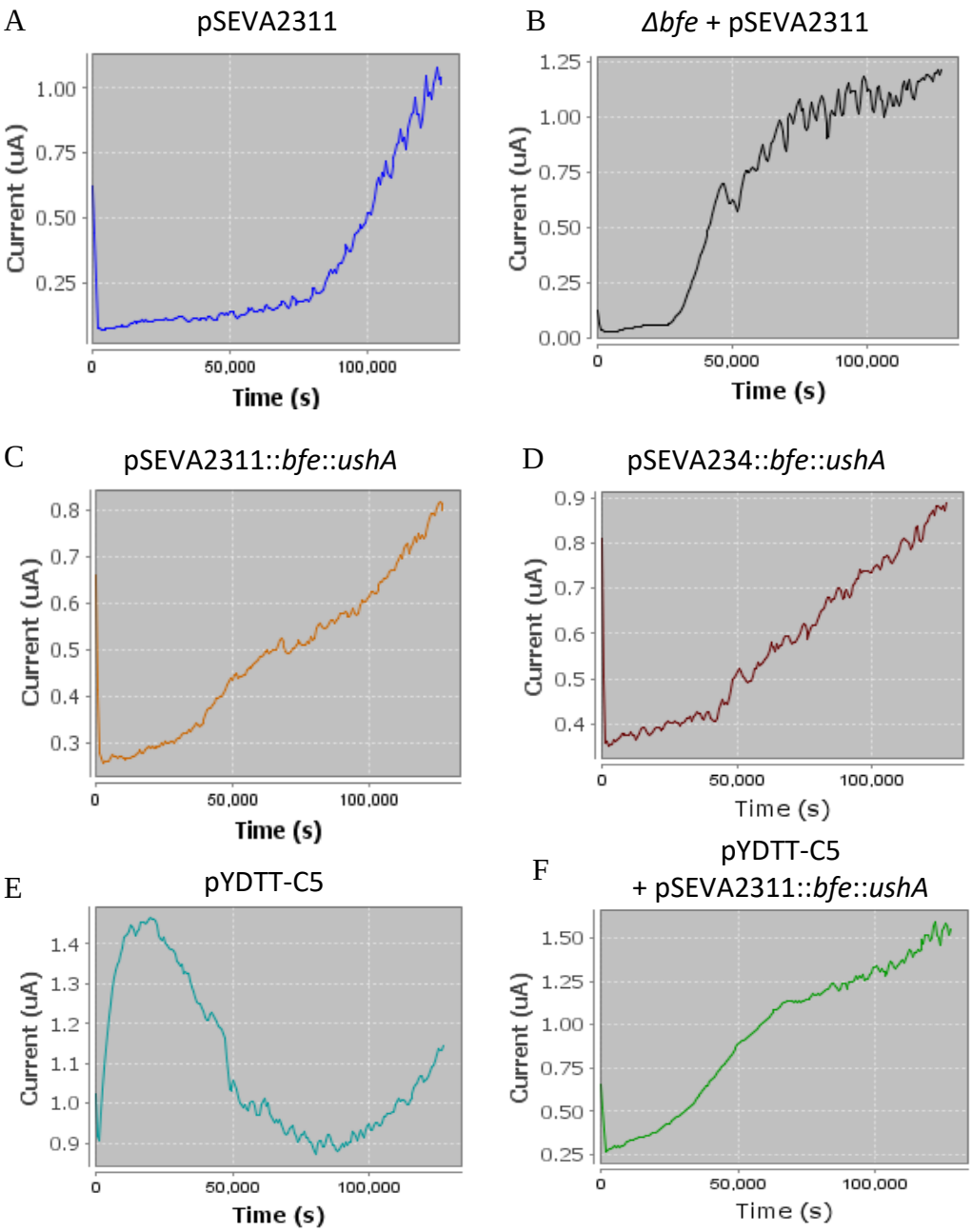

Figure 4.17 Chronoamperometric detection and biofilm growth over ~40 h of SOMR-1 harbouring: (A) empty pSEVA2311 (negative control); (B) Δbfe + empty pSEVA2311 (negative control); (C) pSEVA2311::bfe::ushA; (D) pSEVA234::bfe::ushA; (E) pYDTT-C5; (F) pSEVA2311::bfe::ushA and pYDTT-5. Cultures were set up in anaerobic SBM containing 20 mM sodium, lactate 40 mM sodium fumarate and 30 µg/mL Km. Cultures were induced with 1 mM cyclohexanone and 1 mM IPTG as appropriate.

4.4 Discussion

4.4.1 *Synthetic Operon in SOMR-1 Increases Flavin Production*

Bfe and *ushA* have never been overexpressed together before and overexpression in the newly stablished pSEVA expression systems shows enhanced flavin production compared to what has been reported in the literature (Covington et al. 2010; Kotloski and Gralnick 2013). With only a limited number of studies having realised synthetic biology applications in SOMR-1 (Gao et al. 2010b; Kane 2011; Fried et al. 2012), showed that this novel expression system offers a robust platform that enables increased flavin production, one of the hallmarks to gauge increased current production in SOMR-1. However, it is noteworthy that the bulk flavin production under the transcriptional regulation of $P_{tet/TetR}$ was inferior to that under $P_{Chnb/ChnR}$. Additionally, given the only marginal to up to 1.4-fold difference between induced and uninduced samples indicate that further fine-tuning of the repressor of both $P_{Chnb/ChnR}$ and $P_{trc/lacIq}$ is desirable to strike a better balance between metabolic burden due to and leaky expression to increase flux towards the desired protein expression.

4.4.2 *SPE MFCs in SOMR-1*

The novel set up presented in this work of established voltammetric techniques which are already used to examine electron transfer capabilities from bacteria to electrode material (Ross et al. 2011; Harnisch and Freguia 2012) facilitated conditions for SOMR-1 to allow current production and demonstrated enough sensitivity to provide meaningful data to discern between SOMR-1 WT and known EET knockout mutants.

Screen-printed electrodes have great potential in their application of screening electroactive bacteria. While they have already been tested with *Geobacter spp.*

(Estevez-Canales et al. 2015) in smaller volumes of 75 µL as a bench top application, they have not been used before in miniature MFC with SOMR-1 to understand screen and test electrochemical physiology and current density output of SOMR-1.

4.4.3 *Detection and Fine-tuning of SOMR-1's Current Production*

For the first time the here presented combination of overproduction of the bacterial flavin exporter Bfe and UshA together with riboflavin synthesis genes resulted in significant increase in current density by SOMR-1. By combining the newly developed miniature MFC with novel gene regulation platform and overproduction of key pathway components of SOMR-1's EET mechanism, the detection of difference in current output between different SOMR-1 strains, such as *rib* gene vs *bfe*::*ushA* gene fusion, was realised and thereby allowing for fine-tuning of SOMR-1 current production. However, it should be noted that the unusually high current production of *Δbfe* should be further investigated. These findings are consistent with those described in the literature, however further tests in larger reactor following the initial pre-screen with this technology could be warranted (Covington et al. 2010; Ross et al. 2011; Yang et al. 2015).

4.5 Conclusion

The construction of a synthetic operon which combined the known key proteins involved in flavin production (*bfe* and *ushA*) with the modular pSEVA platform with the novel inducible promoter $P_{Chnb/ChnR}$ showed a significant increase in SOMR-1's flavin production. Further, the heterologous expression of *yedQ* and *yhjH* under $P_{Chnb/ChnR}$ enhanced biofilm formation in SOMR-1. The miniaturisation of SOMR-1 three-electrode MFCs using screen-printed electrode technology, however, needs

further investigation and adaption to be a more robust tool; however the initial screening results of SOMR-1 mutants give indicative results as to what current production can be expected which is in line with the findings from the more common bulk flavin assays further adding to the EET toolbox to discern microbial electrochemical activity.

CHAPTER 5

5 TUNGSTEN TRIOXIDE ASSAYS FOR SOMR-1 PHENOTYPE SCREENING

5.1 Introduction

Traditional EAB characterisation and identification methods, such as voltage-based screening assays in MFC set-ups are laborious, cost and time intensive. Thus, a high-throughput and rapid screening method for the identification of novel characteristics and phenotypes of SOMR-1 is desirable.

Previously, to elucidate the extracellular electron transfer pathway key players in the SOMR-1 Mtr respiratory pathway [see section 1.4.1 and 4.1.1], iron reductions assays were performed using a ferrozine-based assay (Stookey, 1970) where SOMR-1 shuttles electrons to Fe(III), producing quantifiable Fe(II) over time (Coursolle et al. 2010; Kotloski and Gralnick 2013). This has offered insight into SOMR-1 versatile respiratory chains, as it is known to be able to respire on both soluble and insoluble metals. However, comparing iron reduction assay results of various SOMR-1 mutants with their current output when respiring on electrode material are starkly different where for example the *Δbfe* deletion strain only maintains its low current production over time compared to WT, in contrast to data from corresponding the iron reduction assay, the strain increased its Fe(II) production albeit less efficiently than WT (Kotloski and Gralnick 2013). These results indicate that whilst iron reduction assays give a meaningful gauge or SOMR-1's respiratory capabilities, these findings cannot

fully simulate SOMR-1 behaviour and current output with electrode material in a MFC setting.

Recently, Yuan et al. showed a nanoparticle based assay in which the substrate is insoluble and more similar to electrode morphology than iron reduction assays. These nanoparticles made of tungsten trioxide (WO_3) are a biocompatible material that is highly sensitive towards changes in its electrochemical potential. Shaped as clusters of rods, these can be reduced by electroactive bacteria (EABs) and rapidly form a blue-coloured tungsten bronze that is clearly visible with the naked eye, making it a potent electrochromic compound (Yuan et al. 2013; Yuan et al. 2014).

Therefore, this assay could provide the means to quantitatively and qualitatively evaluate electron transfer capabilities and to give mechanistic information on EET pathways similar to that seen in bio-electrochemical reactors to further elucidate and identify key genes and proteins in SOMR-1 electrode reduction mechanism.

It was therefore aimed to establish a tungsten-based electrochromic assay (Yuan et al. 2013; Yuan et al. 2014) that allows quick and simple data acquisition and analysis on electron transfer capabilities of EABs in principle.

5.1.1 *Aims of Work Presented in this Chapter*

The aim of this chapter was to establish a fast-screening, high-throughput method to allow electrochemical screening and selection of multiple phenotypes of SOMR-1 in a small volume with the potential to be automated using tungsten trioxide nanoparticles as an electron acceptor; this way omitting the need to set up large and laborious

electrochemical devices to investigate mutants, constructs or conditions for their EET efficiency in a time saving fashion. The aims were:

- To synthesise tungsten trioxide nanoparticles
- High-throughput screening of electroactive bacteria using WO_3 nanoparticles
- To establish electrochromic detection in multi-well assays
- To demonstrate robustness of the assay
- To test function of/adapt the assay in agar plates
- To identify enhanced EET phenotypes with this assay using transposon and enhancer transposon mutagenesis
- To identify novel genes key to electron transport chain with transposon mutations and WO_3 assay combined

5.2 Results

5.2.1 *Establishment of Electrochromic Detection Method for Electrochemically Active Bacteria (EAB) using a Tungsten Trioxide (WO_3) Assay*

5.2.1.1 *WO_3 Synthesis and Verification of Bioactivity with SOMR-1*

WO_3 nanorods were synthesised as described previously (Yuan et al. 2013; Yuan et al. 2014). The obtained white powder (see Figure 5.1) was and filtered with dH_2O to exclude remaining salts and acids as well as removing WO_3 particles of inadequate size for the assay.

Figure 5.1 Tungsten trioxide powder yield.

On average a WO_3 nanoparticle synthesis yield of ca. 0.4 g was obtained per acid digestion. To ensure that the synthesis set up correctly, i.e. chemicals used, pH accuracy, acid digestion vessel dimensions and crucially oven temperature rising and cooling pattern, to yield the desired WO_3 nanoparticles, X-Ray Diffraction (XRD) was used to confirm that the powder obtained was indeed tungsten trioxide nanorods. The resulting X-Ray powder diffraction spectrum of the newly synthesised WO_3 (see Figure 5.2) was identical with that published by Yuan *et al.*, (2013).

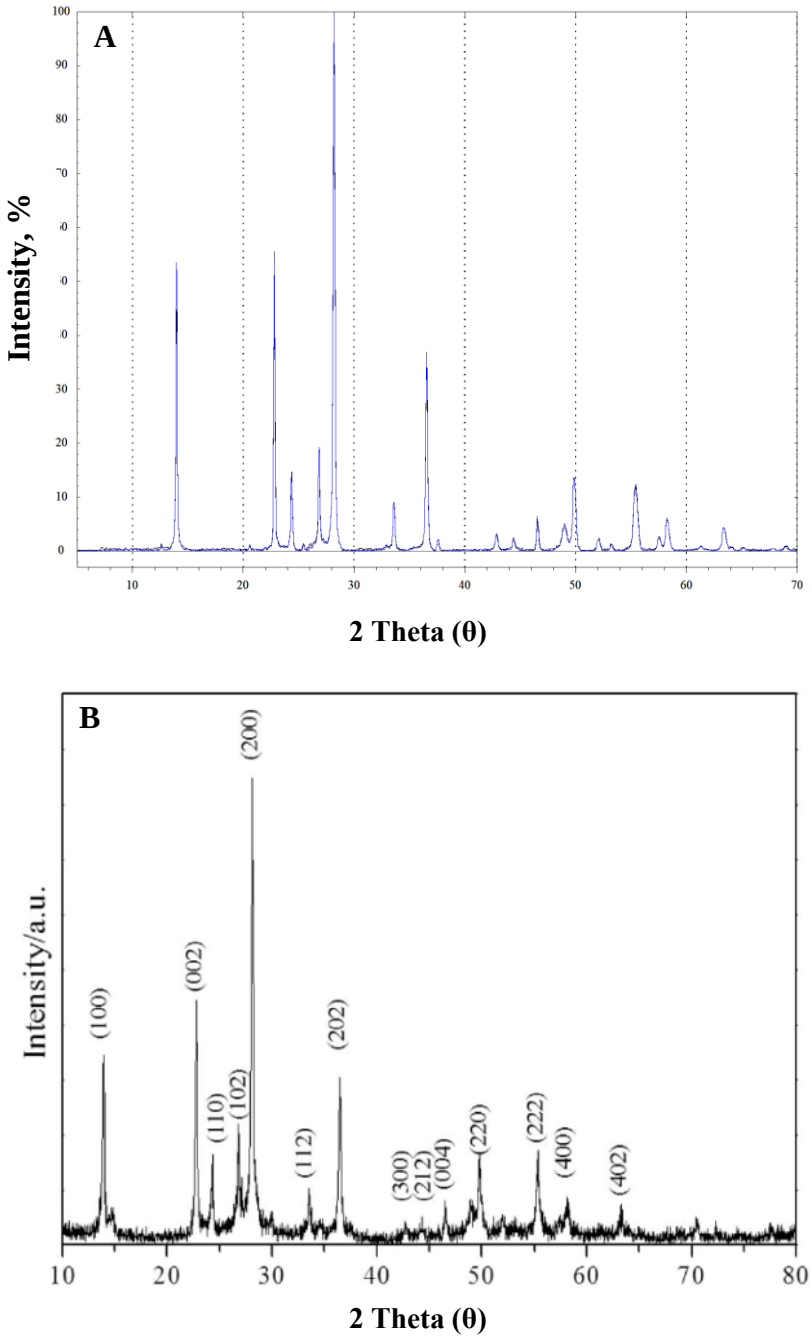

Figure 5.2 X-Ray powder diffraction spectrum of synthesised WO_3. (A) In-house synthesised WO_3 spectrum; (B) reference spectrum, image taken from Yuan et al. (2013).

To further test that the tungsten trioxide had formed into nanorods under these synthesis conditions, scanning electron microscope (SEM) images were taken. These showed the desired morphology of WO_3 nanorod clusters with average size of 2 µm

(see Figure 5.3). Taken together, the protocol established to synthesise WO_3 powder in-house yields the anticipated nanorods morphology that should enable SOMR-1 to be able to reduce them and give a detectable colour-metric change as described in *Yuan et al.* (2013, 2014).

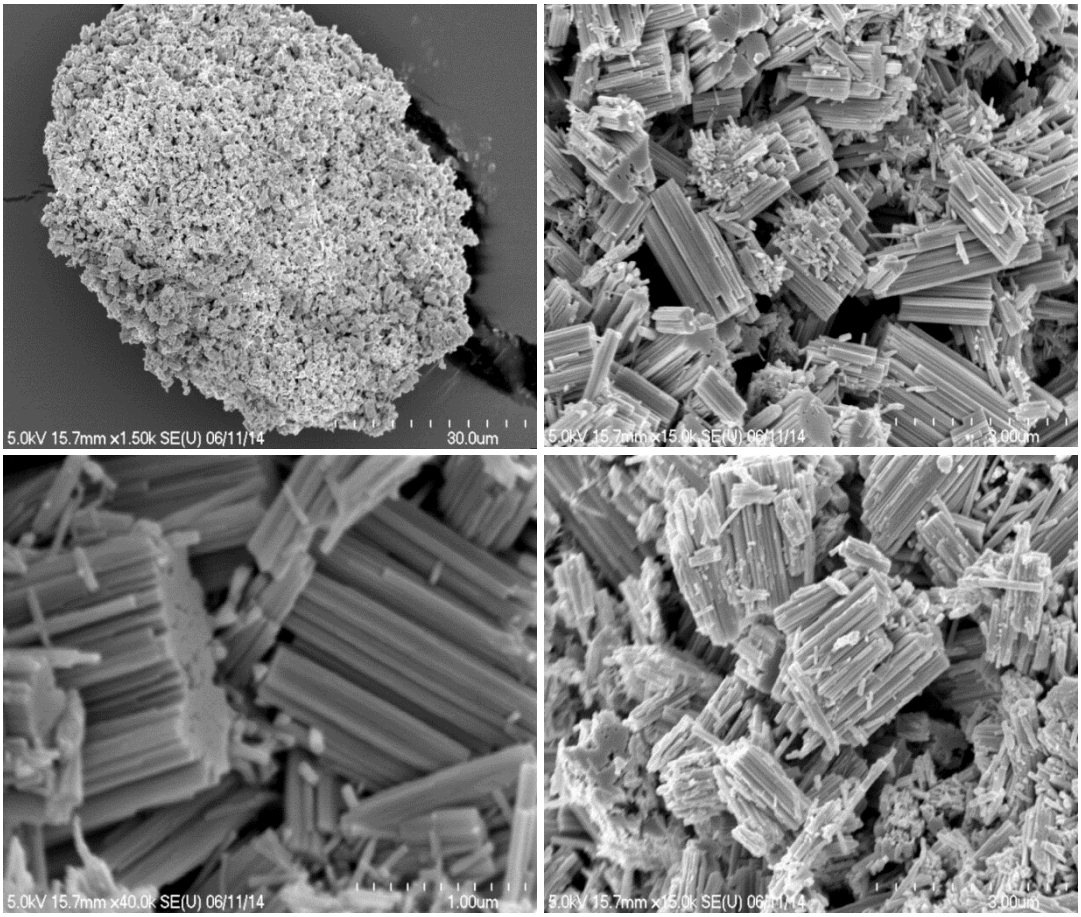

Figure 5.3. SEM images of synthesised WO_3 nanorod clusters with average size of 2 µm.

To test whether our SOMR-1 WT strain was capable of reducing the in-house synthesised WO_3 powder which should result in a colour change of the WO_3 from white to blue, a preliminary test with SOMR-1 culture was carried out. Tungsten trioxide powder was suspended in SBM medium with 20 mM sodium lactate which rapidly sank to the bottom of the tube (see Figure 5.4A). Upon addition of SOMR-1 culture to the reaction and an incubation at 30°C under anaerobic conditions, the

tungsten powder in the tubes with SOMR-1 turned dark blue which can be clearly seen in Figure 5.4B where the cells and tungsten have been pelleted and the supernatant had been removed. Where no bacteria were added, the tungsten remained white indicating that no agent in the medium or environment caused the colour change.

These tests confirmed that the in-house synthesised WO_3 is bio-electrochromically active with our SOMR-1 WT strain evident by the colour change of the probe which only occurred when SOMR-1 was added to the reaction.

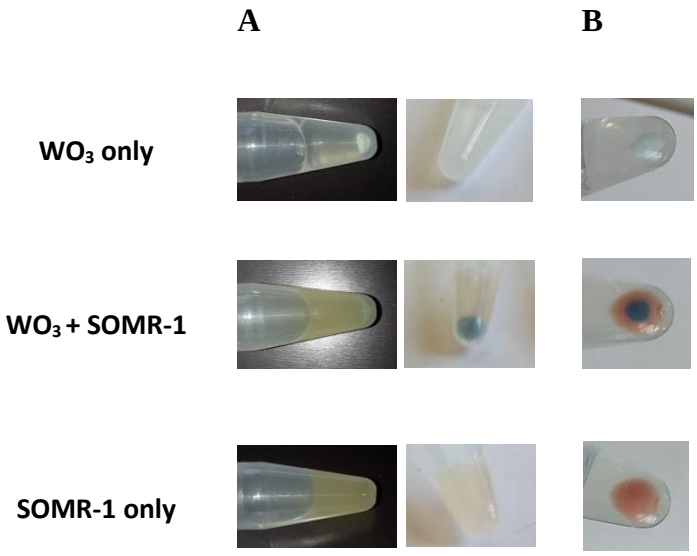

Figure 5.4. Validation of WO_3 reduction by SOMR-1. (A) WO_3 suspended in SBM with and without bacteria;(B) centrifuged microtubes showing white pellet (WO_3 only), orange and blue pellet (WO_3 with SOMR-1) and orange pellet (SOMR-1 only).

5.2.2 *Analysing WO_3 Chromaticity and its Correlation with Bacterial Population Density*

To analyse WO_3 chromaticity, clear flat-bottom 96-well plates were used, as the tungsten particles readily sank to the bottom of each well, as previously seen with mircotubes in Figure 5.4. Due to this, the tungsten nanoparticles block any light detection, making the use of conventional and standard light spectrum absorbance plate readers impossible. To, therefore, obtain numerical data from WO_3 plate assays, the plates were scanned using identical scanning settings under the exclusion of ambient light using a wooden box engulfing the 96-well plate. The mean colorimetric density of each well in biological triplicate was then quantified using ImageJ software and statistically analysed.

Further, as described in Yuan *et al.* (2014) the bio-electrochromic reaction result, i.e. the intensity of the blue-coloured WO_3 bronzes, can correlate with the number of bacterial cells added to each well. This could result strains that would normally be less capable of reduction of the tungsten nanoparticles giving a greater mean density due a higher cell number thereby masking the weaker reduction capabilities and mistakenly be interpreted as a phenotype with greater reduction potential. To assess this, an increasing number of SOMR-1 culture was added to WO_3 wells and incubated under anaerobic conditions, and mean densities analysed after an incubation period (see Figure 5.5). Whereas the first two SOMR-1 inoculated wells show an almost equal density of 58.6 ± 0.8 and 59.0 ± 1.9, respectively, the following four wells show an increase of circa 15% in mean density ranging from 70.8 ± 0.9 to 73.0 ± 1.2 indicating that once a certain bacterial inoculum size was reached the tungsten trioxide reduction

had reached saturation. Therefore, cell numbers for further assays should be adjusted to assure an equal amount of bacterial cells is used to allow for reliant interpretation of results.

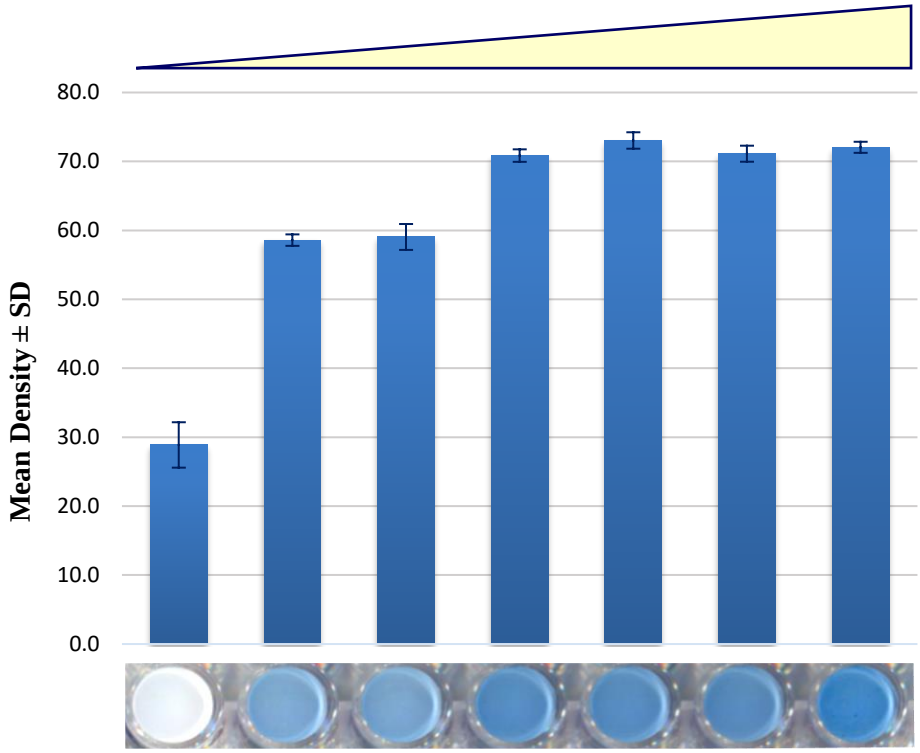

Figure 5.5 Correlation between bacterial inoculum size and mean density of WO_3 chromaticity. Bottom, flat-bottom 96-well plate inoculated with WO_3 only control and increasing number of SOMR-1. Data show biological triplicate with error bars showing standard deviation.

5.2.3 *Is the Difference in Chromaticity of WO_3 Sensitive Enough to Discern Between SOMR-1 Mutations of its Extracellular Electron Transfer Mechanism?*

To test the sensitivity of the in-house synthesised WO_3, the assay was performed with various SOMR-1 mutants lacking major EET pathway components, both in the periplasm (PP) and in the outer membrane (OM). The Mtr pathway (see Figure 5.6) is comprised of the inner membrane-bound tetrahaeme cytochrome CymA (Marritt et al. 2012) which gains electrons from oxidizing menoquinol; it then either reduces periplasmic mediators such as the flavocytochrome FccA or the decahaeme cytochrome MtrA, which forms an outer membrane (OM) complex with MtrB, and decahaeme cytochromes OmcA and MtrC (Myers and Myers 2002). As expected the colour development of the mutant strains inoculated in the 96-well plate is severely impaired compared to the positive control *SOMR-1* WT (well 8, Figure 5.7) and JG 274 (Jeff Gralnick MR-1 strain), especially the ΔPEC strain (see well 2, Figure 5.7A), which has no periplasmic electron carriers, shows a 70% reduction in ET capability (see Figure 5.7B). Further, the Δ*mtrA* and Δ*mtrB* mutants show a considerable decrease in WO_3 reduction capability, as anticipated; whereas Δ*fccA* mutant is still able to transfer electrons effectively, suggesting that there are alternative periplasmic mediators to transfer electron to MtrA. However, the ΔcymA strain should not be capable of such a high transfer rate according to Yuan *et al.* (2013) and Myers & Myers (1997b), therefore this should to be further investigated. As a control to eliminate a false positive reaction, *E. coli* DH5α was used and as can be seen in well 9 (Figure 5.7A) it is not capable to reduce the WO_3. In addition, the prolonged

incubation time of about 30-60 min more is probably due to aerobic inoculation environment; however even after 30 min a clear tendency for the electron transfer capability is visible (see Figure 5.7).

These results are in agreement with those published in Yuan *et al.* (2013, 2014), however, the data also reinforce the high complexity and modularity of the EET and the difficulty to draw conclusions from single knock out mutations. Nonetheless, this approach can be used not only to elucidate novel functions of genes involved in extracellular electron transfer of microorganisms, select an array of mutants which can then be further tested in a MFC setting.

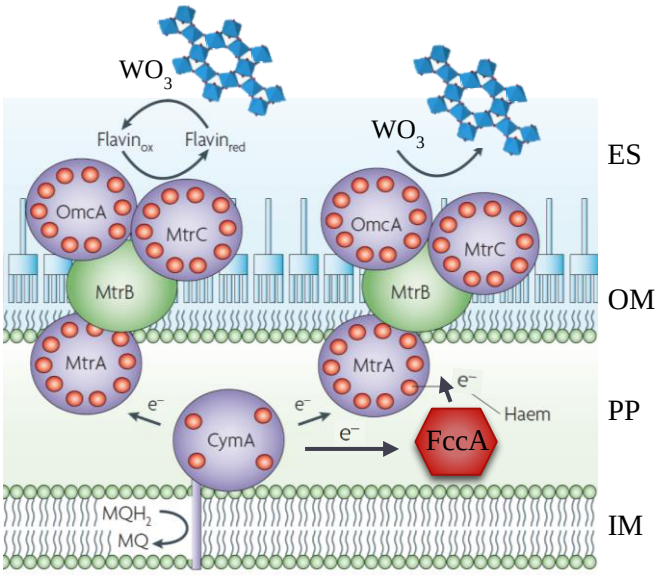

Figure 5.6 Electron transfer pathway from SOMR-1 to WO_3. ES, extracellular space; OM, outer membrane; PP, periplasm; IM, inner membrane; MQH_2, menaquinol; MQ, menaquinone. Image taken and amended from Fredrickson et al., (2008).

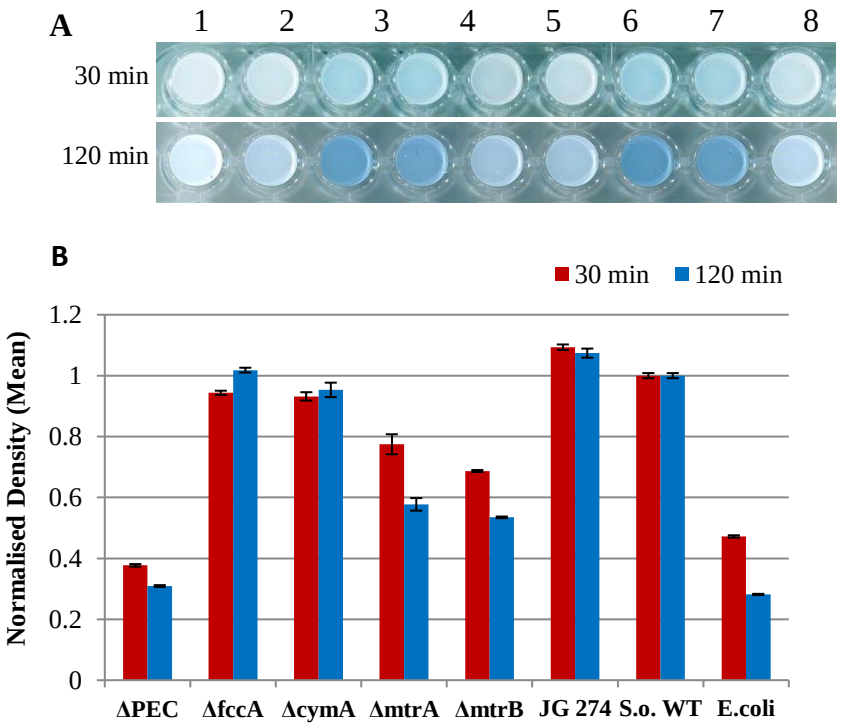

Figure 5.7 Sensitivity validation of WO_3 assay with EET S. oneidensis mutants at different time points. A, images of incubated SOMR-1 mutants (2-6), SOMR-1 WT: JG 274 (6) and NCIMB14063 (7), E.coli DH5α (9) and WO_3 control (1); B, normalised density means, error bars depict standard deviation of three measurements, red: 30 min incubation, blue: 120 min incubation. Data shows triplicate and error bars denote SEM.

5.2.4 *Using WO_3 as a Screening Tool to Identify Enhanced Electricity Production in SOMR-1 Transposon Knockout Mutants*

Based on previous results showing that WO_3 plate assay is providing sufficient sensitivity to discern between SOMR-1 mutants the hypothesis was made whether this assay can be used to identify SOMR-1 mutants that show enhanced electricity production via transposon mutagenesis, thereby allowing to elucidate new genes that are involved in SOMR-1's extracellular electron transport.

Previously, a modified mariner transposon, pMiniHimar RB1, has been constructed for use in SOMR-1 allowing isolation of stable mutants and identification of disrupted genes to find genes involved in cytochrome c biogenesis (Bouhenni et al. 2005). Here, transposon mutagenesis was performed by plasmid conjugation of pMiniHimar RB1 using the donor strain *E. coli* WM3064 (Gao et al. 2010a). Isolation of mutants was performed from LB agar plates containing 50 µg/mL Km. A random selection of colonies was grown overnight aerobically in LB and equal amounts of culture added to SBM in a 96-well plate using SOMR-1 WT, ΔPEC and *E. coli* as positive and negative controls respectively. Freshly prepared WO_3 medium (SBM with 5 g/L of WO_3) was added to the wells at the same time to start the reaction simultaneously and sealed with mineral oil to ensure anaerobic conditions. The plate was transferred into 30 shaking incubator. After only 45 min discernible differences in chromatic changes due to the reduction of WO_3 nanoparticles are already visible (see Figure 5.8). This reaction is amplified over the time course of 24 h.

While the controls of WO_3 medium only and *E. coli* remained starkly white, three out of the 10 mutants exhibited greater density of tungsten bronzes over the first 7 h of the

experiment while the other transposon mutants were showing reduced densities compared to WT.

Similarly this approach is labour intensive with culturing transposon isolates and can lead to higher variation depending on growth speed and cell density on interpreting and correlating densities with EET capabilities. Further, the fast amount of the already scarce yield of WO_3 nanoparticles used per isolate screen makes it uneconomical. A different way of screening multitudes of mutants would be more appropriate.

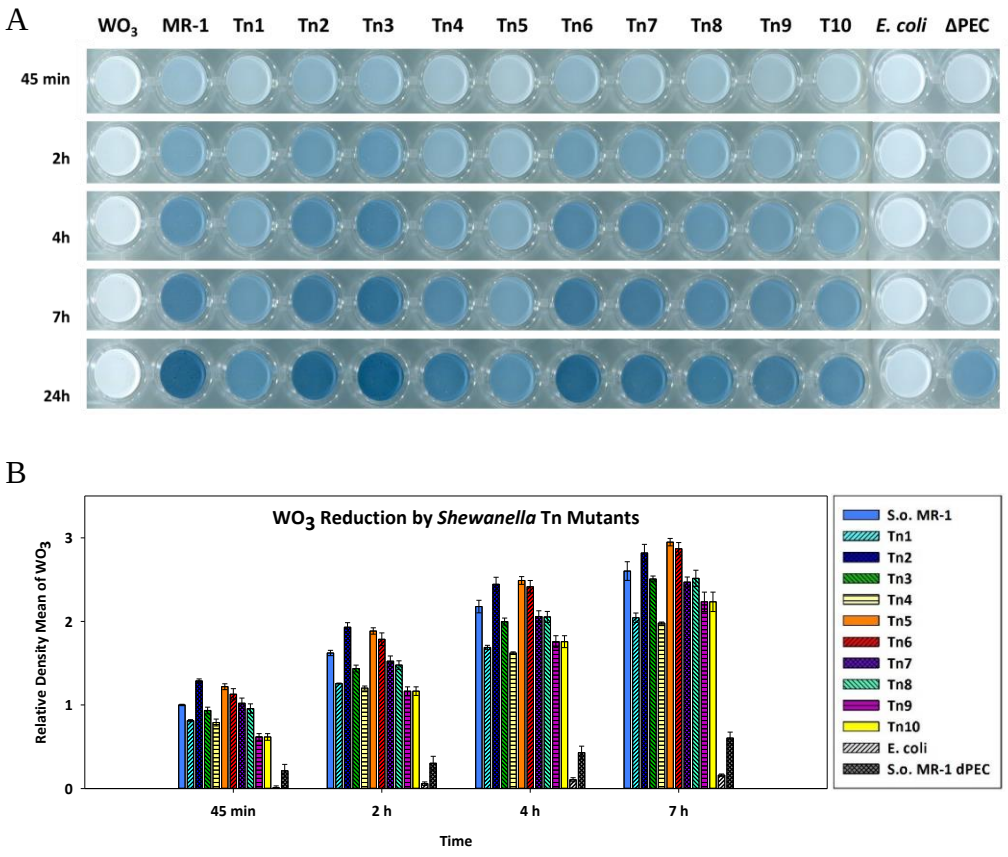

Figure 5.8. WO_3 reduction by SOMR-1 transposon mutants over 24 h. (A) 96-well plate assay showing WO_3 reduction by SOMR-1 WT (well 2), ΔPEC (well 14) and Tn mutants (well 3-12) and E. coli (well 13), un-inoculated control of WO_3 SMB solution (well 1); (B) Relative mean density WO_3 reduction over time. Data show biological triplicate with SD error bars.

5.2.5 *Increasing the SOMR-1 Mutant Screening Capacity by Converting the WO_3 Liquid 96-well Plate Assay into a Plate Screen*

To shorten time and reduced amount of tungsten powder used, to identify potential SOMR-1 mutants of interest, the 96-well plate assay was to be converted into an agar plate based assay where transposon mutants of interest can be directly identified. However, is the intensity of WO_3 bronzes enough in an agar sandwich plate (see Figure 5.9A)?

To test this, SOMR-1 WT and the ΔPEC mutant, which shows the most drastic decline in WO_3 reduction capability, were grown aerobically on SBM medium containing 20 mM sodium lactate as carbon source and then covered in a thin layer of WO_3 agar (5 g/L), both separately and as a mixed culture (see Figure 5.9B). Before addition of the top agar, all colonies appeared of similar size and morphology. After 1 day of incubation, blue halos appeared around the edges of WT and ΔPEC colonies and some colonies of the mixed plate. After 1.5 days of incubation these differences are much starker (see Figure 5.9C). Whereas, the WT colonies exhibited a thick blue halo at the outer edge of each colony (see Figure 5.9C; yellow box), the ΔPEC colonies had a much thinner, more diffused and much less intense tungsten bronze halo compared to the WT (see Figure 5.9C; blue box), which is probably due to the excretion of flavins into the medium. Lastly, the mixed plate displayed a mixed range of tungsten bronzes around the colonies (see Figure 5.9C; red box).

To test, whether it was possible to discern different mutations through the thickness and intensity of the tungsten bronze halos, some colonies were picked and PCR performed from extracted gDNA (see Figure 5.10A). For this, primers that amplify

mtrA were used, as this gene is deleted in ΔPEC giving an easily identifiable band size different of 938 bp (expected band sizes were: WT *mtrA*=1523 bp; ΔPEC Δ*mtrA*=585 bp) [see Figure 5.10B]. Both positive control from stock gDNA of WT and ΔPEC and from gDNA from the split plate resulted in PCR products of the right size. From the 3 colonies picked that showed an increased tungsten halo and were suspected to be WT, all of them showed the corresponding gene size confirming they are indeed WT colonies. From the 3 colonies picked that showed a lesser and more diffused tungsten halo, 2 out 3 were confirmed to be ΔPEC mutants. Both show however, faint bands around 1.5 kb, which leaves room to speculate whether they was any contamination of the sample, as all 4 controls do not show this. Overall, from these results, a tungsten sandwich plate assay could be used to discern different SOMR-1 mutants more rapidly and in great number than the 96-well plate assay.

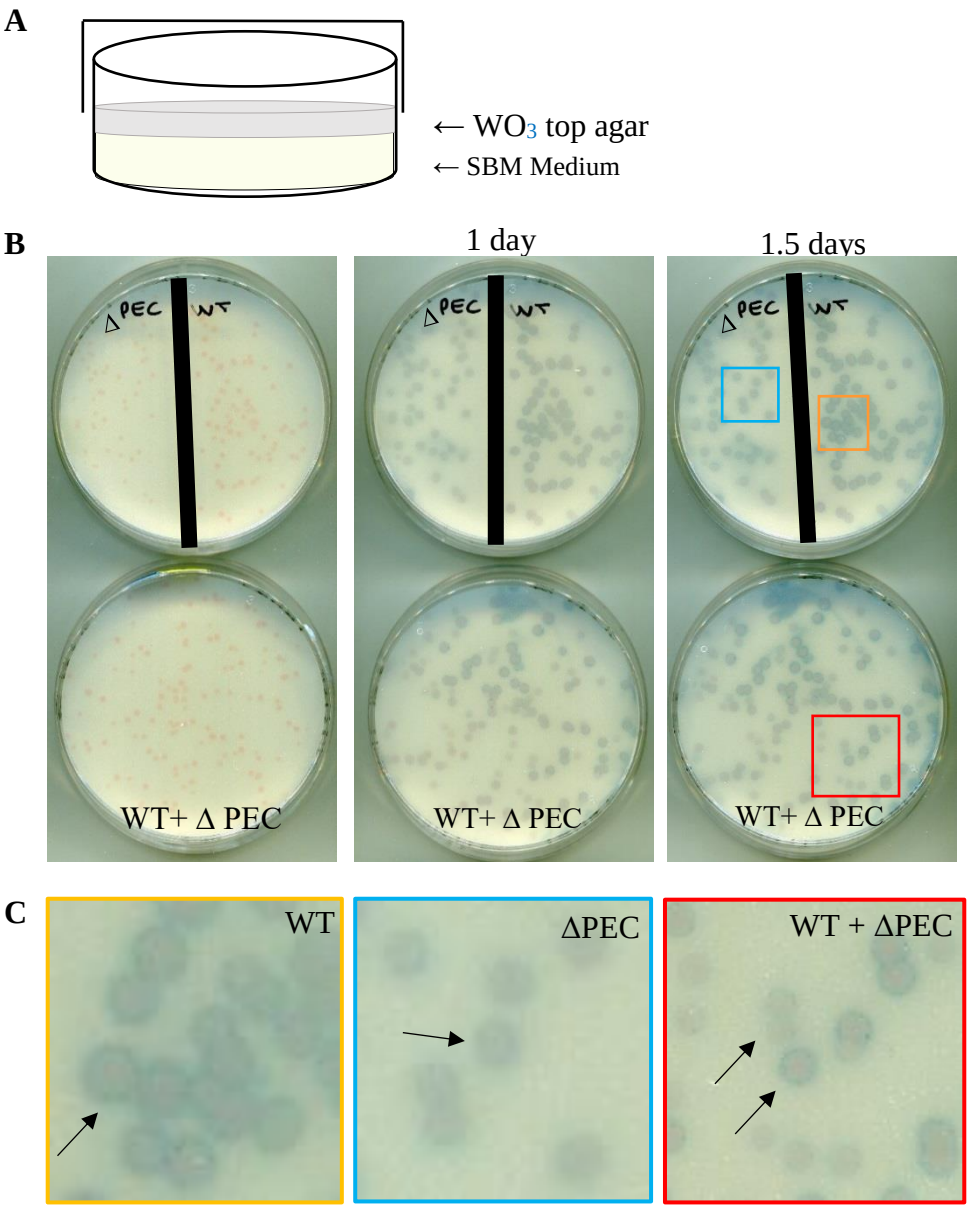

Figure 5.9 WO_3 sandwich plate. (A) Schematic assembly of the assay. (B) SOMR-1 colonies grown on SBM medium-WO_3 sandwich plate over 1.5 days. (C). Magnified images of different SOMR-1 strains reducing WO_3 from (B, 1.5 days, yellow, blue and red box). SOMR-1 SBM agar containing 30 mM sodium lactate, 30 mM sodium fumarate and 0.05% Casamino acids; top agar contained 5 g/L WO_3.

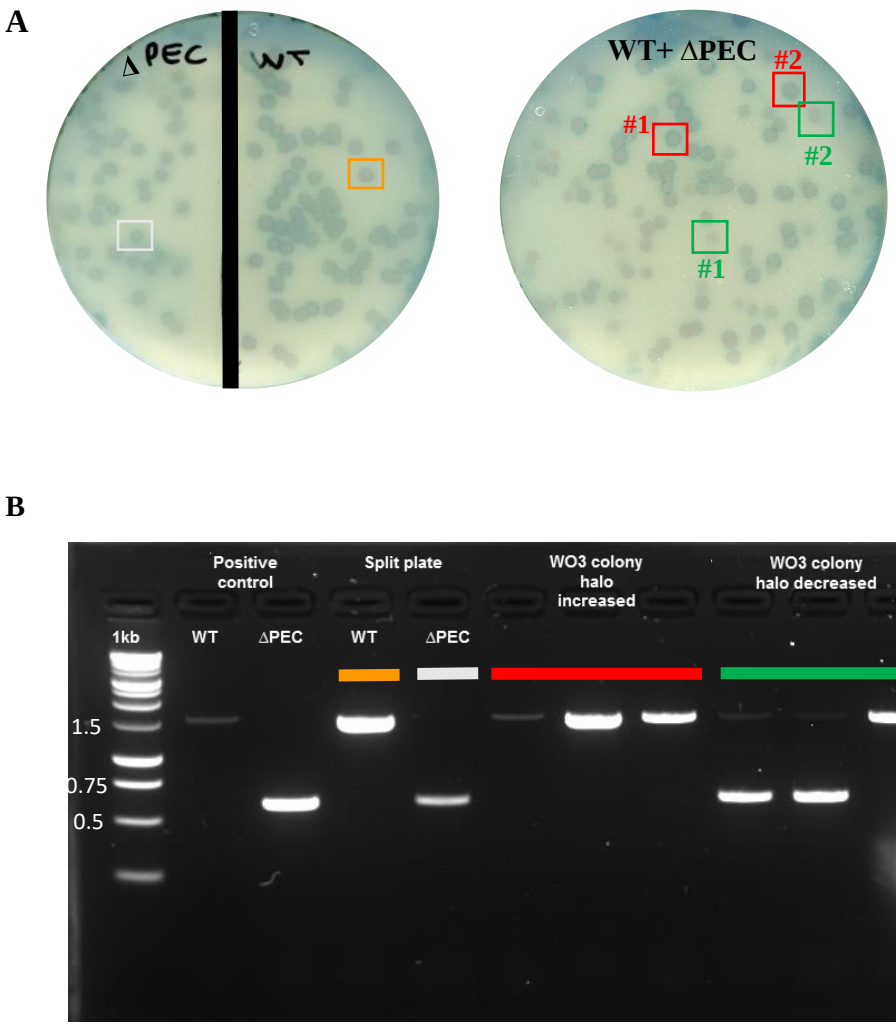

Figure 5.10 PCR Sensitivity test to identify phenotypes with meaningful mutations. (A) WO_3 agar plates with SOM1 WT and delta PEC (left) and mixed culture of these strains (right); (B) 1% agarose gel showing various PCR products of SOMR-1 gDNA PCR amplification of mtrA. Expected band sizes: WT mtrA = 1523 bp; ΔPEC ΔmtrA = 585 bp.

5.2.6 *Enhancer Transposon for Gain of Function in SOMR-1*

5.2.6.1 *Cloning of Enhancer Transposon*

To investigate the simultaneous gene down regulation through knockout by the transposon and gene up-regulation via a strong promoter a the enhancer transposon was designed and constructed, where a strong constitutive promoter (P_{23119}, Anderson series) was cloned into pMiniHimar (Bouhenni et al. 2005), which has been previously been shown to generate stable transposon mutants. Using overlap extension PCR (see oligos in Table 2.4) P_{J23119} was placed directly behind the kanamycin resistance cassette and before the inverted repeat (see Figure 5.11).

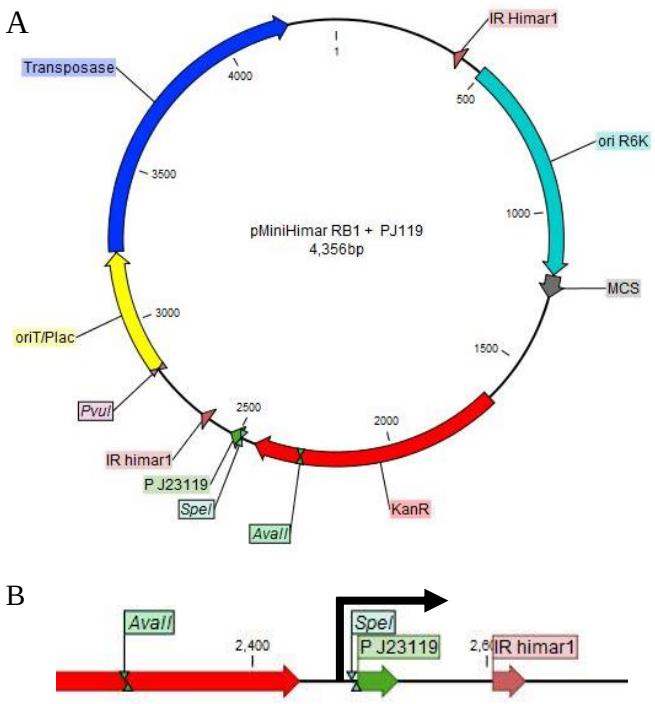

Figure 5.11. Schematic plasmid map of the eenhancer transposon. (A) Plasmid map of pMiniHimar RB1 with constitutive Anderson promoter P_{J23119}; (B) Location of promoter within transposon.

5.2.6.2 *Proof of Concept Control of the Enhancer Transposon Promoter using GFP*

To ensure, that the inverted repeat would not disrupt overexpression of downstream genes a positive control plasmid was constructed to confirm that this placement would be biologically active using GFP as a reporter gene. Here, the promoter region of the reporter gene was designed to have the restriction site KpnI, the constitutive promoter P23119, the inverted repeat from pminiHimar RB1 followed by a RBS (B0034) and the *gfp* gene and *Sal*I restriction site (see Figure 5.12A). This and the first 15 bases of *gfp* gene synthesised as an oligonucleotide and the whole gene amplified using overlap extension PCR and then cloned via restriction digestion and ligation into the multiple cloning site of pSEVA231 backbone (pBBR1 oriV, Kan resistance) using *Kpn*I and *Sal*I. The construct was confirmed by Sanger sequencing. *E. coli* DH5α was chemically transformed with pSEVA23::P23119::IR::RBS::*gfp* and the empty vector, respectively. Overnight cultures in biological triplicate of both SOMR-1 and *E. coli* in LB with 50 µg/mL Km were grown to mid-log phase and washed twice in SMB medium to remove autofluorecent flavins secreted in the medium and relative fluorescence units (fluorescence excitation 485 nm / emission 520 nm / OD_{600}) were measured using (OMG Plate Reader). Both E. coli and SOMR-1 show significant fluorescence compared to the empty vector control (see Figure 5.12)

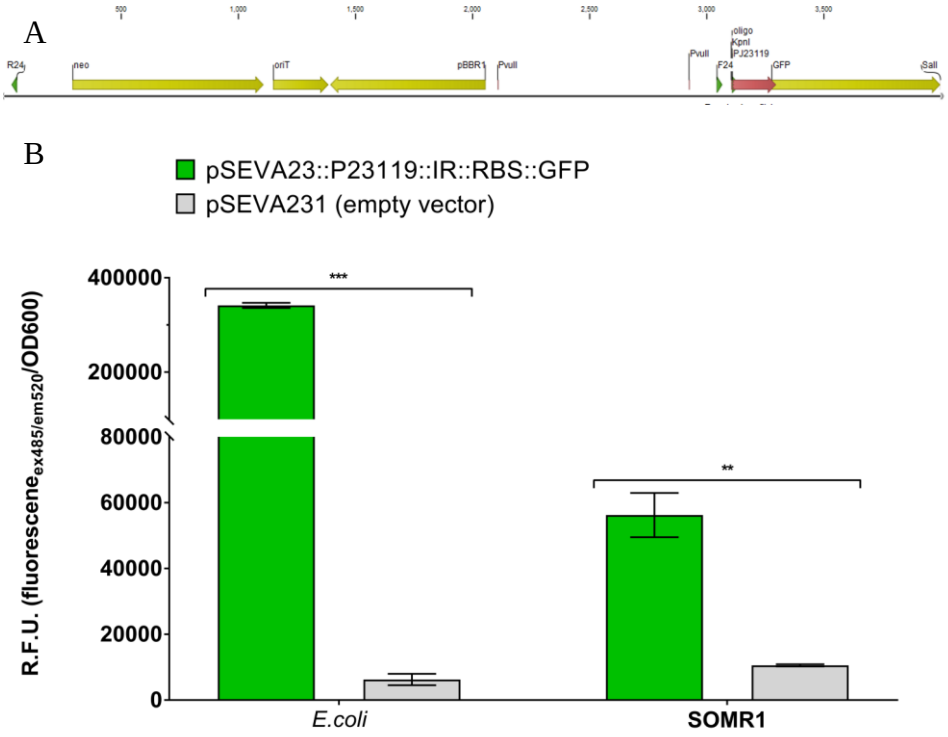

*Figure 5.12. Validation of working enhancer promoter using GFP as a reporter enzyme. (A) Schematic plasmid map pSEVA23::P23119::IR::RBS::gfp; (B) relative fluorescence units (fluorescence excitation 485nm/emission 520nm/OD_{600}) of E .coli and SOMR-1 both harbouring pSEVA23::P_{23119}::IR::RBS::gfp and empty vector backbone pSEVA231. Data are presented as biological triplicated with error bars indicating SEM; ***P≤0.0005; **P≤0.005.*

5.2.6.3 *Does the Enhancer Transposon Yield Viable Mutants?*

pMiniHimar::P23119 was chemically transformed into *E.coli* WM3064 and conjugated into SOMR-1 as previously described in 2.2.2.2.2. Exconjugants of SOMR-1 were selected on SBM plates containing 30 µg/ml Km after washing in SBM to remove residual DAP which sustains *E. coli* growth and nutrients from LB plate. The transposition with pMiniHimar::P_{23119} (see Figure 5.13B).resulted in a large number of colonies with similar morphology compared to transposon mutants generated with pMiniHimar RB1 (see Figure 5.13A). However, a range of colony sizes

is visible on both plates. It could be speculated that this is either due to the position of transposon insertion, but also growth inhibition by lysed *E. coli* cells (see Figure 5.13).

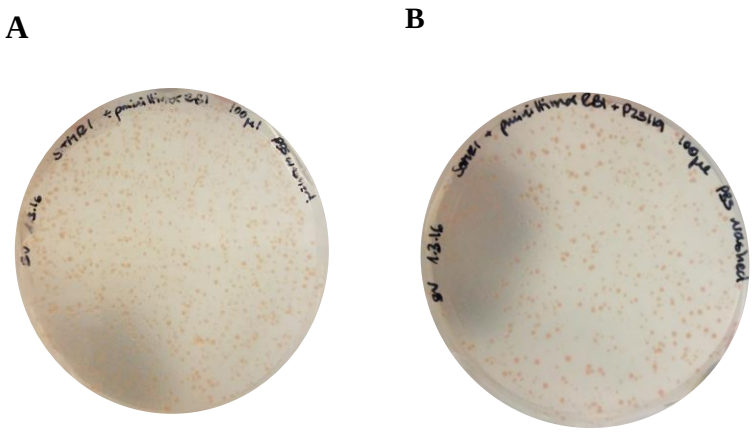

Figure 5.13 Viable exconjugants from mutagenesis with pMiniHimar RB1 (A) and pMiniHimar::P_{23119} (B). A swap of SOMR-1 cells was taken from the DAP LB agar plate and washed 3-times in SBM and resuspended in 1 mL of SBM of which 100 µL were plated and incubated overnight at 30°C on SBM agar containing 30 µg/ml Km.

5.2.6.4 *Selection of Enhancer Transposon Mutants on WO_3 Sandwich Plate*

Transposon mutagenesis as described above was carried out and SOMR-1 transposon mutants were aerobically grown on SBM medium with 20 mM sodium lactate and 0.05 % casamino acids to a visible colony size before being overlaid with the tungsten top agar. The plates were then transferred back into 30°C incubator in a vessel containing anoxic sachet to remove O_2. Figure 5.14 shows the WO_3 sandwich plate of SOMR-1 enhancer transposon mutants. However, no WO_3 reduction by SOMR-1 is visible over the course of 3 days incubation.

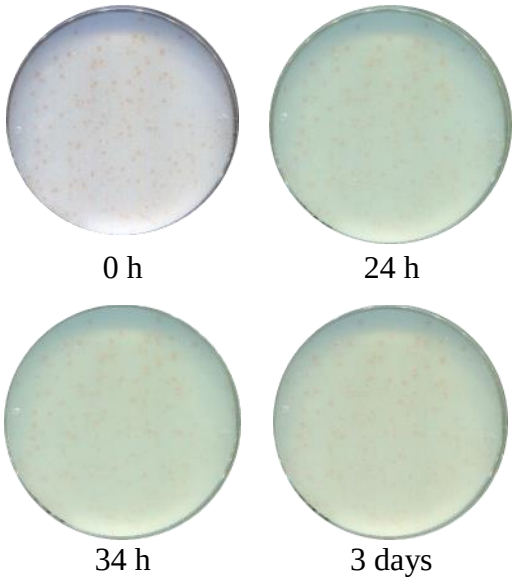

Figure 5.14 WO_3 sandwich plate screen of SOMR-1 enhancer transposon mutants. SOMR-1 colonies were grown on SBM medium containing 20 mM sodium lactate. Colonies were overlaid with tungsten top agar prior to anaerobic incubation at 30°C anaerobically in a 2.5 L-anaerobic jar over the course of 3 days. Plates were scanned and returned back in the anaerobic vessel replacing the anaerobic sachet.

5.3 Discussion

Tungsten trioxide has been shown to be a functional replacement of full set ups of microbial fuel cells and iron reduction assays to measure SOMR-1's EET capabilities (Kotloski and Gralnick 2013; Yong et al. 2013).

Recently, WO_3 nanorods have further been used to screen electrogenic activity of anodic MFC inocula from wastewater sludge to estimate their bioelectrogenic activity (Sharma and Ghangrekar 2018) and to identify novel exoelectrogenic bacteria from lake sediments and a wastewater treatment plants, additionally proving the versatile functionality of this compound. (Yang et al. 2016).

The development of tungsten bronzes in sandwich plates with transposon mutants, both normal gene disruption and those with new enhanced function transposon, would have been desirable and was ultimately the crux of this screening method to identify novel and enhanced gain of function in SOMR-1 strains, as elaborated in this chapter. By using the top agar, the amount of tungsten used per numbers of mutants screened was hugely reduced, making it a more practical and faster screening approach considering the small yields of WO_3 per acid digestion do compete directly with commercially available ferrozine used for iron reduction assays thereby outweighing their increased sensitivity to simulate bacterial behaviour at the electrode material. Although, sodium tungstate is a fairly cheap substrate, the equipment needed to synthesise WO_3 nanorods is rather costly with 500£ for one acid digestion unit and multiple thousand pounds for the oven if not already available in the laboratory or readily available with collaborator on campus, therefore until WO_3 nanorods can be commercially produced it would be unfeasible to upscale these screens and assays.

The reasons why the transposon mutants weren't able to reduce tungsten in the plate assay could be due to a number of reasons, either – due to their prolonged growth on minimal medium – nutrient starvation or carbon source depletion, or as transposon mutants were mated on LB and aerobically, critical gene were disrupted that are essential for anaerobic growth and EET.

Even though WO_3 offers closer condition to replication of anode reduction in MET systems not feasible on a frequent screen for screen a transposon mutant library.

Other biochromic assays that could also be utilised, however using soluble electron acceptor, is the biodecolorisation of Naphthol Green B dye which has been shown to be reducible by SOMR-1 under anaerobic conditions using the Mtr pathway (Xiao et al. 2012).

5.4 Conclusions

Tungsten trioxide assays have been shown to have the sensitivity towards SOMR-1 knock-out mutants in a range of experiments but have failed to demonstrate the capability to discern enhanced EET capabilities in transposon mutants compared with SOMR-1 WT. The pitfalls of nanoparticle synthesis and low yield are outweighing the advantages in identifying novel mutant that would behave similarly on electrode material compared to standard techniques.

CHAPTER 6

6 DISCUSSION, CONCLUSION & FUTURE WORK

6.1 General Discussion and Conclusion

In the past decade the emerging field of microbial electrochemical technologies (METs) has gained increased attention due to its potential for bioenergy production and bioremediation. By utilizing pollutants or waste as carbon sources electroactive bacteria (EAB) can convert chemical energy into electricity, thereby conceivably closing the waste disposal energy generation loop, however to do that genetic tools are needed which are scarce for novel model organisms such as SOMR-1 (Sydow et al. 2014). The presented work focussed on enabling SOMR-1 to become more genetically tractable using synthetic biology approaches to enhance the output of microbial fuel cell technologies. While many research groups work with this organism (Covington et al. 2010; Ross et al. 2011; Yang et al. 2015) and have been successful in manipulating it, taking a step back to basics and providing a set of tools and vectors is crucial to advance research in this field. In this study, it was demonstrated that SOMR-1 is a genetically tractable EAB model organism and feasible as a synthetic biology chassis for which its toolbox has been expanded; however as synthetic gene circuits become more elaborate in size and complexity as demonstrated in Chapter 4, the lack of well-characterized parts that are available for this organism has become more apparent, and precise genetic engineering still remains a bottleneck. The expansion of a SOMR-1 specific synthetic biology toolbox has been shown using a systematic approach to overcome such bottlenecks in SOMR-1's genetic manipulation and has added immense value to increase predictability, stability and novel functionalities of MET

applications. By realising the pSEVA platform (Silva-Rocha et al. 2013; Martinez-Garcia et al. 2014), showing for the first time calculated plasmid copy numbers for SOMR-1 which were in line with copy numbers that have been reported in *E. coli* harbouring pSEVA plasmids (Jahn et al. 2016), characterising new expression systems and reporter tools in SOMR-1. Taken together these results will enable future research with this organism can be more easily realised and will enable more fine-tuned gene expression for MFC set-ups. Furthermore, it has been demonstrated that SOMR-1 is capable to harbour a combination of pSEVA plasmids with different replication systems and yet produce and increased current output (Chapter 4). The development and establishment of transcriptional regulation using oxygen independent inducible & constitutive promoters: $P_{ChnB/ChnR}$, $P_{tet/TetR}$, P_{T7} using *lacZ* assays has added hugely to the SOMR-1 synbio toolbox. However, the oxygen independent reporter phiLOV has not been suitable for studies in this organism due to the large amount of endogenous flavins interfering with the signal intensity compared to studies using it in *Clostridium* (Christie et al. 2012; Buckley et al. 2016).

In this work, it was shown for the first time that the novel cyclohexanone inducible promoter $P_{ChnB/ChnR}$ can be characterised using oxygen independent reporter assays as previously described in *P. putida* (Benedetti et al. 2016a; Benedetti et al. 2016b) Further, heterologous expression of *yedQ* and *yhjH* under $P_{Chnb/ChnR}$ also enhanced biofilm formation in SOMR-1, similar to that seen in *P. putida* (Benedetti et al. 2016a; Benedetti et al. 2016b). Additionally, the construction of a synthetic operon which combined the known key proteins involved in flavin production (*bfe* and *ushA*) with the modular pSEVA platform and its novel inducible promoter $P_{Chnb/ChnR}$, showed a significant increase in SOMR-1's flavin production using the newly developed small-

scale MFCs using screen-printed electrode technology which has only been previously shown for *Geobacter spp*.(Estevez-Canales et al. 2015).

Additional screening methods are presented which were aimed to identify novel EET capabilities in SOMR-1 using a colorimetric tungsten trioxide (WO_3) assay, however, the attempt to utilise WO_3 nanoparticles as high-throughput screening of electroactive bacteria for the discovery of enhanced EET phenotypes with this assay using transposon and enhancer transposon mutagenesis to establish electrochromic detection in multi-well assays, has not been successful owing to laborious and low yield synthesis of the nanorods as well as low dispensability in media.

6.2 Future Research

To further extend the pSEVA plasmid platform for the use in SOMR-1, it would be interesting to sequence the endogenous plasmid from Chapter 3 to identify the replication system and combine it with the SEVA architecture to provide an even more robust expression vector SOMR-1 research and MFC technologies. Additionally, given the limited increase of expression between uninduced and induced cultures with $P_{tet/TetR}$ and even to some extent $P_{Chnb/ChnR}$, it would be interesting to see how these regulation systems affect current production when the repressor was removed, thereby decreasing the metabolic burden of the cell allowing to devote more electron flow towards current production. It would be interesting to also combine the overproduction of flavin with overexpression of *yedQ* to test whether enhancing all notable aspects of known EET components in SOMR-1 will yield in enhanced current density outputs. The SPE technologies could be further investigate and optimised by changing the working electrode material from carbon to graphene or other parameters such as nutrients and carbon source, given the small vessel volume, these could be depleted faster than anticipated.

REFERENCES

Anderson JC, Voigt C a, Arkin AP (2007) Environmental signal integration by a modular AND gate. Mol Syst Biol 3:133 . doi: 10.1038/msb4100173

Andrews JM (2001) JAC Determination of minimum inhibitory concentrations. 5–16

Babauta J, Renslow R, Lewandowski Z, Beyenal H (2012) Electrochemically active biofilms: facts and fiction. A review. Biofouling 28:789–812 . doi: 10.1080/08927014.2012.710324

Baron D, LaBelle E, Coursolle D, Gralnick J a, Bond DR (2009) Electrochemical measurement of electron transfer kinetics by Shewanella oneidensis MR-1. J Biol Chem 284:28865–73 . doi: 10.1074/jbc.M109.043455

Beliaev AS, Saffarini D a., McLaughlin JL, Hunnicutt D (2001) MtrC, an outer membrane decahaem c cytochrome required for metal reduction in Shewanella putrefaciens MR-1. Mol Microbiol 39:722–730 . doi: 10.1046/j.1365-2958.2001.02257.x

Benedetti I, Lorenzo V De, Nikel PI (2016a) Genetic programming of catalytic Pseudomonas putida biofilms for boosting biodegradation of haloalkanes. Metab Eng 33:109–118 . doi: 10.1016/j.ymben.2015.11.004

Benedetti I, Nikel PI, Lorenzo V De (2016b) Data in Brief Data on the standardization of a cyclohexanone-responsive expression system for Gram-negative bacteria. Data Br 6:738–744 . doi: 10.1016/j.dib.2016.01.022

Bertram R, Hillen W (2008) The application of Tet repressor in prokaryotic gene regulation and expression. Microb Biotechnol 1:2–16 . doi: 10.1111/j.1751-7915.2007.00001.x

Beyer P, Al-Babili S, Ye X, Lucca P, Schaub P, Welsch R, Potrykus I (2002) Golden Rice: introducing the beta-carotene biosynthesis pathway into rice endosperm by genetic engineering to defeat vitamin A deficiency. J Nutr 132:506S–510S . doi: 10.1093/jn/132.3.506S

Boesen T, Nielsen LP, Nielsen P (2013) Molecular Dissection of Bacterial Nanowires. MBio 4:e00270-13 . doi: 10.1128/mBio.00270-13.Updated

Bond DR, Lovley DR (2003) Electricity Production by Geobacter sulfurreducens Attached to Electrodes Electricity Production by Geobacter sulfurreducens Attached to Electrodes. Appl Environ Microbiol 69:1548–1555 . doi: 10.1128/AEM.69.3.1548

Bond DR, Strycharz-Glaven SM, Tender LM, Torres CI (2012) On electron transport through Geobacter biofilms. ChemSusChem 5:1099–105 . doi: 10.1002/cssc.201100748

Bouhenni R, Gehrke a, Saffarini D (2005) Identification of genes involved in cytochrome c biogenesis in Shewanella oneidensis, using a modified mariner

transposon. Appl Environ Microbiol 71:4935–7 . doi: 10.1128/AEM.71.8.4935-4937.2005

Brutinel ED, Dean AM, Gralnick JA (2013) Description of a Riboflavin Biosynthetic Gene Variant Prevalent in the. 195:5479–5486 . doi: 10.1128/JB.00651-13

Brutinel ED, Gralnick J a (2012a) Anomalies of the anaerobic tricarboxylic acid cycle in Shewanella oneidensis revealed by Tn-seq. Mol Microbiol 86:273–83 . doi: 10.1111/j.1365-2958.2012.08196.x

Brutinel ED, Gralnick J a (2012b) Shuttling happens: soluble flavin mediators of extracellular electron transfer in Shewanella. Appl Microbiol Biotechnol 93:41–8 . doi: 10.1007/s00253-011-3653-0

Buckley AM, Jukes C, Candlish D, Irvine JJ, Spencer J, Fagan RP, Roe AJ, Christie JM, Fairweather NF, Douce GR (2016) Lighting Up Clostridium Difficile: Reporting Gene Expression Using Fluorescent Lov Domains. Sci Rep 6:1–11 . doi: 10.1038/srep23463

Busalmen JP, Esteve-Núñez A, Berná A, Feliu JM (2008) C-type cytochromes wire electricity-producing bacteria to electrodes. Angew Chem Int Ed Engl 47:4874–7 . doi: 10.1002/anie.200801310

Caccavo F, Lonergan DJ, Lovley DR, Davis M, Stolz JF, McInerney MJ (1994) Geobacter sulfurreducens sp. nov., a hydrogen- and acetate-oxidizing dissimilatory metal-reducing microorganism. Appl Environ Microbiol 60:3752–9

Casadaban MJ, Chou J, Cohen SN (1980) In vitro gene fusions that join an enzymatically active of exogenous proteins : Escherichia coli plasmid vectors for the detection and In Vitro Gene Fusions That Join an Enzymatically Active , B-Galactosidase Segment to Amino-Terminal Fragments of Exogen. 143:971–980

Chamberlin M, Mcgrath J, Waskell L (1970) New RNA polymerase from escherichia coli infected with bacteriophage T7. Nature 228:227–231 . doi: 10.1038/228227a0

Chapman S, Faulkner C, Kaiserli E, Garcia-Mata C, Savenkov EI, Roberts AG, Oparka KJ, Christie JM (2008) The photoreversible fluorescent protein iLOV outperforms GFP as a reporter of plant virus infection. Proc Natl Acad Sci U S A 105:20038–43 . doi: 10.1073/pnas.0807551105

Choi D, Lee SB, Kim S, Min B, Choi I-G, Chang IS (2013) Metabolically engineered glucose-utilizing Shewanella strains under anaerobic conditions. Bioresour Technol 154C:59–66 . doi: 10.1016/j.biortech.2013.12.025

Christie JM, Hitomi K, Arvai AS, Hartfield K a, Mettlen M, Pratt AJ, Tainer J a, Getzoff ED (2012) Structural tuning of the fluorescent protein iLOV for improved photostability. J Biol Chem 287:22295–304 . doi: 10.1074/jbc.M111.318881

Clarke L, Adams J, Sutton P, Bainbridge JW, Birney E, Calvert J, Collis A, Kitney R,

Freemont P, Mason P, Pandya K, Ghaffar T, Rose N, Marris C, Woolfson D, Boyce A (2012) A Synthetic Biology Roadmap for the UK. Technology Strategy Board

Clarke LJ, Kitney RI (2016) Synthetic biology in the UK - An outline of plans and progress. Synth Syst Biotechnol 1:243–257 . doi: 10.1016/j.synbio.2016.09.003

Coursolle D, Baron DB, Bond DR, Gralnick J a (2010) The Mtr respiratory pathway is essential for reducing flavins and electrodes in Shewanella oneidensis. J Bacteriol 192:467–74 . doi: 10.1128/JB.00925-09

Coursolle D, Gralnick J a (2010) Modularity of the Mtr respiratory pathway of Shewanella oneidensis strain MR-1. Mol Microbiol 77:995–1008 . doi: 10.1111/j.1365-2958.2010.07266.x

Covington ED, Gelbmann CB, Kotloski NJ, Gralnick JA (2010) An essential role for UshA in processing of extracellular flavin electron shuttles by Shewanella oneidensis. Mol Microbiol 78(2):519–532 . doi: 10.1111/j.1365-2958.2010.07353.x

Drepper T, Eggert T, Circolone F, Heck A, Krauss U, Guterl J-K, Wendorff M, Losi A, Gärtner W, Jaeger K-E (2007) Reporter proteins for in vivo fluorescence without oxygen. Nat Biotechnol 25:443–5 . doi: 10.1038/nbt1293

El-Naggar MY, Wanger G, Leung KM, Yuzvinsky TD, Southam G, Yang J, Lau WM, Nealson KH, Gorby Y a (2010) Electrical transport along bacterial nanowires from Shewanella oneidensis MR-1. Proc Natl Acad Sci U S A 107:18127–31 . doi: 10.1073/pnas.1004880107

Estevez-Canales M, Berná A, Borjas Z, Esteve-Núñez A (2015) Screen-Printed Electrodes : New Tools for Developing Microbial Electrochemistry at Microscale Level. Energies 8:13211–13221 . doi: 10.3390/en81112366

Franks AE, Malvankar NS, Nevin KP (2010) Bacterial biofilms: the powerhouse of a microbial fuel cell. Biofuels 1:589–604

Frédéricq P, Krčméry V, Kettner M (1971) Transferable colicinogenic factors as mobilizing agents for extrachromosomal streptomycin resistance. Z Allg Mikrobiol 11:11–17 . doi: 10.1002/jobm.19710110103

Fredrickson JK, Romine MF, Beliaev AS, Auchtung JM, Driscoll ME, Gardner TS, Nealson KH, Osterman AL, Pinchuk G, Reed JL, Rodionov D a, Rodrigues JLM, Saffarini D a, Serres MH, Spormann AM, Zhulin IB, Tiedje JM (2008) Towards environmental systems biology of Shewanella. Nat Rev Microbiol 6:592–603 . doi: 10.1038/nrmicro1947

Freemont PS, Kitney RI, Baldwin G, Bayer T, Dickinson R, Ellis T, Polizzi K, Stan G-B (2012) Synthetic Biology - A Primer. Imperial College Press

Fried L, Lassak J, Jung K (2012) A comprehensive toolbox for the rapid construction of lacZ fusion reporters. J Microbiol Methods 91:537–43 . doi: 10.1016/j.mimet.2012.09.023

Gao H, Barua S, Liang Y, Wu L, Dong Y, Reed S, Chen J, Culley D, Kennedy D, Yang Y, He Z, Nealson KH, Fredrickson JK, Tiedje JM, Romine M, Zhou J (2010a) Impacts of Shewanella oneidensis c-type cytochromes on aerobic and anaerobic respiration. Microb Biotechnol 3:455–66 . doi: 10.1111/j.1751-7915.2010.00181.x

Gao H, Wang X, Yang ZK, Chen J, Liang Y, Chen H, Zhou J (2010b) Physiological Roles of ArcA , Crp , and EtrA and Their Interactive Control on Aerobic and Anaerobic Respiration in Shewanella oneidensis. 5: . doi: 10.1371/journal.pone.0015295

Gawthorne J a, Reddick LE, Akpunarlieva SN, Beckham KSH, Christie JM, Alto NM, Gabrielsen M, Roe AJ (2012) Express your LOV: an engineered flavoprotein as a reporter for protein expression and purification. PLoS One 7:e52962 . doi: 10.1371/journal.pone.0052962

Gimkiewicz C, Harnisch F (2013) Waste water derived electroactive microbial biofilms: growth, maintenance, and basic characterization. J Vis Exp 50800 . doi: 10.3791/50800

Gödeke J, Heun M, Bubendorfer S, Paul K, Thormann KM (2011a) Roles of two Shewanella oneidensis MR-1 extracellular endonucleases. Appl Environ Microbiol 77:5342–51 . doi: 10.1128/AEM.00643-11

Gödeke J, Paul K, Lassak J, Thormann KM (2011b) Phage-induced lysis enhances biofilm formation in Shewanella oneidensis MR-1. ISME J 5:613–26 . doi: 10.1038/ismej.2010.153

Goldbeck CP, Jensen HM, TerAvest M a, Beedle N, Appling Y, Hepler M, Cambray G, Mutalik V, Angenent LT, Ajo-Franklin CM (2013) Tuning promoter strengths for improved synthesis and function of electron conduits in Escherichia coli. ACS Synth Biol 2:150–9 . doi: 10.1021/sb300119v

Golitsch F, Bücking C, Gescher J (2013) Proof of principle for an engineered microbial biosensor based on Shewanella oneidensis outer membrane protein complexes. Biosens Bioelectron 47:285–291 . doi: 10.1016/j.bios.2013.03.010

Gorby YA, Yanina S, McLean JS, Rosso KM, Moyles D, Dohnalkova A, Beveridge TJ, Chang IS, Kim BH, Kim KS, Culley DE, Reed SB, Romine MF, Saffarini DA, Hill EA, Shi L, Elias DA, Kennedy DW, Pinchuk GE, Watanabe K, Ishii S, Logan BE, Nealson KH, Fredrickson JK (2006) Electrically conductive bacterial nanowires produced by Shewanella oneidensis strain MR-1 and other microorganisms. Proc Natl Acad Sci 103:11358–11363 . doi: 10.1073/pnas.0905246106

Gralnick JA, Hajimorad M (2016) Towards enabling engineered microbial-electronic systems: RK2-based conjugal transfer system for Shewanella synthetic biology. Electron Lett 52:426–428 . doi: 10.1049/el.2015.3226

Green MR, Sambrook J, MacCallum P (2012) Molecular Cloning: A Laboratory Manual. Cold Spring Harbor Laboratory Press

Hall CW, Mah T-F (2017) Molecular mechanisms of biofilm-based antibiotic resistance and tolerance in pathogenic bacteria. FEMS Microbiol Rev 41:276–301 . doi: 10.1093/femsre/fux010

Harnisch F, Freguia S (2012) A basic tutorial on cyclic voltammetry for the investigation of electroactive microbial biofilms. Chem - An Asian J 7:466–475 . doi: 10.1002/asia.201100740

Hau HH, Gralnick J a (2007) Ecology and biotechnology of the genus Shewanella. Annu Rev Microbiol 61:237–58 . doi: 10.1146/annurev.micro.61.080706.093257

Heidelberg JF, Paulsen IT, Nelson KE, Gaidos EJ, Nelson WC, Read TD, Eisen J a, Seshadri R, Ward N, Methe B, Clayton R a, Meyer T, Tsapin A, Scott J, Beanan M, Brinkac L, Daugherty S, DeBoy RT, Dodson RJ, Durkin a S, Haft DH, Kolonay JF, Madupu R, Peterson JD, Umayam L a, White O, Wolf AM, Vamathevan J, Weidman J, Impraim M, Lee K, Berry K, Lee C, Mueller J, Khouri H, Gill J, Utterback TR, McDonald L a, Feldblyum T V, Smith HO, Venter JC, Nealson KH, Fraser CM (2002) Genome sequence of the dissimilatory metal ion-reducing bacterium Shewanella oneidensis. Nat Biotechnol 20:1118–23 . doi: 10.1038/nbt749

Hernandez ME, Kappler A, Dianne K (2004) Phenazines and Other Redox-Active Antibiotics Promote Microbial Mineral Reduction. Appl Environ Microbiol 70:921–928 . doi: 10.1128/AEM.70.2.921

Hofer U (2014) Milestones in synthetic (micro)biology. Nat Rev Microbiol 12:309

Jahn M, Vorpahl C, Hübschmann T, Harms H, Müller S (2016) Copy number variability of expression plasmids determined by cell sorting and Droplet Digital PCR. Microb Cell Fact 15:211 . doi: 10.1186/s12934-016-0610-8

Jain A, Connolly J (2013) Extracellular electron transfer mechanism in Shewanella loihica PV-4 biofilms formed at indium tin oxide and graphite electrodes. Int J … 8:1778–1793

Jensen HM, Albers AE, Malley KR, Londer YY, Cohen BE, Helms B a, Weigele P, Groves JT, Ajo-Franklin CM (2010) Engineering of a synthetic electron conduit in living cells. Proc Natl Acad Sci U S A 107:19213–8 . doi: 10.1073/pnas.1009645107

Jones KL, Kim SW, Keasling JD (2000) Low-copy plasmids can perform as well as or better than high-copy plasmids for metabolic engineering of bacteria. Metab Eng 2:328–338 . doi: 10.1006/mben.2000.0161

Kane AL (2011) Electrochemical analysis of Shewanella oneidensis engineered to bind gold electrodes.

Kane AL, Bond DR, Gralnick J a (2013) Electrochemical analysis of Shewanella oneidensis engineered to bind gold electrodes. ACS Synth Biol 2:93–101 . doi: 10.1021/sb300042w

Keasling JD (2012) Synthetic biology and the development of tools for metabolic

engineering. Metab Eng 14:189–95 . doi: 10.1016/j.ymben.2012.01.004

Kelly DP, Wood AP (2000) Reclassification of some species of Thiobacillus Acidithiobacillus gen . nov ., Halothiobacillus. 511–516

Kitney R, Freemont P (2012) Synthetic biology - the state of play. FEBS Lett 586:2029–36 . doi: 10.1016/j.febslet.2012.06.002

Kotloski NJ, Gralnick JA (2013) Flavin Electron Shuttles Dominate Extracellular Electron Transfer by Shewanella oneidensis. MBio 4:e00553-12 . doi: 10.1128/mBio.00553-12.Editor

Kovach ME, Elzer PH, Hill DS, Robertson GT, Farris M a, Roop RM, Peterson KM (1995) Four new derivatives of the broad-host-range cloning vector pBBR1MCS, carrying different antibiotic-resistance cassettes. Gene 166:175–6

Kües U, Stahl U (1989) Replication of plasmids in gram-negative bacteria. Microbiol Rev 53:491–516

Kumar A, Katuri K, Lens P, Leech D (2012) Does bioelectrochemical cell configuration and anode potential affect biofilm response? Biochem Soc Trans 40:1308–14 . doi: 10.1042/BST20120130

Leang C, Ueki T, Nevin KP, Lovley DR (2013) A genetic system for Clostridium ljungdahlii: a chassis for autotrophic production of biocommodities and a model homoacetogen. Appl Environ Microbiol 79:1102–9 . doi: 10.1128/AEM.02891-12

Lee C, Kim J, Shin SG, Hwang S (2006) Absolute and relative QPCR quantification of plasmid copy number in Escherichia coli. J Biotechnol 123:273–280 . doi: 10.1016/j.jbiotec.2005.11.014

Lee TS, Krupa R a, Zhang F, Hajimorad M, Holtz WJ, Prasad N, Lee SK, Keasling JD (2011) BglBrick vectors and datasheets: A synthetic biology platform for gene expression. J Biol Eng 5:12 . doi: 10.1186/1754-1611-5-12

Liu H, Logan BE (2004) Electricity generation using an air-cathode single chamber microbial fuel cell in the presence and absence of a proton exchange membrane. Environ Sci Technol 38:4040–4046 . doi: 10.1021/es0499344

Liu T, Yu Y, Deng X, Ng CK, Cao B, Wang J, Rice SA, Kjelleberg S, Song H (2015) Enhanced Shewanella Biofilm Promotes Bioelectricity Generation. Biotechnol Bioeng 112:2051–2059 . doi: 10.1002/bit.25624

Liu W, Lin J, Pang X, Cui S, Mi S, Lin J (2011) Overexpression of rusticyanin in Acidithiobacillus ferrooxidans ATCC19859 increased Fe(II) oxidation activity. Curr Microbiol 62:320–4 . doi: 10.1007/s00284-010-9708-0

Logan BE, Rabaey K (2012) Conversion of wastes into bioelectricity and chemicals by using microbial electrochemical technologies. Science 337:686–90 . doi: 10.1126/science.1217412

Malvankar NS, Lau J, Nevin KP, Franks AE, Tuominen MT, Lovley DR (2012a)

Electrical conductivity in a mixed-species biofilm. Appl Environ Microbiol 78:5967–71 . doi: 10.1128/AEM.01803-12

Malvankar NS, Lovley DR (2012) Microbial nanowires: a new paradigm for biological electron transfer and bioelectronics. ChemSusChem 5:1039–46 . doi: 10.1002/cssc.201100733

Malvankar NS, Tuominen MT, Lovley DR (2012b) Comment on "On electrical conductivity of microbial nanowires and biofilms" by S. M. Strycharz-Glaven, R. M. Snider, A. Guiseppi-Elie and L. M. Tender, Energy Environ. Sci., 2011, 4, 4366. Energy Environ Sci 5:6247 . doi: 10.1039/c2ee02613a

Malvankar NS, Vargas M, Nevin KP, Franks AE, Leang C, Kim B-C, Inoue K, Mester T, Covalla SF, Johnson JP, Rotello VM, Tuominen MT, Lovley DR (2011) Tunable metallic-like conductivity in microbial nanowire networks. Nat Nanotechnol 6:573–9 . doi: 10.1038/nnano.2011.119

Marris C, Calvert J (2019) Science and Technology Studies in Policy: The UK Synthetic Biology Roadmap. Sci Technol Hum Values 0:0162243919828107 . doi: 10.1177/0162243919828107

Marritt SJ, Lowe TG, Bye J, McMillan DGG, Shi L, Fredrickson J, Zachara J, Richardson DJ, Cheesman MR, Jeuken LJC, Butt JN (2012) A functional description of CymA, an electron-transfer hub supporting anaerobic respiratory flexibility in Shewanella. Biochem J 444:465–74 . doi: 10.1042/BJ20120197

Marsili E, Baron DB, Shikhare ID, Coursolle D, Gralnick J a, Bond DR (2008) Shewanella secretes flavins that mediate extracellular electron transfer. Proc Natl Acad Sci U S A 105:3968–73 . doi: 10.1073/pnas.0710525105

Martinez-Garcia E, Aparicio T, Goni-Moreno a., Fraile S, de Lorenzo V (2014) SEVA 2.0: an update of the Standard European Vector Architecture for de-/re-construction of bacterial functionalities. Nucleic Acids Res 43:D1183–D1189 . doi: 10.1093/nar/gku1114

Marx CJ, Lidstrom ME (2001) Development of improved versatile broad-host-range vectors for use in methylotrophs and other Gram-negative bacteria. Microbiology 147:2065–75

Methé B a, Nelson KE, Eisen J a, Paulsen IT, Nelson W, Heidelberg JF, Wu D, Wu M, Ward N, Beanan MJ, Dodson RJ, Madupu R, Brinkac LM, Daugherty SC, DeBoy RT, Durkin a S, Gwinn M, Kolonay JF, Sullivan S a, Haft DH, Selengut J, Davidsen TM, Zafar N, White O, Tran B, Romero C, Forberger H a, Weidman J, Khouri H, Feldblyum T V, Utterback TR, Van Aken SE, Lovley DR, Fraser CM (2003) Genome of Geobacter sulfurreducens: metal reduction in subsurface environments. Science 302:1967–9 . doi: 10.1126/science.1088727

Meyer M, Dehio C (1997) Maintenance of broad-host-range incompatibility group P and group Q plasmids and transposition of Tn5 in Bartonella henselae following conjugal plasmid transfer from Escherichia coli. J Bacteriol 179:538–540

Milewska K, Grzegorz W, Szalewska-Palasz A (2015) Plasmid Transformation of

Shewanella baltica with ColE1-like and P1 plasmids and their maintenance during bacterial growth in cultures. Plas 81:42–49 . doi: 10.1016/j.plasmid.2015.07.001

Miller J (1972) Experiments in Molecular Genetics. Cold Spring Harbor Laboratory Press, Cold Spring Harbor, NY

Mukherjee A, Walker J, Weyant KB, Schroeder CM (2013) Characterization of Flavin-Based Fluorescent Proteins: An Emerging Class of Fluorescent Reporters. PLoS One 8: . doi: 10.1371/journal.pone.0064753

Müller J, Shukla S, Jost K a, Spormann AM (2013) The mxd operon in Shewanella oneidensis MR-1 is induced in response to starvation and regulated by ArcS/ArcA and BarA/UvrY. BMC Microbiol 13:119 . doi: 10.1186/1471-2180-13-119

Murugesan K, Ravindran B, Selvam A, Kurade MB, Yu S-M, Wong JWC (2014) Enhanced dewaterability of anaerobically digested sewage sludge using Acidithiobacillus ferrooxidans culture as sludge conditioner. Bioresour Technol 169:374–9 . doi: 10.1016/j.biortech.2014.06.057

Myers CR, Myers JM (1997a) Replication of plasmids with the p15A origin in Shewanella putrefaciens MR-1. Lett Appl Microbiol 24:221–5

Myers CR, Myers JM (2002) MtrB Is Required for Proper Incorporation of the Cytochromes OmcA and OmcB into the Outer Membrane of Shewanella MtrB Is Required for Proper Incorporation of the Cytochromes OmcA and OmcB into the Outer Membrane of Shewanella putrefaciens MR-1. Appl Environ Microbiol 68:5585–5594 . doi: 10.1128/AEM.68.11.5585

Myers CR, Myers JM (1997b) Cloning and sequence of cymA , a gene encoding a tetraheme cytochrome c required for reduction of iron (III), fumarate , and nitrate by Shewanella putrefaciens MR-1. J Bacteriol 179:1143–1152

Myers CR, Nealson KH (1988) Bacterial manganese reduction and growth with manganese oxide as the sole electron acceptor. Science 240:1319–21 . doi: 10.1126/science.240.4857.1319

Nealson KH, Scott J (2006) Ecophysiology of the Genus Shewanella. Prokaryotes 6:1133–1151

Nevin KP, Lovley DR (2000) Lack of Production of Electron-Shuttling Compounds or Solubilization of Fe (III) during Reduction of Insoluble Fe (III) Oxide by Geobacter metallireducens. Appl Environ Microbiol 66:2248–2251 . doi: 10.1128/AEM.66.5.2248-2251.2000.Updated

Nevin KP, Woodard TL, Franks AE, Summers ZM, Lovley DR (2010) Microbial Electrosynthesis : Feeding Microbes Electricity To Convert Carbon Dioxide and Water to Multicarbon Extracellular Organic Compounds. MBio 1:e00103-10 . doi: 10.1128/mBio.00103-10.Editor

Nielsen AA, Segall-Shapiro TH, Voigt C a (2013) Advances in genetic circuit design: novel biochemistries, deep part mining, and precision gene expression. Curr Opin

Chem Biol 17:878–92 . doi: 10.1016/j.cbpa.2013.10.003

Okamoto A, Hashimoto K, Nealson KH, Nakamura R (2013) Rate enhancement of bacterial extracellular electron transport involves bound flavin semiquinones. Proc Natl Acad Sci U S A 110:7856–61 . doi: 10.1073/pnas.1220823110

Ozawa K, Yasukawa F, Fujiwara Y, Akutsu H (2001) A Simple, Rapid, and Highly Efficient Gene Expression System for Multiheme Cytochromes c. Biosci Biotechnol Biochem 65:185–189 . doi: 10.1271/bbb.65.185

Park DH, Zeikus JG (2000) Electricity generation in microbial fuel cells using neutral red as an electronophore. Appl Environ Microbiol 66:1292–7

Patil SA, Hägerhäll C, Gorton L (2012) Electron transfer mechanisms between microorganisms and electrodes in bioelectrochemical systems. Bioanal Rev 4:159–192 . doi: 10.1007/s12566-012-0033-x

Paulick A, Delalez NJ, Brenzinger S, Steel BC, Berry RM, Armitage JP, Thormann KM (2015) Dual stator dynamics in the Shewanella oneidensisMR-1 flagellar motor. Mol Microbiol 96:993–1001 . doi: 10.1111/mmi.12984

Paulick A, Koerdt A, Lassak J, Huntley S, Wilms I, Narberhaus F, Thormann KM (2009) Two different stator systems drive a single polar flagellum in Shewanella oneidensis MR-1. Mol Microbiol 71:836–50 . doi: 10.1111/j.1365-2958.2008.06570.x

Pirbadian S, Barchinger SE, Leung KM, Byun HS, Jangir Y, Bouhenni RA, Reed SB, Romine MF, Saffarini DA, Shi L, Gorby YA, Golbeck JH, El-Naggar MY (2014) Shewanella oneidensis MR-1 nanowires are outer membrane and periplasmic extensions of the extracellular electron transport components. Proc Natl Acad Sci 1410551111- . doi: 10.1073/pnas.1410551111

Potter MC (1911) Electrical Effects Accompanying the Decomposition of Organic Compounds. Proc R Soc B Biol Sci 84:260–276 . doi: 10.1098/rspb.1911.0073

Qian F, Morse DE (2011) Miniaturizing microbial fuel cells. Trends Biotechnol 29:62–9 . doi: 10.1016/j.tibtech.2010.10.003

Rabaey K, Boon N, Höfte M, Verstraete W (2005) Microbial phenazine production enhances electron transfer in biofuel cells. Environ Sci Technol 39:3401–8

Rachkevych N, Sybirna K, Boyko S, Boretsky Y, Sibirny A (2014) Improving the efficiency of plasmid transformation in Shewanella oneidensis MR-1 by removing ClaI restriction site. J Microbiol Methods 99:35–7 . doi: 10.1016/j.mimet.2014.01.009

Reguera G, McCarthy KD, Mehta T, Nicoll JS, Tuominen MT, Lovley DR (2005) Extracellular electron transfer via microbial nanowires. Nature 435:1098–101 . doi: 10.1038/nature03661

Remington SJ (2006) Fluorescent proteins: maturation, photochemistry and photophysics. Curr Opin Struct Biol 16:714–721 . doi: 10.1016/j.sbi.2006.10.001

Rosenbaum M a, Franks AE (2014) Microbial catalysis in bioelectrochemical technologies: status quo, challenges and perspectives. Appl Microbiol Biotechnol 98:509–18 . doi: 10.1007/s00253-013-5396-6

Rosenbaum M a, Henrich AW (2014) Engineering microbial electrocatalysis for chemical and fuel production. Curr Opin Biotechnol 29:93–98 . doi: 10.1016/j.copbio.2014.03.003

Ross DE, Flynn JM, Baron DB, Gralnick J a, Bond DR (2011) Towards electrosynthesis in shewanella: energetics of reversing the mtr pathway for reductive metabolism. PLoS One 6:e16649 . doi: 10.1371/journal.pone.0016649

Rozendal R a, Hamelers HVM, Rabaey K, Keller J, Buisman CJN (2008) Towards practical implementation of bioelectrochemical wastewater treatment. Trends Biotechnol 26:450–9 . doi: 10.1016/j.tibtech.2008.04.008

Saltikov CW, Newman DK (2003) Genetic identification of a respiratory arsenate reductase. Proc Natl Acad Sci U S A 100:10983–8 . doi: 10.1073/pnas.1834303100

Schmidt CM, Shis DL, Nguyen-Huu TD, Bennett MR (2012) Stable maintenance of multiple plasmids in E. coli using a single selective marker. ACS Synth Biol 1:445–450 . doi: 10.1021/sb3000589

Schneider M, Froggat A (2017) The World Nuclear Industry: Status Report 2017

Schuetz B, Schicklberger M, Kuermann J, Spormann AM, Gescher J (2009) Periplasmic Electron Transfer via the c -Type Cytochromes MtrA and FccA of Shewanella oneidensis MR-1 □. 75:7789–7796 . doi: 10.1128/AEM.01834-09

Segall-Shapiro TH, Sontag ED, Voigt CA (2018) Engineered promoters enable constant gene expression at any copy number in bacteria. Nat Biotechnol 36:352–358 . doi: 10.1038/nbt.4111

Sharma I, Ghangrekar MM (2018) Screening anodic inoculums for microbial fuel cells by quantifying bioelectrogenic activity using tungsten trioxide quantum rods. Bioresour Technol 252:66–71 . doi: 10.1016/j.biortech.2017.12.091

Silva-Rocha R, Martínez-García E, Calles B, Chavarría M, Arce-Rodríguez A, de Las Heras A, Páez-Espino a D, Durante-Rodríguez G, Kim J, Nikel PI, Platero R, de Lorenzo V (2013) The Standard European Vector Architecture (SEVA): a coherent platform for the analysis and deployment of complex prokaryotic phenotypes. Nucleic Acids Res 41:D666-75 . doi: 10.1093/nar/gks1119

Strycharz SM, Glaven RH, Coppi M V, Gannon SM, Perpetua L a, Liu A, Nevin KP, Lovley DR (2011) Gene expression and deletion analysis of mechanisms for electron transfer from electrodes to Geobacter sulfurreducens. Bioelectrochemistry 80:142–50 . doi: 10.1016/j.bioelechem.2010.07.005

Studier FW, Moffatt BA (1986) Use of bacteriophage T7 RNA polymerase to direct selective high-level expression of cloned genes. J Mol Biol 189:113–130 . doi: 10.1016/0022-2836(86)90385-2

Sydow A, Krieg T, Mayer F, Schrader J, Holtmann D (2014) Electroactive bacteria-molecular mechanisms and genetic tools. Appl Microbiol Biotechnol. doi: 10.1007/s00253-014-6005-z

Tabor S (2001) Expression using the T7 RNA polymerase/promoter system. Curr Protoc Mol Biol Chapter 16:Unit16.2 . doi: 10.1002/0471142727.mb1602s11

Thormann KM, Saville RM, Shukla S, Spormann M, Saville M, Spormann AM (2005) Induction of Rapid Detachment in Shewanella oneidensis MR-1 Biofilms. J Bacteriol 187:1014–1021 . doi: 10.1128/JB.187.3.1014

Trubitsyna M, Michlewski G, Cai Y, Elfick A, French CE (2014) PaperClip: rapid multi-part DNA assembly from existing libraries. Nucleic Acids Res 42:e154 . doi: 10.1093/nar/gku829

Tsien RY (1998) The Green Fluorescent Protein. Proteins 67:509–44 . doi: 10.1146/annurev.biochem.67.1.509

United Nations Department of Economic and Social Affairs Population Division (2017) World Population Prospects The 2017 Revision Key Findings and Advance Tables

Vargas M, Malvankar NS, Tremblay P, Leang C, Smith JA, Patel P, Synoeyenbos-West O, Nevin KP, Lovley DR (2013) Aromatic Amino Acids Required for Pili Conductivity and Long- Range Extracellular Electron Transport in Geobacter sulfurreducens. MBio 4:e00105-13 . doi: 10.1128/mBio.00105-13.Editor

von Canstein H, Ogawa J, Shimizu S, Lloyd JR (2008) Secretion of flavins by Shewanella species and their role in extracellular electron transfer. Appl Environ Microbiol 74:615–23 . doi: 10.1128/AEM.01387-07

Wan F, Shi M, Gao H (2017) Loss of OxyR reduces efficacy of oxygen respiration in Shewanella oneidensis. Sci Rep 7:1–14 . doi: 10.1038/srep42609

Wang C, Chen J, Hu W-J, Liu J-Y, Zheng H-L, Zhao F (2014) Comparative proteomics reveal the impact of OmcA/MtrC deletion on Shewanella oneidensis MR-1 in response to hexavalent chromium exposure. Appl Microbiol Biotechnol 9735–9747 . doi: 10.1007/s00253-014-6143-3

Wang H, Ren ZJ (2013) A comprehensive review of microbial electrochemical systems as a platform technology. Biotechnol Adv 31:1796–807 . doi: 10.1016/j.biotechadv.2013.10.001

Webster DP, TerAvest M a., Doud DFR, Chakravorty A, Holmes EC, Radens CM, Sureka S, Gralnick J a., Angenent LT (2014) An arsenic-specific biosensor with genetically engineered Shewanella oneidensis in a bioelectrochemical system. Biosens Bioelectron 62:320–324 . doi: 10.1016/j.bios.2014.07.003

West EA, Jain A, Gralnick JA (2017) Engineering a Native Inducible Expression System in Shewanella oneidensis to Control Extracellular Electron Transfer. ACS Synth Biol 6:1627–1634 . doi: 10.1021/acssynbio.6b00349

Wuebbles DJ, Fahey DW, Hibbard KA, Dokken DJ, Stewart BC, Maycock TK (2017)

Climate science special report: fourth National Climate Assessment

Xiao X, Xu C-C, Wu Y-M, Cai P-J, Li W-W, Du D-L, Yu H-Q (2012) Biodecolorization of Naphthol Green B dye by Shewanella oneidensis MR-1 under anaerobic conditions. Bioresour Technol 110:86–90 . doi: 10.1016/j.biortech.2012.01.099

Yang Y, Ding Y, Hu Y, Cao B, Rice S a., Kjelleberg S, Song H (2015) Enhancing Bidirectional Electron Transfer of Shewanella oneidensis by a Synthetic Flavin Pathway. ACS Synth Biol 4:815–823 . doi: 10.1021/sb500331x

Yang Z-C, Cheng Y-Y, Zhang F, Li B-B, Mu Y, Li W-W, Yu H-Q (2016) Rapid Detection and Enumeration of Exoelectrogenic Bacteria in Lake Sediments and a Wastewater Treatment Plant Using a Coupled WO3 Nanoclusters and Most Probable Number Method. Environ Sci Technol Lett 3:133–137 . doi: 10.1021/acs.estlett.6b00112

Yin J, Sun L, Dong Y, Chi X, Zhu W, Qi S, Gao H (2013) Expression of blaA underlies unexpected ampicillin-induced cell lysis of Shewanella oneidensis. PLoS One 8:e60460 . doi: 10.1371/journal.pone.0060460

Yong Y-C, Yu Y-Y, Yang Y, Liu J, Wang J-Y, Song H (2013) Enhancement of extracellular electron transfer and bioelectricity output by synthetic porin. Biotechnol Bioeng 110:408–16 . doi: 10.1002/bit.24732

Yuan S-J, He H, Sheng G-P, Chen J-J, Tong Z-H, Cheng Y-Y, Li W-W, Lin Z-Q, Zhang F, Yu H-Q (2013) A photometric high-throughput method for identification of electrochemically active bacteria using a WO3 nanocluster probe. Sci Rep 3:1315 . doi: 10.1038/srep01315

Yuan S-J, Li W-W, Cheng Y-Y, He H, Chen J-J, Tong Z-H, Lin Z-Q, Zhang F, Sheng G-P, Yu H-Q (2014) A plate-based electrochromic approach for the high-throughput detection of electrochemically active bacteria. Nat Protoc 9:112–9 . doi: 10.1038/nprot.2013.173